ISSN 2413-5577

№ 1 Январь – Март 2026

Экологическая безопасность прибрежной и шельфовой зон моря

Ecological Safety of Coastal and Shelf Zones of Sea

No. 1 January – March 2026

ecological-safety.ru

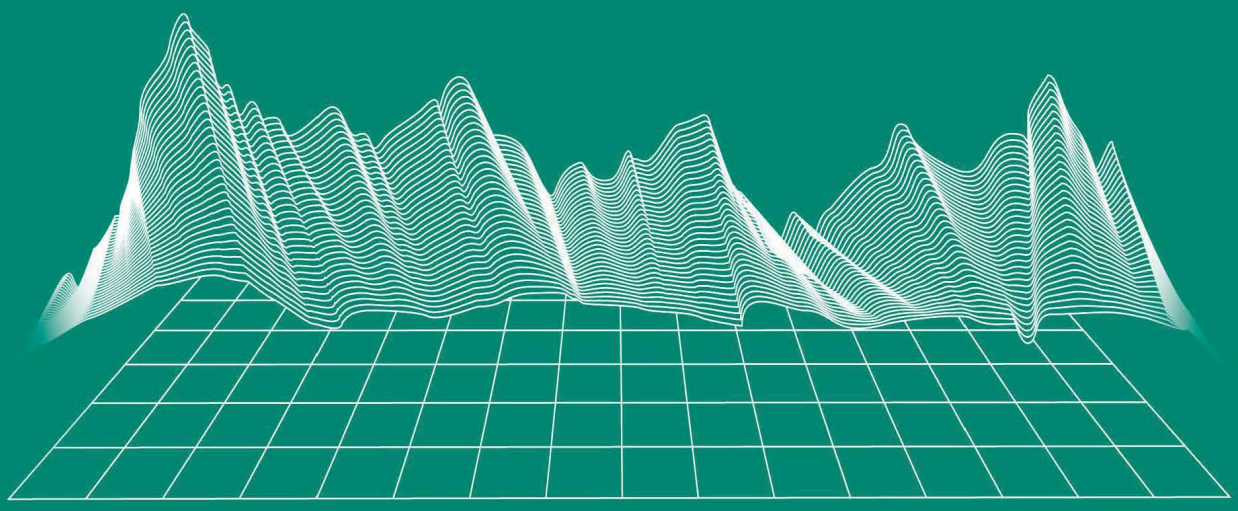

No. 1, 2026
January – March

Publication frequency:
Quarterly

16+

ECOLOGICAL SAFETY OF COASTAL AND SHELF ZONES OF SEA

Scientific and theoretical journal

FOUNDER AND PUBLISHER:
Federal State Budget Scientific Institution
Federal Research Centre
"Marine Hydrophysical Institute of RAS"

Journal is on the list of peer reviewed academic journals of the Higher Attestation Commission of the Russian Federation, where one may publish main research results of a Ph.D. thesis in the following field:

1.6.14 – Geomorphology and paleography (geographical sciences),
1.6.17 – Oceanology (geographical sciences, physical and mathematical sciences, technical sciences),
1.6.18 – Atmosphere and climate sciences (geographical, physical and mathematical sciences),
1.6.20 – Geoinformatics and cartography (geographical sciences),
1.6.21 – Geoecology (geographical sciences),
1.5.16 – Hydrobiology (biological sciences).

Journal is under the scientific and methodological guidance of the Earth Sciences Department of the Russian Academy of Sciences.

Journal is registered by the Federal Service for Supervision of Communications, Information Technology, and Mass Media (registration number ПИ № ФС77-73714 of 21 September 2018 and Эл № ФС77-82679 of 21 January 2022).

Journal coverage: The Russian Federation, other countries.

The Journal is indexed in and reposited at Russian Science Citation Index (RSCI), International Interactive Information and Bibliography System EBSCO.

Journal is in the catalog of scientific periodicals of the RSCI on the platform of the scientific electronic library eLibrary.ru, Cyberleninka.

There is no fee for publishing articles.

e-mail: ecology-safety@mhi-ras.ru

website: http://ecological-safety.ru

Founder, Publisher and Editorial Office address:

2, Kapitanskaya St.,
Sevastopol, 299011, Russia

Phone, fax: + 7 (8692) 54-57-16

EDITORIAL BOARD

Yuri N. Goryachkin – **Editor-in-Chief**, Chief Researcher of FSBSI FRC MHI, Dr.Sci. (Geogr.), Scopus ID: 6507545681, ResearcherID: I-3062-2015, ORCID 0000-0002-2807-201X (Sevastopol, Russia)
Vitaly I. Ryabushko – **Deputy Editor-in-Chief**, Chief Researcher, Head of Department of FSBSI FRC A. O. Kovalevsky Institute of Biology of the Southern Seas of RAS, Dr.Sci. (Biol.), ResearcherID: H-4163-2014, ORCID ID: 0000-0001-5052-2024 (Sevastopol, Russia)
Elena E. Sovga – **Deputy Editor-in-Chief**, Leading Researcher of FSBSI FRC MHI, Dr.Sci. (Geogr.), Scopus ID: 7801406819, ResearcherID: A-9774-2018 (Sevastopol, Russia)
Vladimir V. Fomin – **Deputy Editor-in-Chief**, Chief Researcher, Head of Department of FSBSI FRC MHI, Dr.Sci. (Phys.-Math.), ResearcherID: H-8185-2015, ORCID ID: 0000-0002-9070-4460 (Sevastopol, Russia)
Tatyana V. Khmara – **Executive Editor**, Researcher of FSBSI FRC MHI, Scopus ID: 6506060413, ResearcherID: C-2358-2016 (Sevastopol, Russia)
Sergey V. Berdnikov – Chairman of FSBSI FRC Southern Scientific Centre of RAS, Dr.Sci. (Geogr.), ORCID ID: 0000-0002-3095-5532 (Rostov-on-Don, Russia)
Valery G. Bondur – Director of FSBSI Institute for Scientific Research of Aerospace Monitoring "AEROCOSMOS", vice-president of RAS, academician of RAS, Dr.Sci. (Tech.), ORCID ID: 0000-0002-2049-6176 (Moscow, Russia)
Temir A. Britayev – Chief Researcher of IEE RAS, Dr.Sci. (Biol.), ORCID ID: 0000-0003-4707-3496, ResearcherID: D-6202-2014, Scopus Author ID: 6603206198 (Moscow, Russia)
Elena F. Vasechkina – Deputy Director of FSBSI FRC MHI, Dr.Sci. (Geogr.), ResearcherID: P-2178-2017 (Sevastopol, Russia)
Isaac Gertman – Head of Department of Israel Oceanographic and Limnological Research Institute, Head of Israel Marine Data Center, Ph.D. (Geogr.), ORCID ID: 0000-0002-6953-6722 (Haifa, Israel)
Sergey G. Demyshev – Chief Researcher, Head of Department of FSBSI FRC MHI, Dr.Sci. (Phys.-Math.), ResearcherID C-1729-2016, ORCID ID: 0000-0002-5405-2282 (Sevastopol, Russia)
Nikolay A. Diansky – Chief Researcher of Lomonosov Moscow State University, associate professor, Dr.Sci. (Phys.-Math.), ResearcherID: R-8307-2018, ORCID ID: 0000-0002-6785-1956 (Moscow, Russia)
Vladimir A. Dulov – Chief Researcher of FSBSI FRC MHI, professor, Dr.Sci. (Phys.-Math.), ResearcherID: F-8868-2014, ORCID ID: 0000-0002-0038-7255 (Sevastopol, Russia)
Victor N. Egorov – Scientific Supervisor of FSBSI FRC A. O. Kovalevsky Institute of Biology of the Southern Seas of RAS, academician of RAS, professor, Dr.Sci. (Biol.), ORCID ID: 0000-0002-4233-3212 (Sevastopol, Russia)
Vladimir V. Efimov – Chief Researcher, Head of Department of FSBSI FRC MHI, Dr.Sci. (Phys.-Math.), ResearcherID: P-2063-2017 (Sevastopol, Russia)
Vladimir B. Zalesny – Leading Researcher of FSBSI Institute of Numerical Mathematics of RAS, professor, Dr.Sci. (Phys.-Math.), ORCID ID: 0000-0003-3829-3374 (Moscow, Russia)
Andrey G. Zatsepin – Chief Researcher, Head of Laboratory of P.P. Shirshov Institute of Oceanology of RAS, Dr.Sci. (Phys.-Math.), ORCID ID: 0000-0002-5527-5234 (Moscow, Russia)
Sergey K. Konovalov – Director of FSBSI FRC MHI, corresponding member of RAS, Dr.Sci. (Geogr.), ORCID ID: 0000-0002-5200-8448 (Sevastopol, Russia)
Gennady K. Korotaev – Chief Researcher, Scientific Supervisor of FSBSI FRC MHI, corresponding member of RAS, professor, Dr.Sci. (Phys.-Math.), ResearcherID: K-3408-2017 (Sevastopol, Russia)
Arseniy A. Kubryakov – Leading Researcher, Deputy Director of FSBSI FRC MHI, Ph.D. (Phys.-Math.), ORCID ID: 0000-0003-3561-5913 (Sevastopol, Russia)
Alexander S. Kuznetsov – Leading Researcher, Head of Department of FSBSI FRC MHI, Ph.D. (Tech.), ORCID ID: 0000-0002-5690-5349 (Sevastopol, Russia)
Michael E. Lee – Chief Researcher, Head of Department of FSBSI FRC MHI, Dr.Sci. (Phys.-Math.), professor, ORCID ID: 0000-0002-2292-1877 (Sevastopol, Russia)
Pavel R. Makarevich – Chief Researcher of MMBI KSC RAS, Dr.Sci. (Biol.), ORCID ID: 0000-0002-7581-862X, ResearcherID: F-8521-2016, Scopus Author ID: 6603137602 (Murmansk, Russia)
Ludmila V. Malakhova – Leading Researcher of A. O. Kovalevsky Institute of Biology of the Southern Seas of RAS, Ph.D. (Biol.), ResearcherID: E-9401-2016, ORCID: 0000-0001-8810-7264 (Sevastopol, Russia)
Gennady G. Matishov – Deputy Academician – Secretary of Earth Sciences Department of RAS, Head of Section of Oceanology, Physics of Atmosphere and Geography, Scientific Supervisor of FSBSI FRC Southern Scientific Centre of RAS, Scientific Supervisor of FSBSI Murmansk Marine Biological Institute KSC of RAS, academician of RAS, Dr.Sci. (Geogr.), professor, ORCID ID: 0000-0003-4430-5220 (Rostov-on-Don, Russia)
Ekaterina A. Pozachenyuk – Head of Department in Tavrida Academy of V. I. Vernadsky Crimean Federal University, professor, Dr.Sci. (Geogr.), ORCID ID: 0000-0002-4837-1009 (Simferopol, Russia)
Alexander V. Prazukin – Leading Researcher of FSBSI FRC A. O. Kovalevsky Institute of Biology of the Southern Seas of RAS, Dr.Sci. (Biol.), ResearcherID: H-2051-2016, ORCID ID: 0000-0001-9766-6041 (Sevastopol, Russia)
Anatoly S. Samodurov – Chief Researcher of FSBSI FRC MHI, Dr.Sci. (Phys.-Math.), ResearcherID: V-8642-2017 (Sevastopol, Russia)
Dimitar I. Trukhchev – Institute of Metal Science, equipment, and technologies "Academician A. Balevski" with Center for Hydro- and Aerodynamics at the Bulgarian Academy of Sciences, Dr.Sci. (Phys.-Math.), professor (Varna, Bulgaria)
Naum B. Shapiro – Leading Researcher of FSBSI FRC MHI, Dr.Sci. (Phys.-Math.), ResearcherID: A-8585-2017 (Sevastopol, Russia)

РЕДАКЦИОННАЯ КОЛЛЕГИЯ

Горячкин Юрий Николаевич – **главный редактор**, главный научный сотрудник ФГБУН ФИЦ МГИ, д. г. н., Scopus Author ID: 6507545681, ResearcherID: I-3062-2015, ORCID ID: 0000-0002-2807-201X (Севастополь, Россия)

Рябушко Виталий Иванович – **заместитель главного редактора**, главный научный сотрудник, заведующий отделом ФГБУН ФИЦ ИнБЮМ им. А.О. Ковалевского РАН, д. б. н., ResearcherID: H-4163-2014, ORCID ID: 0000-0001-5052-2024 (Севастополь, Россия)

Совга Елена Евгеньевна – **заместитель главного редактора**, ведущий научный сотрудник ФГБУН ФИЦ МГИ, д. г. н., Scopus Author ID: 7801406819, ResearcherID: A-9774-2018 (Севастополь, Россия)

Фомин Владимир Владимирович – **заместитель главного редактора**, главный научный сотрудник, заведующий отделом ФГБУН ФИЦ МГИ, д. ф.-м. н., ResearcherID: H-8185-2015, ORCID ID: 0000-0002-9070-4460 (Севастополь, Россия)

Хмара Татьяна Викторовна – **ответственный секретарь**, научный сотрудник ФГБУН ФИЦ МГИ, Scopus Author ID: 6506060413, ResearcherID: C-2358-2016 (Севастополь, Россия)

Бердников Сергей Владимирович – председатель ФГБУН ФИЦ ЮНЦ РАН, д. г. н., ORCID ID: 0000-0002-3095-5532 (Ростов-на-Дону, Россия)

Бондур Валерий Григорьевич – директор ФГБНУ НИИ «АЭРОКОСМОС», вице-президент РАН, академик РАН, д. т. н., ORCID ID: 0000-0002-2049-6176 (Москва, Россия)

Британев Темир Аланович – главный научный сотрудник ФГБУН ИПЭЭ, д. б. н., ORCID ID: 0000-0003-4707-3496, ResearcherID: D-6202-2014, Scopus Author ID: 6603206198 (Москва, Россия)

Васечкина Елена Федоровна – заместитель директора ФГБУН ФИЦ МГИ, д. г. н., ResearcherID: P-2178-2017 (Севастополь, Россия)

Гертман Исаак – глава департамента Израильского океанографического и лимнологического исследовательского центра, руководитель Израильского морского центра данных, к. г. н., ORCID ID: 0000-0002-6953-6722 (Хайфа, Израиль)

Демышев Сергей Германович – главный научный сотрудник, заведующий отделом ФГБУН ФИЦ МГИ, д. ф.-м. н., ResearcherID: C-1729-2016, ORCID ID: 0000-0002-5405-2282 (Севастополь, Россия)

Дианский Николай Ардальянович – главный научный сотрудник МГУ им. М. В. Ломоносова, доцент, д. ф.-м. н., ResearcherID: R-8307-2018, ORCID ID: 0000-0002-6785-1956 (Москва, Россия)

Дулов Владимир Александрович – главный научный сотрудник ФГБУН ФИЦ МГИ, профессор, д. ф.-м. н., ResearcherID: F-8868-2014, ORCID ID: 0000-0002-0038-7255 (Севастополь, Россия)

Егоров Виктор Николаевич – научный руководитель ФГБУН ФИЦ ИнБЮМ им. А.О. Ковалевского РАН, академик РАН, профессор, д. б. н., ORCID ID: 0000-0002-4233-3212 (Севастополь, Россия)

Ефимов Владимир Васильевич – главный научный сотрудник, заведующий отделом ФГБУН ФИЦ МГИ, д. ф.-м. н., ResearcherID: P-2063-2017 (Севастополь, Россия)

Залесный Владимир Борисович – ведущий научный сотрудник ФГБУН ИВМ РАН, профессор, д. ф.-м. н., ORCID ID: 0000-0003-3829-3374 (Москва, Россия)

Зацепин Андрей Георгиевич – главный научный сотрудник, руководитель лаборатории ФГБУН ИО им. П.П. Ширшова РАН, д. ф.-м. н., ORCID ID: 0000-0002-5527-5234 (Москва, Россия)

Коновалов Сергей Карпович – директор ФГБУН ФИЦ МГИ, член-корреспондент РАН, д. г. н., ORCID ID: 0000-0002-5200-8448 (Севастополь, Россия)

Коротаев Геннадий Константинович – главный научный сотрудник, научный руководитель ФГБУН ФИЦ МГИ, член-корреспондент РАН, профессор, д. ф.-м. н., ResearcherID: K-3408-2017 (Севастополь, Россия)

Кубряков Арсений Александрович – ведущий научный сотрудник, заместитель директора ФГБУН ФИЦ МГИ, д. ф.-м. н., ORCID ID: 0000-0003-3561-5913 (Севастополь, Россия)

Кузнецов Александр Сергеевич – ведущий научный сотрудник, заведующий отделом ФГБУН ФИЦ МГИ, к. т. н., ORCID ID: 0000-0002-5690-5349 (Севастополь, Россия)

Ли Михаил Ен Гон – главный научный сотрудник, заведующий отделом ФГБУН ФИЦ МГИ, профессор, д. ф.-м. н., ORCID ID: 0000-0002-2292-1877 (Севастополь, Россия)

Макаревич Павел Робертович – главный научный сотрудник ММБИ КНЦ РАН, д. б. н., ORCID ID: 0000-0002-7581-862X, ResearcherID: F-8521-2016, Scopus Author ID: 6603137602 (Мурманск, Россия)

Малахова Людмила Васильевна – ведущий научный сотрудник ФГБУН ФИЦ ИнБЮМ им. А.О. Ковалевского РАН, к. б. н., ResearcherID: E-9401-2016, ORCID ID: 0000-0001-8810-7264 (Севастополь, Россия)

Матишов Геннадий Григорьевич – заместитель академика-секретаря Отделения наук о Земле РАН – руководитель Секции океанологии, физики атмосферы и географии, научный руководитель ФГБУН ФИЦ ЮНЦ РАН, научный руководитель ФГБУН ММБИ КНЦ РАН, академик РАН, профессор, д. г. н., ORCID ID: 0000-0003-4430-5220 (Ростов-на-Дону, Россия)

Празукин Александр Васильевич – ведущий научный сотрудник ФГБУН ФИЦ ИнБЮМ им. А.О. Ковалевского РАН, д. б. н., Researcher ID: H-2051-2016, ORCID ID: 0000-0001-9766-6041 (Севастополь, Россия)

Позаченюк Екатерина Анатольевна – заведующая кафедрой Института «Таврическая академия» ФГАОУ КФУ им. В.И. Вернадского, профессор, д. г. н., ORCID ID: 0000-0002-4837-1009 (Симферополь, Россия)

Самодуров Анатолий Сергеевич – главный научный сотрудник ФГБУН ФИЦ МГИ, д. ф.-м. н., ResearcherID: V-8642-2017 (Севастополь, Россия)

Трухчев Димитър Иванов – старший научный сотрудник Института океанологии БАН, профессор, д. ф.-м. н. (Варна, Болгария)

Шапиро Наум Борисович – ведущий научный сотрудник ФГБУН ФИЦ МГИ, д. ф.-м. н., ResearcherID: A-8585-2017 (Севастополь, Россия)

CONTENTS

№ 1. 2026 January – March, 2026

СОДЕРЖАНИЕ

№ 1. 2026 Январь – Март, 2026

Original paper

Experience in Monitoring Greenhouse Gas Emissions and Uptake in the Coastal Sea Zone

B. V. Divinsky *, S. B. Kuklev, V. V. Kremenetsky, A. A. Nedospasov, V. V. Ocherednik, O. N. Kukleva

Shirshov Institute of Oceanology, Russian Academy of Sciences, Moscow, Russia
* *e-mail: divin@ocean.ru*

Abstract
The study aims to monitor the emissions and uptake of carbon dioxide and water vapour at a specialized carbon polygon near the city of Gelendzhik, Krasnodar Krai. The paper analyses CO_2 and H_2O fluxes along with atmospheric parameters recorded from December 2024 to May 2025 using data from an automatic LI-COR Environmental monitoring station installed 25 m from the shoreline. Gas fluxes were calculated using the eddy covariance method at a frequency of 10 Hz. The main components of the station are atmospheric heat flux sensors, including a photosynthetically active radiation sensor; an ultrasonic anemometer; a gas analyzer; an air temperature and humidity sensor; soil temperature, heat flux and moisture content sensors; and a precipitation gauge. Daytime and nighttime partitioning of the net CO_2 flux into gross primary production and ecosystem respiration was applied. The results of the experiment showed that about 500 g of carbon dioxide per square meter was emitted into the atmosphere from the study area during the specified period. Ecosystem respiration accounted for 1300 g, whereas gross primary production accounted for 800 g. Seasonal dynamics of the exchange were identified: during winter months and in early calendar spring, CO_2 emission into the atmosphere prevails, while from April onward its uptake by the ecosystem is observed. The average CO_2 concentration in the air during the observation period was 423.2 ± 5.2 μmol/mol (with a global average of 420 μmol/mol). Despite the challenging conditions of the station's location in the coastal zone, the obtained results are physically sound and can be used to estimate greenhouse gas fluxes.

Keywords: carbon polygons, Gelendzhik, carbon dioxide flux, eddy covariance method, Li-Cor

Acknowledgements: The work was performed under state assignment topic no. FMWE-2023-0001 of Institute of Oceanology of RAS and funded by the Andrey Melnichenko Foundation.

For citation: Divinsky, B.V., Kuklev, S.B., Kremenetsky, V.V., Nedospasov, A.A., Ocherednik, V.V. and Kukleva, O.N., 2026. Experience in Monitoring Greenhouse Gas Emissions and Uptake in the Coastal Sea Zone. *Ecological Safety of Coastal and Shelf Zones of Sea*, (1), pp. 6–26.

© Divinsky B. V., Kuklev S. B., Kremenetsky V. V., Nedospasov A. A., Ocherednik V. V., Kukleva O. N., 2026

This work is licensed under a Creative Commons Attribution-Non Commercial 4.0 International (CC BY-NC 4.0) License

Опыт мониторинга эмиссии и поглощения парниковых газов в прибрежной зоне моря

Б. В. Дивинский *, С. Б. Куклев, В. В. Кременецкий, А. А. Недоспасов, В. В. Очередник, О. Н. Куклева

Институт океанологии им. П.П. Ширшова РАН, Москва, Россия
* *e-mail: divin@ocean.ru*

Аннотация
Цель работы – мониторинг эмиссии и поглощения углекислого газа и водяного пара на специализированном карбоновом полигоне в районе г. Геленджика Краснодарского края. Проанализированы потоки CO_2 и H_2O, а также параметры состояния атмосферы, зарегистрированные с декабря 2024 г. по май 2025 г. с помощью автоматической станции мониторинга *LI-COR Environmental*, установленной в 25 м от береговой линии. Потоки газов рассчитывались методов турбулентных пульсаций с частотой 10 Гц. Основными компонентами станции являются: датчики потоков атмосферного тепла, включая датчик фотосинтетической активной радиации; ультразвуковой анемометр; газоанализатор; датчик температуры и влажности воздуха; почвенные датчики. Применялось дневное и ночное разделение чистого потока CO_2 на валовую первичную продукцию и экосистемное дыхание. Установлено, что за указанный период на исследуемом участке с квадратного метра в атмосферу поступило около 500 г углекислого газа. При этом на экосистемное дыхание пришлось около 1300 г, на валовую продукцию – 800 г. Выявлена сезонная динамика обмена: в зимние месяцы, а также в начале календарной весны преобладает эмиссия CO_2 в атмосферу, с апреля наблюдается его усвоение экосистемой. Средняя за период наблюдений концентрация CO_2 в воздухе составила 423.2 ± 5.2 мкмоль/моль (при среднемировой в 420 мкмоль/моль). Несмотря на сложные условия расположения станции в прибрежной зоне моря, полученные результаты физически обоснованы и могут использоваться для оценок потоков парниковых газов.

Ключевые слова: карбоновые полигоны, Геленджик, поток углекислого газа, метод турбулентных пульсаций, *Li-Cor*

Благодарности: работа выполнена в рамках темы государственного задания Института океанологии РАН № FMWE-2023-0001 при финансовой поддержке Фонда Мельниченко.

Для цитирования: *Дивинский Б. В., Куклев С. Б., Кременецкий В. В., Недоспасов А. А. и др.* Опыт мониторинга эмиссии и поглощения парниковых газов в прибрежной зоне моря // Экологическая безопасность прибрежной и шельфовой зон моря. 2026. № 1. С. 6–26. EDN PGBTAO.

Introduction

Greenhouse gases that determine the nature of climate change on the planet include water vapour H_2O, carbon dioxide CO_2, methane CH_4, nitrous oxide N_2O, and a group of fluorine-containing gases. Water vapour is the most abundant greenhouse gas in the atmosphere. Its contribution to the climatic fluctuations in air temperature [1)], according to various estimates, is 40–70%. At the same time,

[1)] Atmospheric concentration of greenhouse gases: technical documentation. U.S. Environmental Protection Agency, 2016. 16 p. URL: https://www.epa.gov/sites/default/files/2016-08/documents/ghg-concentrations_documentation.pdf [Accessed: 15 December 2025].

it is believed that human economic activities (such as land reclamation and deforestation) have only a small direct impact on H_2O concentrations. According to the latest bulletin of the World Meteorological Organization [2)], the most important greenhouse gas with a significant anthropogenic footprint is carbon dioxide. Over the period from 1750 (approximately the pre-industrial era) to 2023, the CO_2 share of the anthropogenic temperature increase was about 66%. For comparison: the share of CH_4 was 16%, and that of N_2O was 6%. The global average concentration of carbon dioxide in the atmosphere in 2023 was 420.0 ± 0.1 μmol/mol, with the average growth rate over the last decade reaching 2.4 μmol/mol per year.

In the Russian Federation, research on greenhouse gas fluxes has been developing quite intensively in recent years [1–8]. In 2023, a monograph [9] was published summarizing balance estimates of fluxes of the main greenhouse gases in Russia and concluding that the so-called forest regions of the country (Siberian, Far Eastern, etc.) are net sinks of greenhouse gases, while emission sources are the southern regions with a predominance of pastures and agricultural lands (Southern, North Caucasian, Volga).

In 2021, within the framework of the national system for monitoring greenhouse gas dynamics, the Ministry of Science and Higher Education of the Russian Federation launched the "Carbon Polygons" project (URL: https://carbon-polygons.ru), within which monitoring observations are carried out at nineteen separate sites located in various natural zones of Russia (steppes, taiga forests, swamps, pastures, agricultural lands, forest-tundra). The main task of the carbon polygons is to conduct long-term and, crucially, continuous measurements of greenhouse gas fluxes using modern instrumentation. One such polygon is the measuring site in the area of Gelendzhik, Krasnodar Krai.

Despite the expanding observation network, there is still a lack of detailed data on greenhouse gas fluxes for the coastal resort zones of the Black Sea based on direct instrumental measurements. The features of relief, soils, vegetation, and proximity to the sea form a unique coastal ecosystem whose carbon balance remains poorly understood.

This work aims at studying the fluxes of carbon dioxide and water vapour at the Gelendzhik carbon polygon from December 2024 to May 2025.

Materials and Methods

Gelendzhik carbon polygon. The Gelendzhik polygon, with a total area of 26 hectares, consists of terrestrial and marine parts, where regular instrumental observations of carbon dioxide, water vapour, and methane fluxes, as well as associated atmospheric state parameters, have been conducted since 2022 [10–12].

[2)] The state of greenhouse gases in the atmosphere based on global observations through 2023. Geneva : WMO, 2024. 11 p. (WMO Greenhouse Gas Bulletin ; No. 20). Available at: https://library.wmo.int/idurl/4/69057 [Accessed: 15 December 2025].

According to soil-ecological zoning [3)], the Gelendzhik area is located within the Novorossiysk district of the Western Brown Earth-Forest soil-bioclimatic region of the subboreal geographical belt. The soil cover here is mainly represented by acidic podzolized brown earths and calcareous soddy soils. The herbaceous layer is mainly formed by sheep fescue and heath false brome. Among the plants found are butcher's-broom (sp), three-leaf jasmine (sp), Anatolian blackberry (cop1), and resinous psoralea (un). Coastal vegetation is also represented by Pitsunda pine with an average crown attachment height of 8–9 m, downy oak, growing singly or in clumps, with an average age of about 12 years, as well as hornbeam, dog's bramble, Christ's thorn, and juniper.

In November 2024, the measuring part of the polygon was supplemented with an automatic monitoring station based on the LI-7200 gas analyzer (LI-COR Environmental, USA). The installation is operated by the Southern Branch of the Shirshov Institute of Oceanology, Russian Academy of Sciences. The station is mounted on open natural soil 7 m from a rocky cliff and 25 m directly from the shoreline (Fig. 1). Station coordinates: 44.576657° N, 37.977450° E.

The main components of the station (Fig. 2) are:

1. LI-7550 interface Module (a universal component of all gas measurement systems, containing integrated tools for digital signal processing from gas analyzers).

F i g . 1 . Location of the LI-COR monitoring station at the Gelendzhik polygon

[3)] Information system "Soil-Geographic Database of Russia": [website]. Available at: https://soil-db.ru [Accessed: 15 December 2025] (in Russian).

F i g . 2 . Measuring instruments of the LI-COR monitoring station: *1* – LI-7550 interface module; *2* – atmospheric heat flux sensors, including a photosynthetically active radiation sensor; *3* – ultrasonic anemometer; *4* – gas analyser; *5* – air temperature and humidity sensor; *6* – soil temperature, heat flux and moisture content sensors; *7* – precipitation gauge

2. Atmospheric heat flux sensors, including photosynthetically active radiation sensors (Kipp&Zonen, Netherlands and LI-190R).

3. uSonik-3 ultrasonic anemometer (Metek, Germany).

4. LI-7200 gas analyzer.

5. HMP155 air temperature and humidity sensor (Vaisala, Finland).

6. HydraProbe (Stevens Water Monitoring Systems, USA) and Hukseflux (Hukx, Netherlands) soil temperature, heat flux, and moisture content sensors.

7. TR-525M precipitation gauge (Texas Electronics, USA).

The LI-7200 gas analyzer determines the molar fractions of water vapour and carbon dioxide in an air sample with an accuracy of 2% and 1% of reading, respectively. The station is powered from the laboratory building. The station is connected to a server for acquisition, accumulation and storage of measurement data. The sensor interrogation frequency of the measuring equipment is 10 Hz. All data are processed by standard software and stored on the server.

The data obtained from the station form three separate arrays:

1. Half-hourly data arrays with a sampling interval of 0.1 s (total 18,000 values), containing values of atmospheric carbon dioxide CO_2 and water vapour H_2O, atmospheric pressure, air temperature, and three wind speed components.

2. Processed data arrays with a 1-minute resolution, including the following characteristics: surface albedo; incoming and outgoing shortwave and longwave radiation; Photosynthetic Photon Flux Density (*PPFD*); precipitation amount; air temperature and relative humidity; soil moisture content and temperature; Soil Heat Flux (*SHF*).

3. Statistical parameters characterizing the atmosphere and soil state, obtained by processing the 30-minute raw data. The parameters include: mean values, variance, and higher moments (skewness, kurtosis) of the distributions of three wind speed components (two horizontal and one vertical), carbon dioxide and water vapour concentrations, soil temperature; mean values of surface albedo, incoming and outgoing shortwave and longwave radiation, *PPFD*, precipitation, air humidity and temperature, soil moisture content and temperature, *SHF*; mean values of sensible and latent heat fluxes, carbon dioxide and water vapour fluxes; mean atmospheric state parameters (temperature, humidity, pressure, wind speed and direction, estimate of turbulent kinetic energy, Bowen ratio); estimates of covariance between greenhouse gas fluxes and main meteorological parameters.

The software (EddyPro) allows for correcting flux estimates based on the analysis of outliers, airflow stability, trend components, and time delays of measuring equipment.

Greenhouse gas flux calculations

Eddy covariance method. Currently, the most common and theoretically sound method for calculating greenhouse gas fluxes is the eddy covariance method. The basic principles of the method are outlined in guidelines [4), 5)] and are as follows. The turbulent vertical flux of any substance (e.g., greenhouse gas) can be represented as the covariance of the vertical wind speed and the concentration of that substance. The high frequency of turbulent fluctuations typical of the atmosphere imposes increased requirements on the recording equipment and the operating frequency of sensors (10 Hz in our case). Important limitations of the method are the following assumptions: 1) air density fluctuations are small and can be neglected; 2) over the measurement period (30 min), vertical air mass movements are insignificant. In real natural conditions, especially in areas with complex terrain, these conditions are not always met, which leads to natural errors and measurement uncertainties.

Footprint. An important parameter of the eddy covariance method is so-called footprint – the spatial area from which fluxes are recorded by the station's instruments. The footprint estimate depends on many factors: the height of the instrument installation (4 m in our case), surface roughness, and the nature of atmospheric stratification. The horizontal extent of the footprint, defined as the distance upwind from the sensor installation point, is described statistically in terms of distribution quantiles.

[4)] Aubinet, M., Vesala, T. and Papale, D., eds., 2012. Eddy Covariance: A Practical Guide to Measurement and Data Analysis. Springer Science+Business Media B.V., 438 p. https://doi.org/10.1007/978-94-007-2351-1

[5)] Burba, G.G., Kurbatova, Yu.A., Kuricheva, O.A., Avilov, V.K., etc., 2016. Eddy Covariance Method. Brief Practical Guide. Moscow: A.N. Severtsov Institute of Ecology and Evolution RAS, 223 p. (in Russian).

For example, the 80% footprint is the length (in meters) of the area from which the contribution of a given substance (CO_2 in our case) to the flux is 80%.

Flux partitioning. Carbon dioxide flux calculated by the eddy covariance method represents the Net Ecosystem Exchange (*NEE*) and can be partitioned into the two largest components of the carbon cycle: Gross Primary Production (*GPP*) and ecosystem respiration (R_{eco}). Gross primary production is the total amount of organic matter created by autotrophic organisms during photosynthesis (more precisely, chemosynthesis). *GPP* thus reflects the amount of carbon absorbed by plants during photosynthesis. Ecosystem respiration is associated with the processes of converting organic carbon into CO_2 by organisms and acts as the main pathway for carbon release from terrestrial ecosystems into the atmosphere. In general form, $NEE = R_{eco} - GPP$.

Flux partitioning was performed according to the recommendations outlined in [13]. Currently, several partitioning methods exist. The two most widely used alternative approaches are the so-called nighttime and daytime partitioning:

1. In nighttime partitioning [14], R_{eco} is estimated during nighttime and subsequently extrapolated to the daylight hours. *GPP* is calculated as the difference between R_{eco} and *NEE*. In this case, the stochastic nature of turbulence and noise in the measurement signals can lead to negative *GPP* flux estimates, even though they are positive by definition. However, negative *GPP* fluxes should not be removed (or set to zero), as this would lead to a significant bias in the overall estimates of gross primary production.

2. Daytime partitioning [15] is based on model estimates of NEE_{mod} using light response curves, assuming proportionality between carbon dioxide fluxes and incoming radiation. Given the uncertainty and error of model approximations of fluxes, the resulting model flux, calculated as the difference ($R_{eco} - GPP$), may not exactly match the measured *NEE* value.

An important detail should be noted. Since the natural system is complex and multifactorial, data on primary production and ecosystem respiration fluxes obtained for a specific period are likely to contain significant uncertainty. However, when processed statistically over a long period (months, years), these data will quite correctly reflect the balance components of carbon cycle of the ecosystem under consideration.

Data quality. A key assumption of the eddy covariance method is the stationarity of the mean flow (spatial homogeneity). The initial data quality is assessed according to the approach outlined in [16]. The initial 30-minute observation series is divided into six 5-minute segments. For each segment, the covariance between vertical velocity fluctuations and the parameter under study is calculated.

The flux is considered stationary if the covariances for the individual segments differ from the covariance calculated for the entire series by no more than 30%. Overall, a flag is assigned to each series indicating the quality of the measurements:

– flag 0 (deviation < 30%) – high-quality data;

– flag 1 (deviation < 100%) – medium-quality data but suitable for use in long-term research programs;

– flag 2 (deviation > 100%) – low-quality data to be excluded from analysis.

The proportion of series with low-quality data (flag 2) for carbon dioxide fluxes by month is as follows: December – 22%, January – 15%, February – 26%, March – 21%, April – 19%, May – 22%. Thus, on average across months, about 20% of data are deemed unfit for use due to poor quality, resulting in gaps in the overall time series. The continuity of the time series is achieved by artificially filling these gaps using algorithms described in [13].

Results and Discussion

The main parameters used to estimate the integral values of greenhouse gas emissions (or uptake) are: carbon dioxide flux, sensible and latent heat fluxes, incoming shortwave radiation flux, air and soil temperature, relative humidity, water vapour pressure deficit, and characteristics of the wind flow (wind speed, wind direction, friction velocity, Monin – Obukhov length for turbulent flow).

Fig. 3–5 presents the temporal dynamics of some atmospheric parameters, as well as the carbon dioxide and water vapour content measured over the six-month experimental period.

As follows from Fig. 3, a steady increase in the photosynthetic photon flux density, necessary for photosynthesis, is observed from the end of January. With the onset of calendar spring (March), the soil gradually warms up, and the sign of *SHF* becomes positive. Negative average daily air temperatures were recorded only in the second half of February. Fig. 3 presents the seasonal dynamics of key abiotic factors determining the ecosystem's carbon exchange. Analysis of average daily values shows that from the end of January, a steady increase in *PPFD* is observed, which creates prerequisites for the start of active vegetation. Soil warming, indicated by the change in the SHF sign to positive, becomes stable from March, coinciding with the onset of calendar spring. At the same time, periods with negative average daily air temperature T_a values were noted only in the second half of February. The dynamics of soil temperature T_s corresponded to changes in air temperature and radiation balance. This comprehensive dataset serves as a basis for subsequent analysis of the driving forces and seasonal dynamics of greenhouse gas fluxes.

The distribution of atmospheric precipitation by month during the observation period is uneven (Fig. 4).

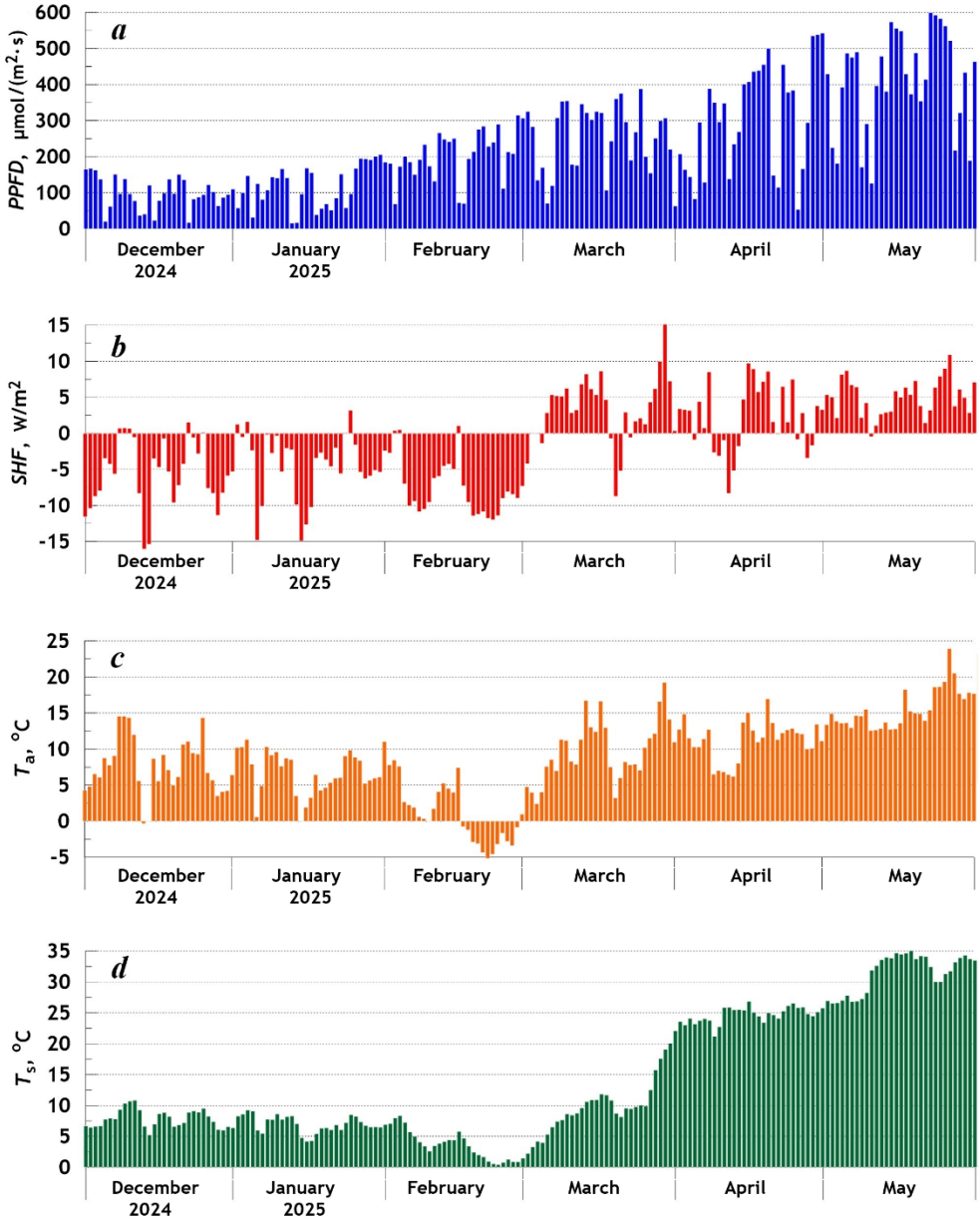

Fig. 3. Daily average values of photosynthetic photon flux density *PPFD*, soil heat flux *SHF*, air temperature T_a and soil temperature T_s from December 2024 to May 2025

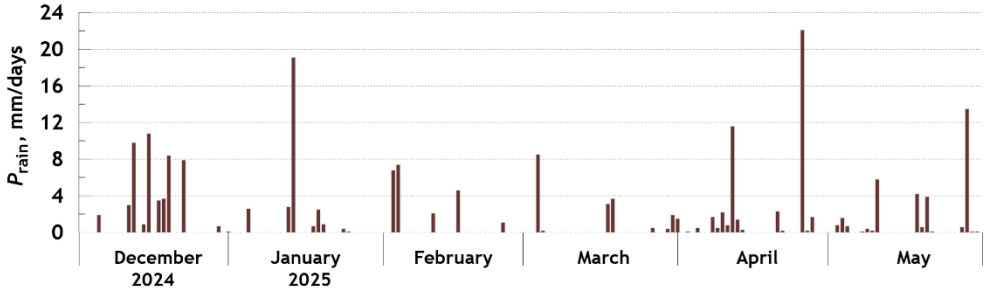

Fig. 4. Daily atmospheric precipitation values from December 2024 to May 2025

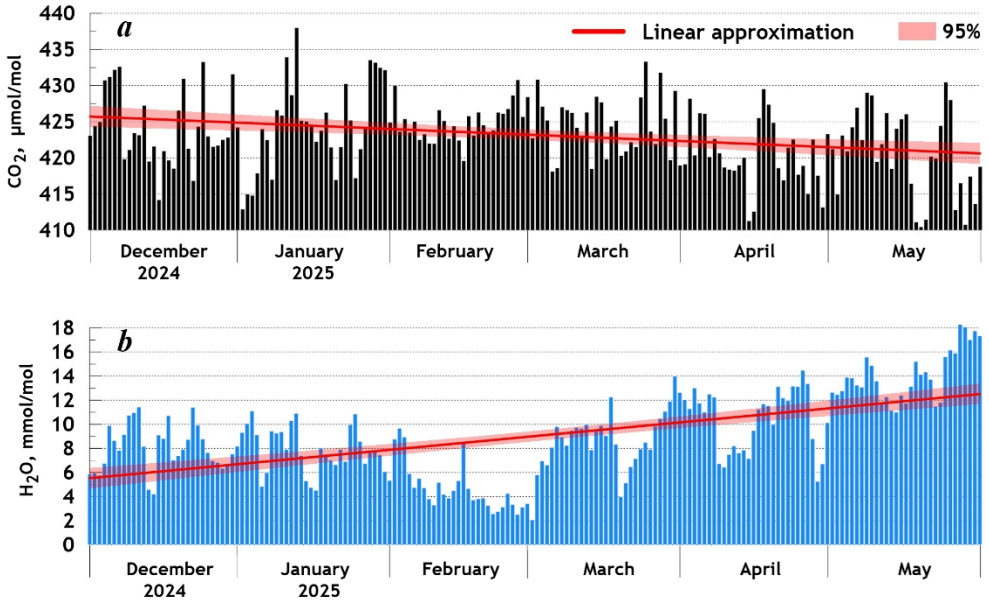

Fig. 5. Daily average concentrations of carbon dioxide and water vapour in the atmosphere from December 2024 to May 2025. The red line represents linear approximation, the pink area shows the 95% confidence interval for the regression line

Total monthly precipitation values were (climatic norms according to the Unified State System of Information on the Situation in the World Ocean [6]) are given in parentheses): December – 50.7 mm (60.1 mm); January – 29.1 mm (40.4 mm); February – 22.0 mm (31.8 mm); March – 19.8 mm (32.3 mm); April – 45.6 mm (30.7 mm); May – 32.7 mm (31.6 mm). December was the wettest month, although precipitation was somewhat below climatological values. January, February, and March were abnormally dry; in April, precipitation exceeded the norm by 1.5 times; May was characterized by average values.

The maximum carbon dioxide content (Fig. 5) was observed in February (437.8 μmol/mol), and the minimum in May (410.5 μmol/mol).

The highest water vapour concentrations were recorded in May (18.1 mmol/mol), the lowest in March (1.9 mmol/mol). The average CO_2 concentration in the air over the observation period was 423.2 ± 5.2 μmol/mol (compared to the global average of 420 μmol/mol), and for H_2O it was 9.0 ± 3.6 mmol/mol. From December to May, a steady negative trend in average daily carbon dioxide concentrations and a positive trend in water vapour were observed. Such seasonal dynamics are typical for all territories with seasonal changes in key atmospheric parameters and vegetation cover, which determine air temperature and photosynthetic activity.

Fig. 6 presents monthly wind roses, characterizing the frequency of average wind speeds across 45-degree directional sectors.

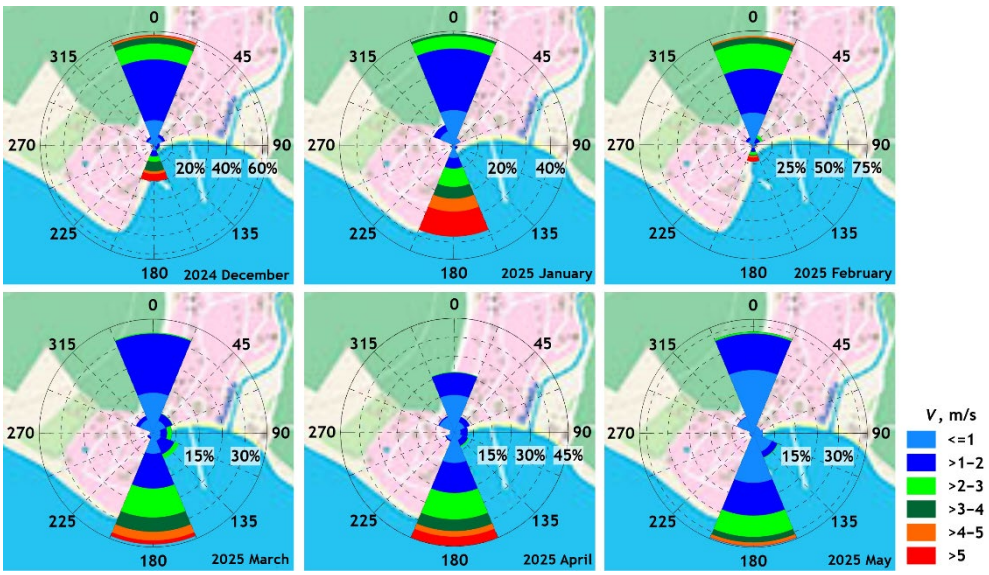

F i g . 6 . Wind speed frequency V (%) by directions in the experiment area

[6] Unified State System of Information on the Situation in the World Ocean (ESIMO). URL: www.esimo.ru (date of access: 10.12.2025) (in Russian).

As follows from Fig. 6, the wind regime is characterized by two pronounced directional sectors: northern and southern. In December and February, winds from northern directions dominated (60% and 73% frequency, respectively), in April – those from southern directions (45% frequency). In January, northern winds slightly prevailed, while in March and May – the southern ones. The average monthly and maximum wind speeds in December were 1.8 and 20.0 m/s, respectively; in January – 2.1 and 17.1 m/s; in February – 1.7 and 18.9 m/s; in March – 1.5 and 15.7 m/s; in April – 1.5 and 18.5 m/s; in May – 1.0 and 12.7 m/s. Despite the fact that climatically the strongest winds in the region are the northern ones (Novorossiysk bora), during the period under review, winds from southern directions exhibited the highest speeds.

The calculated flux footprint areas (Fig. 7) generally reflect the wind conditions discussed above. The footprint is elongated in the meridional direction

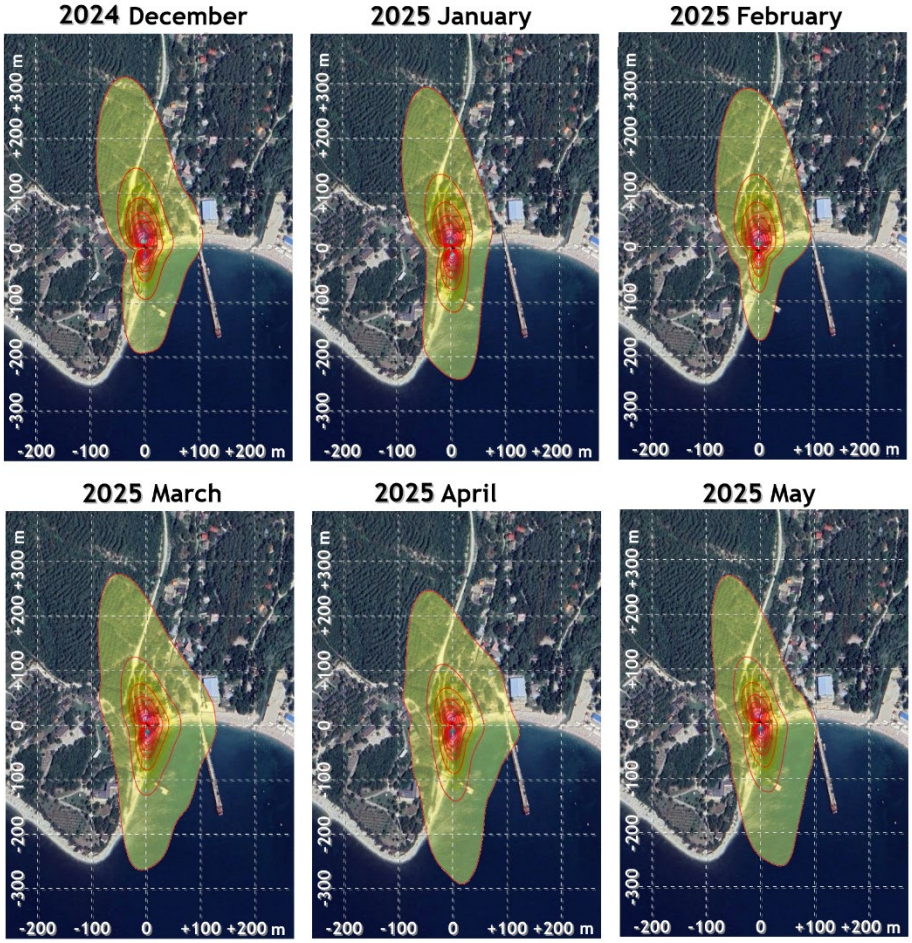

F i g . 7 . Monthly flux footprint coverage areas. Isolines are drawn for 10, 20, …, 90th percentiles of the distributions

(north – south). The average distance contributing most to the measured flux was 60 m from the measuring station, while the distance covering 90% of the contribution (90th percentile) reached 175 m. The monthly average footprint area thus amounts to about 11,000 m² of the underlying surface. In December and February, the footprint extends significantly to the north. In March and May, the footprint expands to the southeast, following the increasing frequency of southeast winds.

Fig. 8 and 9 show the diurnal dynamics of water vapour fluxes and fluctuations in net ecosystem exchange *NEE*, respectively, averaged by month. The graphs show the mean values, 95% confidence intervals for the mean, and the medians of the distributions. Differences between mean and median values indicate deviations of flux distributions from normality. The discrepancies are particularly pronounced in winter months, possibly due to difficulties in interpreting measurement results during this period. Nevertheless, the behavior of mean and median curves generally coincides.

Water vapour fluxes reach their daytime peak from 10:00 to 16:00 in winter; with the onset of spring, the peak period expands. A second maximum of water vapour fluxes, occurring at night (23:00–01:00), is noteworthy, and is discernible in December and (more weakly) in January.

Winter months are characterized by a prevailing emission of carbon dioxide into the atmosphere (Fig. 9) with a relatively weak diurnal cycle.

Starting in March, a stable diurnal cycle of CO_2 flux fluctuations is established: during the daytime, carbon dioxide is actively absorbed, and at night it is released. In May, the time range of carbon dioxide uptake is about 12 hours (from 6:00 to 18:00). The largest CO_2 emission was observed in December, and the largest

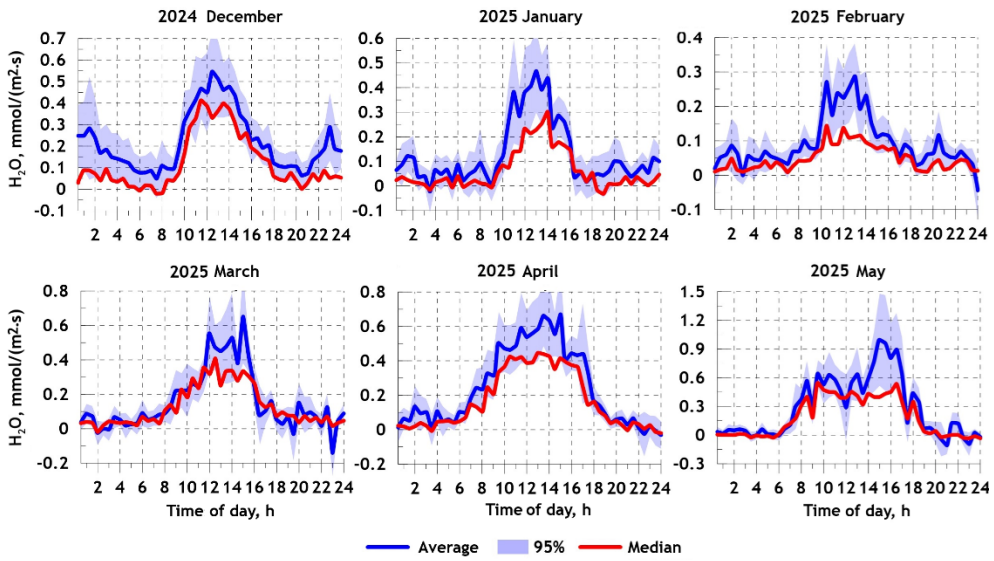

Fig. 8. Diurnal water vapour fluxes

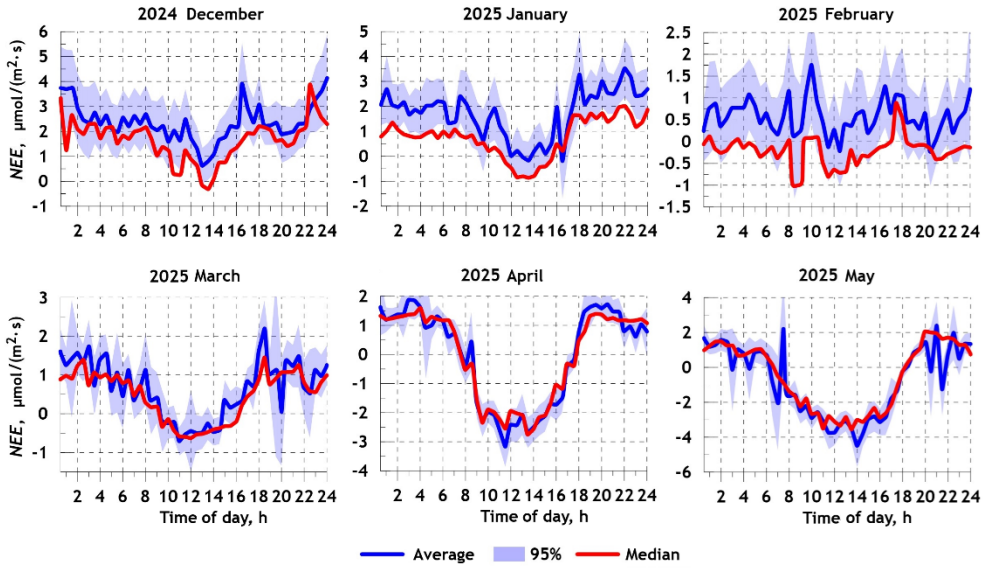

Fig. 9. Diurnal carbon dioxide fluxes

uptake in May, with characteristic flux values of 4–5 and 3–4 μmol/m²·s, respectively. Diurnal fluctuations in water vapour and carbon dioxide fluxes are noted by almost all researchers (e.g., in studies [17–19]). These fluctuations are driven by air temperature and photosynthetic activity. Naturally, the parameters of these fluctuations (amplitude, timing of peaks) depend on many other factors related to soil moisture, the state of the underlying surface, and atmospheric conditions.

As already mentioned, the carbon dioxide flux *NEE* can be partitioned into two important components of the carbon cycle, namely gross primary production *GPP* and ecosystem respiration R_{eco}; the graphs of their diurnal fluctuations are shown in Fig. 10. *GPP* and R_{eco} estimates are calculated using two alternative methods associated with daytime and nighttime partitioning of carbon dioxide fluxes.

Thus, gross primary production *GPP* quantifies the photosynthetic uptake of carbon by the ecosystem. Positive extremes of *GPP* correspond to maximum uptake of carbon dioxide by the ecosystem. In the context of ecosystems, negative respiration R_{eco} refers to the uptake of carbon dioxide, while positive respiration refers to its release. Recall: in the nighttime partitioning scheme, ecosystem respiration R_{eco} is modeled, and gross primary production *GPP* is calculated as the difference between R_{eco} and *NEE*. In daytime partitioning, both *GPP* and R_{eco} are modeled. In this case, the resulting model ecosystem exchange, calculated as $NEE_{mod} = R_{eco}(\text{day}) - GPP(\text{day})$, considering the inevitable modeling error, will differ from the experimentally measured *NEE*.

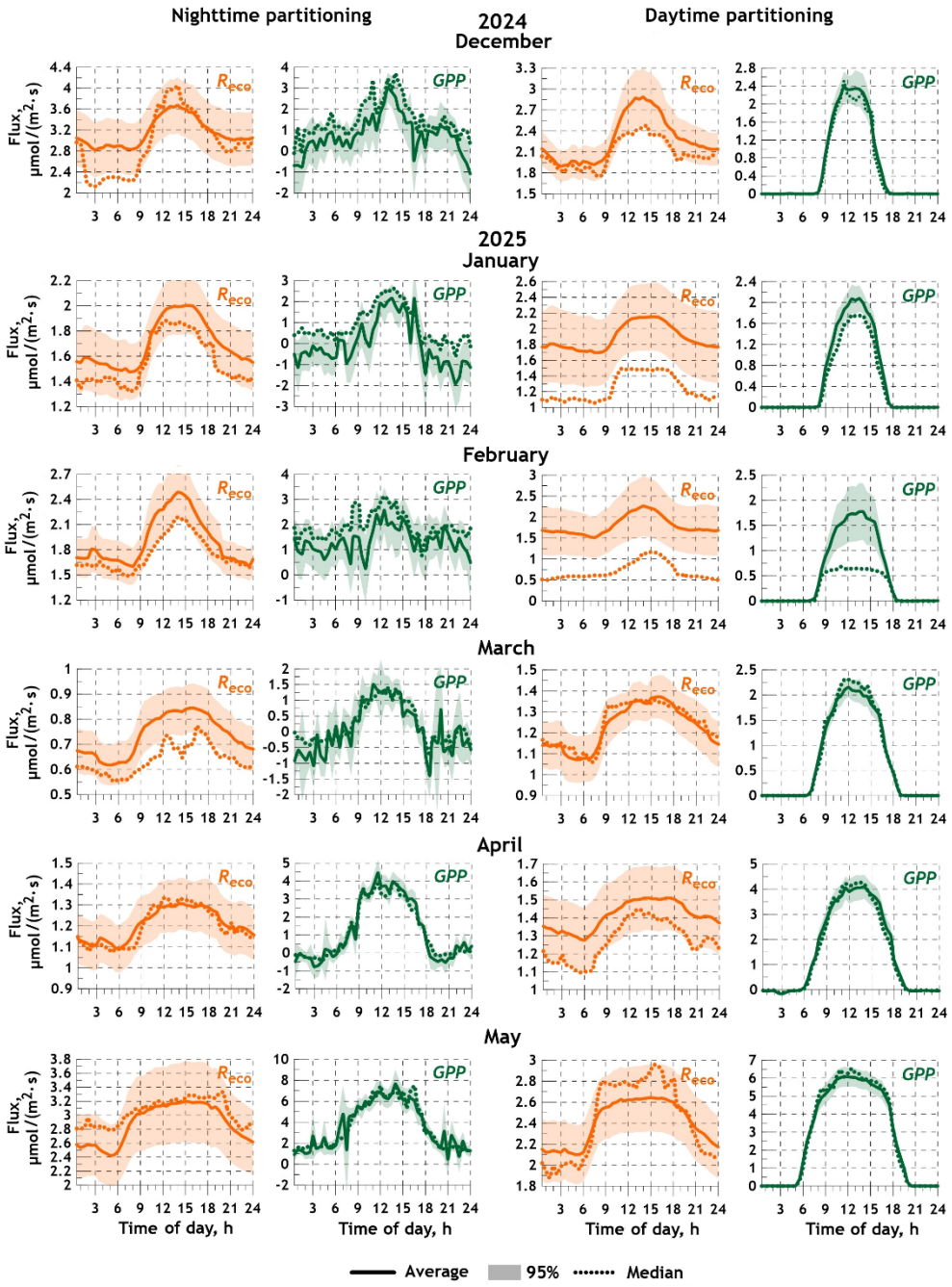

Fig. 10. Diurnal fluxes of gross primary production *GPP* and ecosystem respiration R_{eco} (the solid line is average, the dotted line is median, the shaded area is 95% confidence interval)

In Fig. 10, the second peak of ecosystem respiration occurring at night is quite remarkable. The stepped shape of the *GPP* curve in the daytime partitioning scheme is noteworthy, due to the features of the algorithmic approximation based on light-response curves. Nevertheless, with the onset of calendar spring and the intensification of photosynthesis, the "daytime" and "nighttime" *GPP* estimates show satisfactory agreement, especially in April and May.

Fig. 11 and 12 present the total daily and total monthly masses of carbon dioxide emitted into the atmosphere or absorbed from the atmosphere, respectively. The calculations were performed using the nighttime flux partitioning scheme.

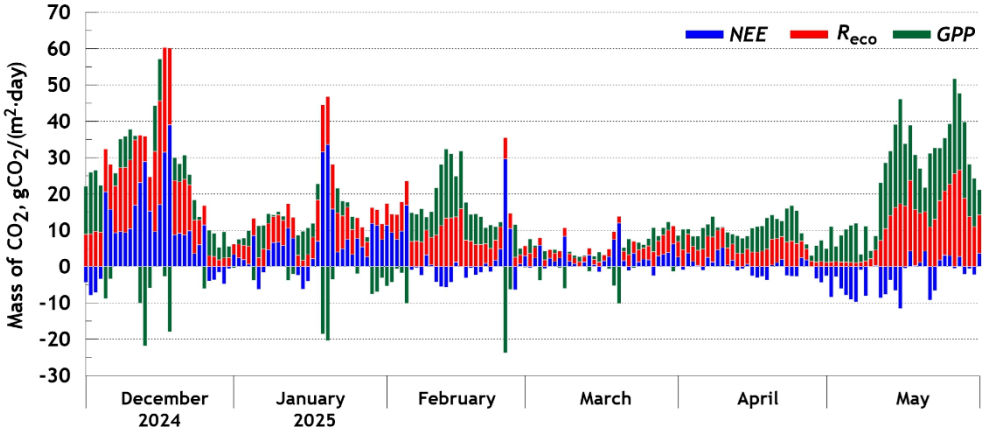

Fig. 11. Daily masses of carbon dioxide corresponding to net ecosystem exchange *NEE*, gross primary production *GPP* and ecosystem respiration R_{eco}

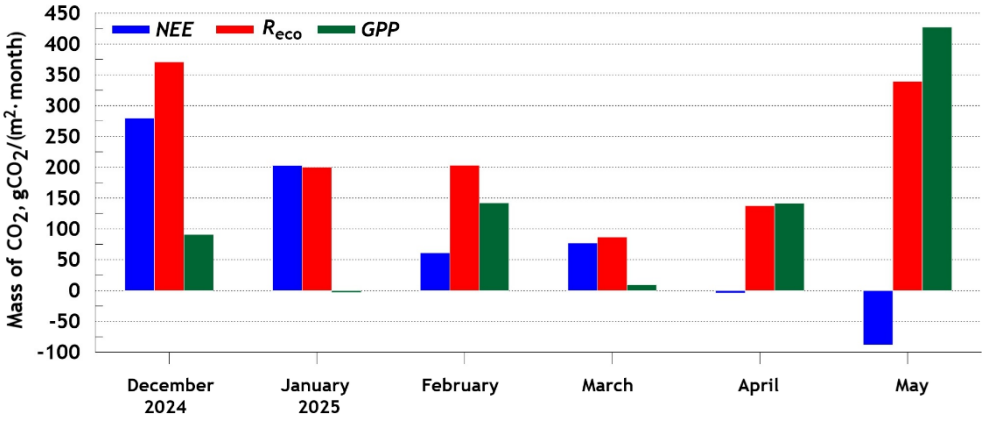

Fig. 12. Total monthly masses of carbon dioxide corresponding to net ecosystem exchange *NEE*, gross primary production *GPP* and ecosystem respiration R_{eco}

Thus, from December to March, CO_2 emission into the atmosphere was observed. Net ecosystem exchange *NEE* in December amounted to 278 $gCO_2/(m^2 \cdot month)$, in March – 76 $gCO_2/(m^2 \cdot month)$. From April onwards, a tendency towards atmospheric carbon dioxide uptake was observed, which reached 88 $gCO_2/(m^2 \cdot month)$ in May.

In total, over the six months of measurements, the net volume of carbon dioxide emissions *NEE* amounted to 529 gCO_2/m^2. Ecosystem respiration accounted for R_{eco}(night) = 1338 gCO_2/m^2, and gross primary production accounted for *GPP*(night) = 809 gCO_2/m^2.

Estimates obtained using the daytime flux partitioning scheme demonstrate comparable results: R_{eco}(day) = 1271 gCO_2/m^2, *GPP*(day) = 768 gCO_2/m^2. These values yield a model estimate of *NEE*(day) = 503 gCO_2/m^2.

Thus, the experimental value of total emissions (*NEE*) for the six months was 529 gCO_2/m^2, while the model value was 503 gCO_2/m^2. The close values suggest the correctness of the measurements and calculations performed.

As a small addition, we are to examine the fluctuations of carbon dioxide and water vapour fluxes in the frequency domain. Fig. 13 shows the frequency spectra of these fluctuations.

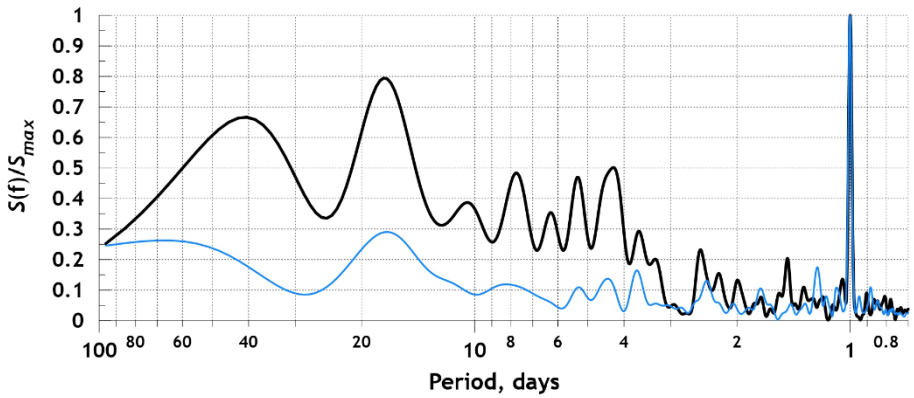

Fig. 13. Normalized spectra of carbon dioxide (black curve) and water vapour (blue curve) concentration fluctuations

For ease of comparison, the spectra are normalized to the spectral density values corresponding to the peak frequencies. Note also that the spectra are constructed from smoothed raw data, which eliminates fluctuation components. As follows from Fig. 13, two periods dominate the spectra of greenhouse gas flux fluctuations: diurnal (24 h) and a period of 17.2 days. For the CO_2 spectrum, these periods are comparable in amplitude, whereas in the H_2O fluctuation spectrum, the diurnal cycle is clearly dominant. Fluctuations in carbon dioxide fluxes on synoptic (several days) and seasonal (about 40 days) variability scales are of independent interest but require more detailed study and will form the subject of a separate task.

Conclusion

In light of the adoption in 2025 of the new national project "Ecological well-being" in Russia, research on greenhouse gas fluxes is an important not only ecological but also economic, social, and political task. At the same time, direct instrumental measurements of fluxes are far from trivial. The eddy covariance method used in this work imposes several significant limitations on the experimental conditions. Here we point out only the most important ones: 1) the site under consideration must be spatially homogeneous, without natural or artificial obstacles; 2) the energy balance (including sensible and latent heat fluxes, as well as soil fluxes) must be closed. Literal adherence to these conditions is practically unattainable, especially in areas of intense economic activity. Vast steppe (or tundra) areas may meet the first condition, but even for them, the energy balance will most likely be unclosed due to unaccounted advective heat fluxes, internal sources or vertical currents associated with uneven surface heating.

Despite the undeniable problematic aspects, we note that the greenhouse gas monitoring station in Gelendzhik is located on a typical site in the resort zone of the Krasnodar Krai Black Sea coast. Measurements at such sites seem necessary from both a scientific and practical point of view. The Gelendzhik carbon polygon is essentially the first experience of measurements under such conditions. Furthermore, the experimental results are based not on single (random) measurements but on long-term continuous data, which lends them a certain statistical reliability. Let us add that currently the eddy covariance method is successfully applied not only to natural environments but also to urban settlements. For example, study [20] uses greenhouse gas measurement data obtained from two stations located directly within the city limits of Basel (Switzerland).

Let us point out the main results obtained:

1. The measuring station of Gelendzhik polygon, operating since December 2024, automatically records the fluxes of the main greenhouse gases, as well as atmospheric state variables. The station is part of the Russian greenhouse gas monitoring project.

2. Based on the experimental results, it was found that from December 2024 to May 2025, about 500 g of carbon dioxide per square meter was emitted into the atmosphere from the study area. Ecosystem respiration accounted for about 1300 g, and gross primary production for 800 g.

3. Seasonal dynamics of carbon exchange were revealed: in the winter months, as well as at the beginning of calendar spring, CO_2 emission into the atmosphere prevails; from April onwards, its uptake by the ecosystem is observed.

Summing up, we note that despite a certain questionability of the station's location, the obtained results can be interpreted from a physical point of view. In particular, the diurnal and seasonal cycle of water vapour and carbon dioxide content agrees well with generally accepted concepts. This confirms the correctness of

the obtained data and the promise of instrumental measurements of greenhouse gas fluxes under complex conditions with further improvement of data processing methods.

The continuation of the experiment and, most importantly, obtaining continuous data will allow for further analysis of greenhouse gas fluxes and associated meteorological elements over a wide range of temporal variability, including seasonal and interannual fluctuations.

REFERENCES

1. Zamolodchikov, D.G., Gytarsky, M.L., Shilkin, A.V., Marunich, A.S. and Karelin, D.V., 2017. Monitoring of Carbon Dioxide and Water Vapor Cycles at the Log Tayozhny Experimental Site (National Park Valdaysky). *Fundamental and Applied Climatology*, 1, pp. 54–68. https://doi.org/10.21513/2410-8758-2017-1-54-68 (in Russian).
2. Khoruzhy, D.S., 2018. Variability of the CO_2 Flux on the Water-Atmosphere Interface in the Black Sea Coastal Waters on Various Time Scales in 2010–2014. *Physical Oceanography*, 25(5), pp. 401–411. https://doi.org/10.22449/1573-160X-2018-5-401-411
3. Krivenok, L.A., Suvorov, G.G., Avilov, V.K. and Sirin, A.A., 2019. Eddy Covariance Measurement of CO_2, CH_4, and H_2O Fluxes: Use of a Mobile Tower and Taking into Account the Changing Fetch. *Optika Atmosfery i Okeana*, 31(11), pp. 942–950. https://doi.org/10.15372/AOO20191111 (in Russian).
4. Fedorov, Yu.A., Sukhorukov, V.V. and Trubnik, R.G., 2021. Review: Emission and Absorption of Greenhouse Gases by Soils. Ecological Problems. *Anthropogenic Transformation of Nature*, 7(1), pp. 6–34. https://doi.org/10.17072/2410-8553-2021-1-6-34 (in Russian).
5. Satosina, E., Zyrianov, V., Prokushkin, A. and Olchev, A., 2022. Temporal Variability of Carbon Dioxide, Methane, Sensible and Latent Heat Fluxes in Forest and Moore Cosystems of Northen Eurasia. *Grozny Natural Science Bulletin*, 7(4), pp. 79–85. https://doi.org/10.25744/genb.2022.41.14.010 (in Russian).
6. Mamkin, V., Avilov, V., Ivanov, D., Varlagin, A. and Kurbatova, J., 2023. Interannual Variability in the Ecosystem CO2 Fluxes at a Paludified Spruce Forest and Ombrotrophic Bog in the Southern Taiga. *Atmospheric Chemistry and Physics*, 23(3), pp. 2273–2291. https://doi.org/10.5194/acp-23-2273-2023
7. Orekhova, N.A., Medvedev, E.V., Mukoseev, I.N. and Garmashov, A.V., 2024. Sea-Air CO_2 Flux in the Northeastern Part of the Black Sea. *Ecological Safety of Coastal and Shelf Zones of Sea*, (1), pp. 57–67.
8. Panov, A.V., Makhnykina, A.V., Urban, A.V., Zyryanov, V.I., Polosukhina, D.A., Kukavskaya, E.A., Aryasov, V.E., Kolosov, R.A., Putilin, I.R. et al., 2024. Carbon Flows in the Ecosystems of the Middle Taiga of Central Siberia. *Siberian Forest Journal*, (3), pp. 37–53. https://doi.org/10.15372/SJFS20240305 (in Russian).
9. Romanovskaya, A.A., ed., 2023. [*Evaluation of Greenhouse Gases Fluxes in Regional Ecosystems of the Russian Federation*]. Moscow: IGKE, OOO Print, 346 p. (in Russian).
10. Kuklev, S.B., Kremenetskiy, V.V., Krylenko, V.V. and Rudnev, V.I., 2022. Digital Model of the "Carbon Test Site in Krasnodar Region" on the Base of SBIO RAS (Gelendzhik). *Hydrosphere Ecology*, (1), pp. 18–28. https://doi.org/10.33624/2587-9367-2022-1(7)-18-28 (in Russian).
11. Varvarova, A.O., Polukhin, A.A., Berdnikova, E.K., Mukhametov, S.S., Borisenko, G.V. and Pronina, Yu.O., 2023. Spatial and Temporal Variability of Carbonate System Parameters at the Gelendzhik Carbon Test Area During the Summer Period. In: MSU,

2024. *Conference Proceedings of the XII International conference "Marine Research and Education" MARESEDU-2023. Moscow, 23–27 October 2023*. Tver: PoliPRESS. Vol. II(IV), pp. 503–507 (in Russian).

12. Rudnev, V.I., Pushkin, V.V. and Kuklev, S.B., 2024. Methodology for Measuring Greenhouse Gas Concentrations at a Test Site near the Blue Bay (Northeast of the Black Sea). *Hydrosphere Ecology*, (2), pp. 91–100. https://doi.org/10.33624/2587-9367-2024-2(12)-91-100 (in Russian).
13. Wutzler, T., Lucas-Moffat, A., Migliavacca, M., Knauer, J., Sickel, K., Sigut, L., Menzer, O. and Reichstein, M., 2018. Basic and Extensible Post-Processing of Eddy Covariance Flux Data with REddyProc. *Biogeosciences*, 15(16), pp. 5015–5030. https://doi.org/10.5194/bg-15-5015-2018
14. Reichstein, M., Falge, E., Baldocchi, D., Papale, D., Aubinet, M., Berbigier, P., Bernhofer, C., Buchmann, N., Gilmanov, T. et al., 2005. On the Separation of Net Ecosystem Exchange into Assimilation and Ecosystem Respiration: Review and Improved Algorithm. *Global Change Biology*, 11(9), pp. 1424–1439. https://doi.org/10.1111/j.1365-2486.2005.001002.x
15. Lasslop, G., Reichstein, M., Papale, D., Richardson, A.D., Arneth, A., Barr, A., Stoy, P. and Wohlfahrt, G., 2010. Separation of Net Ecosystem Exchange into Assimilation and Respiration Using a Light Response Curve Approach: Critical Issues and Global Evaluation. *Global Change Biology*, 16(1), pp. 187–208. https://doi.org/10.1111/j.1365-2486.2009.02041.x
16. Foken, T. and Wichura, B., 1996. Tools for Quality Assessment of Surface-Based Flux Measurements. *Agricultural and Forest Meteorology*, 78(1-2), pp. 83–105. https://doi.org/10.1016/0168-1923(95)02248-1
17. Timokhina, A.V., Prokushkin, A.S. and Panov, A.V., 2014. Daily and Seasonal Dynamics of CO_2 and CH_4 Concentration in the Atmosphere over the Western Siberia (Pri-Yeniseysk Part) Ecosystems. *Bulletin of KSAU*, (12), pp. 83–88 (in Russian).
18. Rastogi, B., Berkelhammer, M., Wharton, S., Whelan, M.E., Meinzer, F.C., Noone, D. and Still, C.J., 2018. Ecosystem Fluxes of Carbonyl Sulfide in an Old-Growth Forest: Temporal Dynamics and Responses to Diffuse Radiation and Heat Waves. *Biogeosciences*, 15(23), pp. 7127–7139. https://doi.org/10.5194/bg-15-7127-2018
19. Gulev, S.K. and Olchev, A.V., eds., 2025. [*Carbon Polygons: Monitoring, Geoinformation Systems, Sequestering Methods*]. Moscow: Nauchny Mir, 419 p. (in Russian).
20. Stagakis, S., Feigenwinter, C., Vogt, R., Brunner, D. and Kalberer, M., 2023. A High-Resolution Monitoring Approach of Urban CO_2 Fluxes. Part 2 – Surface Flux Optimisation Using Eddy Covariance Observations. *Science of the Total Environment*, 903, 166035. https://doi.org/10.1016/j.scitotenv.2023.166035

Submitted 16.09.2025; accepted after review 11.11.2025;
revised 18.12.2025; published 31.03.2026

About the authors:

Boris V. Divinsky, Leading Researcher, Laboratory of Geology and Lithodynamics, Shirshov Institute of Oceanology, Russian Academy of Sciences (36, Nakhimov Ave., Moscow, 117997, Russia), PhD (Geogr.), **ORCID: 0000-0002-2452-1922, ResearcherID: C-7262-2014**, *divin@ocean.ru*

Sergey B. Kuklev, Head of the Laboratory of Hydrophysics and Modeling, Shirshov Institute of Oceanology, Russian Academy of Sciences (36, Nakhimov Ave., Moscow, 117997, Russia), PhD (Geogr.), **ORCID: 0000-0003-4494-9878, ResearcherID: G-5656-2017**, *kuklev@ocean.ru*

Vyacheslav V. Kremenetsky, Deputy Director for Physical Direction, Shirshov Institute of Oceanology, Russian Academy of Sciences (36 Nakhimov Ave., Moscow, 117997, Russia), PhD (Geogr.), *sk@ocean.ru*

Andrey A. Nedospasov, Junior Researcher, Laboratory of Experimental Ocean Physics, Shirshov Institute of Oceanology, Russian Academy of Sciences (36, Nakhimov Ave., Moscow, 117997, Russia), *nedospasov.aa@ocean.ru*

Vladimir V. Ocherednik, Researcher, Laboratory of Hydrophysics and Modeling, Shirshov Institute of Oceanology, Russian Academy of Sciences (36 Nakhimov Ave., Moscow, 117997, Russia), **ORCID: 0000-0002-3593-7114, ResearcherID: G-2850-2017,** *poekperementarium@gmail.com*

Olga N. Kukleva, Researcher, Laboratory of Hydrophysics and Modeling, Shirshov Institute of Oceanology, Russian Academy of Sciences (36, Nakhimov Ave., Moscow, 117997, Russia), **ResearcherID: J-7126-2018,** *kukleva-ola@mail.ru*

Contribution of the authors:

Boris V. Divinsky – problem statement, analysis of the results, article preparation

Sergey B. Kuklev – problem statement, analysis of the literature sources

Vyacheslav V. Kremenetsky – experiment support

Andrey A. Nedospasov – experiment support

Vladimir V. Ocherednik – experiment support

Olga N. Kukleva – preparation of source data, article preparation

All the authors have read and approved the final manuscript.

Original paper

Layering of the Spatial Structure of the Crimean Shelf Pelagic Community in the Summer Season

S. A. Piontkovski [1] *, A. V. Melnik [2], Yu. A. Zagorodnyaya [2], Yu. G. Artemov [2], E. A. Skripaleva [3], E. Yu. Georgieva [2]

[1] *Sevastopol State University, Sevastopol, Russia*

[2] *A. O. Kovalevsky Institute of Biology of the Southern Seas of RAS, Sevastopol, Russia*

[3] *Marine Hydrophysical Institute of RAS, Sevastopol, Russia*

* *e-mail: spiontkovski@mail.ru*

Abstract

Spatial heterogeneity of the thermohaline structure, biotope dynamics and organism interactions form layers of high abundance and biomass. Based on expedition data obtained during the summers of 2010–2024, this paper analyses characteristics of surface and subsurface peaks in phytoplankton biomass, chlorophyll a, total suspended matter, zooplankton (prey and gelatinous), bioluminescence intensity and sound-scattering layers (indicators of the abundance of small pelagic organisms) on the shelf off the coast of Crimea. Characteristic parameter values, layer thicknesses and depths are presented. The mechanisms of layering formation and the relationship between the structural and functional properties of the pelagic community are discussed. It was noted that at lower trophic levels, layering was regulated primarily by thermohaline stratification of the water column. At intermediate trophic levels, represented by copepods and small pelagic fishes, the dominant factor regulating stratification was the organisms' motor activity, associated with feeding behavior, reproductive behavior, defense and other behaviors. In terms of the relationship between the structure and function in a pelagic ecosystem, it was noted that the stratified distribution of organisms created vertical heterogeneity in the density of trophic interactions and consequently vertical heterogeneity in the flow of matter and energy within the community. Trophic interactions were most intense in the layers of maximum thickness due to their greater ecological capacity. These include the surface and subsurface biomass peaks of phytoplankton, zooplankton and small pelagic fishes, primarily common anchovy and sprat.

Keywords: Black Sea, coastal shelf, thermohaline waters structure, phytoplankton, chlorophyll a, total suspended matter concentration, zooplankton, bioluminescence, sound scattering layers, pelagic community

Acknowledgements: The work was funded by the IBSS state assignment no. 124030400057-4, no. 124022400148-4-0556-2024-00, no.124030100127-7, SevSU state assignment no. FEFM-2023-0005, and MHI state assignment no. FNNN-2024-0014. The expeditions were carried out onboard R/V *Professor Vodyanitsky*. Special thanks should be addressed to V. V. Davydov, the research vessel Chief Engineer, with respect to his long-term support of field measurements on board. The figure of station grids was produced by I. A. Minsky.

© Piontkovski S. A., Melnik A. V., Zagorodnyaya Yu. A., Artemov Yu. G., Skripaleva E. A., Georgieva E. Yu., 2026

This work is licensed under a Creative Commons Attribution-Non Commercial 4.0 International (CC BY-NC 4.0) License

For citation: Piontkovski, S.A., Melnik, A.V., Zagorodnyaya, Yu.A., Artemov, Yu.G., Skripaleva, E.A., Georgieva, E.Yu., 2026. Layering of the Spatial Structure of the Crimean Shelf Pelagic Community in the Summer Season. *Ecological Safety of Coastal and Shelf Zones of Sea*, (1), pp. 27–51.

Слоистость пространственной структуры пелагического сообщества крымского шельфа в летний сезон

С. А. Пионтковский [1] *, А. В. Мельник [2], Ю. А. Загородняя [2], Ю. Г. Артемов [2], Е. А. Скрипалева [3], Е. Ю. Георгиева [2]

[1] *Севастопольский государственный университет, Севастополь, Россия*

[2] *ФГБУН ФИЦ «Институт биологии южных морей имени А.О. Ковалевского РАН», Севастополь, Россия*

[3] *Морской гидрофизический институт РАН, Севастополь, Россия*

* *e-mail: spiontkovski@mail.ru*

Аннотация

Пространственная неоднородность термохалинной структуры и динамики биотопа, а также трофические взаимодействия организмов формируют слои их высокой численности и биомассы. На основе экспедиционных данных, полученных в летний период 2010–2024 гг., проанализированы характеристики поверхностного и подповерхностного максимумов биомассы фитопланктона, хлорофилла *a*, общего взвешенного вещества, зоопланктона (кормового и желетелого), интенсивности биолюминесценции и звукорассеивающих слоев (индикаторов обилия мелких пелагических организмов) на шельфе Крыма. Приводятся характерные значения параметров, толщина слоев и глубина их залегания. Обсуждаются механизмы формирования слоистости и взаимосвязь структурных и функциональных свойств пелагического сообщества. Отмечено, что на низших трофических уровнях слоистость регулируется преимущественно термохалинной стратификацией водной толщи. На средних трофических уровнях, представленных копеподами и мелкими пелагическими рыбами, доминирующим фактором в регуляции слоистости выступает двигательная активность организмов, связанная с пищевым, репродуктивным, защитным поведением и прочими его формами. В контексте взаимосвязи структуры и функции в пелагической экосистеме отмечено, что слоистость распределения организмов формирует вертикальную неоднородность плотности трофических взаимодействий и, как следствие, вертикальную неоднородность потока вещества и энергии в сообществе. Трофические взаимодействия наиболее интенсивны в слоях максимальной толщины в связи с их большей экологической емкостью. К таким слоям относятся поверхностный и подповерхностный максимумы биомассы фитопланктона, зоопланктона и мелких пелагических рыб, прежде всего массовых (хамсы и шпрота).

Ключевые слова: Черное море, шельф, термохалинная структура вод, фитопланктон, хлорофилл *a*, концентрация общего взвешенного вещества, зоопланктон, биолюминесценция, звукорассеивающие слои, пелагическое сообщество

Благодарности: работа выполнена в рамках государственных заданий ФИЦ ИнБЮМ № 124030400057-4, 124022400148-4-0556-2024-00, 124030100127-7, СевГУ № FEFM-2023-0005 и ФГБУН ФИЦ МГИ FNNN-2024-0014. Экспедиционные исследования были выполнены в Центре коллективного пользования «НИС Профессор Водяницкий» ФИЦ ИнБЮМ им. А. О. Ковалевского РАН. Особую благодарность

выражаем главному инженеру научного судна В. В. Давыдову за многолетнюю помощь в выполнении экспедиционных измерений. Рисунок схем океанографических станций сделан И. А. Минским.

Для цитирования: *Пионтковский С. А., Мельник А. В., Загородняя Ю. А., Артемов Ю. Г. и др.* Слоистость пространственной структуры пелагического сообщества крымского шельфа в летний сезон // Экологическая безопасность прибрежной и шельфовой зон моря. 2026. № 1. С. 27–51. EDN MBADAW.

Introduction

Numerous global and regional studies have been devoted to the spatial distribution of marine organisms in the pelagic zone [1–3]. Of particular interest are the properties of the vertical component in the spatial structure of pelagic communities, where the steepest gradients in organism abundance and biomass are concentrated. For example, within the upper 100-m layer of the tropical World Ocean, the spatial scales over which mesozooplankton biomass varies by an order of magnitude are approximately 1,000 times smaller vertically than horizontally [4]. This ratio indicates that the vertical variability of biomass is 1,000 times greater than the horizontal variability.

In complex systems, particularly ecosystems, their structure determines their functional properties [5], therefore, the maximum gradients of primary production, organic matter decomposition, bioluminescence, trophic intensity and other functional parameters are also characteristic of the vertical component of spatial distribution.

The layering of the vertical distribution is of significant ecological importance for survival. For example, anchovy larvae obtain their daily food intake by feeding within narrow, dense layers of food concentration. Weak layering or its absence leads to increased larval mortality [6]. On the Crimean shelf, the larvae of *Engraulis encrasicolus* (L., 1758) reach their peak abundance in the surface layers at maximum temperatures, high concentrations of forage zooplankton [7] and minimal water dynamics [8]. “Forage” refers to zooplankton that forms part of the diet of small pelagic fish in the Black Sea. On the Crimean shelf, this diet predominantly includes copepods and pelagic larvae of benthic organisms.

Regional studies help us understand the diverse conditions under which various vertical gradients in the characteristics of the pelagic community develop. In this respect, the Crimean shelf is of interest due to a number of unique features. Firstly, its width varies significantly (from hundreds of metres to tens of kilometres from the coast down to a depth of 200 metres), which affects its ecological capacity, understood as the ecosystem’s carrying capacity with regard to the component under study, e. g., the biomass of organisms [9]. Secondly, the variable shelf geomorphology influences the characteristics of coastal currents and macroscale turbulence, which is reflected in the structural and functional characteristics

of the pelagic community [10, 11]. Thirdly, dynamic processes on the shelf and in its pelagic communities are subject to significant synoptic and seasonal variability [12–14].

The study aims to identify characteristic vertical gradients in the structural and functional parameters of the pelagic community, based on data from expedition surveys conducted on the Crimean shelf during the summers of 2010–2024. This particular season was chosen because the thermohaline stratification of the pelagic community's habitat reaches its maximum during this period.

Materials and methods

This study relies on data from expeditions conducted onboard the research vessel (R/V) *Professor Vodyanitsky*. From the total number of surveyed oceanographic stations, we selected those located in the shelf zone and involving a range of physical, chemical and biological measurements (Table 1, Fig. 1). Some cruises spanned the autumn season, but the data used from those cruises corresponded to the start of the expeditionary measurements.

In the cruises conducted under various departmental programmes, the sets of measured characteristics varied, which made data comparison difficult and also meant that the statistical sufficiency of the data was inconsistent.

T a b l e 1 . A general characteristic of expedition studies aboard R/V *Professor Vodyanitsky*

Number of cruise	Field work period	Number of oceanographic stations	Number of Salpa-M soundings	Number of plankton sampling stations
64	01.07.2010–06.07.2010	31	142	–
70	18.08.2011–29.08.2011	45	451	40
72	21.05.2013–30.05.2013	50	433	49
87	30.06.2016–18.07.2016	106	990	–
95	14.06.2017–04.07.2017	113	–	5
96	19.07.2017–09.08.2017	106	578	49
102	09.06.2018–01.07.2018	122	583	44
103	28.08.2018–20.09.2018	147	–	40
108	11.07.2019–05.08.2019	174	789	40
113	04.06.2020–29.06.2020	164	447	52
123	16.08.2022–10.09.2022	200	–	40
128	03.08.2023–21.08.2023	107	299	66
133	11.09.2024–03.10.2024	100	116	56

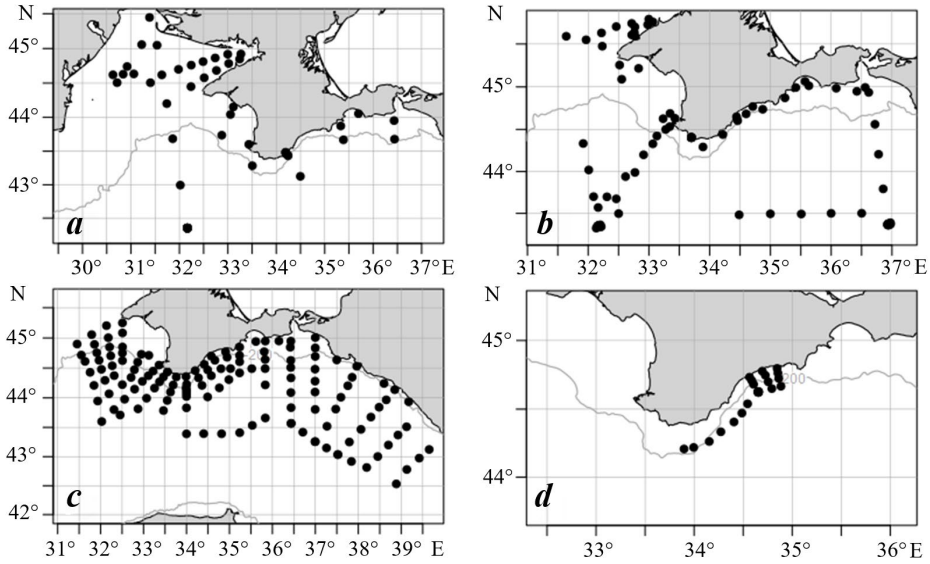

F i g . 1 . Examples of transects and station grids of R/V *Professor Vodyanitsky* summer expeditions: the 70th (*a*), 96th (*b*), 102nd (*c*) and 128th (*d*) cruises. The grey curve marks the shelf boundary (200 m)

Thermohaline structure of the water. The temperature, electrical conductivity and hydrostatic pressure of seawater were measured at each station, generally during daylight hours, at depths of up to 500–1000 m using IDRONAUT OCEAN SEVEN 320 PlusM and SBE 911plus CTD profilers (Available at: http://www.technopolecom.ru/downloads/doc_212.pdf). The zonal and meridional components of current velocity and direction were measured using an ADCP WORKHORSE-300 kHz acoustic Doppler current profiler.

Phytoplankton. Phytoplankton samples of 2 L were collected using the CTD probe's water sampler. Sampling depths were selected based on the vertical temperature profile and water transparency, estimated by the Secchi disc's visibility depth. The species composition and phytoplankton cell sizes were determined under an XY-82 microscope using a Nauman chamber. Cell volumes and phytoplankton biomass were calculated using the standard method [1)].

Chlorophyll a. The fluorescence intensity of chlorophyll a was measured using the IDRONAUT OCEAN SEVEN 320 Plus M, SBE 911plus and Salpa-M [2)]

[1)] Radchenko, I.G., Kapkov, V.I. and Fedorov, V.D., 2010. [*A Practical Guide to the Collection and Analysis of Marine Phytoplankton Samples: A Teaching Guide for University Biology Students*]. Moscow: Mordvintsev, 60 p. (in Russian).

[2)] Available at: http://ecodevice.com.ru/wp-content/manuals/salpa-manual.pdf [Accessed: 10 February 2026] (in Russian).

immersion probes. The fluorescence intensity data obtained from the immersion probes were converted into chlorophyll a concentration using direct proportionality [3)].

Zooplankton. Zooplankton samples collected with a Juday plankton net (entrance diameter 36 cm, mesh size 140 μm) and concentrated to 100 mL were fixed with a neutral formalin solution to a concentration of 4% in the sample. Biomass of forage zooplankton per unit volume of the sampled layer was calculated using size-weight relationships known for Black Sea species [15, 16].

Suspended matter. To determine the concentration of total suspended matter (C_{TSM}) at the stations, the directed light attenuation index (DLAI) was measured using a SIPO 4 spectral probe in the red region of the spectrum at a wavelength of 625 nm, with a vertical resolution of 0.1 m from the surface to a maximum measurement depth of 200 m. C_{TSM} was calculated using the empirical relationship $C_{TSM} = 1.514 \times DLAI(625) - 0.23$, derived for the northern part of the Black Sea [17].

Bioluminescence. Bioluminescent potential (BP) was recorded during vertical casts using the Salpa-M instrument system. BP characterises the maximum luminous flux ($W \cdot cm^{-2} \cdot L^{-1}$) of all organisms entering the instrument's measuring chamber. The system enables synchronous measurements of mechanically stimulated bioluminescence in planktonic organisms. The methodology for measuring BP has been described previously [18].

Small pelagic organisms. Data from hydroacoustic measurements taken using FURUNO FCV 1200 and Lowrance Elite 7 Ti echo sounders at frequencies of 50 and 200 kHz were used to assess the vertical distribution (layering) of small pelagic organisms. The Lowrance Elite 7 Ti echo sounder is equipped with an HST-DFSBL 50/200 kHz Transom Mount Skimmer transducer with a narrow beam angle (12°) at 200 kHz.

Results and discussion

Thermohaline structure and dynamics of the waters

The general thermohaline stratification of the Black Sea waters is known to exhibit thermal stability in the surface layer that exceeds salinity stability by a factor of two to three. Thermal stability is defined as $E_t = \alpha dT/dz$, where α is a coefficient; T is the temperature; z is the depth. Below the core of the cold intermediate layer (at 60 m), the contribution of thermal stability is negligible; from a depth of 40 m, salinity stability predominates, exceeding thermal stability (in the pycnocline) by two orders of magnitude [4)]. This study examines the summer season, which is characterised by a significant (by more than an order of magnitude) prevalence of thermal stability over salinity stability.

[3)] Schmechtig, C., Poteau, A., Claustre, H., D'Ortenzio, F. and Boss, E., 2015. *Processing Bio-Argo Chlorophyll-A Concentration at the DAC Level*. Ifremer, 12 p. https://doi.org/10.13155/39468

[4)] Belokopytov, V.N., 2017. [*Climate Changes of the Black Sea Hydrological Regime. Doctoral Thesis*]. Sevastopol: MGI RAN, 377 p. (in Russian).

According to the data from the summer expeditions, the surface water temperature was 25–27°C, with the upper quasi-homogeneous layer being 5–20 m thick, which corresponds to the climatic norm for the Crimean region. During the studies, the difference in surface temperature between the eastern and western parts of the shelf reached 2–4°C, and on cross-shelf sections within individual field surveys it was 0.5–1.5°C. The summer water structure was characterised by zones of reduced salinity in the surface layer (isohaline 18.1), which extended along the eastern shelf. These areas of desalinated water had formed as the result of the outflow of low-salinity Azov Sea waters from the Kerch Strait and their westward transport by the Rim Current along the Crimean coast, as well as the north-westward advection of the Caucasian coastal waters (which had been desalinated due to river runoff) by the Rim Current coastal flow.

Overall, cyclonic eddies prevailed in the summer water dynamics to the left of the main Rim Current stream, corresponding to the large-scale circulation in the Black Sea. Due to the decrease in the Rim Current velocity in summer, mesoscale and sub-mesoscale anticyclonic eddies were also recorded on the shelf, observed at depths of 10, 25, 75 and 100 m and exhibiting orbital velocities of around 25–30 $cm \cdot s^{-1}$. The number of eddies varied significantly between individual surveys (Fig. 2).

The direction of currents on the Crimean shelf is modulated by prevailing winds (which sometimes cause the flow to reverse by 180°) and the geomorphological features of the coastline. Thus, in the area of the Southern Coast of Crimea, there are a regime of unimodal coastal current and a regime of bimodal modulation of the coastal flow direction. A bimodal structure forms in cases where the magnitude of the orbital velocity of the collinear counter-phase oscillation exceeds the magnitude of the unimodal current velocity, leading to inverse oscillations in the direction and velocity of the current [19]. The average monthly normalised current velocity in the summer season is highest in the surface layer and decreases with depth to 0.3 of its maximum value in the bottom layer [13].

The geomorphology of the bottom, mesoscale eddies and the break of internal gravity waves form a spatially heterogeneous turbulent exchange, where the vertical turbulent diffusion coefficient in the 20–80 m layer along the Crimean shelf can vary by a factor of four [10]. Short-lived coastal upwelling represents dynamic anomalies in the summer turbulent regime. Upwelling events are most pronounced in the surface temperature field in areas of a steep shelf with minimal width. Thus, in the area of the Southern Coast of Crimea during the summer seasons of 2014–2018, 21 events of complete wind-induced upwelling were recorded, with an average temperature decrease of 5°C [20]. Upwelling leads to a 3–6-day erosion of the thermocline and the appearance of associated subsurface maxima in the vertical distribution of plankton biomass.

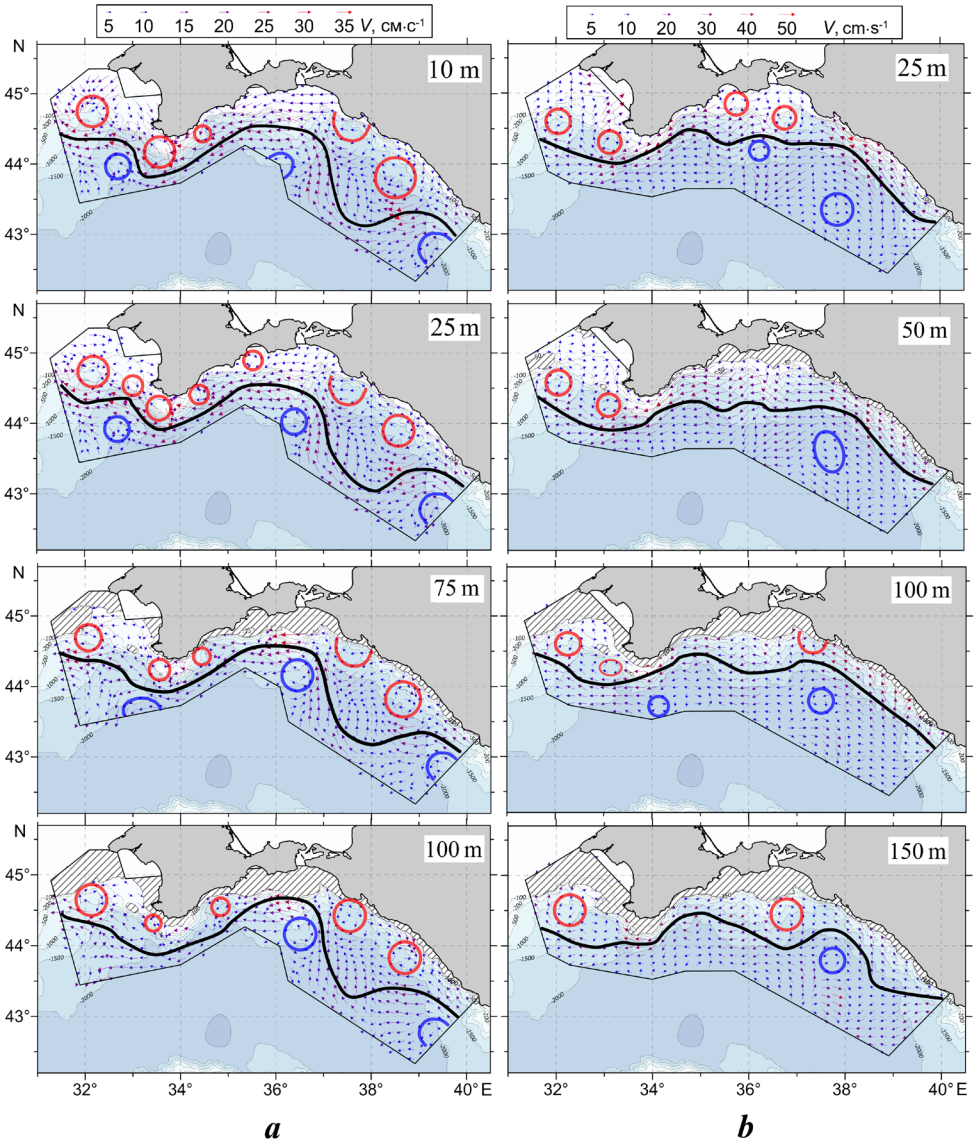

Fig. 2. Vectors of *in situ*-measured currents across various depths according to the 102nd (*a*) and 103rd (*b*) cruises of R/V *Professor Vodyanitsky*. The black curve indicates the location of the Rim Current main stream. The blue ellipses indicate cyclonic eddies and meanders. The red ellipses indicate anticyclonic eddies

Phytoplankton and its pigments

The main contributors to the total phytoplankton biomass were the dinoflagellates (*Dinophyceae*) and diatoms (*Bacillariophyceae*) (Fig. 3).

In the surface layer, the biomass was most often dominated by the diatoms *Pseudosolenia calcar-avis* (Schultze) B. G. Sundström and *Proboscia alata* (Brightwell) Sundström, which accounted for up to 90% of the phytoplankton biomass. In the thermocline, the dinoflagellates *Ceratium furca* (Ehrenberg) Claparède & Lachmann and *Dinophysis rotundatum* Claparède & Lachmann predominated,

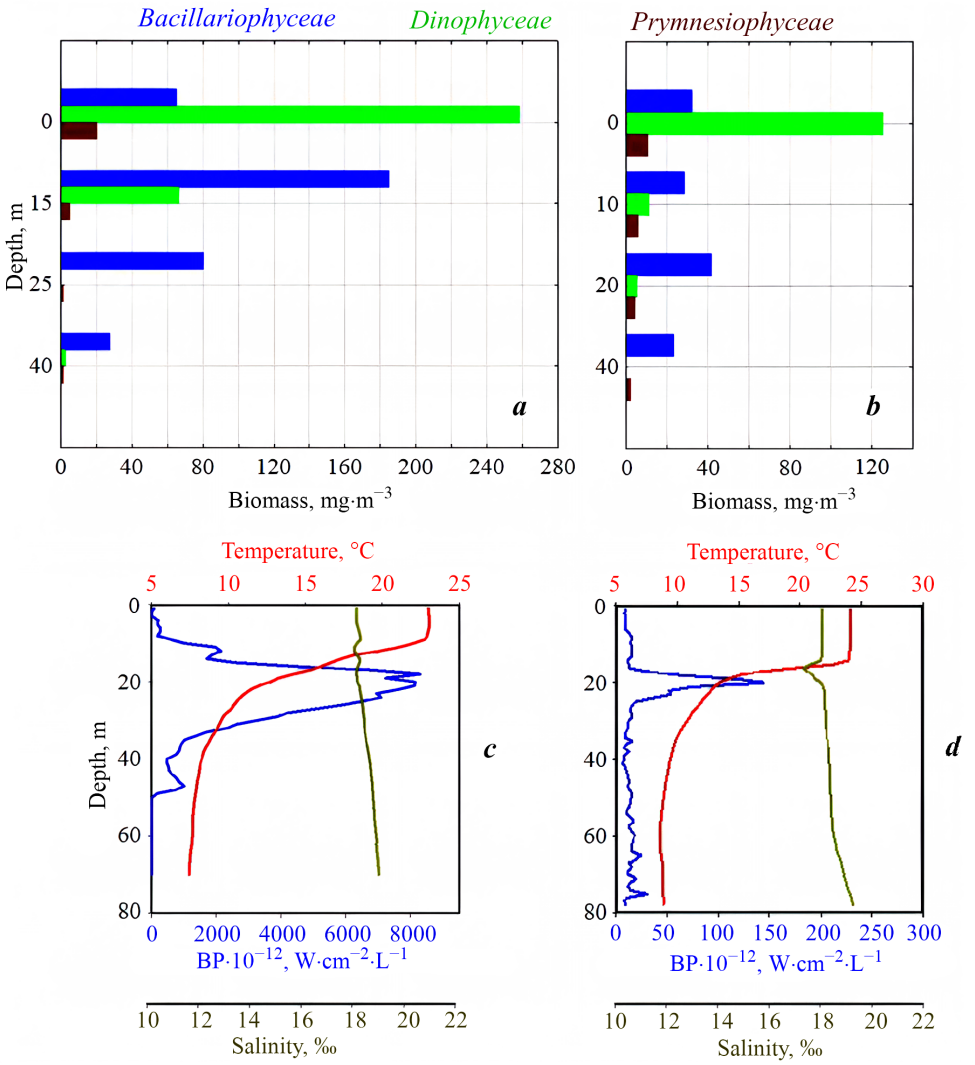

F i g . 3 . Vertical distribution of phytoplankton biomass (*a*, *b*), bioluminescent potential (BP), temperature and salinity (*c*, *d*), during the 64th cruise in July 2010 (*a*, *c*) and 108th cruise in July 2019 (*b*, *d*) of R/V *Professor Vodyanitsky*

accounting for up to 50% of the phytoplankton biomass, along with the diatom *Pseudosolenia calcar-avis* (Schultze) B. G. Sundström, 1986. Many species of dinoflagellates are capable of bioluminescence (light emission). The distribution of total plankton bioluminescence at night was characterised by two types of vertical profiles: one with a maximum at the surface and one with a deep maximum below the thermocline. The unimodal distribution (with a deep maximum) was the most common (Fig. 3). Another widely used indicator of phytoplankton biomass is chlorophyll a fluorescence, from which its concentration is calculated. The vertical distribution of this parameter was also characterised by a deep maximum within or below the seasonal thermocline (Fig. 4).

A deep maximum was also observed in the deep sea, where numerous fluorescence measurements taken by ARGO drifting buoy sensors made it possible to track the seasonal and long-term variability of the deep maximum in chlorophyll concentration [21]. The taxonomic structure of large-celled phytoplankton during the summer season was characterised by a high biomass of the dinoflagellate *Noctiluca scintillans* (Macartney) Kofoid and Swezy, 1921 [13]. Unlike other phytoplankton species, the Black Sea *N. scintillans* is a heterotrophic organism [22, 23]. Its biomass can reach 85% of the total biomass of heterotrophic plankton on the Crimean shelf [23]. The vertical distribution of biomass was characterised by two maxima: at a depth of about 15 m and in the pycnocline.

The presence of a subsurface maximum in summer was also observed on the highly productive north-western shelf, as well as in the north-eastern and southern parts of the highly eutrophic waters of the Marmara Sea [24–26].

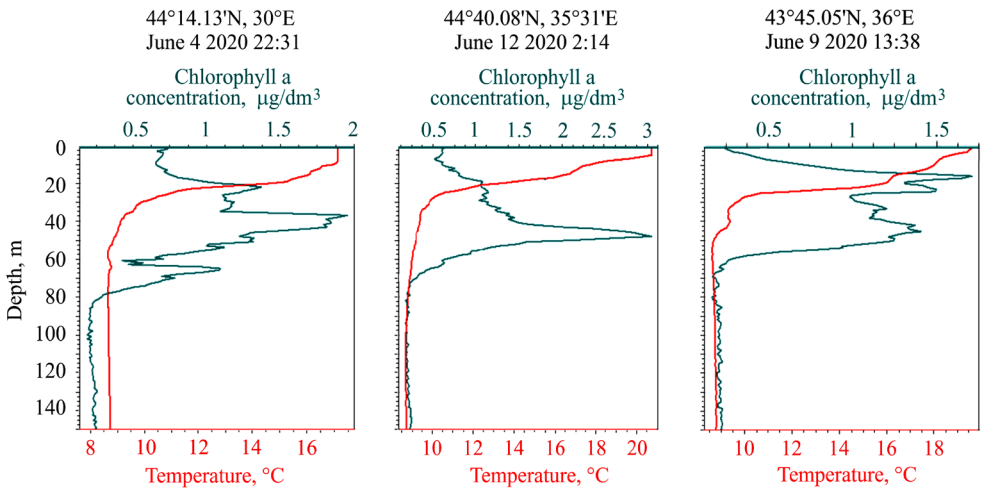

F i g . 4 . Vertical distribution of chlorophyll a concentration and temperature across the Crimean shelf in June 2020 (113th cruise of R/V *Professor Vodyanitsky*) at three stations

Zooplankton

The forage zooplankton included six dominant copepod species, as well as arrow worms, oikopleura and pelagic larvae of benthic organisms (Fig. 5).

In the vertical distribution of the total abundance of forage zooplankton species, a subsurface peak was often observed in early summer, while a more pronounced peak was seen in the layer below the thermocline by late summer (Fig. 5). *Acartia clausi* dominated the surface layer, with *Pseudocalanus elongatus* and *Oithona davisae* acting as subdominants. *A. clausi* also prevailed in the thermocline layer. Below the thermocline, *Pseudocalanus elongatus* dominated in terms of abundance, whereas *Calanus euxinus* dominated in terms of biomass. The vertical distribution of biomass may differ (Fig. 5). Overall, the profiles were characterised by high variability, as the vertical distribution of zooplankton was significantly influenced by its diurnal vertical migrations. This was most evident in the relatively large copepods *C. euxinus* and *P. elongatus*, which rose to the surface at night and descended below the thermocline during the day.

Apart from forage mesoplankton (with organisms typically ranging in size from 0.5 to 2.5 mm), macroplankton–specifically the jellyfish *Aurelia aurita* (L.) – contributed significantly to the total biomass of the planktonic fraction. Their biomass on the shelf exceeded that of the forage mesoplankton by one or two orders of magnitude [25]. With an average size of about 7 cm and high biomass values, individuals formed dense aggregations near the surface and at depth. Fig. 6 exemplifies such an aggregation at a depth of 30 m (light orange) and near the bottom (dark orange). Presumably, the isolated small patches visible on the echogram above the main (light orange) layer are jellyfish of a larger species – the root-mouthed jellies *Rhizostoma pulmo* [Macri, 1778], which are 5–6 times larger than *A. aurita*.

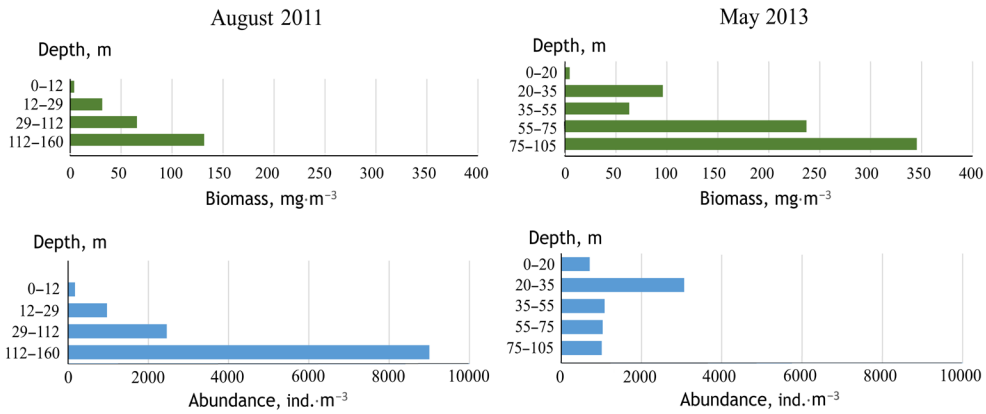

F i g . 5 . Vertical distribution of forage zooplankton total abundance and biomass across the Crimea shelf in May 2013 and August 2011 at night

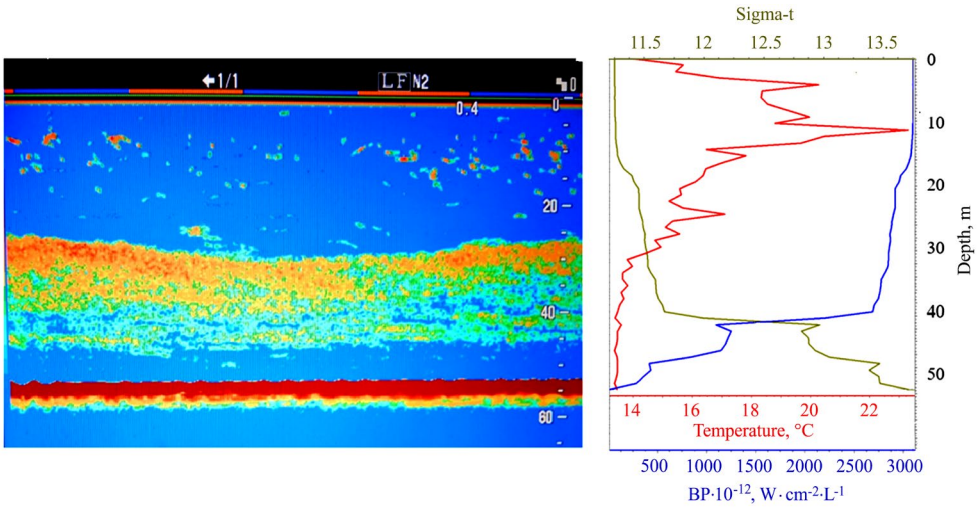

Fig. 6. Vertical stratification according to a *FURUNO FCV* 1200 echo sounder (*left*) at a sound frequency of 50 kHz (wave length from 2.8 cm to 3.0 cm) on 3 October 2024 at 6 a. m. in Laspi Bay, Southern Coast of Crimea (the 133rd cruise of R/V *Professor Vodyanitsky*). Vertical profiles of bioluminescent potential (BP), temperature and relative density (*right*)

The foregoing layer was situated above the pycnocline, which is characterised by sharp gradients in temperature and salinity (Fig. 6). Deep maxima of jellyfish abundance had previously been observed at depths of 11–20 m on the north-western shelf of the Black Sea, where their biomass is at its highest in summer [26]. The dense, deep-water layers of jellyfish are likely to act as a kind of "deep-water bomb", episodically and explosively supplying large amounts of biomass to the waters above the shelf during storms or short-lived coastal upwelling. Simultaneously, reproduction and rapid biomass growth occur due to the high specific productivity of jellyfish [5)]. These peculiarities partly explain the rapid formation of coastal maxima in jellyfish biomass.

Suspended matter

Dying biomass of the pelagic community forms the organic fraction of suspended matter. The mineral fraction of suspended matter in the Crimean shelf waters is formed by erosion of the sandy-clay shores and by suspended matter entering from the Sea of Azov via the Kerch Strait and subsequently transported by the westward-flowing coastal current.

[5)] Greze, V.N., ed., 1979. [*Fundamentals of Biological Productivity in the Black Sea*]. Kiev: Naukova Dumka, 392 p. (in Russian).

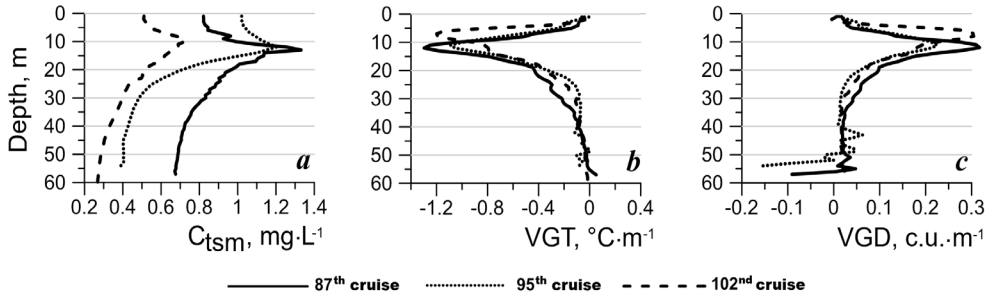

Fig. 7. Vertical profiles of total suspended matter concentration (*a*), vertical gradients of temperature (*b*) and density (*c*) in the upper 60-meter layer

The total concentration of organic and inorganic suspended matter in the water column above the Crimean shelf was relatively high, reaching 1–4 g·m^{-3}, which was comparable to the biomass of plankton. In certain areas, it might be even higher. The vertical distribution of suspended matter was characterised by a subsurface maximum located in the layer of maximum (in absolute terms) vertical gradients of temperature (VGT) and density (VGD), i. e. in the layer of the seasonal thermocline and pycnocline. In this layer, the suspended matter concentration was 1.5 times higher than the background values in the adjacent layers (Fig. 7). The thickness of the layer with the maximum concentration is linearly dependent on the vertical temperature gradient [17]. The results of summer expedition studies revealed a significant negative correlation between the total concentration of suspended matter and the temperature at the lower boundary of the upper quasi-homogeneous layer, and a positive correlation beneath the thermocline [6)].

Small pelagic organisms

The layering of the distribution of nekton organisms, which move actively through the water column, depends significantly on the time of day due to their vertical migrations. The most abundant small pelagic fish actively moving in the waters above the Crimean shelf are anchovy and sprat; they dominate the catches [27].

The Lowrance Elite 7 Ti echo sounder, used to record small pelagic organisms, is classified as a recreational device. However, its full backscatter profile recording function allows it to be used for detecting marine organisms that form sound-scattering layers (SSLs) [28, 29]. SSLs are known to consist of an assembly of spatially random acoustic inhomogeneities: marine organisms capable of varied sound scattering (having backscatter cross-sections). At the same time, the scattering

[6)] Latushkin, A.A., 2022. [*Spatio-Temporal Variability of Total Suspended Solids in the Russian Sector of the Azov–Black Sea Basin Based on Hydro-Optical Measurements. PhD Thesis*]. Sevastopol: MGI RAN, 186 p. (in Russian).

cross-sections of pelagic fish species with gas-filled swim bladders exceed those of other categories of SSL inhabitants (crustaceans, gelatinous organisms, etc.) by several orders of magnitude [7)].

In the single-scattering approximation, the volume backscattering strength SV, in dB, characterises the total backscattering cross-section of all discrete inhomogeneities present, on average, in a unit volume of the medium. Recording the characteristics of SSLs using the Lowrance Elite 7 Ti echo sounder at a frequency of 200 kHz showed that, during the night, small migratory nekton and zooplankton could form a dense layer near the surface and a layered structure, most pronounced down to the depth of the thermocline (Fig. 8). This is evidenced by the positions of the maxima of the volume backscattering strength SV, as this parameter is related to the bioproductivity of the water masses. Notably, the vertical profile roughness of the volume backscattering strength decreases with depth.

Assessments of sprat aggregations using a Simrad EK-400 echo sounder and a SIORS echo integrator, combined with simultaneous sampling of forage zooplankton using plankton nets and analysis of fish stomachs, showed that sprats concentrated in the pycnocline layer, where they fed on copepods [7].

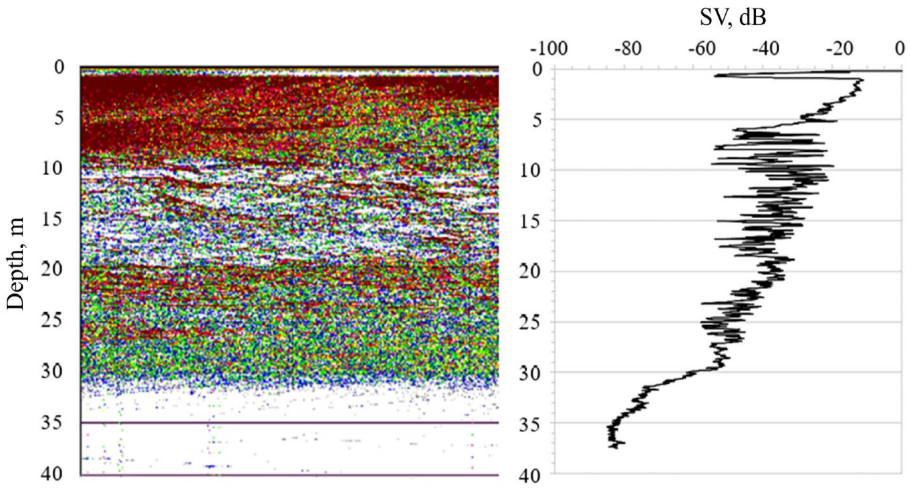

Fig. 8. Echogram of the sound scattering layer (SSL) and the averaged profile of the volume backscattering strength *SV*, dB, at station 190 during the 123rd cruise of R/V *Professor Vodyanitsky* abeam of the Karadag Scientific Biological Station on 1 September 2022 at 1:30 a. m. The data were obtained using a Lowrance Elite 7 Ti mobile echo sounder at a frequency of 200 kHz and processed by the WaveLens program [30]

7) Andreeva, I.B. and Samovolkin, V.G., 1986. [*Acoustic Wave Scattering on Marine Animals*]. Moscow: Agropromizdat, 104 p. (in Russian).

Bioluminescence

The vertical distribution of BP in coastal waters was characterised by surface and deep (at a depth of around 40 m) maxima. The formation of the summer deep maximum is presented in Fig. 9, which shows the peak becoming more pronounced while thermohaline stratification of the water column intensifies seasonally.

The vertical profiles of the BP shown here reveal layers of varying modality and spread: apart from the main seasonal peak, there are numerous less pronounced ones. The thickness of such layers ranges from 3 to 7 m, whereas the horizontal spread of the main layer (the seasonal maximum) is estimated at several kilometres. Therefore, the ratio of the typical dimensions of spatial heterogeneities in the horizontal and vertical directions is approximately 1000 [31].

Bathyphotometers of the used configuration primarily measure the BP of phytoplankton [32–34], in which dinoflagellates generate a significant proportion of the total bioluminescence. This group is also characterised by a high chlorophyll a content. A comparison of chlorophyll a concentrations and BP shows a high correlation in the 1–5, 1–34 and 10–60 m layers, with r values of 0.75, 0.78 and 0.71, respectively, ($p < 0.001$) [35]. The contribution of individual species to BP was difficult to assess, as luminescent dinoflagellates included 38 species [36, 37], the characteristics of which are poorly understood and subject to seasonal and interannual variability.

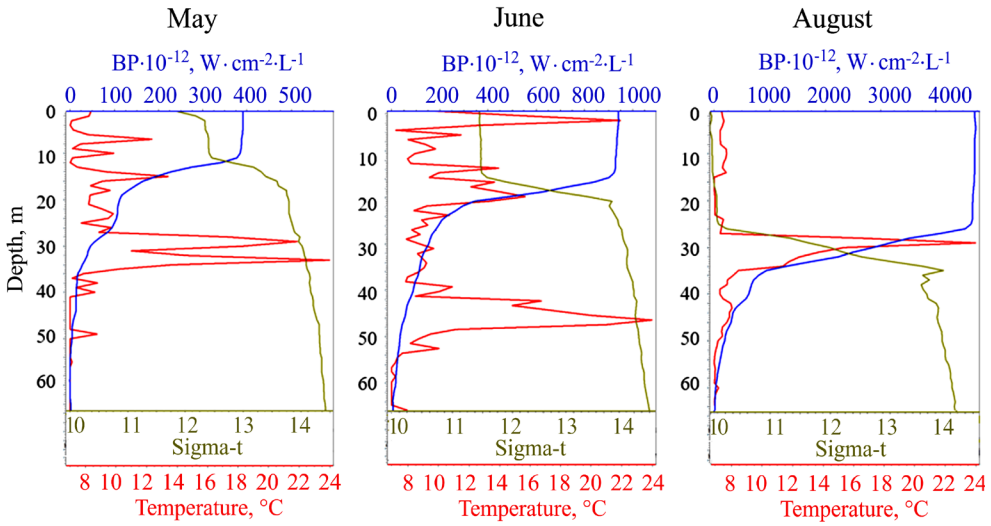

Fig. 9. Vertical distribution of bioluminescent potential (BP), temperature and relative water density in front of the Kruglaya Bay entrance in 2012 two miles off the Sevastopol coast

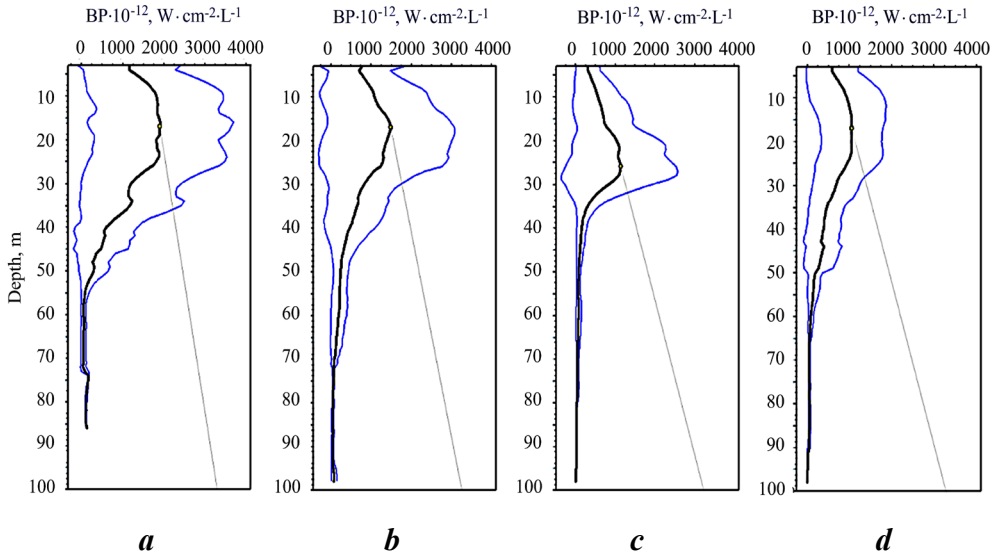

Fig. 10. Averaged profiles of bioluminescent potential (BP) vertical distribution at night: *a* – at the northwestern shelf of Crimea (866 profiles); *b* – at the western shelf of Crimea (752 profiles); *c* – at the Southern Coast of Crimea (267 profiles); *d* – at the eastern shelf of Crimea (556 profiles). The black lines are average values, the blue lines are SD

To analyse the trend in the vertical component of the spatial structure of the plankton community along the shelf, given the influence of microlayering, it is reasonable to smooth the vertical profiles of the parameters. Thus, a positive large-scale trend can be observed in the distribution of BP along the northern Black Sea shelf: the layer with maximum BP values is becoming shallower, while its amplitude is increasing in the direction from the eastern part of the Crimean shelf towards the north-western shelf of the sea (Fig. 10). Primary production also increases in this direction [38]. The coefficient of vertical turbulent diffusion in the upper active layer on the western Crimean shelf is lower than on the eastern shelf [10]. This regime of turbulent diffusion is likely to contribute to the smoothing of the fine-scale layering of bioluminescence.

The estimates of deep maxima obtained during expeditions and found in the literature are summarised in Table 2. It shows that the parameters vary by a factor of two to four during the summer season, whereas for the biomass of forage zooplankton in subsurface maxima, the variation is of the order of one.

Mesoscale variability is likely to account for a significant proportion of the variation, as the calculations included stations covering a relatively large water area (see Fig. 1).

Table 2. Characteristics of deep (subsurface) maxima of investigated parameters in the summer period

Parameter	*D*	*B*	*L*	Data source
Maximum UTB in absolute value (seasonal thermocline)	5–15	N/d	5–12	Measurements during cruises with CTD-complexes IDRONAUT OCEAN SEVEN 320 Plus M, SBE 911plus and Sea-Bird 911plus
Maximum UPB (seasonal pycnocline)	5–15	N/d	5–10	–
Total suspended matter concentration	10–15	N/d	4–16	LAC measurements using SIPO 4
Chlorophyll a concentration	23–54	N/d	3–5	Measurements during cruises with CTD-complex IDRONAUT OCEAN SEVEN 320 Plus M
Phytoplankton biomass	0–20	100–340	10	Cruise reports
Dinophytes biomass (*Dinophyceae*)	15–20	40–190	5–10	Cruise reports

Table 2 concluded

Parameter	*D*	*B*	*L*	Data source
Noctiluca scintillans biomass	35–20*	108	15	Cruise reports
Copepodes biomass	76–104	243	29	Cruise reports
Forage zooplankton biomass	76–104	345	29	Cruise reports
Aurelia aurita biomass	N/d	190 g·m^{-2}	N/d	Cruise reports
Bioluminiscent potential	15–35	N/d	5–10	Salpa-M
SV	20–30	N/d	15–25	Lowrance Elite 7 Ti transducer

Note: D – typical depth of a deep maximum, m; B – biomass at the maximum, mg·m^{-3}; L – maximum layer thickness, m; UTB – the upper thermocline boundary; UPB – the upper pycnocline boundary; *SV* – the sound backscattering volume strength, dB, at a frequency of 200 kHz; N/d – no data.

* Thermocline layer.

General discussion

We have presented the layering of the vertical distribution as individual episodes and trends based on averaged data. It is clear that, in the latter case, the peak amplitudes are smoothed and primarily reflect the main seasonal maximum of the parameter, which is usually associated with the position of the pycnocline. As for the fine structure of the vertical distribution, showing the location of the layers and their amplitudes, such estimates for most biological parameters are limited by the technical capabilities of the measurement methods. Exceptions are vertical profiles of chlorophyll fluorescence, bioluminescence intensity and volume backscattering. However, these provide indirect estimates of organism abundance and biomass.

The factors determining the formation of deep summer maxima for the physical and biological characteristics under consideration are of different natures. Thus, while the depth and thickness of the peak concentration of total suspended matter are linked to vertical gradients of temperature and density, the depth and thickness of the seasonal maximum concentration of chlorophyll a are regulated by phytoplankton adaptation to light conditions and the concentration of nutrients. At the same time, the peaks of chlorophyll a and phytoplankton biomass may not coincide in depth [39]. The mechanism governing the formation of deep zooplankton abundance maxima is different. The heterogeneity in the vertical distribution of copepod abundance is due to their motor activity associated with foraging and to sensory interactions with other zooplankton organisms and small nekton – potential predators [40]. Motor activity and trophodynamic processes also determine the characteristics of aggregations of small pelagic fish (e.g., anchovy and sprat).

In view of further studies, it stands to mention that bioluminescence within layers formed by organisms of varying taxonomic composition is still a poorly understood aspect of the layering of the pelagic community on the Crimean shelf. Due to the complex interactions between organisms, their dense, deep-located aggregations may glow. This applies to deep maxima of phytoplankton, copepods and gelatinous organisms (jellyfish, comb jellies, etc.). The phenomenon requires both visual observations using underwater vehicles and video recording.

This article examines the layering observed in summer. In temperate latitudes, seasonality contributes significantly to the multi-scale spatio-temporal variability of pelagic community characteristics. In this regard, the formation of seasonal subsurface maxima is particularly telling. On the Black Sea shelf, these appear in spring and reach their maximum seasonal amplitudes in July–September. For example, the maximum concentration of chlorophyll a forms by this time at a depth of 30–40 m and accounts for up to 65% of total chlorophyll [41].

Without getting into details about the diurnal variability of the vertical structure, it should be noted that this variability defines the scope of “biological layering”, limiting it to a 24-hour cycle: it is at this interval that nocturnal vertical migrations of zooplankton and small pelagic fish from the depths to the upper layers occur. Migrations and trophic interactions influence abundance and transform the layered structure of zooplankton and small nekton.

Another characteristic feature is the spatial heterogeneity (discontinuity) of the layers, which leads to a patchy distribution of organism abundance. The discontinuity is clearly evident from data from high-frequency measurements of bioluminescence intensity using bathyphotometers and in the sequence of vertical profiles obtained by echo sounders as the vessel was underway. The phenomenon of discontinuity has both hydrophysical (break of internal waves, mesoscale eddies etc.) and biological regulatory mechanisms based on trophic interactions between individuals.

In general, the patchiness of spatial distribution is characterised by an increase in its intensity along the trophic cascade (and thus across the size spectrum of

the pelagic community): from phytoplankton to zooplankton and on to small nekton. In this context, the intensity can be indicated by the variance normalised to the mean [4]. In highly productive areas, the layers exhibit greater contrast in their vertical gradients, since, in terms of statistics (outside the conditions of a normal distribution, which is typical for pelagic community parameters), the parameter variance depends on the mean [42].

In terms of the decadal variability, the layering of the Black Sea's thermohaline structure shows changes that are linear in nature rather than periodic (as with seasonal variability), a phenomenon attributed to the short duration of the time series. For example, the cold intermediate layer, a unique element of the vertical thermohaline structure of the Black Sea waters, has been noted to weaken and gradually disappear [8] [43]. Moreover, model calculations show a gradual decrease in the vertical salinity gradient against its increase in the upper 200-metre layer [44]. Such long-term transformations of the thermohaline structure are likely to be reflected in the layering characteristics of the pelagic community; however, this aspect has been poorly studied.

The spatio-temporal structure of the pelagic community determines the features of its functioning. In the Crimean shelf waters, the organic carbon content in the gelatinous fraction of zooplankton (where *A. aurita* dominates in terms of biomass) is 3–4 times higher than its content in the forage zooplankton, which is dominated by copepods [25]. This indirectly indicates that a significant portion of the organic carbon flux passes through the detritus-based, rather than the grazing, trophic chain of the pelagic ecosystem. The dominance of the detritus pathway has been noted previously [38]. In the grazing chain, the main part of the flux in the link between producers and consumers is accounted for by microzooplankton, which consumes about 50% of primary production [45], as well as by mesozooplankton, including small copepods, phytoplankton filter feeders [46]. The latter include: *Paracalanus parvus*, *Pseudocalanus elongatus* and the copepodid stages of *Acartia clausi*.

Conclusion

The layering of vertical biomass distribution during the summer season, with maxima in the surface layer and the thermocline (or adjacent layers), is characteristic of all the groups of organisms in the studied pelagic community of the Crimean shelf. At the lower trophic levels, this layering is regulated primarily by thermohaline stratification of the water column. At the middle trophic levels, represented by copepods and small pelagic fish, the dominant factor in the layering formation is the motor activity of organisms, associated with feeding behaviour, reproductive, protective and other forms of activity.

---

[8] Vandenbulcke, L., Capet, A., Macé, L., Meulders, C., Mouchet, A. and Grégoire, M., 2023. *Synthesis Quality Overview Document (SQO). Copernicus. CMEMS-BLK-SQO-007-005, iss. 4.0*. Available at: https://catalogue.marine.copernicus.eu/documents/SQO/CMEMS-BLK-SQO-007-010.pdf [Accessed: 22 February 2026].

In the context of the relationship between structure and function in a pelagic ecosystem, the layering of organism distribution forms vertical heterogeneity in the density of trophic interactions and, therefore, vertical heterogeneity in the flow of matter and energy within the community. Trophic interactions appear to be the most intense in the layers of greatest thickness due to their greater ecological capacity. These layers include the surface and subsurface maxima of phytoplankton, zooplankton and small pelagic fish biomass, primarily mass-producing species (anchovies and sprats).

REFERENCES

1. Behrenfeld, M.J., O'Malley, R.T., Boss, E.S., Westberry, T.K., Graff, J.R., Halsey, K.H., Milligan, A.J., Siegel, D.A. and Brown, M.B., 2016. Revaluating Ocean Warming Impacts on Global Phytoplankton. *Nature Climate Change*, 6, pp. 323–330. https://doi.org/10.1038/NCLIMATE2838
2. Longhurst, A., 1998. *Ecological Geography of the Sea*. San Diego: Academic Press, 398 p.
3. Moriarty, R. and O'Brien, T.D., 2013. Distribution of Mesozooplankton Biomass in the Global Ocean. *Earth System Science Data*, 5(1), pp. 45–55. https://doi.org/10.5194/essd-5-45-2013
4. Piontkovski, S.A., 2005. *Multiscale Variability of Mesoplanktonic Fields of the Ocean*. Sevastopol: ECOSI-Gidrophizika, 194 p. (in Russian).
5. Mikhailovsky, G.E., 1984. [Specificity of Ecological Systems and Problems of their Study]. *Zhurnal Obshchei Biologii*, 45(1), pp. 66–77 (in Russian).
6. Lasker, R., 1975. Field Criteria for Survival of Anchovy Larvae: the Relation Between the Inshore Chlorophyll Layers and Successful First Feeding. *Fishery Bulletin*, 73(3), pp. 453–462.
7. Glushchenko, T.I. and Chashchin, A.K., 2008. Peculiarities of Nutrition of the Black Sea Sprat *Sprattus Sprattus Phalericus* (Risso) (Pisces: Clupeidae) and Formation of its Feeding Accumulations. *Marine Ekological Journal*, 7(3), pp. 5–14 (in Russian).
8. Klimova, T.N., Subbotin, A.A., Vdodovich, I.V., Zagorodnyaya, Yu.A. and Zabrodin, D.A., 2024. Ichthyoplankton in the Northern Part of the Black Sea under the Prolongation of Summer Hydrological Season in 2020. *Inland Water Biology*, 17(1), pp. 197–207. https://doi.org/10.1134/S1995082924010085
9. Zaika, V.E., 1981. Environment Capacity: the Content of the Notion and Its Application in Ecology. *Ecology of the Sea*, 7, pp. 3–9 (in Russian).
10. Samodurov, A.S. and Chukharev, A.M., 2017. Intensity of Vertical Turbulent Exchange in the Black Sea Summer Pycnocline Around the Crimean Peninsula. *Journal of Physics: Conference Series*, 899(2), 0220015. https://doi.org/10.1088/1742-6596/899/2/022015
11. Piontkovski, S.A., Al-Oufi, H.S. and Al-Abri, N.M., 2016. Fish Landings and Oman Shelf Area. *Journal of Agricultural and Marine Sciences*, 21(1), pp. 25–32. https://doi.org/10.24200/jams.vol21iss0pp25-32
12. Artamonov, Yu.V., Skripaleva, E.A., Fedirko, A.V., Shutov, S.A., Derjushkin, D.V., Shapovalov, R.O., Shapovalov, Yu. I. and Shcherbachenko, S.V., 2020. Waters Circulation in the Northern Part of the Black Sea in Summer – Winter of 2018. *Ecological Safety of Coastal and Shelf Zones of Sea*, (1), pp. 69–90. https://doi.org/10.22449/2413-5577-2020-1-69-90 (in Russian).
13. Ivanov, V.A., Kuznetsov, A.S. and Morozov, A.N., 2019. Monitoring Coastal Water Circulation along the South Coast of Crimea. *Doklady Earth Sciences*, 485(2), pp. 405–408. https://doi.org/10.1134/S1028334X19040044

14. Zagorodnyaya, Yu.A. and Piontkovski, S.A., 2022. Seasonal and Interannual Variations of the Abundance of the Dinoflagellate *Noctiluca Scintillans* in the Northern Black Sea. *Marine Biology Research*, 18(1-2), pp. 104–116. https://doi.org/10.1080/17451000.2022.2086701

15. Kovalev, A.V., Melnikov, V.V., Ostrovskaya, N.A. and Prusova, I.Yu., 1993. [Macroplankton]. In: A. V. Kovalev and Z. Z. Finenko, eds., 1993. [*Plankton of the Black Sea*]. Kiev: Naukova Dumka, pp. 183–193 (in Russian).

16. Petipa, T.C., 1957. [On Average Weight of Main Zooplankton Forms of the Black Sea]. In: Academy of Sciences of the USSR, 1957. *Trudy Sevastopolskoy Biologicheskoy Stantsii*, 9, pp. 39–57 (in Russian).

17. Latushkin, A.A., Artamonov, Yu.V., Skripaleva, E.A. and Fedirko, A.V., 2022. The Relationship of the Spatial Structure of the Total Suspended Matter Concentration and Hydrological Parameters in the Northern Black Sea According to Contact Measurements. *Fundamental and Applied Hydrophysics*, 15(2), pp. 124–137. https://doi.org/10.48612/fpg/4heu-kxbn-gg7t (in Russian).

18. Melnik, A., Melnik, L., Mashukova, O. and Melnikov, V., 2021. Field Studies of Bioluminescence in the Antarctic Sector of the Atlantic Ocean in 2002 and 2020. *Luminescence*, 36(8), pp. 1910–1921. https://doi.org/10.1002/bio.4125

19. Kuznetsov, A.S. and Ivashchenko, I.K., 2023. Features of Forming the Alongcoastal Circulation of the Coastal Ecotone Waters nearby the Southern Coast of Crimea. *Physical Oceanography*, 30(2), pp. 171–185.

20. Simonova, Yu.V., Stanichny, S.V. and Lemeshko, E.M., 2020. [Characteristics of Upwellings in the Southern coast of Crimea Based on a Comprehensive Analysis of In Situ and Remote Observations]. In: SRI RAS, 2020. *Proceedings of the 19th All-Russian Open Conference "Modern Problems of Remote Probing the Earth from Space"*. Moscow: Space Research Institute of RAS Publishing, p. 335 (in Russian).

21. Kubryakova, E. and Kubryakov, A., 2020. Warmer Winter Causes Deepening and Intensification of Summer Subsurface Bloom in the Black Sea: the Role of Convection and Self-Shading Mechanism, *Biogeosciences Discussions*. [Preprint]. https://doi.org/10.5194/bg-2020-210

22. Drits, A.V., Nikishina, A.B., Sergeeva, V.M. and Solov'ev, K.A., 2013. Feeding, Respiration, and Excretion of the Black Sea *Noctiluca scintillans* MacCartney in Summer. *Oceanology*, 53(4), pp. 442–450. https://doi.org/10.1134/S0001437013040036

23. Zagorodnyaya, Yu.A. and Moryakova, V.K., 2018. [Holoplankton]. In: N. S. Kostenko, ed., 2018. *The Biology of the Black Sea Offshore Area at the South-Eastern Crimea*. Simferopol: PP "ARIAL", pp. 46–59 (in Russian).

24. Mikaelyan, A.S., Malej, A., Shiganova, T.A., Turk, V., Sivkovitch, A.E., Musaeva, E.I., Kogovšek, T. and Lukasheva, T.A., 2014. Populations of the Red Tide Forming Dinoflagellate *Noctiluca scintillans* (Macartney): A Comparison Between the Black Sea and the Northern Adriatic Sea. *Harmful Algae*, 33, pp. 29–40. https://doi.org/10.1016/j.hal.2014.01.004

25. Zagorodnyaya, Yu.A., Piontkovski, S.A. and Gubanov, V.V., 2023. Pelagic Ecosystem of the Black Sea Goes Gelatinous. *Marine Biology Research*, 19(6-7), pp. 317–326. https://doi.org/10.1080/17451000.2023.2235571

26. Zaitsev, Yu.P. and Polishchuk, L.N., 1984. An Increase in the Number of *Aurelia aurita* (L.) in the Black Sea. *Biologiya Morya*, 17, pp. 35–46 (in Russian).

27. Balykin, P.A., Kutsyn, D.N. and Startsev A.V., 2021. Fishing Under Climate Change: Dynamics of Composition and Structure of Catches in the Russian Black Sea in the XXI Century. *Marine Biological Journal*, 6(3), pp. 3–14. https://doi.org/10.21072/mbj.2021.06.3.01 (in Russian).

28. Brough, T., Rayment, W. and Dawson, S., 2019. Using a Recreational Grade Echo-sounder to Quantify the Potential Prey Field of Coastal Predators. *PLoS ONE*, 14(5), e0217013. https://doi.org/10.1371/journal.pone.0217013
29. McInnes, A.M., Khoosal, A., Murrell, B., Merkle, D., Lacerda, M., Nyengera, R., Coetzee, J.C., Edwards, L.C., Ryan, P.G. et al. Recreational Fish-Finders – an Inexpensive Alternative to Scientific Echo-Sounders for Unravelling the Links Between Marine Top Predators and Their Prey. *PLoS ONE*, 10(11), e0140936. https://doi.org/10.1371/journal.pone.0140936
30. Artemov, Yu.G., 2006. Software Support for Investigation of Natural Methane Seeps by Hydroacoustic Method. *Marine Ekological Journal*, 5(1), pp. 57–71.
31. Serikova, I.M., 2020. Algorithm for Mathematical Processing of Bioluminescence Profiles for the Study of Small-Scale Agregation of Plankton. *Monitoring Systems of Environment*, (1), pp. 145–152. https://doi.org/10.33075/2220-5861-2020-1-145-152 (in Russian).
32. Melnik, A.V., Georgieva, E.Iu. and Melnik, L.A., 2019. The Variability of the Spatial Distribution of Bioluminescence and Phytoplankton in the Photic Layer of the Black Sea in Summer 2018. *Monitoring systems of environment*, (3), pp. 120–126. https://doi.org/10.33075/2220-5861-2019-3-120-126 (in Russian).
33. Tokarev, Yu.N., Bityukov, E.P., Vasilenko, V.I. and Sokolov, B.G., 2000. The Bioluminescence Field as a Characteristic Index of the Black Sea Plankton Community Structure. *Ecology of the Sea*, 53, pp. 20–25 (in Russian).
34. Serikova, I.M., Evstigneev, V.P., Tokarev, Yu.N. and Suslin, V.V., 2017. Bioluminescence Field of the Black Sea as Indicator of Dinophyta Aggregation, Its Seasonal and Interannual Dynamics. In: SPIE, 2017. *Proceedings of SPIE*. Vol. 10466: 23rd International Symposium on Atmospheric and Ocean Optics: Atmospheric Physics, 104663X. https://doi.org/10.1117/12.2287964
35. Evstigneev, V.P., Serikova, I.M. and Kyrylenko, N.F., 2019. Biotic and Abiotic Influence on Bioluminescence Field in Summer. In: MEDCOAST, 2019. *14th MEDCOAST Congress on Coastal and Marine Sciences, Engineering, Management and Conservation, MEDCOAST 2019*. Marmaris, 2019. Vol. 1, pp. 307–318.
36. Bityukov, E.P., Evstigneev, P.V. and Tokarev, Yu.N., 1993. Luminescent Dinoflagellata of the Black Sea as Affected by Anthropogenic Factors. *Gidrobiologichesky Zhurnal*, 29(4), pp. 27–34 (in Russian).
37. Serikova, I.M., Bryantseva, Yu.V. and Vasilenko, V.I., 2013. Seasonal Dynamics of the Bioluminescence Field's Structure and Its Connection with the Dinoflagellates Parameters. *Marine Ekological Journal*, 12(4), pp. 87–95 (in Russian).
38. Yunev, O.A., Konovalov, S.K. and Velikova, V., 2019. *Anthropogenic Eutrophication in the Black Sea Pelagic Zone: Long-Term Trends, Mechanisms, Consequences*. Moscow: GEOS, 194 p. (in Russian).
39. Finenko, Z.Z., Churilova, T.Ya. and Lee, R.I., 2005. Vertical Distribution of Chlorophyll and Fluorescence in the Black Sea. *Marine Ekological Journal*, 4(1), pp. 15–46 (in Russian).
40. Piontkovski, S.A. and Seregin, S.A., 2006. *The Behavior of Copepods*. Sevastopol: Ekosi-Gidrophizika, 148 p. (in Russian).
41. Ricour, F., Capet, A., D'Ortenzio, F., Delille, B. and Grégoire, M., 2021. Dynamics of the Deep Chlorophyll Maximum in the Black Sea as Depicted by BGC-Argo Floats. *Biogeosciences*, 18(2), pp. 755–774. https://doi.org/10.5194/bg-18-755-2021

42. Tsou, T., 2011. Determining the Mean-Variance Relationship in Generalized Linear Models – a Parametric Robust Way. *Journal of Statistical Planning and Inference*, 141(1), pp. 197–203. https://doi.org/10.1016/j.jspi.2010.05.029

43. Stanev, E.V., Peneva, E. and Chtirkova, B., 2019. Climate Change and Regional Ocean Water Mass Disappearance: Case of the Black Sea. *Journal of Geophysical Research: Oceans*, 124(7), pp. 4803–4819. https://doi.org/10.1029/2019JC015076

44. Dorofeev, V.L. and Sukhikh, L.I., 2023. Analysis of Long-Term Variability of Hydrodynamic Fields in the Upper 200-Meter Layer of the Black Sea Based on the Reanalysis Results. *Physical Oceanography*, 30(5), pp. 581–593.

45. Stelmakh, L.V., 2013. Microzooplankton Grazing Impact on Phytoplankton Blooms in the Coastal Seawater of the Southern Crimea (Black Sea). *International Journal of Marine Science*, 3(15), pp. 121–127. https://doi.org/10.5376/ijms.2013.03.0015

46. Petipa, T.S., Pavlova, E.V. and Mironov, G.N., 1970. [Food Web Structure, Transfer and Use of Matter and Energy in Black Sea Plankton Communities]. *Biologiya Morya*, 19, pp. 3–43 (in Russian).

Submitted 2.01.2025; accepted after review 21.03.2025;
revised 18.12.2025; published 31.03.2026

About the authors:

Sergey A. Piontkovski, Leading Researcher, Sevastopol State University (33 Universitetskaya St., 299053, Sevastopol, Russia), DSc (Biol.), **ORCID ID: 0000-002-6472-9701**, **Scopus Author ID: 6602165194**, **ResearcherID: ABB-9334-2020**, *spiontkovski@mail.ru*

Aleksandr V. Melnik, Senior Researcher, A. O. Kovalevsky Institute of Biology of the Southern Seas of RAS (2 Nakhimova Ave, Sevastopol, 299011, Russia), PhD (Biol.), **ORCID ID: 0000-0002-4371-384X**, **Scopus AuthorID: 57219127014**, **ResearcherID: X-1393-2019**, *melnikav@ibss-ras.ru*

Yulia A. Zagorodnyaya, Leading Researcher, A. O. Kovalevsky Institute of Biology of the Southern Seas of RAS (2 Nakhimova Ave, Sevastopol, 299011, Russia), PhD (Biol.), **ORCID ID:0000-0002-9502-4923**, **Scopus Author ID: 6506214138**, **ResearcherID: E-3325-2018**, *artam-ant.yandex.ru*

Yuri G. Artemov, Leading Researcher, A. O. Kovalevsky Institute of Biology of the Southern Seas of RAS (2 Nakhimova Ave, Sevastopol, 299011, Russia), PhD (Geogr.), **ORCID ID: 0000-0002-4725-1427**, **Scopus Author ID: 12767058200**, **ResearcherID: G-1797-2015**, *yu.g.artemov@gmail.com*

Elena A. Skripaleva, Senior Researcher, Marine Hydrophysical Institute of RAS (2 Kapitanskaya St., Sevastopol, 299011, Russia), PhD (Geogr.), **ResearcherID: AAC-6648-2020**, **ORCID ID: 0000-0003-1012-515X**, *sea-ant@yandex.ru*

Elena Yu. Georgieva, Leading Engineer, A. O. Kovalevsky Institute of Biology of the Southern Seas of RAS (2 Nakhimova Ave, Sevastopol, 299011, Russia), **ORCID ID: 0000-0002-8177-0781**, **Scopus Author ID: 57193546928**, *e-georgieva@mail.ru*

Contribution of the authors:

Sergey A. Piontkovski – statement of the study objectives, formation of the article structure, analysis and interpretation of the results, preparation of the graphical materials, statistical analysis

Aleksandr V. Melnik – analysis and interpretation of the results, preparation of the graphical materials on bioluminescence

Yulia A. Zagorodnyaya – analysis and interpretation of the results, preparation of the graphical materials on zooplankton

Yuri G. Artemov – preparation of the graphical materials, analysis and interpretation of the results on sound scattering characteristics

Elena A. Skripaleva – preparation of the graphical materials, analysis and interpretation of the results on total suspended matter concentration

Elena Yu. Georgieva – preparation of the graphical materials, analysis and interpretation of the results on phytoplankton

All the authors have read and approved the final manuscript.

Original paper

Hydrocarbons in the Water and Suspended Matter of the Coastal Water Areas of Crimea and Krasnodar Krai after the Fuel Oil Spill in December 2024

E. A. Tikhonova *, O. V. Soloveva, O. A. Mironov, S. V. Alyomov, Yu. S. Klycheva (Tkachenko), G. V. Frolkin

A. O. Kovalevsky Institute of Biology of the Southern Seas of RAS, Sevastopol, Russia
** e-mail: tikhonova_ea@ibss-ras.ru*

Abstract
As a result of the fuel oil spill from *Volgoneft-212* and *Volgoneft-239* tankers in the Kerch Strait on 15 December 2024, the coast of Crimea and the Krasnodar Krai was polluted. The aim of the work is to study hydrocarbon pollution of water and suspended matter in the coastal waters of the Kerch Peninsula and Krasnodar Krai affected by fuel oil emissions from December 2024 to January 2025. Although in the first days after the tanker accident (16–18 December 2024) the hydrocarbon content in the water exceeded the MPC (0.05 mg·L^{-1}) at 70% of the stations, the n-alkanes composition and marker values indicated that the main sources of hydrocarbons in the water and suspended matter of the study water area were natural sources. Signs of degraded petroleum products were noted, indicating chronic oil pollution of the water area. During the petroleum product emissions (January 2025), average hydrocarbon concentrations in the coastal waters of the Kerch Peninsula and Krasnodar Krai did not exceed MPC. The hydrocarbon content in suspended matter in the study area ranged from 13 to 67 μg·L^{-1}, which can be characterised as high. The distribution and composition of n-alkanes in suspended matter in January 2025 indicated probable oil pollution. An analysis of hydrocarbon genesis markers confirmed this conclusion. Thus, the fuel oil pollution that arrived by January 2025 did not cause an increase in hydrocarbon concentrations in the water. In January 2025, evidence of oil pollution was detected only in suspended matter in seawater. Given that the fuel oil spill had a certain impact on individual components of the coastal ecosystem, further studies are needed to assess the long-term impact of hydrocarbons on the ecosystem of these waters.

Keywords: coastal waters, fuel oil spill, petroleum hydrocarbons, petroleum pollution, seawater, suspended matter, Black Sea

Acknowledgments: This work was carried out within the framework of the state assignment on the topic “The state of the marine environment and its capacity for self-purification in the coastal areas of the Crimean Peninsula and Krasnodar Krai after the oil spill in December 2024” (FNNZ-2026-0016).

For citation: Tikhonova, E.A., Soloveva, O.V., Mironov, O.A., Alyomov, S.V., Klycheva (Tkachenko), Yu.S. and Frolkin, G.V., 2026. Hydrocarbons in the Water and Suspended Matter of the Coastal Water Areas of Crimea and Krasnodar Krai after the Fuel Oil Spill in December 2024. *Ecological Safety of Coastal and Shelf Zones of Sea*, (1), pp. 52–72.

© Tikhonova E. A., Soloveva O. V., Mironov O. A., Alyomov S. V., Klycheva (Tkachenko) Yu.S., Frolkin G.V., 2026

This work is licensed under a Creative Commons Attribution-Non Commercial 4.0 International (CC BY-NC 4.0) License

Углеводороды в воде и взвешенном веществе прибрежных акваторий Крыма и Краснодарского края после разлива мазута в декабре 2024 года

Е. А. Тихонова *, О. В. Соловьёва, О. А. Миронов, С. В. Алёмов, Ю. С. Клычёва (Ткаченко), Г. В. Фролкин

ФГБУН ФИЦ «Институт биологии южных морей имени А. О. Ковалевского РАН», Севастополь, Россия

* *e-mail: tikhonova_ea@ibss-ras.ru*

Аннотация

В результате разлива мазута с танкеров «Волгонефть-212» и «Волгонефть-239» в Керченском проливе 15 декабря 2024 г. подверглось загрязнению побережье Крыма и Краснодарского края. Цель работы состоит в исследовании углеводородного загрязнения воды и взвешенного вещества прибрежных акваторий Керченского полуострова и Краснодарского края, подвергшихся выбросам мазута с декабря 2024 г. по январь 2025 г. Хотя в первые дни после аварии танкеров (16–18 декабря) содержание углеводородов в воде на 70 % станций превышало ПДК (0.05 мг·л$^{-1}$), состав н-алканов и значения маркеров указывают, что основными источниками обнаруженных углеводородов в воде и взвешенном веществе исследуемой акватории были природные источники. Отмечены признаки наличия деградированных нефтепродуктов, что свидетельствует о хроническом нефтяном загрязнении акватории. В период выбросов нефтепродуктов (январь 2025 г.) средние концентрации углеводородов в воде побережья Керченского полуострова и Краснодарского края не превышали ПДК. Содержание углеводородов во взвеси исследуемого района, колебавшееся в диапазоне 13–67 мкг·л$^{-1}$, можно характеризовать как высокое. Распределение и состав н-алканов во взвешенном веществе в январе 2025 г. указывают на вероятное нефтяное загрязнение. Анализ маркеров генезиса углеводородов подтверждает данный вывод. Таким образом, мазут, поступивший к январю 2025 г. в результате аварии, не вызвал повышения концентрации углеводородов в воде. Признаки нефтяного загрязнения в январе 2025 г. зафиксированы только во взвешенном веществе в морской воде. С учетом того, что разлив мазута оказал определенное влияние на отдельные компоненты прибрежной экосистемы, необходимы дальнейшие исследования в данном направлении для оценки долговременного воздействия углеводородов на компоненты экосистемы акваторий.

Ключевые слова: прибрежная акватория, разлив мазута, углеводороды нефти, загрязнение нефтепродуктами, морская вода, взвешенное вещество, Черное море

Благодарности: работа выполнена в рамках госзадания ФИЦ ИнБЮМ по теме «Состояние морской среды и ее способность к самоочищению в прибрежных районах Крымского полуострова и Краснодарского края после разлива нефтепродуктов в декабре 2024 г.» (FNNZ-2026-0016).

Для цитирования: *Тихонова Е. А., Соловьёва О. В., Миронов О. А., Алёмов С. В. и др.* Углеводороды в воде и взвешенном веществе прибрежных акваторий Крыма и Краснодарского края после разлива мазута в декабре 2024 года // Экологическая безопасность прибрежной и шельфовой зон моря. 2026. № 1. С. 52–72. EDN KOVTFI.

Introduction

The Kerch Strait is a key transport route connecting the ports of the Sea of Azov and the Don and Volga River basins with the Black and Mediterranean Seas. The Kerch Sea Port and the Port of Kavkaz operate in its waters, with petroleum cargoes accounting for the major part of their cargo turnover [1, 2]. According to the Association of Sea Commercial Ports, in December 2024, oil and petroleum products were 30.2 and 20.3% of the total transshipment volume, respectively [1)]. Due to the fact that the Kerch Strait has recently become one of the main thoroughfares for Russian oil exports [2)], the risk of accidents has increased significantly.

During a storm on 15 December 2024, two oil tankers (*Volgoneft-212* and *Volgoneft-239*) suffered shipwreck in the Kerch Strait. As a result of the hulls breaking apart, some of the transported fuel oil leaked into the Black Sea. The fuel oil spill had serious consequences. On 17 December, a state of emergency was declared in Anapa and several settlements in the Temryuk District of the Krasnodar Krai, which was raised to the federal level on 26 December. By mid-January, at least 54 km of the Krasnodar Krai coastline (from the village of Veselovka in the Temryuk District to the village of Blagoveshchenskaya near Anapa) and 15 km of the Crimean coast (including the Kerch, Feodosia, Sudak, Alushta and Sevastopol areas) had been polluted with fuel oil.

The volume of fuel oil spilled as a result of the accident has not yet been determined. However, preliminary estimates suggest that it exceeds the amount leaked in a similar disaster that took place in the Kerch Strait in November 2007 after the wreckage of the tanker *Volgoneft-139*, which resulted in approximately 1,300 tonnes of fuel oil entering the water area [3–5]. These incidents not only harm the ecosystem of the strait, but also highlight critical issues concerning the safety of maritime transportations, corporate responsibility and the necessity for strict enforcement of environmental standards.

The relevance of the oil pollution problem cannot be overrated. Organic substances in petroleum products have a devastating effect on marine flora and fauna, causing irreparable damage to living organisms and ecosystems. Oil spills negatively affect biochemical processes in water bodies, which can lead to long-range effects, including loss of biodiversity and deterioration of water quality [6].

Hydrocarbons (HCs) in water and suspended matter are key indicators of pollution levels and sources. Analysis of these HCs allows for a rapid assessment of the scale of pollution and its spread. Given the increasing frequency of oil spills around the world, it is necessary to study the consequences of such disasters and develop strategies to prevent and minimise damage. In this article, we study the state of individual components of the coastal ecosystem in the affected water areas caused by the fuel oil spill in the Kerch Strait in December 2024.

[1)] Available at: https://www.morport.com/rus/news/gruzooborot-morskih-portov-rosszayanvar-dekabr-2024-goda [Accessed: 13 May 2025] (in Russian).

[2)] Grogoriev, L., ed., 2016. [*Energy Bulletin*]. Analytical Centre under the Government of the Russian Federation, 10 p. Iss. 36: Development of Oil Transportation (in Russian). Available at: https://ac.gov.ru/files/publication/a/9072.pdf [Accessed: 12 February 2026] (in Russian).

The work is aimed to assess the condition of water and suspended matter in the coastal waters of the Kerch Peninsula and Krasnodar Krai, which were polluted with fuel oil from December 2024 to January 2025.

In accordance with the objective, the following tasks have been stated:

1) to study the content and composition of HCs, as well as to identify the most probable sources of HCs in the water and suspended matter off the coast of the Kerch Peninsula and Krasnodar Krai immediately after the accident (16–18 December 2024) and one month after it (20–23 January 2025) to obtain baseline data on the pollution of the studied coast and indicators corresponding to the period of intensive petroleum product wash up;

2) to assess changes in the studied parameters as a result of fuel oil entering the water area after the accident.

Material and methods

Water samples from the surface layer were collected during two expeditions conducted on 16–18 December 2024 (immediately after the accident) and 20–23 January 2025 (Fig. 1). Seawater samples were collected at 10 stations on 16–18 December 2024. Since fuel oil spills continued on the coast a month after the tanker wreckage, we added areas where, according to media reports, volunteers had recorded spills to the station map (Fig. 1).

Sample preparation for determining HCs in water. A water sample and 20 mL of n-hexane were placed in a separating funnel and the mixture was shaken for 10 minutes. After separation of water and n-hexane, the water was poured back into the container, and the hexane extract was poured into a flask for concentration through a chemical funnel filled with freshly calcined sodium sulphate on a cotton wool plug. The water samples were re-extracted for 10 minutes in a separating funnel with the addition of 15 mL of n-hexane. After separation of the water and n-hexane layers, the water layer was discarded and the hexane extracts were combined. The vessel and separating funnel were rinsed with 2–3 mL of n-hexane and added to the extract. The resulting extract was passed through a glass column filled with aluminium oxide and concentrated to a volume of 1 mL.

Sample preparation for determining HCs in suspension. Membrane nitrocellulose filters 0.45 μm were weighed on a VLR-200 analytical scale, then 1 L of water was passed through the filtration unit. The suspension obtained on the filters was dried under natural conditions. The analysis for determining HCs was based on the extraction of HCs from the suspension collected on the filters with an alkaline solution of ethyl alcohol, with the transfer of the analysed ingredient to hexane and the removal of interfering compounds by sorption on aluminium oxide. The resulting extract was concentrated to a volume of 1 mL.

Determination of HCs and n-alkanes. An aliquot of the concentrated extract (1 μL) was injected with a microsyringe into a Crystal 5000.2 gas chromatograph evaporator heated to 250°C with a flame ionisation detector. HCs were separated on a TR-1MS tubular column 30 m long, 0.32 mm in diameter, with a stationary

Fig. 1. Location of sampling stations off the coast of the Kerch Peninsula and Krasnodar Krai, December 2024 and January 2025. The inset shows the study area (red box)

phase film thickness of 0.25 μm (Thermo Scientific). The column temperature was programmed from 70 to 280°C (temperature rise rate: 8°C/min). The carrier gas (nitrogen) flow in the column was 2.5 mL/min without flow splitting. The detector temperature was 320°C.

The total HC content was quantified by absolute calibration with a flame ionisation detector using a HC mixture prepared by the gravimetric method with a HC content in the range of 0.02–5.0 mg/L. A standard sample of ASTM D2887 Reference Gas Oil (SUPELCO, USA) was used as the HC mixture. The total HC content was determined by the sum of the n-alkanes peak areas. The results were processed using the Chromatec Analyst 3.0 software, the absolute calibration method and percentage normalisation.

N-alkanes were identified using a standard sample of a mixture of paraffin hydrocarbons in hexane with a mass concentration of each component of 200 μg/mL. Pristane (Pr) and phytane (Ph) were identified using a sample with a concentration of 100 μg/mL in hexane (SUPELCO, USA).

Identification of the HC origin. The origin of HCs was determined based on the chromatographic pattern, the distribution of n-alkanes and biogeochemical markers (Table 1).

Statistical analysis of data. The difference between the mean values of the two samples was determined based on box plots (Microsoft Excel) with outlier fences showing the distribution of data by quartiles with the median and outliers highlighted.

T a b l e 1. Diagnostic molecular ratios and their typical values

Diagnostic index (calculation formula)	Value	Typical value interpretation
$LWH/HWH = \sum(C_{11}-C_{21})/\sum(C_{22}-C_{35})$	> 1	Oil origin
	< 1	Terrigenous, higher plant
$CPI_2 = (1/2)\{(C_{25}+C_{27}+C_{29}+C_{31}+C_{33}+C_{35})/(C_{24}+C_{26}+C_{28}+C_{30}+C_{32}+C_{34}) + (C_{25}+C_{27}+C_{29}+C_{31}+C_{33}+C_{35})/(C_{26}+C_{28}+C_{30}+C_{32}+C_{34})\}$	~ 1	Large portion of petroleum hydrocarbons
	< 1	Mainly biogenic origin
	> 1	Biogenic, influence on hydrocarbon composition of terrigenous organic matter
$Ki = (Pr + Ph)/(\text{n-}C_{17} + C_{18})$	$0.8 \le Ki \le 1.5$	Presence of moderately degraded oil
	$0.3 \le Ki \le 0.8$	Presence of mildly degraded oil
	$Ki \le 0.3$	Presence of fresh oil
Pr/Ph	< 1	Presence of oil in bottom sediments

Table 1 concluded

Diagnostic index (calculation formula)	Value	Typical value interpretation
$P_{aq} = (C_{23} + C_{25})/(C_{23} + C_{25} + C_{29} + C_{31})$	0.1	Traces of terrigenous degraded plants
	$0.1 < P_{aq} < 0.4$	Fresh macrophytes
	$0.4 < P_{aq} < 1.0$	Water macrophytes
$TAR = (C_{27} + C_{29} + C_{31})/(C_{15} + C_{17} + C_{19})$	High TAR	Prevalence of terrigenous material
$ACL = [25C_{25} + 27C_{27} + 29C_{29} + 31C_{31} + + 33C_{33}]/[C_{25} + C_{27} + C_{29} + C_{31} + C_{33}]$	Lowered ACL	Oil emissions

Sampling stations were grouped according to their HC content and alkane composition using tree-type clustering with the Euclidean distance as a measure. The Statistica 12 software package was used for statistical data processing.

Results and discussion

Results of the expedition to the coast of the Kerch Peninsula and Krasnodar Krai, December 2024 (after the accident)

Seawater. The content of HCs in water ranged from 0.029 to 0.103 $mg \cdot L^{-1}$ (Fig. 2), averaging 0.061 $mg \cdot L^{-1}$ along the coast. In 70% of samples, the maximum permissible concentration (MPC) (0.05 $mg \cdot L^{-1}$) was exceeded. At station *8*, where oil spills were recorded on the coast immediately prior to sampling, the HC content in water did not exceed the MPC and amounted to 0.048 $mg \cdot L^{-1}$. The proportion of n-alkanes in HCs was typical of seawater and ranged from 0.31 to 0.48, with an average of 0.37.

Isoalkane Pr was absent or found in low concentrations (around 10^{-4} $mg \cdot L^{-1}$), while Ph was found in concentrations of the order of 10^{-3} $mg \cdot L^{-1}$.

These indicators show no recent input of petroleum HCs [7].

The distribution of n-alkanes was generally bimodal (Fig. 3). The first maximum occurred at odd-numbered C_{17} and C_{19}, characterising the development of the phyto-community [8]. The second group of maxima was in the C_{24}–C_{32} range and included

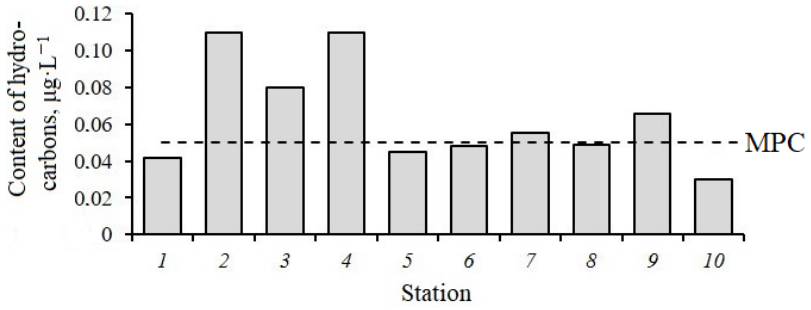

Fig. 2. Hydrocarbons content in the water off the coast of the Kerch Peninsula and Krasnodar Krai, December 2024 (after the accident)

both even-numbered compounds of bacterial origin [9] and odd-numbered allochthonous compounds [10]. This distribution of n-alkanes indicates active bacterial transformation processes and the input of organic matter from land, which is typical of coastal areas [7].

Of note, at certain stations in the Kerch water area (stations *2*, *3*, *9*) and the village of Taman (station *7*), the proportion of C_{17} was reduced. This can be attributed both to anthropogenic pollution, which inhibits the growth of green microalgae [11], and to the rapid biotransformation of this homologue [12]. The high content of the even-numbered homologue C_{30} at most of the mentioned stations [7] may indicate the activity of the microbial community.

To specify the sources of heavy metal input into the water of the studied area, so-called biogeochemical markers were calculated (Table 2).

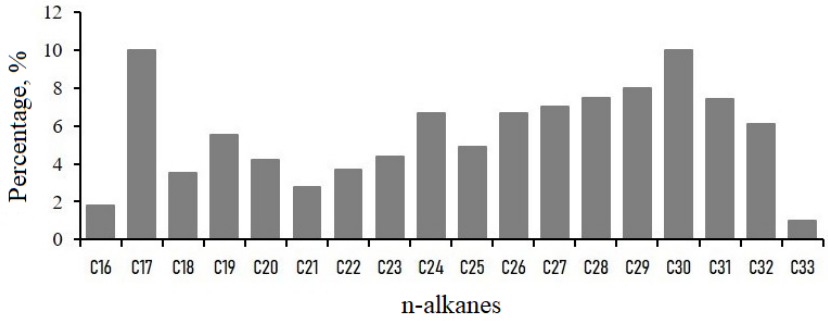

Fig. 3. Average distribution of n-alkanes in the water off the coast of the Kerch Peninsula and Krasnodar Krai, December 2024 (after the accident)

Table 2. Values of hydrocarbons genesis markers in the water off the coast of Kerch Peninsula and Krasnodar Krai, December 2024 (after the accident)

Station number	Marker					
	P_{aq}	TAR	ACL	LWH/HWH	$C_{17}+C_{19}+C_{21}$/ n-alkanes	CPI_2
1	0.4	1.3	28	0.6	0.2	1.3
2	0.5	1.4	28	0.4	0.2	0.7
3	0.1	3.0	30	0.3	0.1	1.1
4	0.4	6.1	28	0.1	0.1	0.4
5	0.5	0.4	27	0.9	0.4	0.9
6	0.4	1.6	28	0.3	0.2	0.9
7	0.5	1.0	28	0.3	0.2	0.6
8	0.4	1.3	28	0.4	0.2	0.8
9	0.2	4.8	29	0.1	0.1	1.1
10	0.3	1.0	28	0.4	0.3	1.1
Average	0.4	2.2	28	0.4	0.2	0.9

The main marker for diagnosing oil pollution, CPI_2, had values characteristic of the presence of petroleum products (≈ 1) at stations *3*, *5*, *6*, *8*, *9* and *10*. This may be due to chronic oil pollution of the Azov-Black Sea coast. However, the chromatographic pattern and the low content of isoprenoid alkanes indicate the predominance of a biogenic background. Even if oil pollution is present, which is typical of this area [11], it is not accident-induced but chronic in nature and is transformed.

Another sign of fresh petroleum product input may be an elevated LWH/HWH ratio (> 1). This ratio averaged 0.4 and did not reach unity at any of the stations, confirming the absence of fresh oil input. Stations *1* (0.6) and *5* (0.9) stood out with an elevated proportion of low-molecular-weight homologues. However, these values result from the high content of C_{17} and C_{19} and are therefore related to natural primary production processes [13]. The increased content of autochthonous compounds at stations *5* and *10* is further supported by the ratio of these compounds to the total n-alkanes in water.

The P_{aq} moisture index values corresponded to the presence of traces of both fresh and degraded aquatic vegetation, which is typical of coastal areas [14].

The average terrigenous/aquatic ratio (TAR) value was 2.2, indicating a predominance of terrigenous organic matter. At stations *5*, *7* and *10*, this indicator had

lower values, suggesting a low proportion of allochthonous matter. Given the composition of n-alkanes at these stations, such values are likely to be formed due to the high proportion of autochthonous compounds (C_{17}, C_{19}) in the composition of n-alkanes. Two of the three stations with reduced allochthonous substance content are located in the Sea of Azov, and one station is located in the Kerch Strait. The peculiarities of n-alkane distribution may be determined by the character of the production processes in the Sea of Azov.

Clustering stations based on the composition of alkanes in water allows stations *2–4* and *9* to be placed into a separate cluster. At these stations, the HC content exceeded the MPC for fishery water bodies. All stations are located in the water area adjacent to the Kerch Peninsula. This water area is under significant anthropogenic pressure [15] as a result of the city's activities and intensive shipping in the strait.

Thus, the HC content in the water of the studied water area exceeded the MPC due to the combined effect of natural and anthropogenic factors. The main sources of HCs were primary and bacterial production, as well as allochthonous matter. Oil pollution was present in a transformed form. This fact probably indicates a constant input of pollutants into the water area and a high rate of their biotransformation. A similar phenomenon was observed in the Kerch Strait before, when, despite permanent pollution of the water area, there were no signs of fresh oil pollution in the water due to its active biodegradation [16].

Suspended matter. The HC content in the suspended matter ranged from 31 to 495 μg·L^{-1} (Fig. 4), with an average of 121 μg·L^{-1}. These concentrations are considered high [16]. Elevated values relative to the average were recorded at stations *3*, *5* and *8*. Stations *3* and *5* are located in the Kerch Strait.

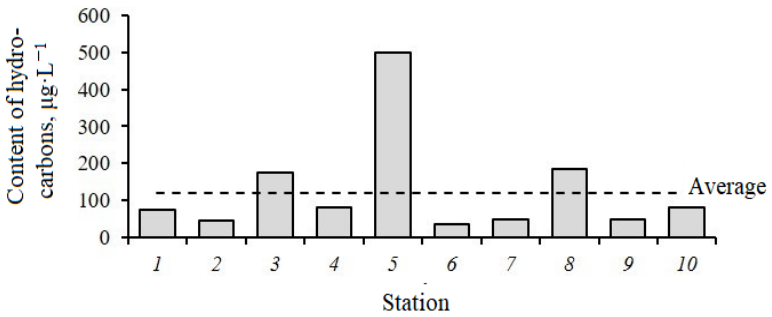

Fig. 4. Content of hydrocarbons in the suspended matter off the coast of the Kerch Peninsula and Krasnodar Krai, December 2024 (after the accident)

At station *8*, located near the village of Veselovka (Krasnodar Krai), petroleum products were spilled onto the coast during the sampling period, while the sea was stormy. This could have led to resuspension of coastal sediments and emulsification of the floating fuel oil.

The proportion of n-alkanes in the HC composition ranged from 0.22 to 0.42, with an average of 0.31. The average values were mildly elevated at stations *6*, *7* and *9*, which suggests an intense input of this class of compounds into the suspended matter.

Compounds C_{15}–C_{33} were recorded in the n-alkane composition in the suspension (Fig. 5), with a bimodal distribution of n-alkanes. The first maximum was dominated by C_{17} and C_{19} of phytoplankton origin [8]. The second maximum was in the C_{24}–C_{31} range, which included both bacterial even-numbered peaks and C_{25}, the presence of which is associated with the presence of aquatic macrophytes [17]. Allochthonous C_{27}, C_{29} and C_{31}, coming from the coast, stood out particularly in this group of peaks [7].

A quite high content of Pr and Ph was recorded comparable to that of individual n-alkanes, which suggests oil pollution [7].

The values of the P_{aq} marker (Table 3) indicate the presence of traces of aquatic macrophytes in the suspended matter [14].

The TAR marker averaged 3.2, which is due to the predominance of terrigenous organic matter. However, at station *1*, its value was less than unity, which is typical of the predominance of autochthonous compounds. This station also showed elevated P_{aq} (0.5), characterising the input of organic matter from macrophytes, and an increased proportion of autochthonous n-alkanes (0.3).

The average length of the hydrocarbon chain was quite high (30) and ranged from 29 to 31. This fact indicates an increased proportion of high-molecular-weight compounds and a small proportion of low-molecular-weight n-alkanes, which are indicators of fresh oil pollution [18].

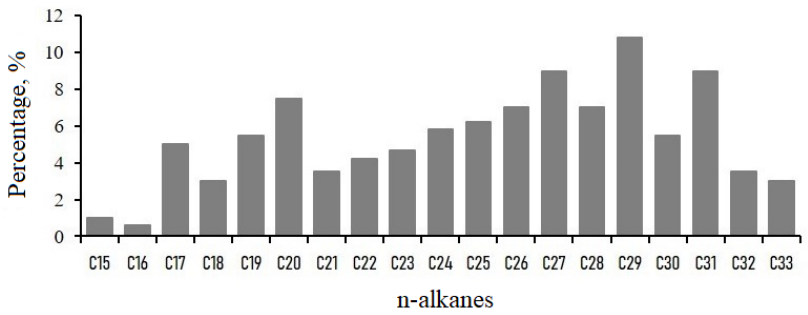

Fig. 5. Average distribution of n-alkanes in the suspended matter off the coast of the Kerch Peninsula and Krasnodar Krai, December 2024 (after the accident)

Table 3. Values of markers of hydrocarbons genesis in suspended matter off the coast of the Kerch Peninsula and Krasnodar Krai, December 2024 (after the accident)

Station number	Marker							
	P_{aq}	TAR	ACL	LWH/HWH	$C_{17}+C_{19}+C_{21}$/n-alkanes	CPI_2	Pr / Ph	K_i
1	0.5	0.7	30	0.7	0.3	1.4	0.3	1.1
2	0.4	1.9	31	0.3	0.2	1.2	0.3	1.3
3	0.4	3.2	29	0.4	0.1	1.5	0.2	1.9
4	0.3	4.2	29	0.3	0.1	1.5	0.2	2.0
5	0.2	4.7	30	0.2	0.1	1.1	0.1	1.5
6	0.2	4.5	30	0.2	0.1	1.9	0.3	1.1
7	0.4	3.9	31	0.2	0.1	1.4	0.1	0.8
8	0.3	2.2	30	0.6	0.2	1.8	0.1	1.8
9	0.4	4.0	31	0.2	0.1	1.3	–	–
10	0.4	2.4	30	0.3	0.2	1.6	0.2	1.6
Average	0.4	3.2	30	0.4	0.2	1.5	0.2	1.4

High-molecular-weight compounds prevailed at most stations. The exceptions were station *1* (LWH/HWH = 0.7) due to the high content of autochthonous C_{15}, C_{17} of phytoplankton origin [10] and C_{20} of bacterial origin [19], as well as station *8* (LWH/HWH = 0.6) due to the high content of C_{19} of phytoplankton origin [7] and C_{20} of bacterial origin. The proportion of compounds of phytoplankton origin at these stations was also elevated, amounting to 0.3 and 0.2, respectively, with an average value of 0.2. Consequently, signs of actively developing phytoplankton and bacterial communities were recorded in these areas.

The Pr/Ph ratio values indicate oil pollution in the suspended matter. The isoprenoid coefficient value (K_i = 0.8...2.0) aligns with the presence of moderately to highly degraded petroleum products.

The main marker of oil pollution, CPI_2, had values in the range of 1.1–1.9, which is typical of suspended matter. Slightly elevated values at stations *6* and *8* were associated with the high content of allochthonous n-alkanes in the composition of the suspended matter at these stations.

From the cluster analysis, the composition of alkanes at station *1* differed significantly from that at other stations, where the proportion of low-molecular-weight n-alkanes, starting with C_{15}, was increased. At the other stations, the hydrocarbon background was fairly uniform.

Seawater. The HC concentration in the water (Fig. 6) ranged from 0.012 to 0.097 mg·L^{-1}, with an average of 0.035 mg·L^{-1}. The MPCs were exceeded at two stations: *12* (1.3 times the MPC) and *16* (2 times the MPC). At the remaining sites, the sanitary standards for fishery waters were not exceeded.

There was no statistically significant difference in the HC content in the water at stations around which fuel oil was detected and at stations where it was not present.

The proportion of n-alkanes in the HCs ranged from 0.26 to 0.54, with an average of 0.41. An elevated value (0.54) was recorded at station *5*, indicating a recent input of n-alkanes in this area. A reduced value (0.26) was observed at station *16*, which most likely indicates active transformation of n-alkanes.

We identified n-alkanes ranging from C_{17} to C_{33}, with C_{17}–C_{31} compounds being present almost throughout the study area, while C_{32}–C_{33} compounds were found only in a few samples. The distribution of n-alkanes was bimodal (Fig. 7), with the first peak corresponding to C_{17}, an n-alkane of phytoplankton origin (its average proportion was 16%), and the second peak corresponding to C_{29} of allochthonous origin (16%). This distribution pattern indicates that natural pathways prevail in the HC input into the coastal waters.

At station *12*, where peaks were observed in the C_{29}–C_{32} range (11–21%), the distribution of n-alkanes in the high-molecular-weight fraction may correspond to the presence of transformed petroleum products, as well as to the active development of certain components of the microbial community. At the other stations, the distribution of n-alkanes corresponded to the average value for the study area.

The isoprenoid alkanes Pr (10^{-5} mg·L^{-1}) and Ph (10^{-3} mg·L^{-1}) were detected at low concentrations, which corresponds to their natural levels.

The P_{aq} marker values (Table 4) indicate the presence of traces of macrophytes; however, at station *12*, its reduced value can be attributed to a significant contribution from degraded terrestrial vegetation.

The TAR value generally indicates a slight predominance of terrigenous n-alkanes. At stations *5*, *6* and *9*, the TAR values were less than unity, which indicates

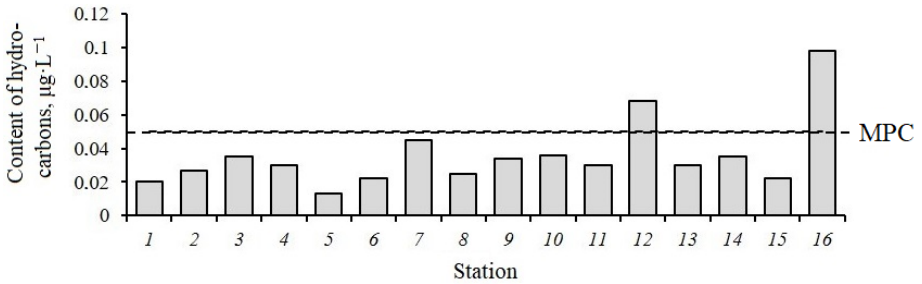

Fig. 6. Content of hydrocarbons in the water off the coast of the Kerch Peninsula and Krasnodar Krai, January 2025

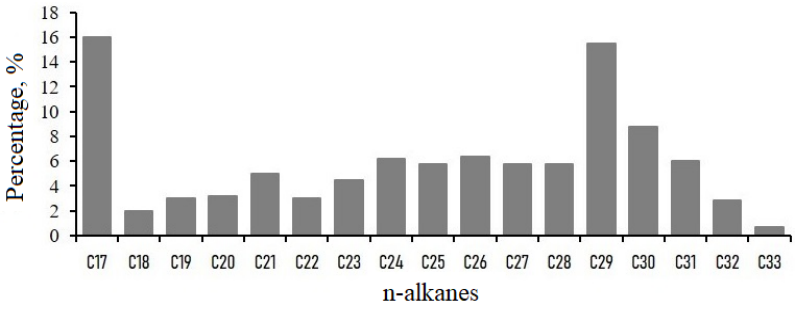

Fig. 7. Average distribution of n-alkanes in the water off the coast of the Kerch Peninsula and Krasnodar Krai, January 2025

Table 4. Values of markers of hydrocarbons genesis in the water off the coast of the Kerch Peninsula and Krasnodar Krai, January 2025

Station number	Marker					
	P_{aq}	TAR	ACL	LWH/HWH	$C_{17}+C_{19}+C_{21}$/ n-alkanes	CPI_2
1	0.4	1.1	28	0.5	0.2	1.1
2	0.2	1.7	29	0.3	0.2	0.8
3	0.2	1.6	29	0.3	0.2	0.9
4	0.3	1.5	28	0.4	0.2	1.4
5	0.3	0.8	28	0.8	0.4	1.6
6	0.7	0.3	27	0.6	0.4	0.5
7	0.3	1.4	28	0.3	0.2	1.2
8	0.4	1.6	28	0.5	0.3	1.5
9	0.4	0.9	28	0.7	0.4	1.8
10	0.3	1.8	28	0.4	0.2	1.7
11	0.3	1.6	28	0.6	0.3	2.6
12	0.1	5.5	30	0.1	0.1	1.3
13	0.3	3.5	29	0.2	0.1	1.7
14	0.4	1.5	28	0.4	0.2	1.4
15	0.3	1.9	28	0.3	0.2	2.0
16	0.4	2.3	28	0.3	0.1	1.0
Average	0.3	1.8	28	0.4	0.2	1.4

a high proportion of autochthonous components. At station *12*, the TAR was at its highest (5.5) and indicated a significant contribution from allochthonous matter.

The average HC chain length (ACL) was 28, ranging from 27 to 30. In December, this figure was higher, at 30. A decrease in ACL may be due to the entry of petroleum products into the water.

The average LWH/HWH ratio was 0.4 (0.1–0.7). Lower values of this parameter, characteristic of terrigenous matter predominance, were recorded at station *12* (0.1) and station *13* (0.2). Overall, this parameter was rather high, indicating an elevated content of low-molecular-weight n-alkanes.

The proportion of autochthonous n-alkanes was low (0.2 on average), which is consistent with the data obtained in December 2024.

The CPI_2 averaged 1.4, ranging from 0.5 to 2.6. Most of the values were consistent with the biogenic nature of the HCs. At stations *1* (1.1), *3* (0.9) and *16* (1.0), the values of the carbon preference index were characteristic of oil pollution. However, the distribution pattern of n-alkanes indicates that the HCs were mainly of biogenic origin.

Thus, the composition of alkanes suggests the HC sources are predominantly natural, consisting largely of autochthonous and allochthonous materials. Clustering of stations based on the alkane composition did not reveal any distinct groupings, indicating a fairly homogeneous alkane composition in the study area.

Suspended matter. The HC concentration in the suspended matter of the study area ranged from 13 to 67 $\mu g \cdot L^{-1}$, with an average of 34 $\mu g \cdot L^{-1}$ (Fig. 8). A decrease in the average compared to December values was noted, which is associated with the absence of a sharp exceedance of the average (by 5–10 times) at some stations, as observed in December 2024. Overall, this HC concentration in the suspended matter can be seen as high [16]. There were no statistically significant differences in the HC concentrations in the suspended matter between the areas where petroleum product wash up was recorded in the coastal zone and those with no wash up.

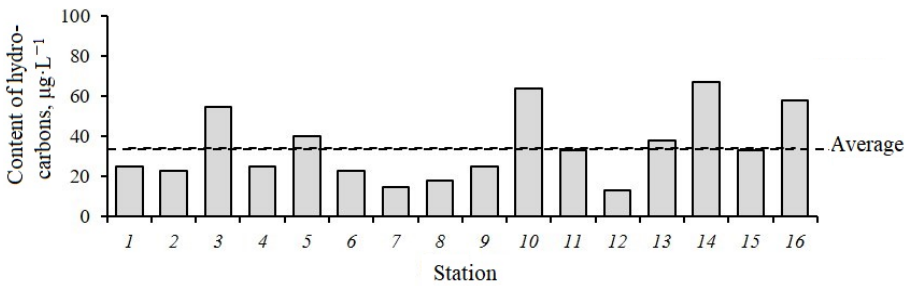

Fig. 8. Content of hydrocarbons in the suspended matter off the coast of the Kerch Peninsula and Krasnodar Krai, January 2025

The proportion of n-alkanes in the HCs ranged from 0.25 to 0.57, with an average of 0.44. At certain stations, this figure was slightly higher. These figures indicate a fresh input of n-alkanes.

The identified n-alkanes included homologues ranging from C_{16} to C_{33}. Namely, C_{16} and C_{33} were recorded at certain stations (stations *14–16*), while C_{17}–C_{32} were present at the others. The insignificant proportion of phytoplankton-derived C_{17} (on average 5%) (Fig. 9) indicates a low contribution of phytoplankton to the formation of HCs of the suspended matter. The maxima were located in the high-molecular-weight region of the n-alkane spectrum. The major peaks (> 10%) were the allochthonous C_{27} and C_{29} [7] and the bacteria-derived C_{26} [17].

At the same time, a relatively high concentration of isoprenoid alkanes Pr and Ph was recorded, which may indicate oil pollution. The distribution pattern of n-alkanes and the high concentration of Pr and Ph may indicate the presence of transformed oil pollution in the suspended matter. Consequently, due to self-purification, the coastal ecosystem copes with the input of petroleum products. A similar phenomenon has been described for this area previously [16].

Compared with the December data, the proportion of phytoplankton-derived n-alkanes in the suspension decreased, suggesting a reduction in phytoplankton production, which is the main source of low-molecular-weight odd-numbered n-alkanes. This decline in production could have occurred both as part of the annual dynamics of phytoplankton development [20] and as a result of the inhibitory effect of oil on its growth [21]. Another reason for the decrease in the proportion of phytoplankton-derived peaks may be the intensive transformation of the corresponding homologues by the micro-community, the activity of which is evidenced by the high proportions of C_{24}, C_{26} and C_{28} homologues [7].

The P_{aq} moisture index ranged from 0.5 to 0.8, with an average of 0.7 (Table 5). These relatively high values indicate the presence of traces of transformed macrophytes at all sampling stations. These values align with the high C_{25} content, which is associated with macrophytes, and also indicate the active development

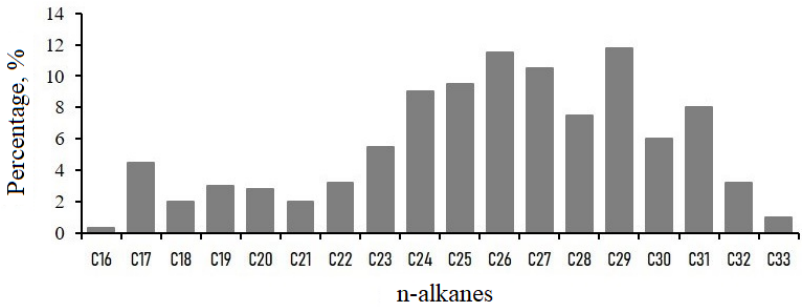

Fig. 9. Average distribution of n-alkanes in the suspended matter off the coast of the Kerch Peninsula and Krasnodar Krai, January 2025

Table 5. Values of markers of hydrocarbons genesis in the suspended matter off the coast of the Kerch Peninsula and Krasnodar Krai, in January 2025

Station number	Marker							
	P_{aq}	TAR	ACL	LWH/HWH	$C_{17}+C_{19}+C_{21}$/n-alkanes	CPI_2	Pr / Ph	K_i
1	0.5	2.9	28	0.2	0.1	0.4	0.7	1.0
2	0.5	5.0	28	0.2	0.1	0.7	2.1	0.6
3	0.7	4.9	27	0.2	0.1	0.7	0.6	0.8
4	0.7	5.2	27	0.2	0.1	0.8	0.2	0.8
5	0.7	4.2	27	0.3	0.1	0.9	1.6	0.3
6	0.7	1.5	27	0.5	0.1	0.7	0.5	1.0
7	0.6	8.8	27	0.2	0.1	0.8	0.1	1.3
8	0.8	3.6	27	0.3	0.1	0.8	0.2	0.6
9	0.7	8.5	27	0.2	0	0.8	0.1	1.8
10	0.6	6.0	27	0.2	0.1	0.9	0.4	1.6
11	0.8	7.6	27	0.1	0	0.9	0.3	1.2
12	0.7	10.4	27	0.2	0	0.9	0.1	1.1
13	0.8	8.7	26	0.1	0	1.2	0.4	1.1
14	0.8	10.5	26	0.1	0	1	0.2	1.3
15	0.5	3.0	28	0.4	0.1	0.7	2.3	1.9
16	0.7	2.8	27	0.1	0.1	0.8	1.6	0.4
Average	0.7	5.8	27	0.2	0.1	0.8	0.7	1.1

of the bacterial community (C_{24}, C_{26}, C_{28}) [7], which contributes to the transformation of organic matter.

The TAR marker ranged from 1.5 to 10.5, with an average of 5.8, indicating a moderate to strong predominance of terrigenous material in the suspension. The hydrocarbon chain length ranged from 26 to 28, with an average of 27. Lower values (26) were recorded at stations *13* and *14*, located in the area where petroleum products were massively washing ashore. This may indicate the presence of petroleum products in the suspended matter.

Overall, the mixture was dominated by high-molecular-weight n-alkanes (LWH/HWH = 0.1–0.5). The proportion of phytoplankton-derived homologues was low and did not exceed 0.1.

The CPI_2 marker of petroleum origin in the suspended matter had low values ranging from 0.4 to 1.2 (average 0.8). For suspended matter, these are somewhat low figures. At most stations, except for station *1*, these values may indicate oil pollution.

The marked predominance of Pr over Ph at stations *4*, *7–9*, *11*, *12* and *14* may indicate oil pollution. The isoprenoid coefficient ranged from 0.3 to 1.9 (mean 1.1). Such indicators characterise the presence of oil at various stages of degradation (from slightly degraded to degraded). The average values show that, overall, the oil was at an intermediate stage of degradation. At station *5*, the isoprenoid ratio corresponded to the presence of fresh oil. At this same station, a predominance of Pr over Ph was noted, which is characteristic of the presence of terrigenous organic matter. At stations *2–4*, *8* and *16*, the marker value corresponded to the presence of degraded petroleum products. Most of these stations are located on the coast of the Kerch Strait. Chronic oil pollution in this area has been noted previously [11, 16].

Thus, the markers indicate a predominance of allochthonous compounds in the suspended matter, as well as probable oil pollution. In January, the oil pollution in the suspended matter had degraded to a lesser extent than in December 2024, which may indicate a more active influx of oil.

The cluster analysis revealed a fairly compact grouping of stations, with only station *15* standing out, where a reduced proportion of C_{24}–C_{28} homologues (which are predominantly of bacterial origin) was observed. Thus, the composition of the suspended matter at the stations where wash up was recorded and at the stations with no wash up differed only slightly. This means that the location of the probable source of oil pollution in the suspended matter is not related to fuel oil wash up onto the coast.

In January 2025, the proportion of n-alkanes in the HC composition increased, although the total HC concentration in the suspended matter remained at the December 2024 level. The composition of n-alkanes also changed: the proportion of autochthonous compounds decreased, while the distribution and composition of the alkanes indicate probable oil pollution. The analysis of HC origin markers supports this conclusion.

Conclusion

With the exception of station *8*, the samples collected in December 2024 were taken from water areas that had not yet been affected by pollution resulting from the emergency petroleum product spill. This allowed us to obtain data on the baseline condition of the study area prior to its pollution by fuel oil.

In December 2024, the HC concentration in the waters around the Kerch Peninsula and Krasnodar Krai exceeded the MPC (0.05 $mg \cdot L^{-1}$) in 70% of samples. The main sources of HCs in the water were primary and bacterial production, as well as allochthonous matter. Oil pollution was present in a transformed form. Given the composition of n-alkanes and marker values, the main sources of HC formation in the suspended matter of the studied water area in December 2024 were phytoplankton and bacterial production, as well as the input of allochthonous compounds. Signs of degraded oil pollution were noted, indicating chronic oil pollution of the water body. Thus, the studied coastal site was under chronic oil pollution, which was more pronounced in the composition of suspended matter than in the water.

In January 2025, petroleum products were massively entering into the coastal zone. Based on average concentrations that did not exceed the MPC, it can be concluded that the coastal waters of the Kerch Peninsula and Krasnodar Krai were not polluted with HCs. The HC composition in the studied water area was determined primarily by natural factors: autochthonous production, the input of allochthonous compounds and the bacterial degradation of organic matter. Consequently, fuel oil spills at the time of the study (January 2025) did not have a negative impact on the degree of HC pollution of the water. In January 2025, the HC composition in the suspended matter changed, whereas the HC concentration remained comparable to that of December 2024: the proportion of n-alkanes increased and the proportion of autochthonous compounds decreased. The distribution and composition of alkanes indicate oil pollution, and the analysis of HC origin markers supports this conclusion.

As the fuel oil spill has affected certain components of the coastal ecosystem, further studies are needed in this area to assess the long-term impact of HCs on the aquatic ecosystem.

References

1. Ivanov, A.Yu., Kucheiko, A.A., Filimonova, N.A., Kucheiko, A.Yu., Evtushenko, N.V., Terleeva, N.V. and Uskova, A.A., 2017. Spatial and Temporal Distribution of Oil Spills in the Black Sea and the Caspian Sea Based on SAR Images: Comparative Analysis. *Issledovanie Zemli iz Kosmosa*, (2), pp. 13–25 (in Russian).
2. Tikhonova, E.A., Burdiyan, N.V., Soloveva, O.V. and Doroshenko, Ju.V., 2015. Chemical and Microbiological Parameters of the Kerch Strait Sea Bottom Sediments after the Accident of "Volgoneft-139" Ship. *Environmental Protection in Oil and Gas Complex*, (4), pp. 12–16 (in Russian).
3. Korpakova, I.G. and Agapov, S.A., eds., 2008. *The Oil Spill Accident in the Kerch Strait: Its Effects on the Water Ecosystems*. Rostov-na-Donu: FSUE AZNIIRKH, 229 p.
4. Matishov, G.G., Berdnikov, S.V. and Savitsky, R.M., 2008. [*Ecosystem Monitoring and Assessment of the Impact of Oil Spills in the Kerch Strait. Ship Accidents in November 2007*]. Rostov-on-Don: Yuzhny Nauchny Zentr RAN, 80 p. (in Russian).
5. Kuznetsov, A.N., Fedorov, Yu.A. and Zagranitchny, K.A., 2011. About the Results of Three-Year Monitoring of a Fuel Oil Spill in the Kerch Strait. *Bulletin of Higher Educational Institutions. North Caucasus Region. Natural Sciences*, (4), pp. 90–95 (in Russian).
6. Mironov, O.G. and Alyomov, S.V., eds., 2018. *Sanitary and Biological Studies of the South-Western Crimea Coastal Waters at the Beginning of XXI Century*. Simferopol: ARIAL, 276 p. https://doi.org/10.21072/978-5-907118-89-8 (in Russian).
7. Nemirovskaya, I.A., 2013. *Oil in the Ocean (Pollution and Natural Flow)*. Moscow: Nauchny Mir, 432 p. (in Russian).
8. Tashlikova, N.A., Kuklin, A.P. and Bazarova, B.B., 2009. Primary Production of Phytoplancton, Epiphytic Seaweed and the Higher Water Plants in the Channels of the Selenga River Delta. *Bulletin of KSAU*, (9), pp. 106–112 (in Russian).

9. Bieger, T., Abrajano, T.A. and Hellou, J., 1997. Generation of Biogenic Hydrocarbons During a Spring Bloom in Newfoundland Coastal (NW Atlantic) Waters. *Organic Geochemistry*, 26(3–4), pp. 207–218. https://doi.org/10.1016/S0146-6380(96)00159-3
10. Nemirovskaya, I.A., 2021. Distribution and Origin of Hydrocarbons on a Transarctic Transect. *Oceanology*, 61(2), pp. 183–192. https://doi.org/10.1134/S0001437021020144
11. Tikhonova, E.A., Burdiyan, N.V. and Soloveva, O.V., 2017. The Chemical-Microbiological Characteristics of Sea Water and Bottom Sediments of the Kerch Strait and Adjacent Water Areas. *Marine Biological Journal*, 2(3), pp. 75–85. https://doi.org/10.21072/mbj.2017.02.3.07 (in Russian).
12. Yáñez-Arancibia, A. and Day, J., 1982. Ecological Characterization of Terminos Lagoon. A Tropical Lagoon-Estuarine System in the Southern Gulf of Mexico. *Oceanologica Acta*, 5(4), pp. 431–440.
13. Wang, X.-C., Sun, S., Ma, H.-Q. and Liu, Y., 2005. Sources and Distribution of Aliphatic and Polyaromatic Hydrocarbons in Sediments of Jiaozhou Bay. Qingdao. China. *Marine Pollution Bulletin*, 52(2), pp. 129–138. https://doi.org/10.1016/j.marpolbul.2005.08.010
14. Ficken, K.J., Li, B., Swain, D.L. and Eglniton, G., 2000. An N-Alkane Proxy for the Sedimentary Input of Submerged / Floating Freshwater Aquatic Macrophytes. *Organic Geochemistry*, 31(7–8), pp. 745–749. https://doi.org/10.1016/S0146-6380(00)00081-4
15. Sapozhnikov, V.V., Arzhanova, N.V., Lapina, N.M., Agatova, A.I., Torgunova, N.I., Zozulya, N.M., Bondarenko, L.G., Vishnevsky, S.L., Radchenko, S.V. et al., 2013. Complex Ecological Studies in Kerch Strait and Taman' Bight after Oil Spill (2007–2010). *Trudy VNIRO*, 150, pp. 65–77 (in Russian).
16. Nemirovskaya, I.A., Khaustov, A.P. and Redina, M.M., 2022. Distribution and Genesis of Hydrocarbons in Water and Sediments of the Kerch Strait. *Geochemistry International*, 60(1), pp. 43–51. https://doi.org/10.1134/S0016702922010098
17. Mead, R., Xu, Yu., Chong, J. and Jaffé, R., 2005. Sediment and Soil Organic Matter Source Assessment as Revealed by the Molecular Distribution and Carbon Isotopic Composition of N-Alkanes. *Organic Geochemistry*, 36(3), pp. 363–370. https://doi.org/10.1016/j.orggeochem.2004.10.003
18. Simoneit, B.R.T., Pisani, O., Ekpo, B.O., Fubara, E.P., Nna, P.J. and Ekpa, O.D., 2017. Lipid Biomarker Analysis of Suspended Particulate Matter from the Great Kwa River, SE Nigeria: Origins and Environmental Implications of Biogenic and Anthropogenic Organic Compounds. *Aquatic Geochemistry*, 23(2), pp. 89–108. http://doi.org/10.1007/s10498-017-9311-0
19. Yunker, M.B., Macdonald, R.W., Ross, P.S., Johannessen, S.C. and Dangerfield, N., 2015. Alkane and PAH Provenance and Potential Bioavailability in Coastal Marine Sediments Subject to a Gradient of Anthropogenic Sources in British Columbia, Canada. *Organic Geochemistry*, 89–90, pp. 80–116. https://doi.org/10.1016/j.orggeochem.2015.10.002
20. Yasakova, O.N. and Makarevich, P.R., 2023. *Current State of Phytoplankton in the North-Eastern Black Sea*. Rostov-on-Don: SSC RAS, 232 p. (in Russian).
21. Kustenko, N.G. and Imnadze, N.O., 1988. The Effect of Oil and Nitrogen on Phytoplankton in the Eastern Coast of the Black Sea. *Ecology of the Sea*, 29, pp. 73–77 (in Russian).

Submitted 19.09.2025; accepted after review 06.10.2025;
revised 18.12.2025; published 31.03.2026

About the authors:

Elena A. Tikhonova, Leading Researcher, A. O. Kovalevsky Institute of Biology of the Southern Seas of RAS (2 Nakhimov Ave., Sevastopol, 299011, Russia), PhD (Biol.), **ORCID ID: 0000-0002-9137-087X, Scopus Author ID: 57208495804, ResearcherID: X-8524-2019**, *tikhonova_ea@ibss-ras.ru*

Olga V. Soloveva, Leading Researcher, A. O. Kovalevsky Institute of Biology of the Southern Seas of RAS (2 Nakhimov Ave., Sevastopol, 299011, Russia), PhD (Biol.), **ORCID ID: 0000-0002-1283-4593, Scopus Author ID: 57208499211, ResearcherID: X-4793-2019**, *soloviova@ibss-ras.ru*

Sergey V. Alyomov, Leading Researcher, A. O. Kovalevsky Institute of Biology of the Southern Seas of RAS (2 Nakhimov Ave., Sevastopol, 299011, Russia), PhD (Biol.), **ORCID ID: 0000-0002-3374-0027, Scopus Author ID: 24070027300,** *numa_63@mail.ru*

Oleg A. Mironov, Senior Researcher, A. O. Kovalevsky Institute of Biology of the Southern Seas of RAS (2 Nakhimov Ave., Sevastopol, 299011, Russia), PhD (Biol.), **Scopus Author ID: 56227568700**, **ResearcherID: ABH-9273-2020**, *mironov_oa@ibss-ras.ru*

Yulia S. Klycheva (Tkachenko), Junior Researcher, A. O. Kovalevsky Institute of Biology of the Southern Seas of RAS (2 Nakhimov Ave., Sevastopol, 299011, Russia), **ORCID ID: 0009-0001-1752-1043, Scopus Author ID: 1220495**, *tkachenko_90@ibss-ras.ru*

Georgy V. Frolkin, Junior Researcher, Research Center for Freshwater and Saltwater Hydrobiology, Branch of IBSS, (2 Nakhimov Ave, Sevastopol, 299011, Russia), **ORCID ID: 0009-0002-2260-5230**, **ResearcherID: NIU-5117-2025**, *frean1k@yandex.ru*

Contribution of the authors:

Elena A. Tikhonova – statement of the objectives and tasks of a comprehensive study, manuscript writing

Olga V. Soloveva – participation in fieldwork, analysis of the results obtained regarding the hydrocarbon composition of the ecosystem components under study, calculation of diagnostic indices, discussion of the results, article writing

Sergey V. Alyomov – sampling, involvement in sample preparation, article revision

Oleg A. Mironov – water sampling, water filtration to obtain suspended matter

Yulia S. Klycheva (Tkachenko) – preparation of water samples for the qualitative and quantitative analysis of hydrocarbons, article writing and formatting

Georgy V. Frolkin – water sampling, preparation of samples

All the authors have read and approved the final manuscript.

Original paper

The Influence of Temperature on the Formation of Caspian Sprat Aggregations During Hydroacoustic Surveys in the Central Caspian Sea in Summer

T. V. Pomogaeva

A. O. Kovalevsky Institute of Biology of the Southern Seas of RAS, Sevastopol, Russia
e-mail: pomogtatyana@mail.ru

Abstract
The paper aims to identify distribution patterns of Caspian sprats (the main commercial fish in the Caspian Sea) in the epipelagic zone of the Central Caspian Sea in summer and to assess the relationship between the fish aggregation density and the temperature gradient, based on hydroacoustic and hydrological data for 2014–2021. Hydroacoustic surveying was carried out in the deep sea (depth up to 800 m) using a Simrad EK-60 hydroacoustic complex installed on R/V *Caspian Explorer* with stationary split-beam antennas operating at frequencies of 38 and 120 kHz. Biomass was calculated for standard 10-metre layers from 0 to 50 m. The water temperature was measured at depths of 10, 20, 25, 30 and 50 m. The vertical temperature gradient was calculated for the 20–30 m layer. The relationship between the aggregation density and the gradient was assessed using linear regression analysis. It was found that in summer, the bulk of Caspian sprats, migrating for feeding, concentrates in the middle part of the Caspian Sea, in the upper 50-metre layer. From the results of the 2021 summer hydroacoustic survey, a map of the sprat distribution in the middle part of the Caspian Sea was constructed. The maximum concentrations of sprats were observed in the 20–30 m layer. A significant linear relationship ($R^2 = 0.802$) was found between the density of sprat aggregations (over 30 t/mile^2) and the vertical temperature gradient ($R^2 = 0.802$) in this layer. It was shown that dense commercial aggregations form at a gradient of no less than 0.3 °C/m and a temperature above 9.0°C at a depth of 30 m. The results can be used to estimate the location of commercial sprat aggregations in the deep-water part of the Central Caspian Sea in summer.

Keywords: Caspian Sea, Central Caspian, Caspian sprat, *Clupeonella*, hydroacoustic studies, hydroacoustic survey, sounding graph, temperature gradient, water temperature, commercial aggregations

Acknowledgements: The work was carried out as part of the state assignment of A.O. Kovalevsky Institute of Biology of the Southern Seas of RAS on the topic “Study of the biogeochemical patterns of radioecological and chemoecological processes in the ecosystems of the Azov-Black Sea basin water bodies in comparison with other water areas of the World Ocean and individual aquatic ecosystems of their catchment basins to ensure sustainable development in the southern seas of Russia” (no. 124030100127-7). The author is grateful to the management and staff of the Volga-Caspian Branch of the Russian State

© Pomogaeva T. V., 2026

This work is licensed under a Creative Commons Attribution-Non Commercial 4.0 International (CC BY-NC 4.0) License

Research Center of Fisheries and Oceanography (VNIRO) for the material collected during the survey on R/V *Caspian Explorer* in accordance with clause 78 of the R&D programme using the sea vessels of the Volga-Caspian Branch of the Russian State Research Center of Fisheries and Oceanography (VNIRO) for 2021. “Assessment of the status of sturgeon, mullet and other fish and crayfish stocks in the summer period based on the results of trawl-acoustic and net surveys. Assessment of the ecological conditions of the habitat of water bioresources. Research on the hydrological, hydrochemical, ecological and toxicological characteristics of the habitat and water bioresources, the state of the food base and the abundance of commercial fish species in the Caspian Sea. Assessment of the *Mnemiopsis* population status”.

For citation: Pomogaeva, T.V., 2026. The Influence of Temperature on the Formation of Caspian Sprat Aggregations During Hydroacoustic Surveys in the Central Caspian Sea in Summer. *Ecological Safety of Coastal and Shelf Zones of Sea*, (1), pp. 73–84.

Влияние температурного фактора на образование скоплений каспийских килек при проведении гидроакустических исследований в Среднем Каспии в летний период

Т. В. Помогаева

ФГБУН ФИЦ «Институт биологии южных морей имени А.О. Ковалевского РАН», Севастополь, Россия

e-mail: pomogtatyana@mail.ru

Аннотация

Цель работы – на основе гидроакустических и гидрологических данных за 2014–2021 гг. выявить особенности распределения каспийских килек (основных промысловых рыб в Каспийском море) в эпипелагиали Среднего Каспия в летний период и оценить связь плотности их скопления с температурным градиентом. Гидроакустическую съемку производили в глубоководной части моря (глубина до 800 м) установленным на НИС «Исследователь Каспия» гидроакустическим комплексом *Simrad EK*-60, оборудованным стационарно установленными антеннами с расщепленным лучом на частоте 38 и 120 кГц. Расчет биомассы выполнен для стандартных 10-метровых слоев от 0 до 50 м. Температуру воды измеряли на горизонтах 10, 20, 25, 30 и 50 м. Вертикальный температурный градиент рассчитывали для слоя 20–30 м. Связь между плотностью скоплений и градиентом оценивали методом линейного регрессионного анализа. Установлено, что в летний период основная масса каспийских килек, совершая нагульные миграции, концентрируется в средней части Каспийского моря в верхнем 50-метровом слое. По результатам летней гидроакустической съемки 2021 г. построена карта распределения килек в средней части Каспийского моря. Максимальные концентрации килек были отмечены в слое 20–30 м. Выявлена значимая линейная зависимость ($R^2 = 0.802$) между плотностью скоплений кильки (свыше 30 т/миля^2) и вертикальным температурным градиентом ($R^2 = 0.802$) в этом слое. Показано, что плотные промысловые скопления формируются при градиенте не ниже 0.3 °С/м и температуре на горизонте 30 м выше 9.0 °С. Результаты могут быть использованы для прогнозирования локализации промысловых скоплений кильки в глубоководной части Среднего Каспия в летний период.

Ключевые слова: Каспийское море, Средний Каспий, каспийские кильки, *Clupeonella*, гидроакустические исследования, гидроакустическая съемка, эхограмма, температурный градиент, температура воды, промысловые скопления

Благодарности: работа выполнена в рамках государственного задания ФИЦ ИнБЮМ по теме «Изучение биогеохимических закономерностей радиоэкологических и хемоэкологических процессов в экосистемах водоемов Азово-Черноморского бассейна в сравнении с другими акваториями Мирового океана и отдельными водными экосистемами их водосборных бассейнов для обеспечения устойчивого развития на южных морях России» (№ 124030100127-7). Автор выражает благодарность руководству и коллективу ВКФ ФГБНУ «ВНИРО» («КаспНИРХ») за материал, собранный в ходе съемки на НИС «Исследователь Каспия» согласно п. 78 программы НИР с использованием морских судов ВКФ ФГБНУ «ВНИРО» («КаспНИРХ») на 2021 г. «Оценка состояния запасов осетровых, кефали и других видов рыб, раков в летний период по результатам тралово-акустической и сетной съемок. Оценка экологических условий среды обитания ВБР. Исследования гидролого-гидрохимических, эколого-токсикологических характеристик среды обитания и ВБР, состояния кормовой базы и численности промысловых видов рыб Каспийского моря. Оценка состояния популяции мнемиопсиса».

Для цитирования: *Помогаева Т. В.* Влияние температурного фактора на образование скоплений каспийских килек при проведении гидроакустических исследований в Среднем Каспии в летний период // Экологическая безопасность прибрежной и шельфовой зон моря. 2026. № 1. С. 73–84. EDN FZNAUP.

Introduction

Hydroacoustic surveys to assess sprat stocks have been conducted in the Caspian Sea since the 1970s. Scientific hydroacoustic research in the Caspian Sea has enabled fishing companies to obtain recommendations and start fishing for Caspian sprats off the coast of Dagestan. Trawl fishing for Caspian sprats off the Dagestan coast, which began in 2019, is efficient only during the autumn-winter and spring periods, before spawning temperatures rise in the area and the wintering sprat aggregations disperse [1), 2)].

Hydroacoustic surveys of Caspian sprats conducted between 2014 and 2021 showed that the majority of sprats, undertaking feeding migrations from the Dagestan shelf to the deep-water part of the Central Caspian Sea, are concentrated in the central part of the Caspian Sea above depths of 100 to 700 m during the summer period (June to early September). In September–October, the return migration to the coast begins, where the fish stay until March–April.

Each year, the total recommended catch for the three species of Caspian sprats (common sprats, anchovy sprats and big-eyed sprats) is determined on the basis of annual surveys conducted by the Volga-Caspian Branch of the Federal State Budget Scientific Institution “Russian Federal Research Institute of Fisheries and Oceanography” in the Caspian Sea, and is set at 100,000 t [1, 2]. The current commercial

---

[1)] Available at: https://casp-geo.ru/astrahanskij-kaspnirh-opublikoval-obzor-kilechnogo-promysla/ [Accessed: 25 February 2025] (in Russian).

[2)] Available at: http://kaspnirh.vniro.ru/news/2024-12-25/2683/ [Accessed: 25 February 2025] (in Russian).

exploitation rate of the recommended catch is around 30%. The reasons for this low level of exploitation remain poorly understood.

Studies on sprat biomass in the deep-water section of the Central Caspian Sea will help resolve the issue of achieving the recommended catch for Caspian sprats.

The study aims to identify, using the data obtained during the summer months of 2014–2021, the influence of temperature and temperature gradients on the formation of dense aggregations of sprats.

Materials and methods

The hydroacoustic surveys were conducted in accordance with standard procedures [3)] [3]. All research work was carried out on R/V *Caspian Explorer* using a Simrad EK-60 dual-frequency scientific echo sounder with permanently mounted four-section antennas operating at 38 and 120 kHz, and a GPS navigation system.

When working with the Simrad EK-60 hydroacoustic system, the Simrad ER-60 and Simrad BI-60 software packages (version 2.1.1) were used. The Simrad BI-60 post-processing software allows for the assessment of fish aggregations by layer, taking into account the species composition and size groups, as well as NASC and Ts (target strength of sprats) and reference catch data. Using the Simrad BI-60, the density of fish aggregations was calculated for predefined 10-metre layers.

Between 2014 and 2021, 13 expeditions were carried out, each lasting on average 25 days. The surveys took place from early June to mid-September. While conducting hydrological studies in the deep-water area of the Central Caspian Sea, the water temperature at the surface and at depths of 10, 20, 25, 30 and 50 metres at each station was measured using an SBE-19 profiler.

Results and discussion

According to the results of hydroacoustic surveys conducted in the Central Caspian Sea during the summer months of 2014–2021, dense commercial aggregations of Caspian sprats [4)] were predominantly found in the upper 50-metre layer of the sea [4–8].

According to data from test trawls carried out in July 2015, which supported the hydroacoustic survey results, the following average size and weight characteristics were obtained: the average length and weight of common sprats were 9.9 cm and 9.5 g, respectively, and those of anchovy sprats were 11.4 cm and 13.2 g, respectively. Common sprats predominated in the catches (82%), whereas the proportion of anchovy sprats was 18%.

One of the main factors influencing the size and reproduction of Caspian sprat populations is water temperature [9, 10]. The formation of dense aggregations of sprat is also influenced by the vertical temperature gradient.

In all surveys conducted between 2014 and 2021, the vertical temperature gradient was calculated for each station (the number of stations varied between 23 and 43 over the years) as the difference between the temperatures at the 10-metre and

---

[3)] Ermolchev, V.A. and Sedov, S.I., 1990. [*Guidelines for Conducting Hydroacoustic Surveys of Sprat Stocks in the Caspian Sea*]. Murmansk: PINRO, 92 p. (in Russian).

[4)] Pomogaeva, T.V., 2024. [*Improving and Organising the Caspian Sprat Fishery in the Central Caspian Sea. PhD Thesis*]. Astrakhan: AGTU, 159 p. (in Russian).

25-metre depths. The minimum and maximum gradients for each survey were considered, as well as the difference between the values. At the 25-metre depth, the minimum and maximum temperature values were determined, as well as the difference between them.

The formation of dense aggregations of sprats was revealed to depend on the vertical temperature gradient in the 10–25 m layer and the temperature range at the 25-metre depth [4)].

Since 2019, after visual identification of the layer with dense sprat aggregations, temperature has been measured at depths of 20 and 30 m.

According to the 2017 survey data, the biological productivity of sprats was significantly higher than in previous and subsequent years. During that period, high vertical and horizontal temperature gradients were observed: at a depth of 10 m, the difference between the minimum (10.3°C) and maximum (27.9°C) temperatures was 17.6°C at stations located approximately 30 nmi apart; at a depth of 25 m, the corresponding difference was 13.4°C (from 8.8 to 22.2°C) over a distance of about 40 nmi. The thermocline contributed to the formation of very dense sprat aggregations in 2017, which is clearly visible in the echo sounder profile as of 29 July 2017 (42°21′ N, 48°38′ E) in the 15–35 m layer: a very high concentration of sprats was recorded at the 20-metre depth (Fig. 1).

In 2021, the survey took place from 11 August to 13 September. Water temperatures during that period were typical for summer: at a depth of 10 m, the values ranged from 14.4 to 28.6°C (average 26.6°C), and at a depth of 25 m, they ranged from 8.9 to 25.3°C (average 14.1°C).

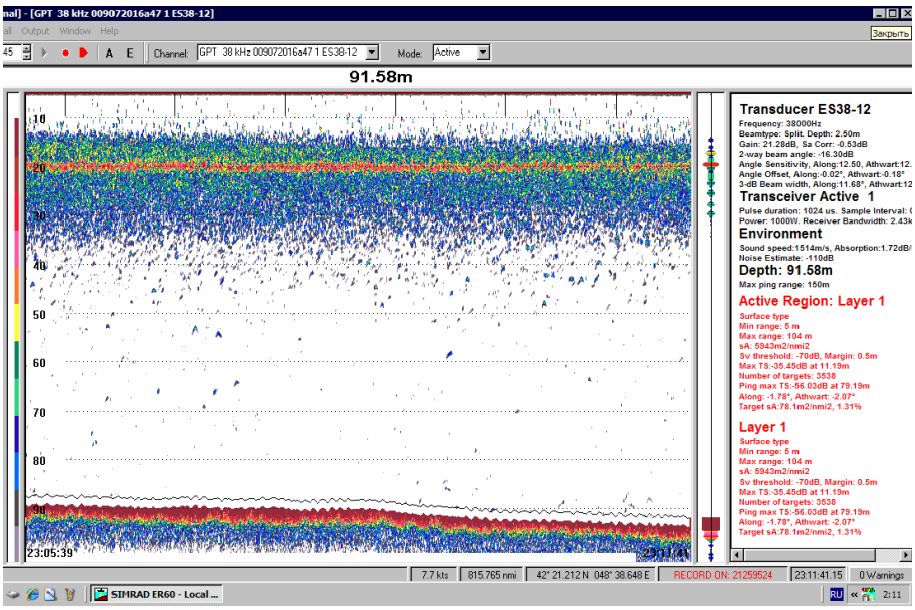

Fig. 1. Part of an echogram showing Caspian sprat aggregations at a depth of 91 m. A nighttime record on 29 July 2017. *NASC* 5943 m^2/nmi^2

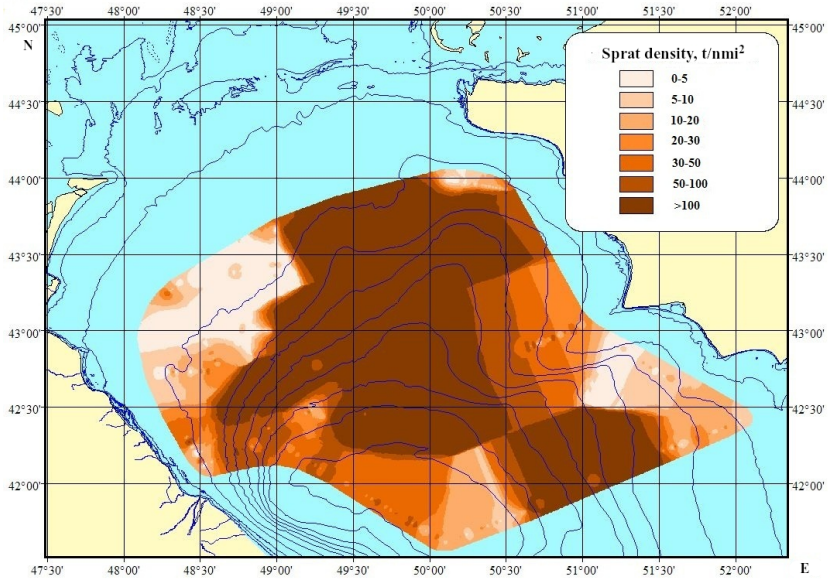

F i g . 2 . Sprat total biomass distribution in the Central Caspian Sea, August–September 2021

The distribution of sprat biomass in August–September 2021 (Fig. 2), determined in total (from the water surface to the bottom), was heterogeneous: in the northern and central parts of the surveyed area, the values exceeded 100 t/nmi^2, which corresponds to very dense aggregations of Caspian sprats.

Studies conducted in 2019–2021 showed that the largest proportion of sprat biomass was found in the 20–30 m layer [7]. In 2021, the biomass in the 20–30 m layer accounted for 60% of the total biomass in the upper 50-metre layer (Fig. 3).

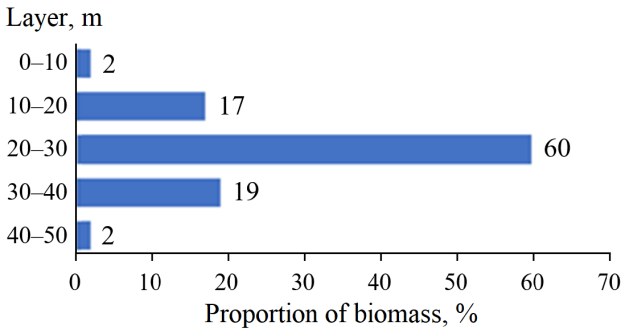

F i g . 3 . Sprat biomass distribution by water layers in the Central Caspian Sea in summer 2021

The relationship between sprat aggregation density and temperature in August–September 2021 was revealed by measuring temperature at depths of 20 and 30 metres, where the aggregation density was highest.

The temperature at the 20 m depth (t_{20}) ranged from 11.0 to 27.2°C, and at the 30 m depth (t_{30}) it varied from 7.2 to 15.3°C, with values of 11–13°C prevailing over most of the water area. The temperature gradient $\Delta t_{20–30}$ in the 20–30 m layer varied from 1.2 to 17.1°C.

Fig. 4 shows the distribution of sprat biomass in the 20–30 m layer, with isotherms at the 30 m depth. At temperatures ranging from 7.5 to 11°C in this layer, the sprat biomass density did not exceed 5 t/nmi^2. In the southern part of the water area, at temperatures of 14–15°C, the density of sprat aggregations increased to 20 t/nmi^2. The densest aggregations, i. e. exceeding 50 t/nmi^2 (at temperatures ranging from 10 to 13°C), were recorded in the central, northern and south-eastern parts of the water area.

For the further analysis, data were selected from stations where the sprat biomass density exceeded 30 t/nmi^2 (Fig. 5). The t_{20} values at these stations ranged from 12.3 to 26.5°C, t_{30} was within 8.9 and 14.7°C and $\Delta t_{20–30}$ varied from 2.8 to 13.7°C.

In the 20–30 m layer, the relationship between the density of sprat aggregations and the vertical temperature gradient $\Delta t_{20–30}$ is approximated by the linear equation $y = 1.917x - 13.059$ ($R^2 = 0.802$), where x is the temperature at the 30 m depth; y is the difference between the temperatures at the 20 m and 30 m depths. High commercial concentrations (over 30 t/nmi²) were observed at the vertical

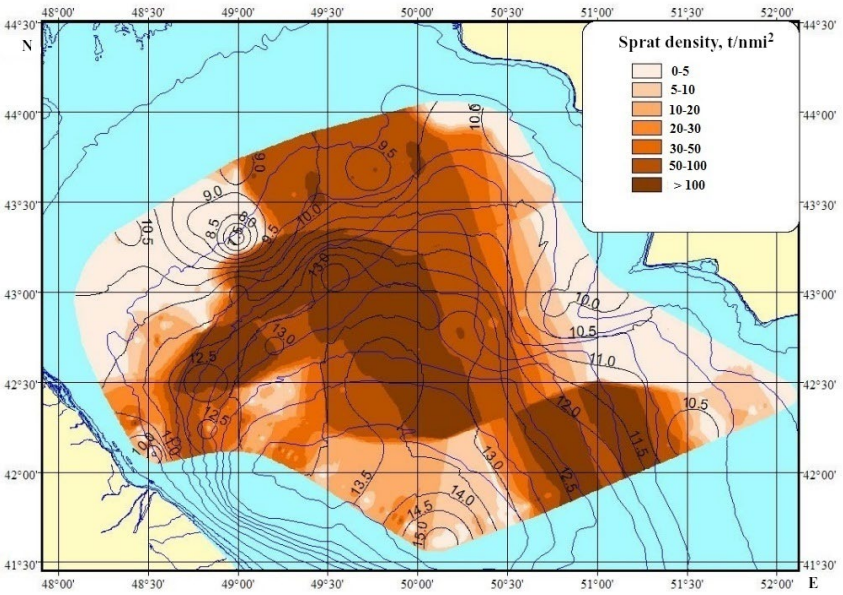

Fig. 4. Sprat biomass distribution in the Central Caspian Sea in the 20–30 m water layer, August–September 2021. The isolines denote temperature at a depth of 30 m

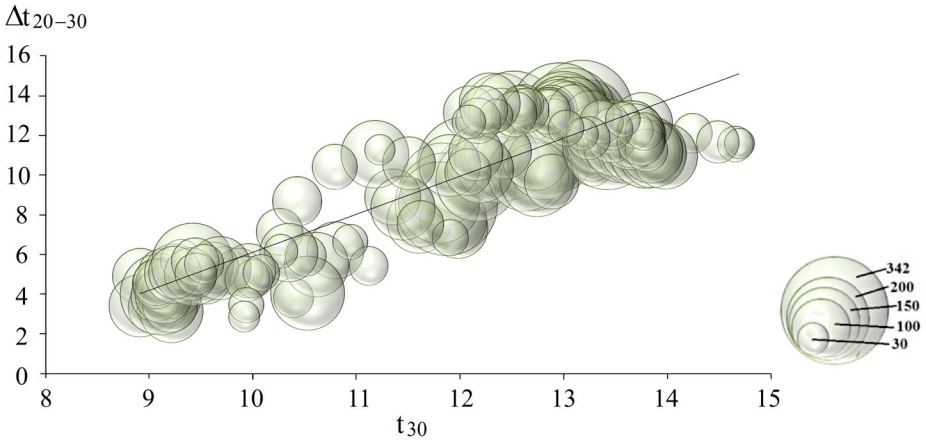

Fig. 5. Dependence of sprat aggregation density on temperature at a depth of 30 m (t_{30}) and vertical temperature gradient in the 20–30 m layer ($\Delta t_{20–30}$), August–September 2021. The circle diameter is proportional to the aggregation density (t/nmi²); only values over 30 t/nmi² were considered

gradient at least 0.3°C/m and t_{30} values above 9.0°C. The conversion of NASC (m²/nmi²) to the Caspian sprat biomass density (t/nmi²) was performed using size-weight coefficients ranging from 0.1 to 0.2 depending on the characteristics of the fish [8].

Fig. 6 and 7 show fragments of the echogram as of 18 and 15 August 2021, taken on the approach to stations with coordinates 42°10′ N, 48°39′ E and 43°05′ N, 49°31′ E, respectively. In the first case, t_{20} = 24.8, t_{30} = 12.1°C ($\Delta t_{20–30}$ = 12.7°C); in the second case, t_{20} = 26.4, t_{30} = 13.3 °C ($\Delta t_{20–30}$ = 13.1°C). Despite the considerable distance between the areas, similar water temperatures and a comparable vertical gradient in the 20–30 m layer facilitate the formation of dense aggregations of sprats.

The shown echograms clearly illustrate the distribution pattern of sprat aggregations in the 20–30 m layer, which is typical for the summer period: during the day, the fish remain in small shoals (see Fig. 6), while at night they form dense aggregations (Fig. 7). A comparison with the 2017 echogram (see Fig. 1) confirms that in 2017, the thermocline contributed to the formation of dense aggregations.

Thus, the results of hydroacoustic surveys in the Central Caspian Sea show that the bulk of the sprat biomass was concentrated in the upper 50-metre layer, predominantly at depths of 20–30 metres, and allowed the identification of a relationship between dense aggregations of sprats and the vertical temperature gradient.

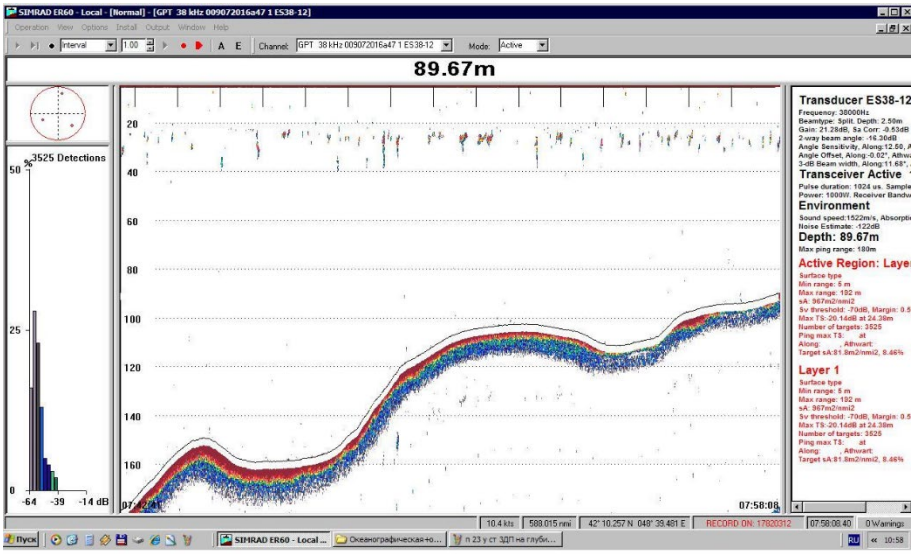

Fig. 6. Part of an echogram showing sprat aggregations at a depth of 89 m. A daytime record on 18 August 2021. *NASC* 967 m^2/nmi^2

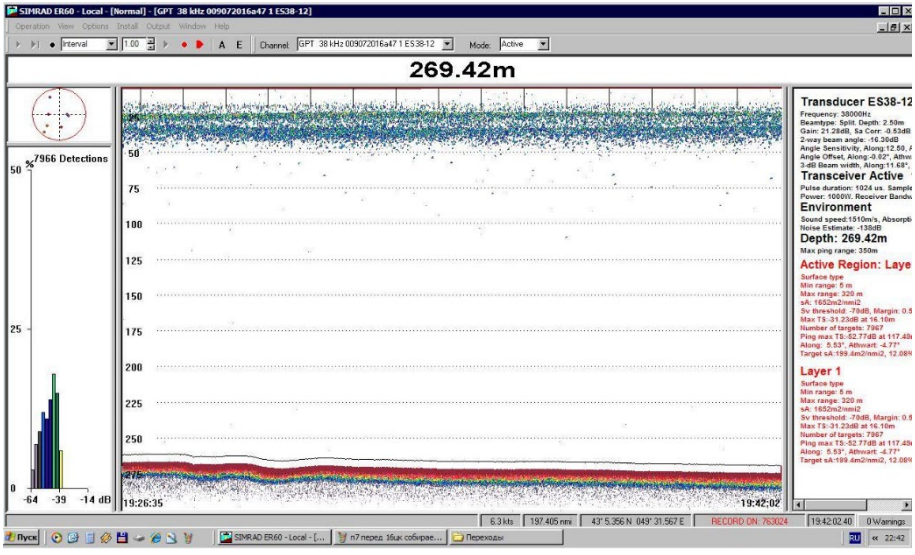

Fig. 7. Part of an echogram showing sprat aggregations at a depth of 269 m. A nighttime record on 15 August 2021. *NASC* 1652 m^2/nmi^2

The findings of hydroacoustic surveys conducted in the Caspian Sea can be applied to the study of the distribution of commercial fish species in the Black Sea [5)] [11–13], where the influence of the thermocline and the thermal structure of the water on the formation of pelagic fish aggregations, such as sprats and anchovies, has been also noted [14–19]. This suggests the potential for applying similar methodological approaches to different marine basins.

The study results, which take into account the influence of temperature during the summer months on the formation of dense commercial concentrations in the 20–30 m layer below the water surface, allow us to identify promising areas for Caspian sprat fishing in the deep-water part of the Caspian Sea during different seasons of the year. This served as the basis for amendments to the Fisheries Regulations (Order of the Ministry of Agriculture of the Russian Federation no. 695 of 13 October 2022 "On the Approval of Fisheries Regulations for the Volga-Caspian Fisheries Basin"): from 1 March 2023, year-round fishing for sprat using multi-depth trawls is permitted in the Central Caspian fishery sub-district in waters with depths of over 80 m.

Conclusions

1. In the deep-water section of the Central Caspian Sea, the highest concentrations of Caspian sprats were found at a depth of 20–30 metres during the summer months.

2. Dense aggregations of sprats (30 t/nmi^2 or more) start to form when the vertical temperature gradient is at least 0.3°C per metre in the 20–30 m layer and the temperature at the 30-metre depth is at least 9.0°C.

3. Identification of promising fishing grounds requires taking into account both data from hydroacoustic surveys and the influence of temperature factors on the formation of dense sprat aggregations.

References

1. Paritckij, Yu.A. and Razinkov, V.P., 2018. Forming Caspian Sprat Stocks in Modern State of the Sea Ecosystem. *Vestnik of Astrakhan State Technical University. Series: Fishing Industry*, (2), pp. 70–80. https://doi.org/10.24143/2073-5529-2018-2-70-80 (in Russian).
2. Paritskiy, Yu.A., Kanatev, S.V., Aseinova, A.A. and Razinkov, V.P., 2018. Some Behaviour Patterns and Distribution of Caspian Ordinary Sprat Species – Clupeonella Delicatula Caspia Svetovidov. *Vestnik of Astrakhan State Technical University. Series: Fishing Industry*, (3), pp. 70–80. https://doi.org/10.24143/2073-5529-2018-3-27-38 (in Russian).
3. Zare, P., Shibaev, S.V., Kasatkina, S.M. and Fazli, H., 2016. An Improved Approach for Assessing of Kilka Biomass by Acoustic Surveys in the Caspian Sea. *KSTU News*, (43), pp. 34–44 (in Russian).
4. Pomogaeva, T.V., 2018. Allocation of Fishing Features Clusters of Sprats and an Average of Caspian Sea in Summer. In: KGTU, 2018. [*Proceedings of the 6th International Baltic Marine Forum, in 6 Volumes. Kaliningrad, 03–06 September 2018*]. Kaliningrad: KGTU. Vol. 2. [Marine Engineering and Technology. Maritime Industry Safety], pp. 405–410 (in Russian).

[5)] Doray, M., Masse, J. and Petitgas, P., 2012. *Pelagic Fish Stock Assessment by Acoustic Methods at Ifremer*. 18 p. https://doi.org/10.13155/11446

5. Pomogaeva, T.V., 2018. [Results of Hydroacoustic Surveys of Caspian Sprats in the Central Caspian Sea, June 2018]. In: I. I. Gordeev, F. V. Lishchenko and K. K. Kivva, eds., 2018. [*Current Issues and Prospects for the Development of the Fisheries Sector: Proceedings of the 6th Scientific and Practical Conference of Young Scientists with International Participation, Moscow, 11–12 October 2018*]. Moscow: VNIRO, pp. 221–226 (in Russian).
6. Pomogaeva, T.V., 2019. [Results of Hydroacoustic Surveys of Caspian Sprats in the Central Caspian Sea, June 2018]. In: I. I. Gordeev, K. A. Zhukova, K. K. Kivva, A. M. Sytov and D. M. Palatov, eds., 2019. [*Current Issues and Prospects for the Development of the Fisheries Sector: Proceedings of the 7th Scientific and Practical Conference of Young Scientists with International Participation, Moscow, 14–15 October 2019*]. Moscow: VNIRO, pp. 400–404 (in Russian).
7. Pomogaeva, T., 2021. Deep-Water Part of the Middle Caspian Sea as a Promising Area of Operation of the Caspian Sprats. *Fisheries*, (4), pp. 48–52. https://doi.org/10.37663/0131-6184-2021-4-48-52 (in Russian).
8. Pomogaeva, T.V. and Tatarnikov, V.A., 2021. Features of the Spatial Distribution of the Caspian Sprats in the Middle Part of the Caspian Sea in the Summer Period According to the Results of Sonar Studies. *Trudy VNIRO*, 184, pp. 87–98. https://doi.org/10.36038/2307-3497-2021-184-87-98 (in Russian).
9. Aseynova, A.A. and Sedov, S.I., 1999. [The Influence of Environmental Factors on the Population Size of the Common Sprat]. In: VNIRO, 1999. *XI All-Russian Conference on Commercial Oceanology: Abstracts (Kaliningrad, 14–18 September 1999)*. Moscow: VNIRO, pp. 61–62 (in Russian).
10. Razinkov, V., Paritsky, Yu., Mikhailova, A., Khursanov, A. and Grozesku, Yu.N., 2021. Stock Status, Environmental Factors and Reproduction Efficiency of the Anchovy Sprat Population (Clupeonella Engrauliformis Borodin) in Modern Conditions. *Fisheries*, (6), pp. 76–79. https://doi.org/10.37663/0131-6184-2021-6-76-79 (in Russian).
11. Panov, B.N., Spiridonova, E.O., Piatinskii, M.M. and Stytsyuk, D.R., 2020. On the Role of Temperature as a Factor Influencing the Behavior of the European Sprat and the Efficiency of Its Fishing. *Aquatic Bioresources & Environment*, 3(1), pp. 106–113. https://doi.org/10.47921/2619-1024_2020_3_1_106 (in Russian).
12. Panov, B.N., Spiridonova, E.O., Pyatinsky, M.M. and Arutyunyan, A.S., 2020. Results of Monitoring of Temperature Conditions of Migration and Fishing of the Azov Khamsa. *Bulletin of Higher Educational Institutions. North Caucasus Region. Natural Sciences*, (1), pp. 71–77. https://doi.org/10.18522/1026-2237-2020-1-71-77 (in Russian).
13. Panov, B.N., Smirnov, S.S. and Spiridonova, E.O., 2023. Oceanographic Conditions for Autumn Migration and Fishing of the Black Sea Anchovy off the Coast of Crimea in 2021. *Aquatic Bioresources & Environment*, 6(2), pp. 30–39. https://doi.org/10.47921/2619-1024_2023_6_2_30 (in Russian).
14. Panov, B.N., Smirnov, S.S. and Spiridonova, E.O., 2023. Multiyear Changes in Oceanographic Factors of the Autumn Migration of the Black Sea Anchovy to the Shores of Crimea from Satellite Data in 2000–2021. *Trudy VNIRO*, 192. pp. 152–161. https://doi.org/10.36038/2307-3497-2023-192-152-161 (in Russian).
15. Belousov, V.N., Piatinskii, M.M., Shlyakhov, V.A. and Kulba, S.N., 2024. Role of Water Temperature Spatio-Temporal Variability in European Anchovy Catches Dynamics in the Northwestern Black Sea. *Trudy VNIRO*, 198, pp. 75–86. https://doi.org/10.36038/2307-3497-2024-198-75-86 (in Russian).

16. Shlyakhov, V.A., Negoda, S.A., Pyatinskii, M.M. and Shlyakhova, O.V., 2023. Stock Assessment of the European Anchovy and European Sprat in the Russian Waters of the Black Sea in 2022–2023. In: Belousov V.N., ed., 2023. *Proceedings of AzNIIRKH*. Rostov-on-Don: AzNIIRKH. Vol. 4, pp. 9–27 (in Russian).
17. Malakhova, T.V., Artemov, Yu.G., Khurchak, A.I., Reshetnik, L.V., Fedirko, A.V. and Egorov, V.N., 2023. Studying Diurnal Dynamics of Vertical Methane Distribution in the Black Sea Aerobic Zone Combined with Acoustic Research of the Sound-Scattering Layers. *Physical Oceanography*, 30(2), pp. 229–244.
18. Artemov, Yu.G. and Egorov, V.N., 2024. The Potential of High-Frequency Hydroacoustic Methods in Oceanography. *Monitoring Systems of Environment*, (4), pp. 57–72. https://doi.org/10.33075/2220-5861-2024-4-57-72 (in Russian).
19. Panayotova, M., Marinova, V., Raykov, V., Stefanova, K., Shtereva, G. and Krastev, A., 2014. Pilot Acoustic Study of Fish Stocks Distribution in the Northern Bulgarian Black Sea Area. *Proceedings of the Bulgarian Academy of Sciences*, 67(8), pp. 959–964.

Submitted 24.07.2025; accepted after review 27.08.2025;
revised 18.12.2025; published 31.03.2026

About the author:

Tatiana V. Pomogaeva, Junior Researcher, A. O. Kovalevsky Institute of Biology of the Southern Seas of RAS (2, Nakhimov Ave., Sevastopol, 299011, Russia), PhD (Agric.), *pomogtatyana@mail.ru*

The author has read and approved the final manuscript.

Original paper

The Influence of Flood Runoff on the Content of Trace Elements in the Water of the Kacha, Belbek and Chernaya Rivers

O. D. Chuzhikova *, V. Yu. Proskurnin, A. A. Paraskiv, N. Yu. Mirzoeva

A. O. Kovalevsky Institute of Biology of the Southern Seas of RAS, Sevastopol, Russia
* *e-mail: chuzhikova@ibss-ras.ru*

Abstract

The article studies the impact of flood runoff on the content of trace elements (metals and metalloids) in the water of the Kacha, Belbek and Chernaya rivers near Sevastopol in 2024. During the flood (March 2024) and dry (July 2024) periods, the concentrations of a number of elements (Be, V, Fe, Co, Ni, Cu, Zn, As, Se, Mo, Cd, Sb, Tl, Pb, Ag), including heavy metals, as well as their total concentrations including dissolved forms and those associated with suspended matter were determined in river water. The content of all studied elements was determined in their acidic concentrates and leachates from samples in accordance with State Standard of Russia 56219-2014 by mass spectrometry with inductively coupled plasma on a PlasmaQuant MS Elite mass spectrometer (Analytik Jena, Germany). It was found that during the flood period, the suspended matter concentration in the Kacha and Belbek Rivers increased by over 100 times, while in the Chernaya River it increased by 2.5 times. The obtained data allowed identification of critical elements whose dissolved or total concentrations exceeded the established standards. Thus, the dissolved copper and zinc were detected to exceed the maximum permissible concentrations for fishery waters. An analysis of total trace elements concentrations using Dutch standards resulted in a wider list of pollutants during the flood: the nickel, zinc, copper and vanadium concentrations in the Kacha and Belbek Rivers exceeded the MPC. The cobalt and beryllium contents were also higher than the MPC (only in the Kacha River). An integral assessment by pollution index confirmed the water quality deterioration by 1–2 classes during the flood: down to class III (moderately polluted) in the Kacha and Belbek Rivers and down to class II (clean) in the Chernaya River. Moreover, the paper analyses trace elements distribution in the water–suspended matter system and shows a predominant contribution of suspended matter to the total content of trace elements in the river water during the flood and low water. The accumulation capacity of suspended matter in relation to the studied trace elements was assessed. The concentration factor for various elements varied from $n \cdot 10^3$ to $n \cdot 10^7$, which confirmed the leading role of suspended matter in processes of water self-purification from pollutants and redistribution of trace elements among the components of aquatic ecosystems. The results ground the necessity to consider suspended forms of trace elements within monitoring the drinking water quality, especially during floods.

© Chuzhikova O. D., Proskurnin V. Yu., Paraskiv A. A., Mirzoeva N. Yu., 2026

This work is licensed under a Creative Commons Attribution-Non Commercial 4.0 International (CC BY-NC 4.0) License

Keywords: heavy metals, element dissolved form, element suspended form, total element concentration, suspended matter, concentration factor, maximum permissible concentration, water pollution index, flood runoff, low water, Chernaya River, Sevastopol, Crimea

Acknowledgments: The work was carried out under the state assignment of the FRC IBSS RAS “Study of biogeochemical patterns of radioecological and chemoecological processes in the ecosystems of water bodies of the Azov-Black Sea basin in comparison with other water areas of the World Ocean and individual aquatic ecosystems of their catchment basins to ensure sustainable development in the southern seas of Russia” (state registration number 124030100127-7).

For citation: Chuzhikova, O.D., Proskurnin, V.Yu., Paraskiv, A.A. and Mirzoeva, N.Yu., 2026. The Influence of Flood Runoff on the Content of Trace Elements in the Water of the Kacha, Belbek and Chernaya Rivers. *Ecological Safety of Coastal and Shelf Zones of Sea*, (1), pp. 85–104.

Влияние паводкового стока на содержание микроэлементов в воде рек Кача, Бельбек и Черная

О. Д. Чужикова *, В. Ю. Проскурнин, А. А. Параскив, Н. Ю. Мирзоева

ФГБУН ФИЦ «Институт биологии южных морей имени А. О. Ковалевского РАН», Севастополь, Россия

* *e-mail: chuzhikova@ibss-ras.ru*

Аннотация

Исследовано влияние паводкового стока на содержание микроэлементов (металлов и металлоидов) в воде рек Кача, Бельбек и Черная в окрестностях Севастополя в 2024 г. В паводковый (март 2024 г.) и засушливый (июль 2024 г.) периоды в речной воде были определены концентрации растворенных форм ряда элементов (Be, V, Fe, Co, Ni, Cu, Zn, As, Se, Mo, Cd, Sb, Tl, Pb, Ag), в том числе тяжелые металлы, а также их общие концентрации, включающие растворенные формы и связанные со взвешенным веществом. Содержание всех изучаемых элементов определяли в их кислотных концентратах и минерализатах в соответствии с ГОСТ Р 56219–2014 методом масс-спектрометрии с индуктивно-связанной плазмой на масс-спектрометре *PlasmaQuant MS Elite* (*Analytik Jena*, Германия). Установлено, что в паводковый период в р. Кача и Бельбек концентрация взвешенного вещества увеличилась более чем в 100 раз, в то время как в р. Черной этот показатель вырос в 2.5 раза. Полученные данные позволили выявить критические элементы, у которых концентрации растворенных форм или общие концентрации превышали установленные нормы. Так, обнаружено превышение ПДК в воде рыбохозяйственных водоемов для растворенных форм меди и цинка. Анализ общих концентраций микроэлементов с использованием нормативов «Голландских листов» показал более широкий перечень загрязнителей в паводок: в реках Кача и Бельбек зафиксированы превышения ПДК никеля, меди, цинка, ванадия, а также кобальта и бериллия (только в реке Кача). Интегральная оценка по индексу загрязненности подтвердила ухудшение качества воды в паводковый период на 1–2 класса: в реках Кача и Бельбек до III класса (умеренно загрязненная), в реке Черной – до II класса (чистая). Кроме того, проанализировано распределение микроэлементов в системе вода – взвешенное вещество и установлен преобладающий вклад взвешенного

вещества в общее содержание микроэлементов в речной воде в паводковый и сухой периоды. Оценена аккумулирующая способность взвешенного вещества в отношении исследуемых микроэлементов: коэффициенты накопления для различных элементов варьировали от $n \cdot 10^3$ до $n \cdot 10^7$, что подтвердило ведущую роль взвеси в процессах самоочищения вод от загрязнителей и перераспределения микроэлементов между компонентами водных экосистем. Полученные результаты обосновывают необходимость учета взвешенных форм микроэлементов при мониторинге качества вод, используемых для питьевого водоснабжения, особенно в паводковые периоды.

Ключевые слова: тяжелые металлы, растворенная форма элемента, взвешенная форма элемента, общая концентрация элемента, взвешенное вещество, коэффициент накопления, предельно допустимая концентрация, индекс загрязненности воды, паводковый сток, межень, река Черная, Севастополь, Крым

Благодарности: работа выполнена по теме госзадания ФИЦ ИнБЮМ «Изучение биогеохимических закономерностей радиоэкологических и хемоэкологических процессов в экосистемах водоемов Азово-Черноморского бассейна в сравнении с другими акваториями Мирового океана и отдельными водными экосистемами их водосборных бассейнов для обеспечения устойчивого развития на южных морях России» (№ гос. регистрации 124030100127-7).

Для цитирования: *Чужикова О. Д., Проскурнин В. Ю., Параскив А. А., Мирзоева Н. Ю.* Влияние паводкового стока на содержание микроэлементов в воде рек Кача, Бельбек и Черная // Экологическая безопасность прибрежной и шельфовой зон моря. 2026. № 1. С. 85–104. EDN DXWQGC.

Introduction

The Kacha, Belbek and Chernaya Rivers are among the main rivers of Crimea and Sevastopol, each with an annual runoff volume of 50–75 million m^3 of fresh water. Due to the water deficit on the peninsula, river runoff is regulated by reservoirs, ponds, and water intakes used both for irrigation and for water supply to populated areas [1]. The rivers of Crimea belong to the rivers with a flood regime of the Crimean subtype, characterized by winter and autumn rainfall floods and prolonged summer (June–August) or summer-autumn (May–October) periods with very low water flow [2]. During the dry period, the water level in the rivers drops sharply, up to complete drying up, while during flood periods, the level rises by 1 m or more, in some cases up to 2–6 m [3]. During the flood period, river turbidity increases sharply, and water quality is formed under the influence of the products of water erosion of the soil cover of the drainage basin (wash-off products) and channel erosion (scour products) [4–6]. Thus, floods pose a real threat to public health, as the quality of water in drinking water sources may temporarily deteriorate [1)] due to the influx of chemical, organic, and biological pollutants with flood runoff waters [7].

[1)] Goncharov, S.F., Batrak, N.I., Sakhno, I.I., Suranova, T.G. et al., 2014. Monitoring of the Sanitary-Epidemiological Situation in Zones of Flooding and Catastrophic Flood. Ed. by L.I. Ivanishina. Moscow: All-Russian Center for Disaster Medicine “Zashchita” of the Ministry of Health of Russia, 36 p. EDN YABMRP (in Russian).

One of the main indicators of drinking water quality is the content of trace elements, including a number of heavy metals, which can have toxic effects on the human body [2)]. Systematic monitoring of surface water pollution in the regions is carried out by laboratories under the guidance of Roshydromet, summarizing the data in the annual publication "Quality of Surface Waters of the Russian Federation" [3)]. However, the existing accounting system considers only the dissolved forms of trace elements.

At the same time, during the flood period, the content of suspended matter in river water can increase significantly. Existing water treatment systems used in the urban water supply system may fail to completely remove suspended particles at critical moments, and water with residual suspended matter containing sorbed chemical substances may be supplied to the population. This substantiates the expediency of studying the total concentration of trace elements in river water, taking into account their dissolved and suspended forms, as well as changes in river water quality during the flood period.

Full-scale monitoring of the Sevastopol rivers in different seasons of the year with simultaneous sampling of water and suspended matter for the analysis of trace element content was previously carried out on the Chernaya River [8]. Similar studies have not been conducted on the Kacha and Belbek Rivers, which determines the relevance of this work.

This study is aimed at investigating the distribution of trace elements (in dissolved and suspended forms) in the water of the Sevastopol rivers Kacha, Belbek, and Chernaya during the flood and dry periods and assessing the impact of flood runoff on the water quality of the studied rivers.

Materials and methods

In order to determine trace elements, including heavy metals (HMs), water and suspended matter samples were collected in the lower reaches of the Kacha, Belbek, and Chernaya Rivers near Sevastopol (Fig. 1) in March and July 2024, corresponding to the periods of high and low water – the difference in water levels in all rivers was about half a meter (Fig. 2).

Immediately after water sample collection, in the laboratory, suspended matter was separated by vacuum filtration through cellulose acetate membrane filters with a pore diameter of 0.45 μm. The total suspended matter concentration was determined by the gravimetric method in accordance with PND F 14.1:2:3.110-97 [4)].

[2)] Chertko, N.K., Taranchuk, A.V., Chertko, E.N. and Budko, D.A., 2012. Biological Function of Chemical Elements: A Reference Guide. Ed. by N.K. Chertko. Minsk: Chetyre chetverti, 172 p. EDN IQXSRX (in Russian).

[3)] Trofimchuk, M.M., ed., 2024. Quality of Surface Waters of the Russian Federation. Yearbook. 2023. Rostov-on-Don: Hydrochemical Institute, 597 p. (in Russian).

[4)] PND F 14.1:2:3.110-97, 2016. Method for Measuring the Mass Concentration of Suspended Solids in Samples of Natural and Waste Waters by the Gravimetric Method. Moscow, 15 p. (in Russian).

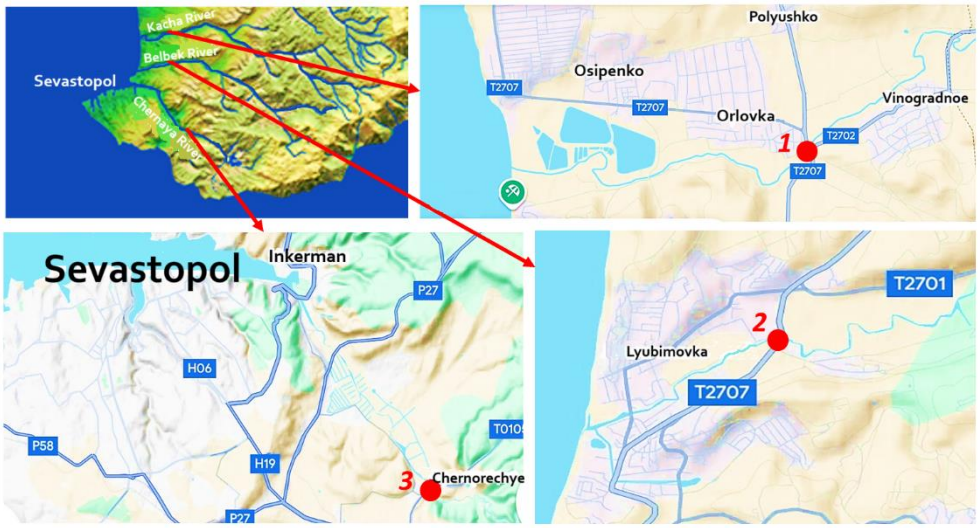

Fig. 1. Schematic map of the study area and sampling points around Sevastopol: *1* – the Kacha River (Orlovka Bridge, 44.726500° N, 33.590981° E), *2* – the Belbek River (Lyubimovka Bridge, 44.669705° N, 33.564247° E), *3* – Chernaya River (gauging station near the village of Khmelnitskoye, 44.545080° N, 33.662357° E)

Dissolved forms of the studied elements were extracted from water by extraction concentration in the form of diethyldithiocarbamates using carbon tetrachloride in accordance with RD 52.10.243-92 [5]. The determined elements were extracted from suspended matter by acid digestion followed by filtration in accordance with PND F 16.2.2:2.3.71-2011 [6]. Concentrations of the studied elements (Be, V, Fe, Co, Ni, Cu, Zn, As, Se, Mo, Ag, Cd, Sb, Tl, Pb) in acid concentrates and leachates were measured by inductively coupled plasma mass spectrometry on a PlasmaQuant MS Elite mass spectrometer (Analytik Jena, Germany) in accordance with the Russian State Standard R 56219-2014 [7] at the Center for Collective Use "Spectrometry and Chromatography" of the FRC IBSS. The mass spectrometer was calibrated using

[5] RD 52.10.243-92, 1993. Guidelines for the Chemical Analysis of Marine Waters. Saint Petersburg: Gidrometeoizdat, 264 p. (in Russian).

[6] PND F 16.2.2:2.3.71-2011, 2011. Method for Measuring Mass Fractions of Metals in Sewage Sludge, Bottom Sediments, Samples of Plant Origin by Spectral Methods. Moscow: Federal Center for Analysis and Assessment of Technogenic Impact (in Russian).

[7] GOST R 56219-2014, 2015. Water. Determination of the Content of 62 Elements by Inductively Coupled Plasma Mass Spectrometry. Moscow: Standartinform, 36 p. (in Russian).

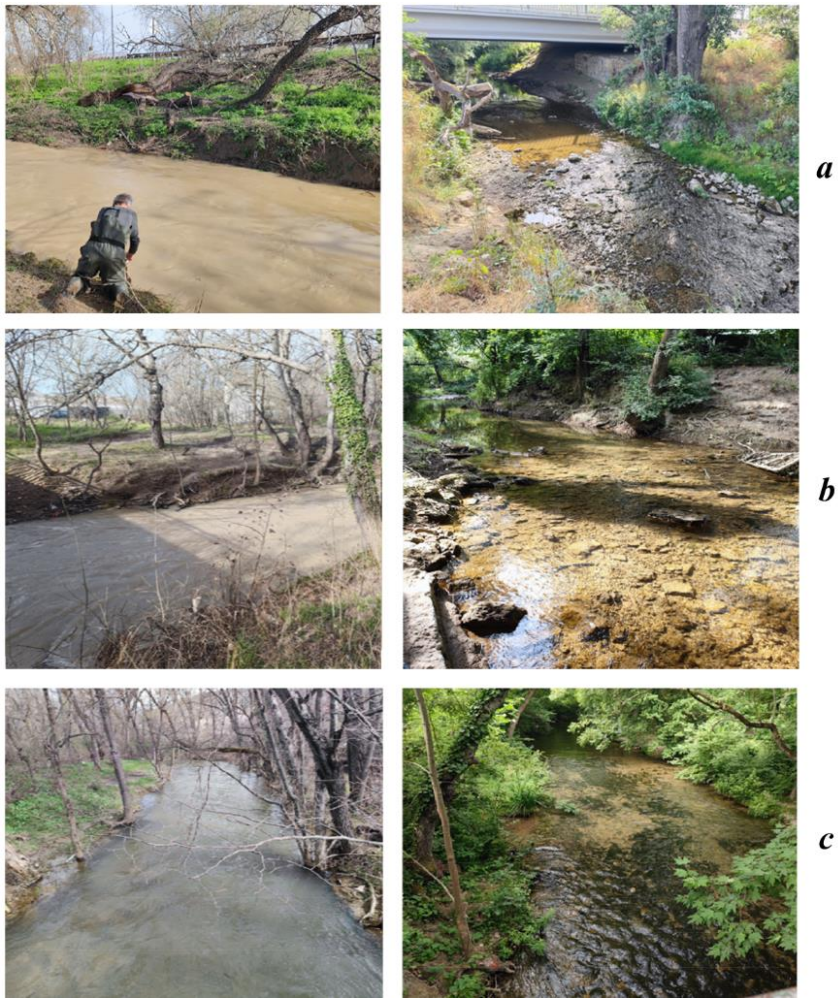

Fig. 2. State of the Kacha (*a*), Belbek (*b*) and Chernaya (*c*) Rivers during sampling: the flood period (*left*) and low-water period (*right*)

a standard solution "Calibration Standard Multi-element IV-28, HNO_3/HF, 125 mL" (Inorganic Ventures) by constructing a calibration curve using solutions with dilutions of the standard covering the entire range of concentrations of the determined elements. The measurement procedure included at least seven replicates for each measured element in each sample. The measurement time was determined by the intensity of the detector response to the presence of a particular element in the solution and varied from 0.01 to 0.1 s. For all measured elements, the relative measurement error was determined, which did not exceed 10%.

To assess the degree of pollution of river waters, the obtained concentrations of elements were compared with the maximum permissible concentrations (MPC)

established by SanPiN 1.2.3.3685-2 [8] for surface water bodies used for domestic drinking and cultural-household use (MPC_{DD}), as well as with the MPC for harmful substances in water bodies of fishery importance (MPC_{fish}), recommended by the order of the Federal Agency for Fisheries (Rosrybolovstvo) [9]. For comparison with foreign standards, the Dutch standards were used [10].

Unlike Russian regulatory documents, the Dutch standards regulate not only the concentrations of dissolved forms of trace elements in water (MPC_{DS}), but also their total concentrations (MPC_{tot}), including their dissolved and suspended forms. This is especially relevant during the flood period, when river water turbidity increases sharply. The standard values from the above-mentioned documents for a number of elements are given in Table 1.

River water quality was assessed by calculating the index of water pollution (IWP) for priority pollutants [11]. Priority pollutants included those elements for which the ratio of the measured concentration to the MPC was the highest. In cases where the concentrations of all elements did not exceed the MPC, the elements with values closest to the standard were included among the priority ones. The IWP necessarily includes indicators such as dissolved oxygen and biochemical oxygen demand over five days (BOD_5). In the present work, these indicators were not assessed, and the IWP was calculated exclusively for the content of heavy metals in water (IWP_{HM}) according to the formula [9]

$$\mathrm{IWP_{HM}} = \frac{1}{n}\sum_{i=1}^{n}\frac{C_i}{\mathrm{MPC}_i},$$

where C_i is the actual concentration of the i-th pollutant metal; MPC_i is the maximum permissible concentration of the i-th pollutant metal; n is the number of priority pollutant metals. MPC_{fish} was applied as the MPC, and in the absence of this indicator for any element, MPC_{DD} or MPC_{DS} was used.

The parameter n in the formula should not exceed 6 and is usually taken as 4–6. In the present work, $n = 6$.

---

[8] SanPiN 1.2.3.3685-21, 2022. Hygienic Standards and Requirements for Ensuring the Safety and (or) Harmlessness of Environmental Factors to Humans (as amended on December 30, 2022) (in Russian).

[9] Order of the Federal Agency for Fisheries (Rosrybolovstvo) No. 296 dated May 26, 2025. On Approval of Water Quality Standards for Water Bodies of Fishery Importance, Including Standards for Maximum Permissible Concentrations of Pollutants in Waters of Water Bodies of Fishery Importance (in Russian).

[10] Warmer, H. and van Dokkum, R., 2002. Water Pollution Control in the Netherlands. Policy and Practice 2001. RIZA report 2002.009, 76 p. Available at: https://edepot.wur.nl/674312 (date of access: 28.02.2026).

[11] Temporary Methodological Recommendations for the Comprehensive Assessment of the Quality of Surface and Marine Waters by Hydrochemical Indicators. Moscow: State Committee for Hydrometeorology of the USSR, 8 p., 1986 (in Russian).

Table 1. Maximum permissible concentrations (MPC) of some elements in surface waters according to various standards

Element	MPC_{DD}, $\mu g \cdot L^{-1}$	MPC_{fish}, $\mu g \cdot L^{-1}$	MPC_{DS}, $\mu g \cdot L^{-1}$	MPC_{tot}, $\mu g \cdot L^{-1}$
Pb	10	6	11	220
Cu	1000	1	1.5	3.8
Zn	5000	10	9.4	40
Ni	20	10	5.1	6.3
Co	100	10	2.8	3.1
V	100	1	4.3	5.1
As	10	50	25	32
Ag	50	–	0.08	–
Mo	70	1	290	300
Cd	1	5	0.4	2
Se	10	2	5.3	5.4
Sb	5	–	6.5	7.2
Fe	300	100	–	–
Be	0.2	0.3	0.2	0.2
Tl	0.1	–	1.6	1.7

Note: MPC_{DD} – maximum permissible concentration of the element in water of surface water bodies for domestic and drinking water use; MPC_{fish} – MPC of the element in fisheries; MPC_{DS} – MPCs from Dutch standards; MPC_{tot} – total MPCs of elements.

Water quality classification was carried out according to the scale [11], where the obtained IWP values correspond to the following classes:

– less than or equal to 0.3 – very clean water, Class I;

– more than 0.3 to 1.0 – clean water, Class II;

– more than 1.0 to 2.5 – moderately polluted water, Class III;

– more than 2.5 to 4.0 – polluted water, Class IV;

– more than 4.0 to 6.0 – dirty water, Class V;

– more than 6.0 to 10.0 – very dirty water, Class VI;

– more than 10.0 – extremely dirty water, Class VII.

Results and discussion

The change in the content of trace elements in river water during the flood period is primarily associated with an increase in the suspended matter concentration, which can increase many times compared to the low-water period. These changes are visible to the naked eye – the water in the rivers becomes turbid, and transparency sharply decreases (Fig. 2).

The composition and amount of suspended matter can vary greatly in different rivers or in different periods in the same river. During the flood period in mountain rivers, characterized by high flow velocity, suspended matter is predominantly represented by lithogenic material due to the influx of terrigenous runoff, erosion of the flooded shoreline, and resuspension of bottom sediments.

Analysis of field observations and measurement results showed that during the dry period (July 2024), the concentrations of total suspended matter in the water of the Kacha, Belbek, and Chernaya Rivers were low and ranged from 2.5 to 3.2 mg·L^{-1} (Fig. 3). The photographs (Fig. 2, *right*) reveal that the water in the rivers was clear. During the flood period, the suspended matter concentration in the Chernaya River increased by 2.5 times, while in the Kacha and Belbek Rivers this indicator increased by more than 100 times (Fig. 3).

Suspended matter in river water can be both a source of trace elements, which can be transferred into dissolved forms through leaching from suspension particles, and a sorbent for dissolved trace elements from water. Different trace elements may behave differently with respect to suspended matter. Thus, complex processes of redistribution of trace elements in water between dissolved forms and forms associated with suspended matter occur [10].

According to the obtained data, the observed concentrations of all regulated trace elements in river water did not exceed MPC_{DD}. Comparison of the results with the standard concentration values for water bodies of fishery importance revealed a number of exceedances. Concentrations of dissolved copper (1.06–1.83 μg·L^{-1} at MPC_{fish} = 1 μg·L^{-1}) exceeded the standard in all river water samples in both seasons, except for the summer sample from the Chernaya River. Concentrations of dissolved zinc (21.84–66.36 μg·L^{-1} at MPC_{fish} = 10 μg·L^{-1}) were above the MPC during the spring sampling in all rivers and in summer in the Kacha River (Fig. 4).

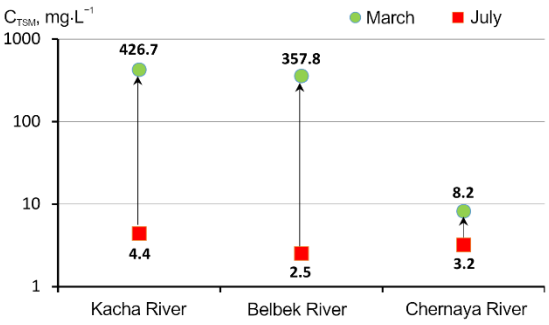

Fig. 3. Concentration of total suspended matter (C_{TSM}) in the Kacha, Belbek and Chernaya Rivers in March (flood) and July (low-water period) 2024

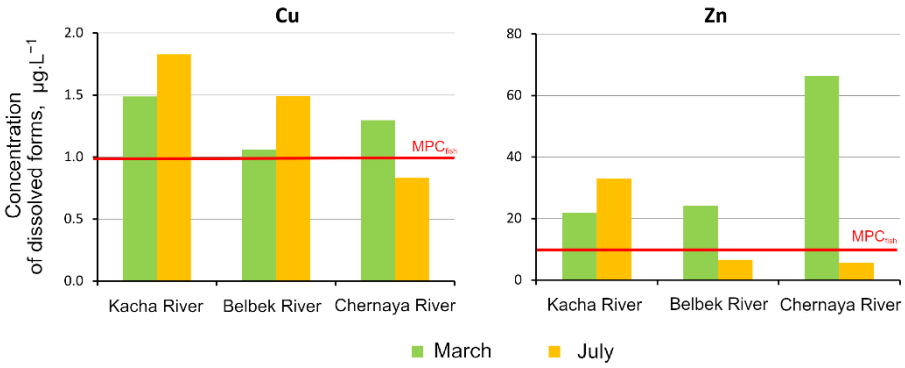

Fig. 4. Concentrations of dissolved copper (*left*) and zinc (*right*) in the Kacha, Belbek and Chernaya Rivers during flood (March) and low-water (July) periods of 2024

Analysis of total trace element concentrations showed that in the water of the Kacha and Belbek Rivers during the flood period, exceedances of MPC_{tot} were recorded for nickel (12.79 and 9.27 μg·L^{-1} at MPC_{tot} = 6.3 μg·L^{-1}), copper (9.45 and 6.88 μg·L^{-1} at MPC_{tot} = 3.8 μg·L^{-1}), zinc (47.93 and 44.44 μg·L^{-1} at MPC_{tot} = 40 μg·L^{-1}), and vanadium (8.43 and 6.25 μg·L^{-1} at MPC_{tot} = 5.1 μg·L^{-1}), and in the Kacha River – also for cobalt (3.17 μg·L^{-1} at MPC_{tot} = 3.1 μg·L^{-1}) and beryllium (0.22 μg·L^{-1} at MPC_{tot} = 0.2 μg·L^{-1}) (Fig. 5). In the Chernaya River, an exceedance of MPC_{tot} was found only for zinc (68.64 μg·L^{-1} at MPC_{tot} = 40 μg·L^{-1}) in the spring season.

Concentrations of the other studied elements did not exceed the established standards and in most cases amounted to less than 20% of the corresponding MPCs (Fig. 6).

It should be noted that when analyzing the total concentrations of trace elements in water, a greater number of critical elements whose concentrations exceeded the MPC were recorded than when analyzing their dissolved forms. This indicates that trace elements associated with suspended matter have a significant impact on water quality in rivers, and consequently, on the well-being of aquatic organisms inhabiting them and on the safety of using river water by the population for economic purposes.

To assess water quality with respect to heavy metals and other trace elements, indices of water pollution (IWP_{HM}) were calculated for dissolved forms and total concentrations in water (Table 2). The calculation included six elements whose concentrations exceeded the MPC in at least one case – zinc, copper, cobalt, nickel, vanadium, and beryllium.

Analysis of the results revealed that when assessing the dissolved forms of trace elements in the Kacha and Belbek Rivers during the flood period, no deterioration in water quality was observed – it remained clean (Class II). In the Chernaya

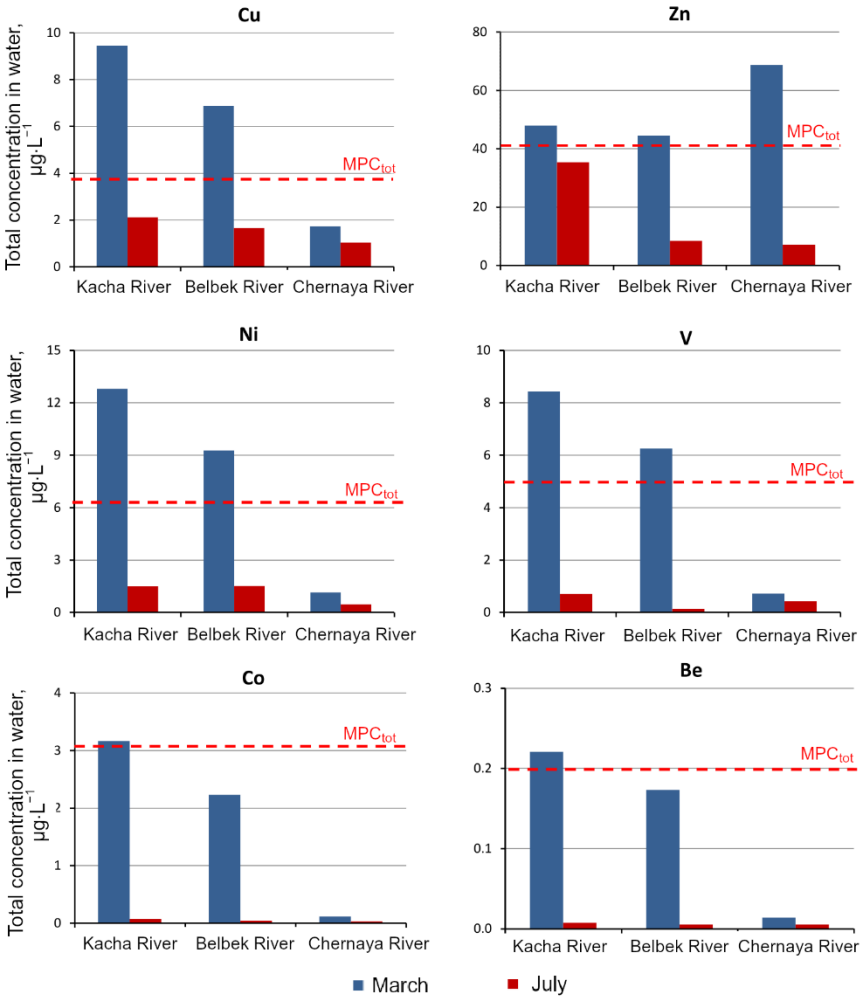

Fig. 5. Total concentrations of trace elements in the Kacha, Belbek and Chernaya Rivers during the flood (March) and low-water (July) periods of 2024

River, the result was different: during the flood period, water quality with respect to dissolved metal forms deteriorated to Class III (moderately polluted) compared to Class I (very clean) in the dry period. This result is explained by the anomalously high concentration of dissolved zinc, which exceeded MPC_{fish} by 6.6 times during the flood period.

The IWP_{HM} calculated from the total metal concentrations in water unequivocally indicates a lower quality of river waters during the flood period compared to the dry period. In the Kacha and Belbek Rivers, water quality during the flood period was defined as “moderately polluted” (Class III), and in the Chernaya River – as “clean” (Class II). During the dry period, water quality in all studied rivers was

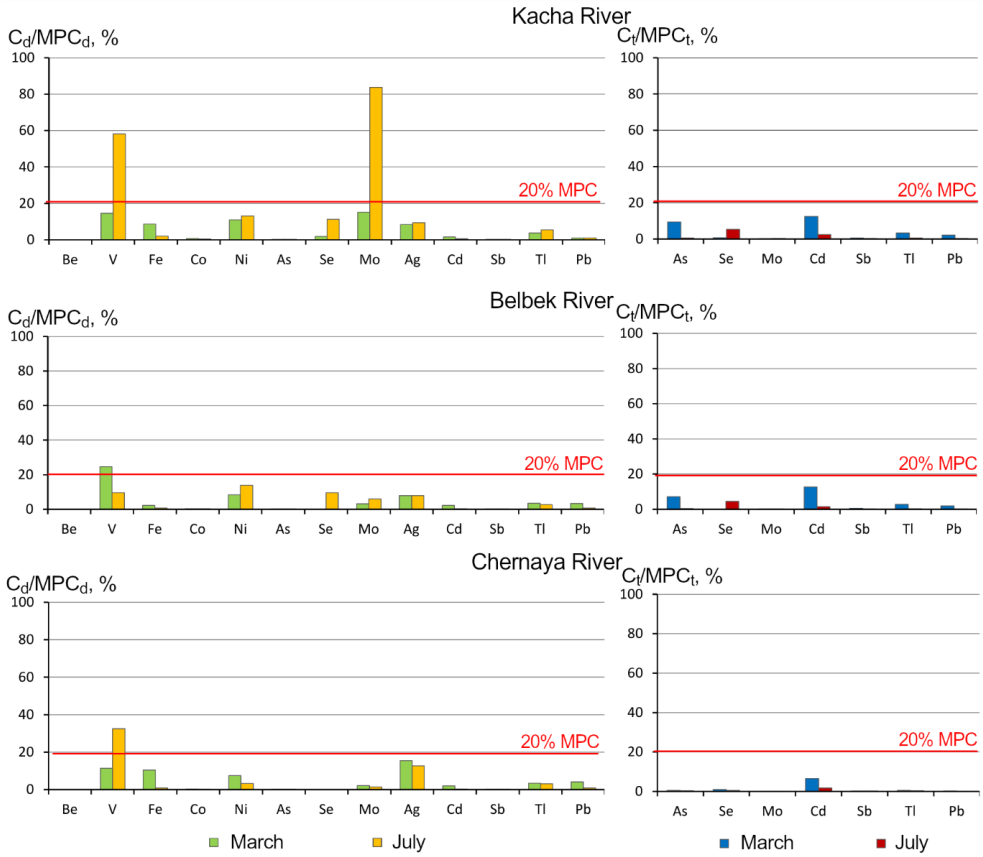

Fig. 6. Relative concentrations of dissolved forms (*C*d/MPCd) and relative total concentrations (*C*t/MPCt) of trace elements in the Kacha, Belbek and Chernaya Rivers during the flood (March) and low-water (July) periods of 2024

defined as "very clean water" (Class I). The obtained IWP_{HM} values correlate with the concentration of suspended matter in the rivers.

The performed water quality assessment of the rivers under study shows that it is advisable to study not only the concentrations of dissolved forms of trace elements, but also their total concentrations in water.

Sedimentation processes in aquatic ecosystems play an important role in the self-purification of the aquatic environment from pollutants and in ensuring water quality [11, 12]. Therefore, when assessing the ecological state of aquatic ecosystems, it is important to study the accumulation properties of suspended matter with respect to pollutants of various types. In the water of the Kacha, Belbek, and Chernaya Rivers, in addition to the amount of total suspended matter and the concentration of trace elements associated with suspended matter, the contribution

Table 2. Water quality assessment in the Kacha, Belbek and Chernaya Rivers in relation to trace elements during the flood (March) and low-water (July) periods of 2024

Assessment criterion	Kacha River		Belbek River		Chernaya River	
	March	July	March	July	March	July
Dissolved form						
IWP_{HM}	0.7	1.0	0.6	0.4	1.4	0.3
Water quality class	II	II	II	II	III	I
Total content						
IWP_{HM}	1.6	0.3	1.2	0.2	0.4	0.1
Water quality class	III	I	III	I	II	I

Note: IWP_{HM} – index of water pollution with heavy metals.

of suspended forms of elements to their total content in water was assessed, and concentration factors were calculated to evaluate the accumulation properties of suspended matter with respect to 15 trace elements, including heavy metals.

The ratios of dissolved and suspended forms of trace elements in the Kacha, Belbek, and Chernaya Rivers during the flood and dry periods are shown in Fig. 7 and Fig. 8, respectively. Analysis of the results revealed that these ratios have only slight differences in the different studied rivers within the same study period and describe the general trends of the redistribution of trace elements between their dissolved forms and the forms associated with suspended matter [13, 14].

During the flood period, most elements are characterized by a predominance of suspended forms (Fig. 7). Exceptions are zinc, molybdenum, cadmium, and silver, for which the ratio of forms is closer to the average values. Slightly different results were obtained during the flood period in the Chernaya River – here, dissolved forms dominated for half of the elements. This is probably due to the fact that the amount and composition (ratio of lithogenic and biogenic components) of suspended matter in the Chernaya River and in the Kacha and Belbek Rivers differ significantly.

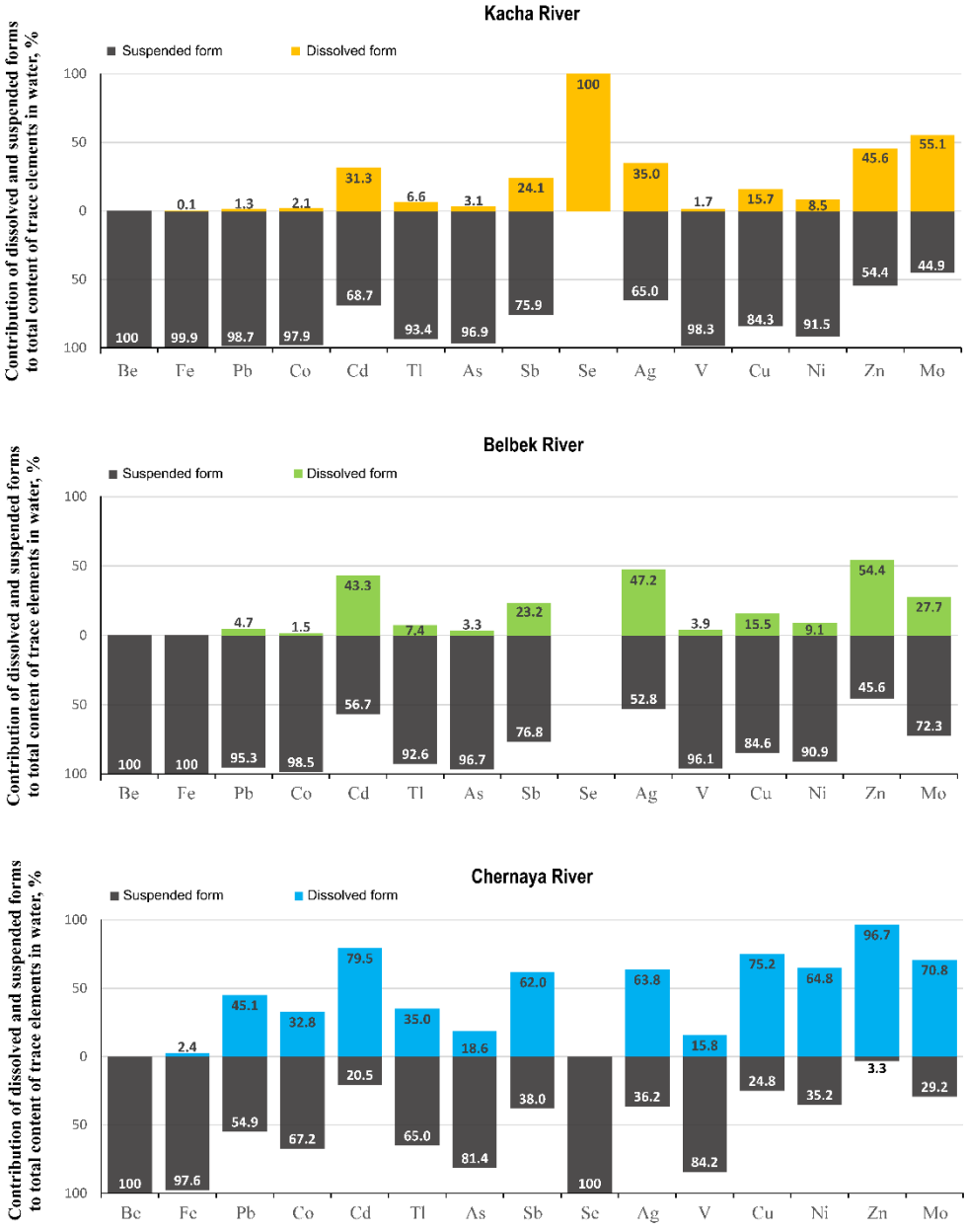

Fig. 7. Contribution of dissolved and suspended forms to the total content of trace elements in the Kacha, Belbek and Chernaya Rivers during the flood (March 2024)

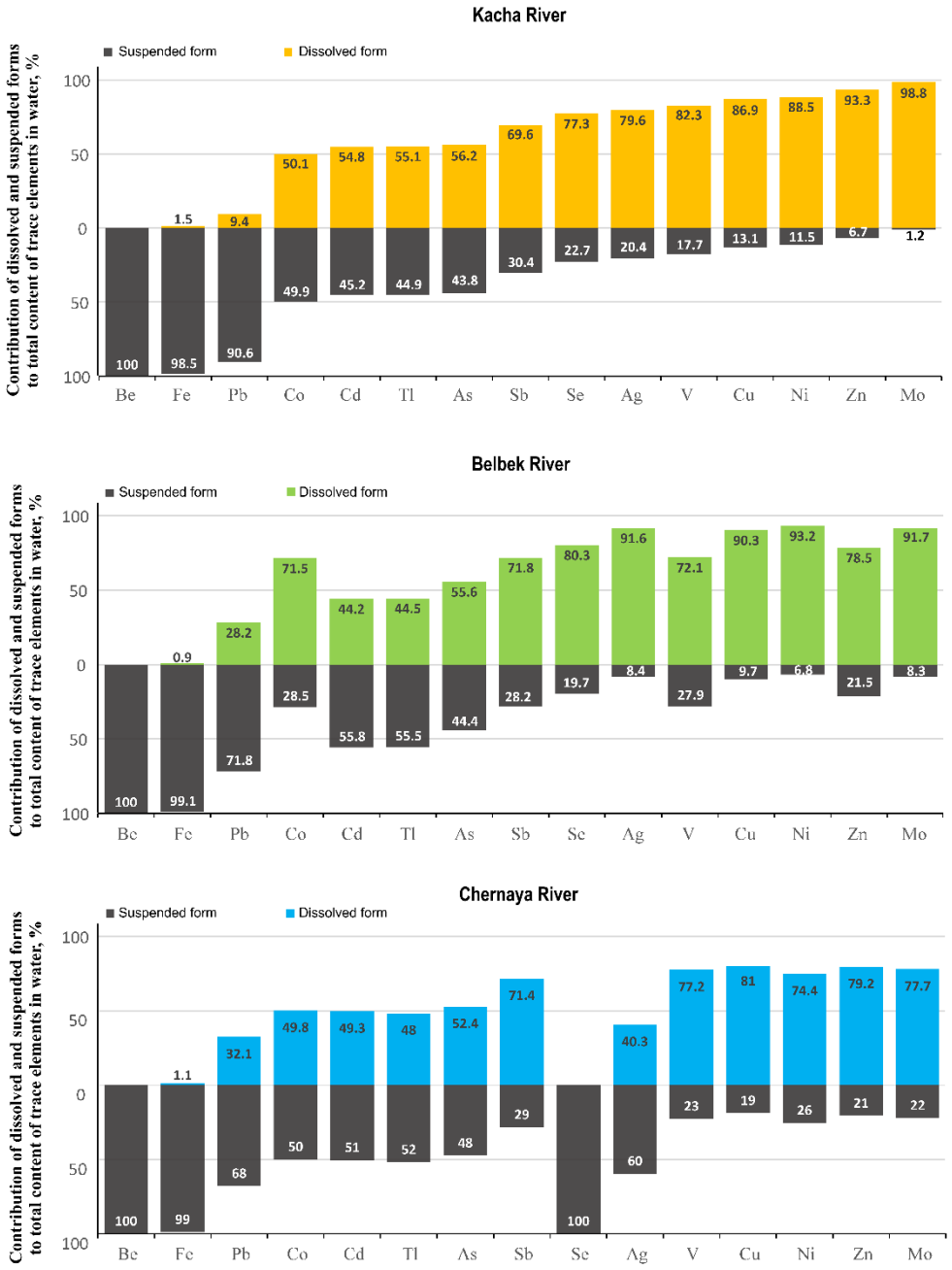

Fig. 8. Contribution of dissolved and suspended forms to the total content of trace elements in the Kacha, Belbek and Chernaya Rivers during the low-water period (July 2024)

During the dry period, the predominance of dissolved forms is characteristic of most trace elements, and the distribution itself differs little among the studied rivers (Fig. 8). During this period, iron, beryllium, and lead are mainly found in suspended form. For cobalt, arsenic, cadmium, and thallium, the distribution between dissolved and suspended forms is approximately equal.

A quantitative assessment of the accumulation capacity of suspended matter regarding trace elements was carried out by calculating the concentration factor (C_f), which shows the ratio of the concentration of an element in suspended matter to its concentration in dissolved form.

The large values of the concentration factor of most trace elements for suspended matter indicate its high accumulation capacity, and consequently, its significant role in the redistribution of substances entering river ecosystems [10].

On the one hand, suspended matter contributes to the rapid removal of pollutants from the aquatic environment as a result of sedimentation. On the other hand, during hydrodynamic processes, pollutants associated with suspended matter can be transported to other parts of the river, and also be carried out of the river ecosystem by the water flow. As noted earlier, resuspension of bottom sediments can lead to desorption of substances from bottom sediment particles, which leads to secondary pollution of river waters. The efficiency of all these processes concerning a specific element largely depends on the ability of suspended matter to accumulate that element [10, 14]

As evidenced by the data presented in Fig. 9, the C_f values for different elements differed by four orders of magnitude. The lowest C_f values ($n \cdot 10^3$) were noted for zinc, molybdenum, silver, cadmium, and antimony during the flood period in the Kacha and Belbek Rivers. In the Chernaya River, C_f for these elements was an order of magnitude higher, indicating a different composition of suspended matter in this river during the flood period. The highest C_f values ($n \cdot 10^6$–$n \cdot 10^7$) were obtained for iron in both seasons and for lead in the dry season. Accordingly, the smallest and largest transport fluxes of these elements with suspended matter will be formed [8]. For the remaining trace elements (vanadium, cobalt, nickel, copper, arsenic, and thallium), the concentration factors C_f were in the range of $n \cdot 10^4$–$n \cdot 10^5$.

In general, for all rivers, similar C_f values of elements in the suspended matter of river water can be noted for both the flood period and the dry season. The studied elements can be arranged in a series in decreasing order of C_f: Fe > Co > V > Pb > As > Tl > Ni > Cu > Sb > Mo > Ag > Cd > Zn – during the flood period; Fe > Pb > Cd > Tl > As > Co > Sb > V > Zn > Se > Cu > Ag > Ni > Mo – during the dry period. Concentration factors for beryllium by suspended matter could not be estimated due to its low, undetectable dissolved concentrations in water.

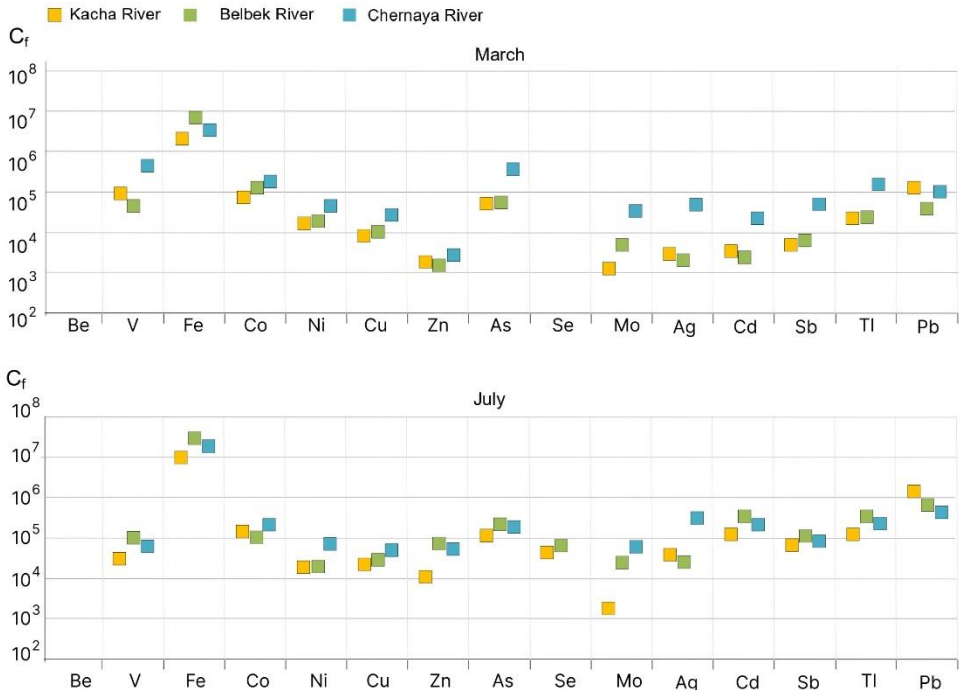

Fig. 9. Concentration factors of trace elements by suspended matter in the Kacha, Belbek and Chernaya Rivers during the flood (March) and low-water (July) periods of 2024

Conclusion

The high interest in studies of the pollution of ecosystem components in the Sevastopol rivers Kacha, Belbek, and Chernaya is due to the fact that these rivers are the main sources of fresh water in the region and are used for drinking water supply to Sevastopol. In the analysis of river water quality carried out by Roshydromet, only dissolved forms of trace elements are determined, without taking into account those associated with suspended matter.

When assessing water quality by dissolved forms, exceedances of MPC_{fish} were recorded only for copper (in all samples except the summer one in the Chernaya River) and zinc (in all rivers in spring and in the Kacha River in summer). Analysis of total trace element concentrations in water revealed a greater number of pollutants during the flood period: in the Kacha and Belbek Rivers, exceedances of MPC_{tot} were noted for copper, zinc, nickel, vanadium, as well as beryllium and cobalt (only in the Kacha River).

Assessment of water quality by IWP with respect to the studied trace elements, performed considering their total concentrations in water, showed a deterioration in river water quality during the flood period by 1–2 classes – from very clean water (Class I) to clean water (Class II) (in the Chernaya River) and to moderately polluted water (Class III) (in the Kacha and Belbek Rivers). This indicates that

trace elements associated with suspended matter have a significant impact on water quality in rivers (especially during the flood period), and consequently, on the well-being of aquatic organisms inhabiting them and on the safety of using river water by the population for economic purposes.

Analysis of the distribution of trace elements in the water – suspended matter system revealed that suspended matter plays an important role in the self-purification of river ecosystems from trace elements, including a number of heavy metals and metalloids. The values of the concentration factor C_f of elements in suspended matter for different elements varied by four orders of magnitude from $n \cdot 10^3$ (zinc, molybdenum, silver, cadmium, and antimony) to $n \cdot 10^7$ (iron, lead). This indicates the high accumulation capacity of suspended matter, and consequently, its significant role in the redistribution of trace elements entering river ecosystems.

It was determined that the flood period significantly affects the content of trace elements in river water, especially in the Kacha and Belbek Rivers, where the concentration of total suspended matter increases substantially, and some portion of trace elements associated with suspended matter may transfer into dissolved form. During this period, for the safe use of river water for economic purposes, it is necessary to pre-filter or let it settle. Furthermore, it is advisable to monitor the content of copper and zinc as critical elements in all studied rivers regardless of the season.

The obtained results can be applied in developing measures for preventing chemical pollution of river waters used as the main source of water supply for the population, with regard to water quality deterioration during the flood period.

REFERENCES

1. Degterev, A.Kh., 2022. [*Filling Capacity of Crimean Reservoirs During the Closure of the North Crimean Canal*]. Sevastopol: SevGU, 70 p. (in Russian).
2. Kuksina, L.V., Golosov, V.N., Zhdanova, E.Yu. and Tsyplenkov, A.S., 2021. Hydrological and Climatological Factors of Extreme Erosion Events in the Crimean Mountains. *Vestnik Moskovskogo Universiteta. Seria 5, Geografia*, (5), pp. 36–50 (in Russian).
3. Nikolenko, I.V., Kopachevskii, A.M. and Karimov, E.A., 2022. Analysis of the Filling of Naturally Flowing Reservoirs for Substantiating Ways to Solve the Problems of Water Supply Security in the Republic of Crimea and City of Sevastopol. *Water Resources*, 49(4), pp. 567–581. https://doi.org/10.1134/S0097807822040157
4. Istomina, M.N., Kocharyan, A.G., Lebedeva, I.P. and Nikitskaya, K.E., 2004. [Ecological Consequences of Floods]. *Inzhenernaya Ekologiya*, (4), pp. 3–19 (in Russian).
5. Demidov, V.V. and Mushaeva, T.I., 2014. [The Impact of Erosion Processes During the Spring Snowmelt on the Chemical Composition of River Runoff]. *Prioritetnye Nauchnye Napravlenia: Ot Teorii k Praktike*, (10), pp. 71–76 (in Russian).
6. Mushaeva, T.I. and Demidov, V.V., 2015. Regularities of Formation and Erosion Processes During Spring Snowmelt on the Territory of Agrolandscape and Their Impact on the Quality of River Water. *Live and Bio-Abiotic Systems*, (11), 9 (in Russian).
7. Krzhizh, L., Vittlingerova, Z., Pashkovskii, I.S. and Khaloupka, D., 2006. Impact of Flood Situations on the Water Quality in Subsurface Sources of Water Supply. *Geoekologiya. Inzhenernaya Geologiya, gidrogeologiya, geokriologiya*, (5), pp. 440–445 (in Russian).

8. Malakhova, L.V., Proskurnin, V.Yu., Egorov, V.N., Chuzhikova-Proskurnina, O.D. and Bobko, N.I., 2020. Trace Elements in the Chernaya River Water and Evaluation of their Income with the Riverine Inflow into the Sevastopol Bay in Winter 2020. *Ecological Safety of Coastal and Shelf Zones of Sea*, (3), pp. 77–94. https://doi.org/10.22449/2413-5577-2020-3-77-94 (in Russian).
9. Chuzhikova-Proskurnina, O.D., Proskurnin, V.Yu., Tereshchenko, N.N. and Kobechinskaya, V.G., 2022. Heavy Metals in the Coastal Waters of Russian Sector of the Black Sea and the Sea of Azov. *Ekosistemy*, (31), pp. 111–122 (in Russian).
10. Egorov V.N., 2019. *Theory of Radioisotope and Chemical Homeostasis of Marine Ecosystems*. Sevastopol: IBSS, 356 p. (in Russian).
11. Egorov, V.N., Gulin, S.B., Malakhova, L.V., Mirzoeva, N.Yu., Popovichev, V.N., Tereshchenko, N.N., Lazorenko, G.E., Plotitsina, O.V., Malakhova, T.V. et al., 2018. Rating Water Quality in Sevastopol Bay by the Fluxes of Pollutant Deposition in Bottom Sediments. *Water Resources*, 45(2), pp. 222–230. https://doi.org/10.1134/S0097807818020069
12. Egorov, V.N., Gulin, S.B., Malakhova, L.V., Mirzoeva, N.Yu., Popovichev, V.N., Tereshchenko, N.N., Lazorenko, G.E., Plotitsina, O.V., Malakhova, T.V. et al., 2018. Biogeochemical Characteristics of the Sevastopol Bay Sedimentation Self-Purification from Radionuclides, Mercury and Chlorogenic Contaminants. *Marine Biological Journal*, 3(2), pp. 40–52 (in Russian).
13. Savenko, V.S., 2006. [The Chemical Composition of Suspended Sediment of the Rivers of the World]. Moscow: GEOS, 173 p. (in Russian).
14. Gordeev, V.V., 2018. Features of River Flow Geochemistry in the Black Sea. In: Lisitsyn, A.P., ed., 2018. *The Black Sea System*. Moscow: Nauchny Mir, pp. 247–286 (in Russian).

Submitted 26.06.2025; accepted after review 06.08.2025;
revised 18.12.2025; published 31.03.2026.

About the authors:

Olga D. Chuzhikova, Junior Researcher, A. O. Kovalevsky Institute of Biology of the Southern Seas of RAS (2, Nakhimov Ave., Sevastopol, 299011, Russia), **ORCID ID: 0000-0002-4518-2624, Scopus AuthorID: 57205198922, ResearcherID: X-4583-2019,** *chuzhikova@ibss-ras.ru*

Vladislav Yu. Proskurnin, Researcher, A. O. Kovalevsky Institute of Biology of the Southern Seas of RAS (2, Nakhimov Ave., Sevastopol, 299011, Russia), **ORCID ID: 0000-0002-2176-9228, Scopus Author ID: 55653290000, ResearcherID: H-4611-2018,** *v_proskurnin@ibss-ras.ru*

Artem A. Paraskiv, Researcher, A. O. Kovalevsky Institute of Biology of the Southern Seas of RAS (2, Nakhimov Ave., Sevastopol, 299011, Russia), PhD (Biology), **ORCID ID: 0000-0001-9874-5382, Scopus Author ID: 57205196196, ResearcherID: K-1314-2018**, *paraskiv@ibss-ras.ru*

Natalya Yu. Mirzoeva, Leading Researcher, Head of the Department of Radiation and Chemical Biology, A. O. Kovalevsky Institute of Biology of the Southern Seas of RAS (2, Nakhimov Ave., Sevastopol, 299011, Russia), PhD (Biology), **ORCID ID: 0000-0002-8538-2436, Scopus Author ID: 55623414000, ResearcherID: Q-9393-2016,** *mirzoyevanyu@ibss-ras.ru*

Contribution of the authors

Olga D. Chuzhikova – participation in expeditions, sample preparation and chemical analysis for determining trace element concentrations, analytical data processing, writing the manuscript, article formatting

Vladislav Yu. Proskurnin – participation in expeditions, performing chemical analysis and measuring concentrations for trace element determination, analytical data processing, editing the article

Artem A. Paraskiv – participation in expeditions, sampling and sample preparation, participation in chemical analysis for determining trace element concentrations, editing the article

Natalya Yu. Mirzoeva – setting the goal and objectives, analysis of the obtained results, discussion of the results, editing the article

All the authors have read and approved the final manuscript.

ISSN 2413-5577, Ecological Safety of Coastal and Shelf Zones of Sea, 2026, No. 1, pp. 105–113.

Original paper

Long-Term Dynamics of Sea Surface Temperature in the Area of the Oyster and Mussel Farm (Outer Harbour of Sevastopol)

M. A. Popov

A. O. Kovalevsky Institute of Biology of the Southern Seas of RAS, Sevastopol, Russia
e-mail: mark.a.popov@mail.ru

Abstract

The paper uses long-term *in situ* measurement data for 2000–2024 to analyse sea surface temperature variability in the water area near the oyster and mussel farm near the eastern cape of Karantinnaya Bay (Cape Lokhanochka, Sevastopol). This study is a continuation of previously published data for 2000 to 2013. Sea surface temperature measurements were taken once daily using a TM-10 mercury meteorological thermometer. Verification was performed using standard publicly available data from the Chersonesus Lighthouse Marine Hydrometeorological Station. Data comparison revealed similar results at these two observation points. Long-term (25 years) observations in the area of Cape Lokhanochka showed significant sea surface temperature fluctuations on interseasonal and interannual scales. The difference between the maximum and minimum sea surface temperatures over the entire measurement period reached 26°C. The maximum absolute sea surface temperature value (29.8°C) was recorded on 12 August 2010, and the minimum (3.8°C) was registered on 24 January 2006. The average long-term sea surface temperature for the observation period was 15.9 ± 0.2°C. The year of 2024 was noted to be the warmest year in terms of average annual sea surface temperature (17.6 ± 0.7°C), breaking the record of the previous extreme year of 2010 (17.1 ± 0.7°C). The magnitude of the positive linear trend in average annual sea surface temperature was 0.07°C/year. It was noted that climatic sea surface temperature seasons lagged behind the atmospheric ones by one month, whereas the summer season increased to four months due to September. Spring was reduced to two months. It is shown that an increase in winter sea surface temperature values prevents the formation of the cold intermediate layer in its classical definition (temperature ≤8°C). The paper presents average monthly sea surface temperatures for the entire observation period.

Keywords: average annual temperature, sea surface temperature, in situ measurements, Black Sea, coastal zone, cold intermediate layer, climate trend

Acknowledgments: The work was carried out within the framework of the state assignment of the A. O. Kovalevsky Institute of Biology of the Southern Seas of RAS on the topic: “Comprehensive study of the mechanisms of functioning of marine biotechnological complexes in order to obtain biologically active substances from aquatic organisms” (2024–2026), no. 124022400152-1.

© Popov M. A., 2026

This work is licensed under a Creative Commons Attribution-Non Commercial 4.0 International (CC BY-NC 4.0) License

For citation: Popov, M.A., 2026. Long-Term Dynamics of Sea Surface Temperature in the Area of the Oyster and Mussel Farm (Outer Harbour of Sevastopol). *Ecological Safety of Coastal and Shelf Zones of Sea*, (1), pp. 105–113.

Многолетняя динамика температуры поверхности моря в районе устрично-мидийной фермы (внешний рейд города Севастополя)

М. А. Попов

ФГБУН ФИЦ «Институт биологии южных морей имени А. О. Ковалевского РАН», Севастополь, Россия

e-mail: mark.a.popov@mail.ru

Аннотация

На основе многолетних контактных измерений 2000–2024 гг. проанализирована изменчивость температуры поверхности моря в районе устрично-мидийной фермы, расположенной у восточного мыса Карантинной бухты (мыс Лоханочка, г. Севастополь). Работа продолжает опубликованные ранее исследования за 2000–2013 гг. Температуру поверхности моря измеряли один раз в сутки метеорологическим ртутным термометром ТМ-10. Верификация была проведена по стандартным данным наблюдений морской гидрометеостанции «Херсонесский маяк», опубликованным в открытой печати. Сравнение данных показало сходные результаты в этих двух пунктах наблюдения. Многолетние (25 лет) наблюдения в районе м. Лоханочка показали значительные колебания температуры поверхности моря на межсезонном и межгодовом масштабах. Разность между максимальной и минимальной температурами поверхности моря за весь период измерений достигала 26 °С. Максимальное абсолютное значение температуры поверхности моря (29.8 °С) зафиксировано 12 августа 2010 г., а минимальное (3.8 °С) – 24 января 2006 г. Среднемноголетняя температура поверхности моря за период наблюдения составила (15.9 ± 0.2) °С. Отмечено, что 2024 г. стал максимально теплым по среднегодовой температуре поверхности моря – (17.6 ± 0.7) °С, побив рекорд предыдущего экстремального 2010 г. – (17.1 ± 0.7) °С. Положительный линейный тренд среднегодовой температуры поверхности моря равен 0.07 °С/год. Отмечено, что климатические сезоны температуры поверхности моря запаздывают относительно атмосферных на один месяц, а летний сезон увеличился до четырех месяцев за счет сентября. Весна сокращается до двух месяцев. Показано, что повышение зимних значений температуры поверхности моря препятствует формированию холодного промежуточного слоя в его классическом понимании (температура ≤ 8 °С). Приведены среднемесячные значения температуры поверхности моря за весь период наблюдения.

Ключевые слова: среднегодовая температура, температура поверхности моря, контактные измерения, Черное море, прибрежные зоны, холодный промежуточный слой, климатический тренд

Благодарности: работа выполнена в рамках госзадания ФГБУН ФИЦ ИнБЮМ по теме: «Комплексное исследование механизмов функционирования морских биотехнологических комплексов с целью получения биологически активных веществ из гидробионтов» (2024–2026 гг.) № 124022400152-1.

Для цитирования: *Попов М. А.* Многолетняя динамика температуры поверхности моря в районе устрично-мидийной фермы (внешний рейд города Севастополя) // Экологическая безопасность прибрежной и шельфовой зон моря. 2026. № 1. С. 105–113. EDN ICIOXI.

Introduction

Seawater temperature is the most significant factor impacting marine biota. This was noted by S. A. Zernov in one of the first classical works on hydrobiology [1]. Subsequent studies confirmed this conclusion, showing that water temperature exerts a dominant influence on the distribution of organisms, their behavior, physiology, reproduction, and biochemistry [2, 3].

Recently, remote sensing methods have become popular, operational, and fairly accurate tools for measuring sea surface temperature (SST). However, in coastal waters, where the largest errors in temperature measurement by remote methods occur [4], contact methods for measuring SST remain relevant.

We will leave aside debates about the existence or absence of global warming. This work does not aim to analyze global climate change. The local nature of the observations allows for the assessment of regional trends but does not provide a basis for extrapolation to a global scale. According to data from [5], a 25-year time series is quite sufficient for assessing the climatic norm and calculating interannual trends; however, it does not allow us to predict whether the warming trend will continue in the future or be replaced by a cooling trend after the warming peak has passed.

This paper focuses on the long-term variability of SST on seasonal and interannual scales in a specific area off the coast of Sevastopol.

An oyster-mussel farm is located in the area under consideration. The applied significance of this water area has led to numerous hydrobiological studies by researchers from the IBSS (A. O. Kovalevsky Institute of Biology of the Southern Seas of RAS, Sevastopol, Russia) and other scientific institutions. During these works, a large amount of experimental data has been accumulated and important results have been obtained [6–8]. Sufficiently long time series make it possible to assess the interannual variability of SST, calculate linear trends, and identify the long-term average seasonal variability of SST. These estimates are necessary for the successful management of the oyster-mussel farm and for identifying patterns in the temporal variability of the productivity of shellfish aquaculture species. The results of this work will also be useful to hydrobiologists conducting research in the water area adjacent to the area under consideration.

The aim of this work is to study the long-term dynamics of SST in the area of Cape Lokhanochka (nonofficial geographic name) based on contact measurements.

Materials and methods

SST was measured in the area of Cape Lokhanochka from 2000 to 2024 daily at 12:00 local time on working days using a TM-10 meteorological mercury thermometer according to the method [1)]. In favorable weather, measurements were carried out at point *1*. During stormy winds, icy conditions, or rain, when observations at point *1* involved a risk, observations were carried out at point *2* (Fig. 1).

[1)] Ivanov, G.S., ed., 1977. *Guidelines for Hydrological Surveys in Oceans and Seas*. Leningrad: Gidrometeoizdat, 725 p. (in Russian).

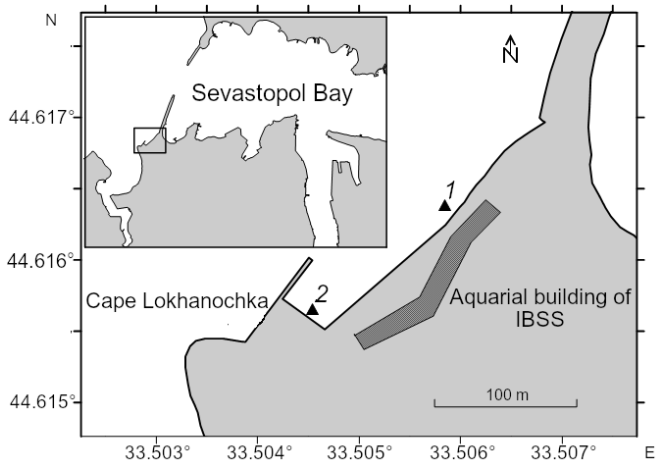

Fig. 1. Layout of observation points [9]

A total of 4449 SST measurements were carried out. Minor gaps of 1–2 days were filled using average values calculated from the nearest SST measurements [10]. For longer gaps, data for the nearest representative point (usually Pobedy Park Beach, Sevastopol) from the website https://watsen.info/ were used. The observations were verified by comparing the average monthly measured SST in the Cape Lokhanochka area with data from [11], obtained at the Chersonesos Lighthouse Marine Hydrometeorological Station (Fig. 2). Statistical processing was performed using the Microsoft Excel software package.

Results and discussion

SST was measured once a day, so the question of data verification arose. For comparison, publicly available observational SST data [11] from the nearest Chersonesos Lighthouse Marine Hydrometeorological Station, located in the open sea, were used. These were compared with the data obtained in the Cape Lokhanochka area. The verification showed similar results at these two observation points (Fig. 2). The maximum discrepancy was recorded in June 2000 and amounted to 1.1°C. The lower SST values in the Cape Chersonesos area can be explained by the activation of upwelling in this region.

The Black Sea, particularly the waters adjacent to the southwestern part of the Crimean Peninsula, is characterized by significant intra-annual variability in SST. The main factor determining this variability is solar radiation, which reaches its maximum in the summer months and its minimum in winter [12]. The difference between the maximum and minimum SST values over the entire measurement period reached 26°C. The maximum absolute SST value (29.8°C) was recorded on August 12, 2010, and the minimum (3.8°C) was recorded on January 24, 2006.

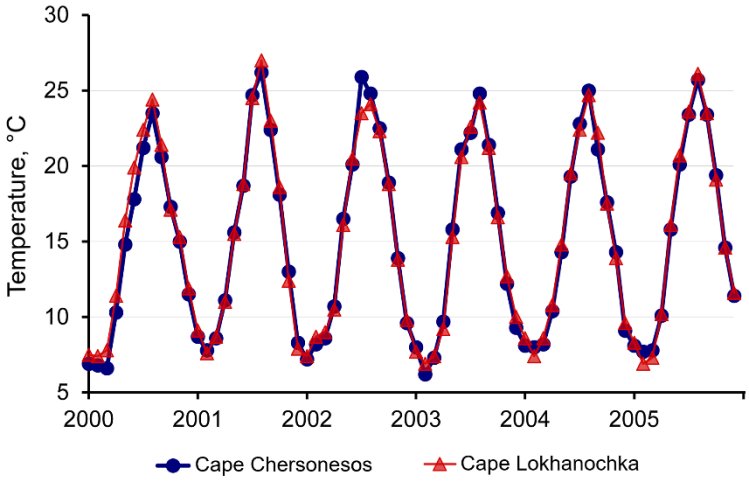

Fig. 2. Average monthly sea surface temperatures (SST) in the vicinity of Cape Chersonesos [11] and Cape Lokhanochka

The intra-annual course of average monthly SST values over the 25-year period is shown in Fig. 3. The average SST was calculated from data for each month over 25 years. The minimum and maximum SST values correspond to the absolute minimum and maximum temperatures recorded in each month over the entire observation period. The winter months (January, February, and March) are characterized by low average temperatures, with a minimum in February. In spring, from April to May, intensive warming of the water column occurs under the influence of solar radiation. In the summer months (June – September), SST reaches its maximum values, with August being the warmest month. September can also be considered part of the summer season: temperatures in this month are close to those in June, and sometimes exceed them.

A shift of seasonal phenomena by approximately one month relative to land was recorded. Therefore, October, November, and December are considered autumn months. During this period, the surface layer of the sea cools monotonically. The largest standard deviations from the average monthly SST values were observed in May and June due to intra-monthly heterogeneity in the rate of temperature increase during the period of intensive warming of the sea surface layer, which is consistent with an increase in the level of synoptic (intra-monthly) SST variability during these months according to satellite data [13]. Isolated significant deviations of minimum temperatures from the monthly averages were recorded in September. Such a deviation can be explained by upwelling events. For instance, on September 20, 2007, SST reached 20.5°C, and on September 25, 2007, it dropped to 13.0°C, only to rise to 21.0°C by October 3. According to the authors of [14], the coastal upwelling was caused by intense winds from the northern quadrant. Such events are quite rare for this area. Almost all upwelling cases here are latent and are only detected by variations in the depth of the seasonal thermocline.

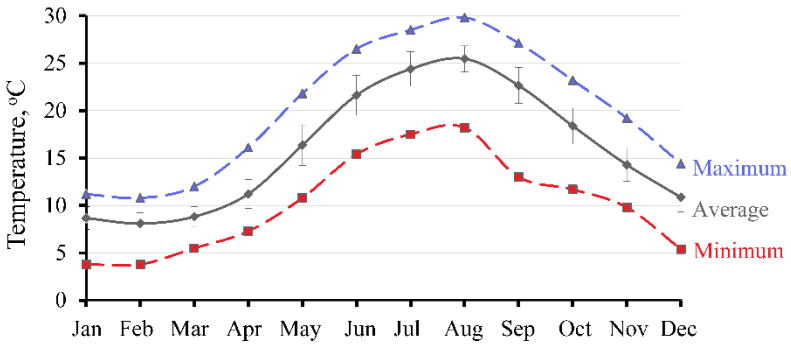

Fig. 3. Intra-annual variation of SST for 2000–2024. The error in average monthly temperatures is represented by the standard deviation

A previous analysis [9] of 13-year SST variability in the Cape Lokhanochka area revealed a steady positive trend in average annual SST values. Observations up to the present have confirmed the persistence of this trend. The magnitude of the positive linear trend in average annual SST for 2000–2024 was 0.07°C/year, with an approximation reliability of $R^2 = 0.546$ (Fig. 4).

The long-term average annual SST for 2000–2024 was 15.9 ± 0.2°C (here and below, the error represents the 95% confidence interval). Extremely warm years were 2010 (17.1 ± 0.7°C) and 2024 (17.6 ± 0.7°C). The summer of 2010 was the warmest over the entire observation period. In 2024, the summer was not extremely warm, but the average annual temperature was higher due to the other seasons. The years 2018 (16.7 ± 0.7°C) and 2020 (16.8 ± 0.7°C) can also be considered warm (Fig. 4).

The coldest years were 2003 (14.5 ± 0.6°C) and 2006 (14.9 ± 0.6°C). A feature similar to that observed in the warmest years was also noted here. The winter of 2006 was extremely cold, while in 2003, lower temperatures were recorded throughout the year. The years 2004 (15.0 ± 0.6°C) and 2011 (15.2 ± 0.6°C) can be considered cold years. Against the background of the overall warming trend, 2017 (15.7 ± 0.7°C) and 2022 (16.0 ± 0.7°C) can also be considered relatively cold.

Recently, due to the increase in SST, the cold intermediate layer (CIL) in its classical sense (temperature ≤ 8°C) has almost disappeared [15]. The CIL forms in winter when the SST drops below 8°C. As can be seen from the table, such SST values have been observed less and less frequently in recent years. The last renewal of the CIL occurred only in 2017. An increase in winter SST may lead to a decrease in the dissolved oxygen content in the CIL core due to a reduction in the intensity of winter convective mixing [16]. Such exceedances of 8°C in the CIL core have been recorded before, in the late 1930s and in 1962–1972 [17].

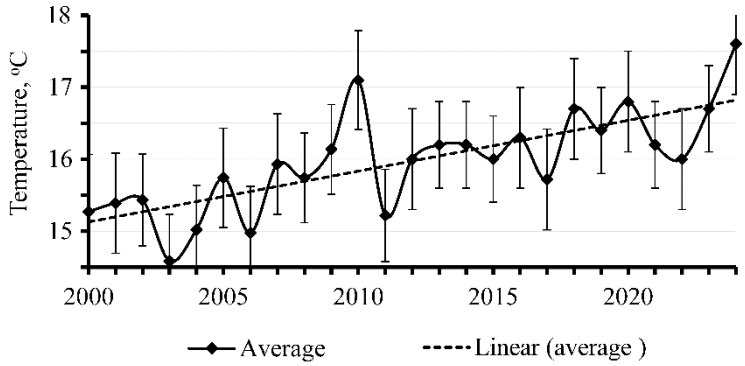

Fig. 4. Average annual SST values and their linear trend, the error of average annual SST is presented by the 95% confidence interval

Average monthly temperature (°C) of the sea surface

Year	Months											
	I	II	III	IV	V	VI	VII	VIII	IX	X	XI	XII
2000	7.5	7.4	7.8	11.4	16.4	19.9	22.4	24.4	21.4	17.1	15.3	11.9
2001	9.1	7.6	8.7	11	15.5	18.8	24.5	27	23	18.6	12.4	7.9
2002	7.4	8.7	9	10.5	16.1	20.5	23.5	24.1	22.3	18.8	13.8	9.8
2003	7.7	6.9	7.4	9.2	15.3	20.6	22.6	24.2	21.2	16.6	12.7	10
2004	8.6	7.4	8.6	10.8	14.8	19.5	22.4	24.7	22.2	17.5	13.9	9.6
2005	8.3	6.9	7.3	10.2	16.1	20.7	23.6	26.1	23.5	19.1	14.6	11.6
2006	7.4	6.4	7.9	10.8	15.2	20.3	23.7	24.8	19.8	18.4	13.3	10.9
2007	8.7	7.9	8.1	10.5	16.6	23.2	24.9	26.4	21.8	18.4	13.8	10.1
2008	8.6	8	8.6	11.1	16	21.1	24.1	24.9	21.7	18	15.3	11.3
2009	8.3	8.4	9.2	11.8	15.6	21.2	25.7	24.4	21.8	18.9	15.4	12.3
2010	9.9	8.9	9.6	12	17.4	23.3	27	28	23.4	17.7	15.3	12.2
2011	9.3	7.7	7.8	10.5	15.8	21.9	23.5	24.2	22	17.3	12.1	10.1
2012	8	5.9	7.6	10	18.2	22.1	24.8	24.7	22.4	20.2	15.8	11.5
2013	8.7	8.7	8.9	11.2	18.5	22.5	24.4	24.5	20.7	16.1	13.6	9.8
2014	9.1	8.7	10.1	12.5	17.0	21.7	24.2	26.0	22.6	17.6	13.1	11.2
2015	9.3	8.4	9.3	10.8	16.0	21.4	23.8	25.2	23.9	18.8	13.8	10.7
2016	8.8	8.8	9.7	11.8	17.1	22.5	26.5	26.3	23.7	18.0	12.9	8.8
2017	6.8	7.4	9.3	11.0	15.9	21.7	23.8	25.0	23.1	17.8	13.3	10.8
2018	8.8	8.4	8.8	12.8	18.8	23.2	25.6	25.9	23.4	18.9	14.9	10.7
2019	9.1	8.9	9.1	11.5	16.4	24.4	23.9	24.9	22.6	18.2	15.3	11.7

Continued

Year	Months											
	I	II	III	IV	V	VI	VII	VIII	IX	X	XI	XII
2020	9.2	8.7	9.8	11.7	15.5	21.9	25.5	25.0	24.2	21.3	15.8	11.9
2021	10.3	9.3	9.5	11.0	15.8	20.9	24.5	26.6	22.4	17.1	14.6	11.5
2022	8.6	8.5	8.1	10.6	15.3	21.2	23.7	26.0	23.1	18.8	18.8	15.1
2023	10.2	8.9	9.5	11.9	16.2	22.0	24.3	26.4	24.2	19.4	15.4	13.5
2024	9.5	9.8	10.9	14.1	16.9	23.5	26.3	26.4	24.8	20.9	16.0	12.0

Note. The data for 2000–2013 are taken from paper [10].

Conclusion

Analysis of SST in the area of the oyster-mussel farm showed that the warming trend in 2000–2024 was 0.07°C/year. The same trend was recorded in 2000–2013. The year 2024 became an extremely warm year (average annual SST 17.6 ± 0.7°C), surpassing the anomalously warm year 2010 (average annual SST 17.1 ± 0.7°C). However, such high temperatures as those observed in the summer of 2010 were not observed in the summer of 2024.

The long-term average annual SST for 2000–2024 was 15.9 ± 0.2°C. A shift in the seasonal cycle of SST relative to the atmospheric seasons by one month and an extension of the summer season to four months, due to September, were noted.

The increase in winter SST values has led to the degradation of the CIL in its classical sense. This creates prerequisites for changes in the oxygen regime of coastal waters and must be taken into account when managing the oyster-mussel farm in the studied water area.

References

1. Zernov, S.A., 1913. [*On Studying Life of the Black Sea*]. In: IAS, 1913. Zapiski Imperatorskoy Akademii Nauk. Saint Petersburg: Imperatorskaya Akademiya Nauk. Vol. 32, iss. 1, 304 p. (in Russian).
2. Shulman, G.E. and Finenko, Z.Z., eds., 1990. [*Biopower of Hydrobionts*]. Kiev: Naukova Dumka, 246 p. (in Russian).
3. Mitra, A., Abdel-Gawad, F.K., Bassem, S., Barua, P., Assisi, L., Parisi, C., Temraz, T.A., Vangone, R., Kajbaf, K. et al., 2023. Climate Change and Reproductive Biocomplexity in Fishes: Innovative Management Approaches towards Sustainability of Fisheries and Aquaculture. *Water*, 15(4), 725. https://doi.org/10.3390/w15040725
4. Zakharova, E.V. and Fomin, V.V., 2024. Assessment of the Accuracy of the Sea Surface Temperature of the Baltic Sea. *InterCarto. InterGIS*, 30(1), pp. 604–616. https://doi.org/10.35595/2414-9179-2024-1-30-604-616 (in Russian).
5. Monin, A.S., 1999. [*Hydrodynamics of the Ocean Atmosphere and Earth's Interior*]. Saint Petersburg: Gidrometeoizdat, 523 p. (in Russian).

6. Lisitskaya, E.V., 2017. Taxonomic Composition and Seasonal Dynamics of Meroplankton in the Area of Mussel-Oyster Farm (Sevastopol, Black Sea). *Marine Biological Journal*, 2(4), pp. 38–49. https://doi.org/10.21072/mbj.2017.02.4.04
7. Mashukova, O.V., Skuratovskaya, E.N. and Shilova, J.B., 2019. Biophysical and Biochemical Techniques in Monitoring the Coastal Waters of Sevastopol (Black Sea). *Monitoring Systems of Environment*, (1), pp. 55–62 (in Russian).
8. Shakhmatova, O.A., Milchakova, N.A. and Kovardakov, S.A., 2018. Catalase Activity of Some Red Gelling Algae in the Different Environmental Condition of the Sevastopol Coastal Zone (Black Sea). *Ekosistemy*, (14), pp. 91–102 (in Russian).
9. Popov, M.A., 2014. [Variability of Sea Surface Temperature in the Area of Cape Lokhanochka (Sevastopol, Black Sea)]. In: MHI, 2014. *Ekologicheskaya Bezopasnost' Pribrezhnykh i Shel'fovykh Zon i Kompleksnoe Ispol'zovanie Resursov Shel'fa* [Ecological Safety of Coastal and Shelf Zones and Comprehensive Use of Shelf Resources]. Sevastopol: ECOSI-Gidrofizika. Iss. 28, pp. 172–175 (in Russian).
10. Abramenkova, I.V. and Kruglov, V.V., 2005. [Methods of]Restoring Gaps in Data Arrays]. *Software & Systems*, (2), pp. 18–22 (in Russian).
11. Giragosov, V.E., Zuev, G.V. and Repetin, L.N., 2006. Variability of Reproductive Potential of the Black Sea Sprat (*Sprattus sprattus Phalericus*) in Connection with Temperature Environmental Conditions. *Marine Ekological Journal*, 5(4), pp. 5–22 (in Russian).
12. Ivanov, V.A. and Belokopytov, V.N., 2013. *Oceanography of Black Sea*. Sevastopol: ECOSI-Gidrofizika, 210 p.
13. Artamonov, Yu.V., Skripaleva, E.A. and Fedirko, A.V., 2020. Regional Features of the Temperature Field Synoptic Variability on the Black Sea Surface from Satellite Data. *Physical Oceanography*, 27(2), pp. 186–196. https://doi.org/10.22449/1573-160X-2020-2-186-196
14. Dzhiganshin, G.F., Polonskii, A.B. and Muzyleva, M.A., 2010. Upwelling in the northwest part of the Black Sea at the end of the summer season and its causes. *Physical Oceanography*, 20(4), pp. 281–293. https://doi.org/10.1007/s11110-010-9084-0
15. Polonskii, A.B. and Novikova, A.M., 2020. Interdecadal Variability of the Black Sea Cold Intermediate Layer and Its Causes. *Russian Meteorology and Hydrology*, 45(10), pp. 694–700. https://doi.org/10.3103/S1068373920100039
16. Vidnichuk, A.V. and Konovalov, S.K., 2021. Changes in the Oxygen Regime in the Deep Part of the Black Sea in 1980–2019. *Physical Oceanography*, 28(2), pp. 180–190. https://doi.org/10.22449/1573-160X-2021-2-180-190
17. Belokopytov, V.N. and Zhuk, E.V., 2024. Climatic Variability of the Black Sea Thermohaline Characteristics (1950–2023). *Physical Oceanography*, 31(6), pp. 788–801.

Submitted 24.07.2025; accepted after review 11.08.2025;
revised 18.12.2025; published 31.03.2026

About the author:

Mark A. Popov, Senior Researcher, A.O. Kovalevsky Institute of Biology of the Southern Seas of the Russian Academy of Sciences (2, Nakhimov Ave., Sevastopol, 299011, Russia), PhD (Geogr.), **Scopus Author ID: 57197871255**, **ORCID ID: 0000-0003-0220-1298**, *mark.a.popov@mail.ru*

The author has read and approved the final version of the manuscript.

Original paper

Pollution of Crimean Coastal Towns Soil with Heavy Metals and Petroleum Products

A. V. Baranenko [1], E. I. Golubeva [1], E. S. Kashirina [2] *

[1] *Lomonosov Moscow State University, Moscow, Russia*

[2] *A. O. Kovalevsky Institute of Biology of the Southern Seas of RAS, Sevastopol, Russia*

* *e-mail: e_katerina.05@mail.ru*

Abstract

The paper is devoted to the peculiarities of soil pollution in small seaside towns with resort specialization using Crimea as a case study. The specifics of soil pollution in resort towns are related to the active use of motor vehicles, the operation of infrastructure enterprises and the development of agriculture in adjacent areas. Heavy metals and petroleum products occupy a leading place among pollutants. The purpose of the work is to assess the level of soil pollution in the coastal towns of the Southern Coast of Crimea with heavy metals and petroleum products using the example of Yalta, Alushta and Sudak. The research methodology included soil sampling in different functional zones of the towns and beyond their limits. Samples for determining background levels were collected at a distance from highways in forested areas. The content of heavy metals in the soil was determined by the X-ray fluorescence method, and petroleum products by the luminescent-bituminological method. In the soils of residential areas of the three studied towns, elevated concentrations of lead (Pb) and zinc (Zn) were recorded. The highest exceedances of background levels for heavy metals were recorded in Yalta (3.5–4 times). In addition, copper (Cu), strontium (Sr), manganese (Mn) and vanadium (V) actively accumulate in the soils of resort towns of the Southern Coast of Crimea. Pb, Zn, Cu, Sr, Mn and V accumulate in the soils of suburban areas of the Southern Coast of Crimea near highways. The content of petroleum products in soils is, as expected, higher along major suburban highways than within town limits. The main source of pollutants is motor vehicles. Their impact increases in the summer season with the influx of vacationers to the Southern Coast of Crimea, whose number reached 3.85 million people in 2021. Another source of pollution is heat and power facilities, including stoves in low-rise residential buildings. The total pollution index (Zc) indicates a low level of soil pollution in the studied towns; however, the concentrations of some pollutants exceed background levels. The results of the study can be used in the environmental monitoring system and in the formulation of regional environmental policy in resort towns.

Keywords: environmental problems of resort towns, soil pollution with heavy metals and metalloids, petroleum products, Black Sea coast

Acknowledgments: The study was conducted under the state assignment of Lomonosov Moscow State University “Geographical approach to optimizing environmental management in sustainable development models” and IBSS state research assignment (No. 124030100030-0).

© Baranenko A. V., Golubeva E. I., Kashirina E. S., 2026

This work is licensed under a Creative Commons Attribution-Non Commercial 4.0 International (CC BY-NC 4.0) License

For citation: Baranenko, A.V., Golubeva, E.I. and Kashirina, E.S., 2026. Pollution of Crimean Coastal Towns Soil with Heavy Metals and Petroleum Products. *Ecological Safety of Coastal and Shelf Zones of Sea*, (1), pp. 114–128.

Загрязнение почв приморских городов Крыма тяжелыми металлами и нефтепродуктами

А. В. Бараненко [1], Е. И. Голубева [1], Е. С. Каширина [2] *

[1] *Московский государственный университет имени М.В. Ломоносова, Москва, Россия*

[2] *ФГБУН ФИЦ «Институт биологии южных морей имени А.О. Ковалевского РАН, Севастополь, Россия*

* *e-mail: e_katerina.05@mail.ru*

Аннотация

На примере Крыма рассмотрены особенности загрязнения почв в небольших приморских городах с курортной специализацией. Специфика загрязнения почв городов связана с активным использованием автотранспорта, работой предприятий инфраструктуры и развитием сельского хозяйства на прилегающих территориях. Ведущее место среди загрязняющих веществ занимают тяжелые металлы и нефтепродукты. Цель работы – оценить уровень загрязнения почв городов Южного берега Крыма тяжелыми металлами и нефтепродуктами на примере Ялты, Алушты и Судака. Методика исследования включала отбор проб почвы в разных функциональных зонах городов и за их пределами. Пробы для определения фоновых значений отбирали в отдалении от автотрасс в лесной зоне. Содержание тяжелых металлов в почве определяли рентгенофлуоресцентным методом, нефтепродуктов – люминесцентно-битуминологическим методом. В почвах селитебных зон трех рассмотренных городов отмечается превышение концентраций свинца (Pb) и цинка (Zn). Максимальные превышения фоновых значений тяжелых металлов зафиксированы в Ялте (в 3.5–4 раза). Кроме того, в почвах курортных городов Южного берега Крыма активно аккумулируются медь (Cu), стронций (Sr), марганец (Mn), ванадий (V). В почвах пригородных районов Южного берега Крыма возле автодорог накапливаются Pb, Zn, Cu, Sr, Mn, V. Содержание нефтепродуктов в почвах ожидаемо выше вдоль крупных загородных автотрасс по сравнению с городской чертой. Главным источником загрязняющих веществ является автотранспорт. Его влияние возрастает в летний сезон с притоком на Южный берег Крыма отдыхающих, численность которых в 2021 г. достигала 3.85 млн человек. Другим источником загрязнения выступают объекты теплоэнергетики и печное отопление малоэтажных зданий. Суммарный показатель загрязнения *Zc* свидетельствует о низком уровне загрязнения почв исследуемых городов, однако концентрации некоторых загрязняющих веществ превышают фоновые. Результаты исследования могут быть использованы в системе экологического мониторинга, при формировании региональной экологической политики в курортных городах.

Ключевые слова: экологические проблемы, курортные города, загрязнение почвы тяжелыми металлами, тяжелые металлы и металлоиды, нефтепродукты, побережье Черного моря

Благодарности: исследование выполнено в рамках государственного задания МГУ имени М. В. Ломоносова «Географический подход к оптимизации природопользования в моделях устойчивого развития» и государственного задания ФИЦ ИнБЮМ (№ гос. регистрации 124030100030-0).

Для цитирования: *Бараненко А. В., Голубева Е. И., Каширина Е. С.* Загрязнение почв приморских городов Крыма тяжелыми металлами и нефтепродуктами // Экологическая безопасность прибрежной и шельфовой зон моря. 2026. № 1. С. 114–128. EDN BNZOQJ.

Introduction

Urbanization contributes to the growth of demand for recreational activities and tourism among the population, which increases the anthropogenic load on natural ecosystems. This problem is especially relevant for the Crimean Peninsula, which is characterized by a high concentration of valuable and vulnerable landscapes.

Crimea is one of the major tourist centers of our country, and its attractiveness is based on unique natural conditions. During the summer period, resort towns on the Southern Coast of Crimea (SCC) experience a large influx of vacationers, which leads to an increase in anthropogenic impact on the natural environment. Thus, in 2021, the number of tourists visiting Crimea amounted to 9.39 million people, 41% (3.85 million) of whom vacationed on the SCC [1)]. At the same time, the SCC is distinguished by its unique nature with characteristic sub-Mediterranean ecosystems, a large number of rare and protected plants and animals, and a high proportion of specially protected natural areas (more than 220 sites with a total area of over 250 thousand hectares) [1]. Thus, intensive economic use contradicts the need to preserve the natural environment, which determines the relevance of assessing anthropogenic impact, particularly soil pollution.

The pollution of resort towns by individual chemical elements can be affected by many factors. For example, a study of Cd content in resorts revealed that the element enters the environment (air, soils, and water bodies) during the construction of hotels, with wastewater from tourist infrastructure facilities, and from vehicle exhaust [2].

An increased content of certain chemical elements in the soils of resort towns may be associated with the lithological composition of the area's rocks. For example, in the soils of resort towns on the Canary Islands, the contents of Co, Cr, Ga, Mn, Mo, Ni, Ti, and V are naturally elevated due to the predominance of basaltic volcanic tuffs and lava flows. The content of Ag, Ba, Ge, Li, Pb, Sn, and Sr in the soils is low, which is associated with the deposition of a significant amount of wind-borne light particles [3].

The soils of the resorts of the Caucasian Mineral Waters, located in the complex geological conditions of the Mineralovodsk uplift, are distinguished by high levels of certain chemical elements. In the soils of Kislovodsk, Zheleznovodsk, Essentuki, and Pyatigorsk, increased concentrations of Pb, Cd, and Ni have been reported. The natural background in the area of the resort towns of the Caucasian Mineral Waters includes concentrations of not only heavy metals but also radionuclides [4, 5].

[1)] Report "On the state and protection of the environment on the territory of the Republic of Crimea in 2021". Available at: https://meco.rk.gov.ru/uploads/txteditor/meco/attachments//d4/1d/8c/d98f00b204e9800998ecf8427e/phpPrPviN1.pdf [Accessed: 14 April 2023] (in Russian).

Agriculture can be a source of soil pollution in resort towns, but its actual contribution is not always significant. For example, in the banana cultivation area on the Canary Islands, a slightly increased phosphorus content in the soil was indeed noted, which is explained by the application of mineral fertilizers. However, overall, this had little effect on changes in the concentrations of chemical elements in the resort soils [3].

A significant role in the pollution of cities, including resort towns, is played by motor vehicles. For example, in the large resort city of Dehradun (India), elevated concentrations of Zn, Cu, Pb, Cd, and As were noted in road dust [6]. A similar trend is observed in other resort towns [7, 8].

The specifics of soil pollution in resort towns are associated with the active use of motor vehicles, the operation of electric and thermal power facilities, and the development of agriculture. In the resort towns of Crimea (Yalta, Alushta, and Sudak), the major soil pollutants are heavy metals, metalloids (HMM), and petroleum products.

The resort towns selected as models are located on the SCC, have access to the sea area, and possess a number of similar natural and socio-economic features: they are situated in the lower part of steep slopes in a mountain-forest zone with broad-leaved and coniferous communities. The dominant soils on the SCC are brown forest soils (*Dystric Cambisols*) and cinnamonic soils (*Eutric Cambisols*) [9]. The industrial specialization of the cities is also similar: it includes thermal power facilities, construction material production enterprises, food industry enterprises, and vineyards.

Despite the absence of large industrial sources of soil pollution in resort towns, elevated HMM content may be noted on agricultural lands, particularly in vineyards. The input of HMM into vineyard soils is also due to the use of pesticides. The leading place among toxicants used in vineyards is occupied by Cu. According to a global review [10], the average Cu content in vineyard soils is 63 mg/kg.

For the Crimean Peninsula, the Cu content in soils has been studied for various types of agricultural landscapes and varies widely. The total Cu content in cinnamonic soils of SCC vineyards reaches 140 mg/kg, which is explained by the introduction of the element with fungicides [11]. It should be noted that the Cu content in calcareous soils of the SCC is higher than in leached soils – 48 and 22 mg/kg, respectively [12].

Ni, Cr, Pb, V, Fe, Zn, As, and Ba enter the soils of agricultural lands in the SCC in addition to Cu; their content in soils under vineyards exceeds the MPC, APC for Fe, and threshold values for Ba given in the literature [12].

The study is aimed at assessing the level of soil pollution in the coastal towns of the SCC with heavy metals and petroleum products using the example of the towns of Yalta, Alushta, and Sudak.

Materials and methods

The study objects are the soils of the resort towns on the SCC – Yalta, Alushta, and Sudak. During field work in the summer of 2022, samples were collected for geochemical studies. To compare the levels of soil pollution, urban and suburban areas were studied: slopes of southern (profile along route *1*) and eastern (profile along route *2*) exposures (Fig. 1). Observation points on the slopes adjacent to the cities were selected at approximately equal height intervals. For a more accurate assessment, a height interval from sea level to 600 m was chosen in all towns due to the difference in the amplitudes of the mountain ranges (maximum elevation

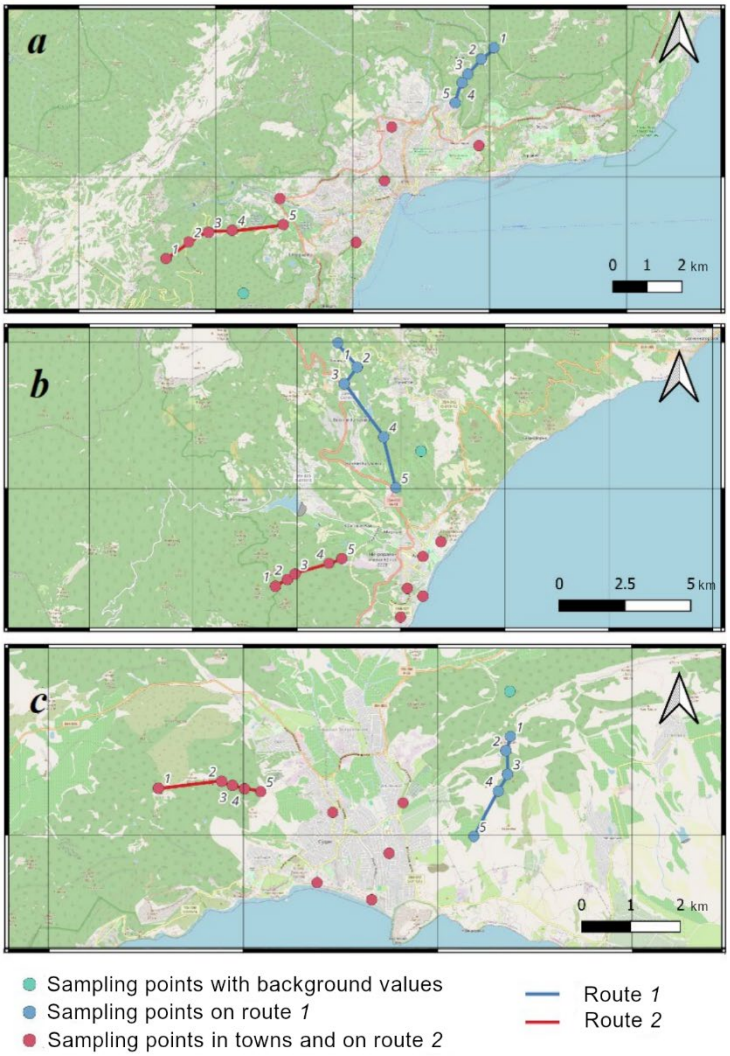

F i g . 1 . Location of routes and sampling points in: *a* – Yalta; *b* – Alushta; *c* – Sudak

marks in Sudak are about 500 m). HMM content in the soils of the Yalta Nature Reserve, located at a distance from pollution sources in the mountain-forest zone, was taken as the background value for HMM content in soils.

Soil samples were taken using the envelope method from the upper humus horizon over an area of 1 m^2. The samples were dried at a temperature of 40°C for 12 hours and sieved through sieves with mesh sizes of 1 mm and 0.25 mm, then the samples were ground in an agate mortar to a dusty structure.

The content of 11 HMM (Pb, Zn, Cu, Cr, Sr, Mn, V, Fe, As, Cd, Ni) was determined in the samples. Determination was carried out by X-ray fluorescence analysis with sample preparation according to the standard method M-049-PDO/18 FR.1.31.2018.32143. Two parallel measurements were performed for each sample using a portable X-ray fluorescence analyzer, the Olympus Innov-X SDD 25 Delta Professional.

Analysis of the petroleum product content in soils was carried out using the luminescent-bituminological method on a Fluorat-02 instrument [2), 3)].

The concentration coefficient was calculated as the ratio of the chemical element content in the soil to its content under background conditions.

The total pollution coefficient *Zc* was calculated as the sum of concentration coefficients with a value greater than 1 minus the number of elements minus 1 and is expressed by the formula

$$Zc = \sum_{i=1}^{n} \mathrm{Cc}_i - (n - 1),$$

where n is the number of determined substances being summed with $\mathrm{Cc}_i > 1$; Cc_i is the concentration coefficient of the i-th chemical element [13, p. 38].

The pollution level with a *Zc* value in the range of 0–16 is considered low (non-hazardous); 16–32 is considered medium (moderately hazardous); in the range of 32–128 it corresponds to a high (hazardous) level; more than 128 is considered very high (extremely hazardous) [13].

To assess the level of soil pollution by petroleum products, a classification based on their concentration was adopted [4)]: less than 1000 mg/kg corresponds to a permissible pollution level; 1000–2000 mg/kg to a low level; 2000–3000 mg/kg to a medium level; 3000–5000 mg/kg to a high level; more than 5000 mg/kg to a very high level.

Maps were constructed in the freely accessible software environment QGIS.

[2)] Baranova, T.E., Ilina, A.A. and Florovskaya, V.N., eds., 1966. [*Guidelines for Luminescent-Bituminological Research*]. Leningrad: Nedra, 1966, 112 p. (in Russian).

[3)] PND F 16.1:2.21-98. Quantitative Chemical Analysis of Soils. Method for Measuring the Mass Fraction of Petroleum Products in Soil and Ground Samples by the Fluorimetric Method Using a "Fluorat-02" Liquid Analyzer: Approved by FGU "TSEKA" 18 March 2003. Available at: https://gostrf.com/normadata/1/4293799/4293799929.pdf [Accessed: 10 April 2023] (in Russian).

[4)] *Procedure for Determining the Amount of Damage from Land Pollution by Chemicals*: Letter of the Ministry of Natural Resources of Russia dated 27 December 1993 No. 04-25/61-5678: Approved by Roskomzem on 10 November 1993 and the Ministry of Natural Resources of the Russian Federation on 18 November 1993. Available at: https://legalacts.ru/doc/pismo-minprirody-rossii-ot-27121993-n-04-2561-5678/ [Accessed: 10 April 2023] (in Russian).

Results and Discussion

In the composition of the surface horizons of Yalta soils, increased concentrations of Pb, Zn, and Cu are observed; they exceed background values at certain points by up to 7.0, 5.0, and 2.5 times, respectively. The average concentration coefficients for Pb, Zn, and Cu in the city are 4.0, 3.5, and 1.7, respectively (Table 1). No significant exceedances of the background are noted in the soils of the studied mountain slopes. The input of Pb, Zn, and Cu into Yalta soils is primarily associated with the operation of vehicles, particularly private cars. This is confirmed by samples taken in summer, when the intense influx of vacationers by personal transport leads to an increase in the concentrations of these elements, especially Pb, which is a typical indicator (topophilic element) of pollution from motor vehicles.

The priority pollutants for Yalta are Zn, Pb, and Cu (in descending order of significance), accounting for up to 60% of the mass of the determined chemical elements,

Table 1. Contents of heavy metals, metalloids and petroleum products in soils of Yalta and adjacent areas

Substance	C_f, mg/kg	Town		Route *1*		Route *2*	
		C_{avg}, mg/kg	C_c	C_{avg}, mg/kg	C_c	C_{avg}, mg/kg	C_c
Pb	24.0	95.6	**4.0**	23.7	1.0	24.8	1.0
Zn	72.0	249.0	**3.5**	76.3	1.1	76.3	1.1
Cu	30.0	52.0	**1.7**	22.0	0.7	24.3	0.8
Cr	54.0	69.4	1.3	48.7	0.9	60.3	1.1
Sr	165.0	207.0	1.3	165.3	1.0	117.1	0.7
Mn	462.0	574.4	1.2	375.0	0.8	537.7	1.2
V	49.0	58.9	1.2	40.7	0.8	56.7	1.2
Fe	22 302.0	26 135.8	1.2	19 623.7	0.9	21 758.0	1.0
As	13.3	12.8	1.0	12.8	1.0	10.7	0.8
Cd	26.0	24.3	0.9	27.0	1.0	N/D	N/D
Ni	73.0	57.2	0.8	46.7	0.6	50.7	0.7
PP	780	586.0	0.8	1675	**2.1**	1987.0	**2.5**

Note: C_f – background concentration; C_{avg} – average concentration or median concentration of petroleum products; C_c – concentration coefficient; PP – petroleum products; N/D – no data. Figures in bold show a significant exceedance over the background concentration of a chemical element or the median concentration of petroleum products.

while for the suburban area of the Yalta Nature Reserve they are Zn, Cr, Pb, and V with a total mass fraction of up to 50%.

In addition, two soil samples were taken near the town's industrial district in the northwestern part of Yalta (Darsan area), where sources of Pb and Zn may also be present. The elements enter the soil as a result of coal combustion in private houses, as well as the operation of thermal power plants. The high level of soil pollution in the Darsan area is consistent with data reported in the literature [14].

The calculated total soil pollution coefficient *Zc* is 6.47, which generally indicates an overall low level of pollution in the area.

Analysis of the collected soil samples for the presence of petroleum products revealed that in Yalta their concentration varies from 35 to 4450 mg/kg. The highest concentrations were noted on mountain slopes near roads and parking lots. The level of petroleum product concentration along the highway is characterized as high. On route *1*, the upper observation point was located near a parking lot at the Grushevaya Polyana cordon (entrance to the Crimean National Park). Along the other studied slope runs a road leading to Mount Ai-Petri – a frequently visited place. Parking lots are also located here, which determines the observed medium and high content of petroleum products (Fig. 2).

In the urbanized central part of Yalta, at two points, the petroleum product content is slightly above the permissible level and above the median value (1100 and 1275 mg/kg). The remaining sampling areas are characterized by permissible levels of petroleum products in soils. In new districts of the town and

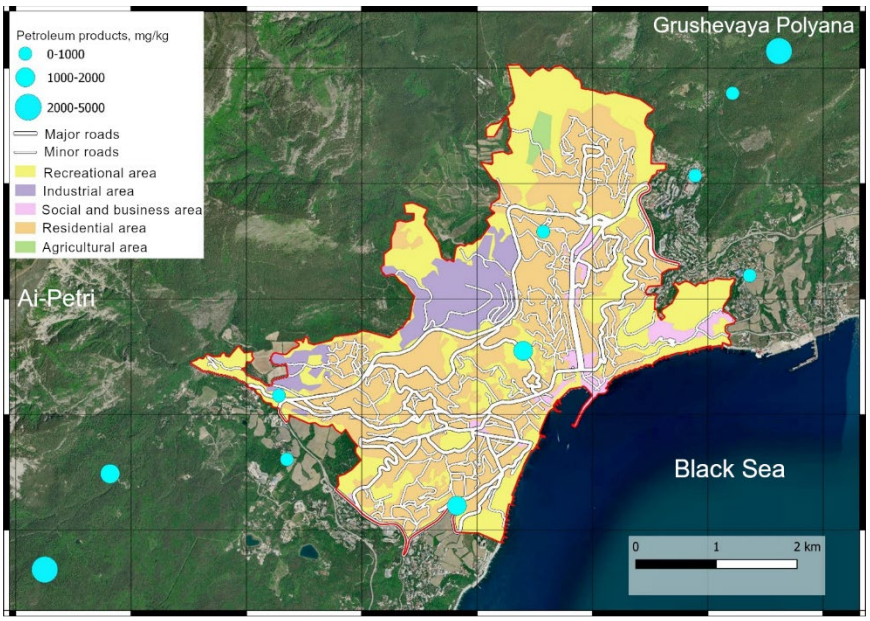

F i g . 2 . Petroleum product content in the soils of Yalta and adjacent mountain landscapes

the mountain-forest area, a permissible level of soil pollution by petroleum products was recorded (120–850 mg/kg). Only at one point on the highway does the median value of petroleum product content in soils slightly exceed the background one (by 10%).

In the soils and road dust of Alushta, Zn, Sb, Pb, Cu, Cd, and benzo(a)pyrene accumulate, which is associated with the use of motor vehicles [15, 16]. The leading role of motor vehicles in soil pollution is evidenced by the seasonality of chemical element concentrations – they increase during the summer tourist season. At the same time, the total pollution of soils and road dust by heavy metals is at a low level [17].

Fuel combustion at thermal power enterprises and in stoves for heating private houses are also a source of pollutants entering the soil. In the cold period of the year, an increase in the content of Mo and Bi, coming from the operation of heating

Table 2. Contents of heavy metals, metalloids and petroleum products in soils of Alushta and adjacent areas

Substance	C_f, mg/kg	Town		Route *1*		Route *2*	
		C_{avg}, mg/kg	C_c	C_{avg}, mg/kg	C_c	C_{avg}, mg/kg	C_c
Pb	40.0	63.6	**1.6**	69.3	**1.7**	44.3	1.1
Zn	159.0	225.2	**1.4**	248.3	**1.6**	108.7	0.7
Sr	134.0	184.4	**1.4**	200.3	**1.5**	128.0	1.0
Cr	68.0	75.2	1.1	38.3	0.6	85.7	1.3
Cu	55.0	60.2	1.1	156.0	**2.8**	44.3	0.8
Cd	22.0	23.0	1.0	22.0	1.0	24.0	1.1
Mn	674.0	634.6	0.9	675.3	1.0	828.7	1.2
Ni	65.0	60.8	0.9	36.3	0.6	75.7	1.2
As	17.0	15.6	0.9	8.4	0.5	15.2	0.9
V	77.0	67.8	0.9	43.0	0.6	87.0	1.1
Fe	32 143.0	26 832.0	0.8	20 165.0	0.6	35 311.0	1.1
PP	310.0	254.1	0.8	2783.3	**9.0**	185.0	0.6

Note: C_f – background concentration; C_{avg} – average concentration or median concentration of petroleum products; C_c – concentration coefficient; PP – petroleum products. Figures in bold show a significant exceedance over the background concentration of a chemical element or the median concentration of petroleum products.

systems, is observed in the soils of Alushta [17]. Pb source are coal combustion emissions [18]. Stove heating leads to significant accumulation of pollutants in low-rise residential areas of Yalta, where anomalies in the Pb, Zn, Sb, Sr, and Sn content have been noted [19].

On the territory of Alushta, at individual points in the soils, an excess of background concentrations of Pb, Zn, Sr, and Cu of up to four times is noted. The average concentration coefficients of Pb, Zn, and Sr for the soils of both the town and route *1* do not exceed 2.8 (Table 2).

The presence of Pb, Zn, and Sr in the soils of the mountain slopes along route *1* is explained by the proximity of the observation points to the villages of Lavanda, Verkhnyaya, and Nizhnyaya Kutuzovka. The busy Alushta – Simferopol highway passes through the latter two villages. In addition, a high content of Cu was noted on route *1*, which may be associated with the use of copper sulfate for spraying vineyards.

The priority pollutants for the urban territory of Alushta are Sr, Zn, and Pb (in descending order of significance), accounting for up to 40% of the mass of the determined chemical elements.

The priority chemical elements found in the soils of the suburban area of the mountain-forest zone on route *1* are Cu, Zn, Pb, and Sr. No priority chemical elements stand out in soil samples taken on route *2*.

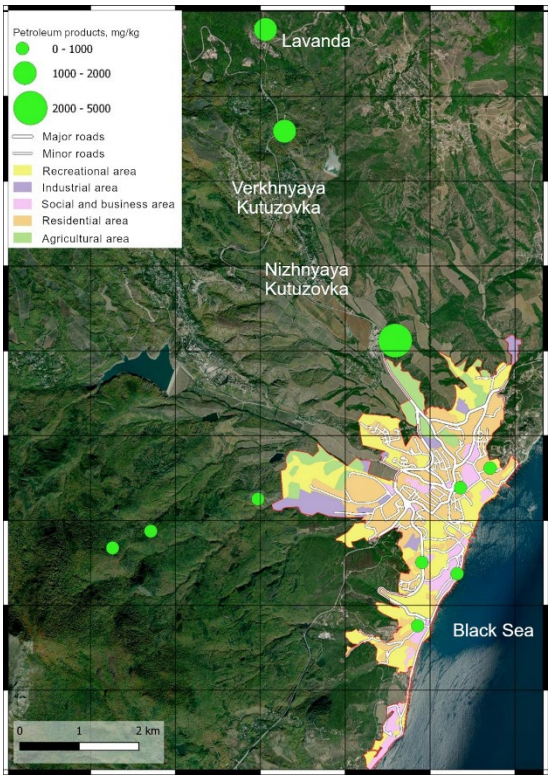

Fig. 3. Petroleum product content in the soils of Alushta and adjacent mountain landscapes

The total soil pollution coefficient *Zc* in Alushta and its suburbs is 4.48, indicating a low level of pollution.

On the territory of Alushta, both in the urbanized and mountain-forest zones, a permissible level of soil pollution by petroleum products was noted, except for areas along the Alushta – Simferopol highway (route *1*) (Fig. 3).

For Alushta, the highest concentrations of petroleum products (4750 mg/kg) are found on route *1*, near the busy Alushta – Simferopol highway and the adjacent villages of Lavanda, Verkhnyaya, and Nizhnyaya Kutuzovka.

At other points on the highway, the content of petroleum products in soils is 1600 and 2000 mg/kg (low level). The median content of petroleum products in soils along the highway exceeds the background value by nine times. This is explained by the large amount of traffic passing through the area. The concentration of petroleum products at points on route *2*, which has less intense traffic, is significantly lower (5–350 mg/kg). In the urbanized area, the petroleum product content is within permissible limits (20–630 mg/kg), but at one point exceeds the background value by two times.

In the soils of Sudak, an excess of background values for five elements (Mn, Cu, Zn, Pb, and V) is noted (Table 3). The increased content of Mn and Cu is likely

T a b l e 3 . Contents of heavy metals, metalloids and petroleum products in soils of Sudak and adjacent areas

Substance	C_f, mg/kg	Town		Route *1*		Route *2*	
		C_{avg}, mg/kg	C_c	C_{avg}, mg/kg	C_c	C_{avg}, mg/kg	C_c
Mn	193.0	532.2	**2.8**	517.0	**2.7**	617.7	**3.2**
Cu	17.0	40.4	**2.4**	39.0	**2.3**	30.3	**1.8**
Zn	53.0	118.2	**2.2**	97.3	**1.8**	76.3	1.4
Pb	16.0	30.2	**1.9**	29.3	**1.8**	26.7	**1.7**
V	40.0	58.4	**1.5**	66.7	**1.7**	54.7	1.4
Ni	55.0	65.4	1.2	71.3	1.3	66.3	1.2
Fe	24 206.0	26 387.6	1.1	28 824.3	1.2	20 722.7	0.9
As	11.6	12.0	1.0	12.9	1.1	12.6	1.1
Cr	65.0	60.0	0.9	72.7	1.1	56.3	0.9
Sr	227.0	204.2	0.9	201.3	0.9	159.0	0.7
PP	35.0	243.4	7.0	251.7	7.1	33.0	0.9

Note: C_f – background concentration; C_{avg} – average concentration or median concentration of petroleum products; C_c – concentration coefficient; PP – petroleum products. Figures in bold show a significant exceedance over the background content of a chemical element or the median content of petroleum products.

related to agricultural activities. On the slope of Mount Lysaya, located to the west of the town, near agricultural lands, a jump in Mn concentration is noted.

Cu, Zn, and Pb sources in Sudak, as in other SCC cities, are motor vehicles and thermal power facilities. In general, the concentrations of these elements are low compared to the concentrations in Yalta and Alushta. The priority pollutants for Sudak are Mn, Cu, Zn, and Pb, accounting for up to 60% of the mass of the determined chemical elements. The concentrations of priority elements in the suburban and urban areas of Sudak differ insignificantly. On Mount Lysaya on route *2*, a noticeable increase in the share of Mn – up to 40% – is observed.

Samples taken in the area of Sudak contain from 5 to 1125 mg/kg of petroleum products, which corresponds to a permissible and low level of soil pollution. In Sudak, petroleum product concentrations are significantly lower than in the other towns considered. This may be due to some isolation of the city from the main Crimean highways and the barrier role of the mountains, protecting the built-up area from the influence of northern winds. The median concentration of petroleum products in Sudak is very low at 35 mg/kg.

The maximum concentration of petroleum products (1125 mg/kg) is noted in the center of Sudak between two main roads with heavy intra-city and transit traffic (Fig. 4). The pollution level at this point, located in a residential area, can be

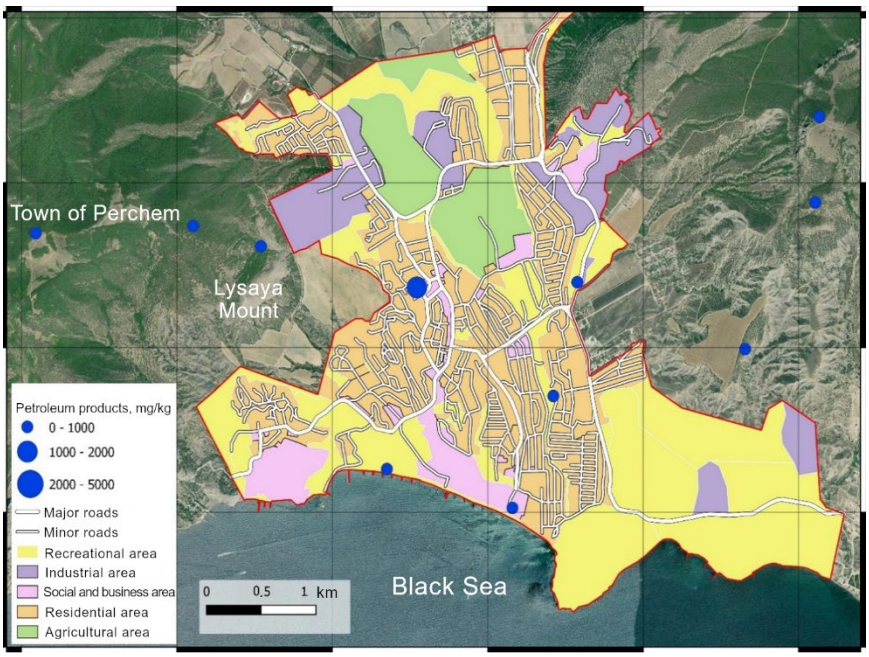

Fig. 4. Petroleum product content in the soils of Sudak and adjacent mountain landscapes

classified as low. When compared with the median value, a significant increase in the pollution level is noticeable – in the town and on route *1*, the petroleum product content is 7 and 7.1 times higher than the background value, respectively.

The calculated total soil pollution coefficient *Zc* for Sudak is 6.93, which also indicates a low level of pollution.

Conclusion

The assessment of soil pollution in three resort towns of the SCC – Yalta, Alushta, and Sudak – by heavy metals and petroleum products allowed us to draw the following conclusions.

In the soils of residential areas of the three towns under study, an excess of Pb and Zn concentrations is noted. In Yalta, their maximum concentrations exceed the background by 3.5–4 times. In addition, Cu, Sr, Mn, and V are actively accumulated in the soils of resort towns on the SCC. The number of soil pollutants is higher in Sudak, where five elements accumulate (Mn, Cu, Zn, Pb, and V).

In the soils of suburban areas of the SCC near roads, Pb, Zn, Cu, Sr, Mn, and V accumulate. The content of petroleum products in soils is an order of magnitude higher along major suburban highways compared to the city limits.

The main source of heavy metals and metalloids, as well as petroleum products, in the studied cities is motor vehicles. Its influence increases in the summer season with the influx of vacationers – their number reached 9.39 million people, with 41% of them visiting the SCC. Another source of pollution is thermal power facilities and stoves in low-rise buildings.

The calculated total pollution index *Zc* for Yalta, Alushta, and Sudak does not exceed 6.93, which indicates a relatively low level of soil pollution in the studied cities.

The results of the study can be used in environmental monitoring for the formulation of regional environmental policy in resort towns and for addressing the problem of soil pollution.

REFERENCES

1. Golubeva, E.I., Kashirina, E.S. and Novikov, A.A., 2025. Regional System of Natural Protected Areas of the Crimea: State and Geoecological Problems. *Bulletin of the Russian Geographical Society*, 157(1), pp. 28–43. https://doi.org/10.7868/S3034538325010033 (in Russian).
2. Mikhailenko, A.V., Ruban, D.A., Ermolaev, V.A. and van Loon, A.J. (Tom), 2020. Cadmium Pollution in the Tourism Environment: A Literature Review. *Geosciences*, 10(6), 242. https://doi.org/10.3390/geosciences10060242
3. Alekseyenko, V.A., Puzanov, A.V., Alekseyenko, A.V. and Shvydkaya, N.V., 2017. On Some Ecologic and Geochemical Features of Soils of Canary Islands Resorts. *Bulletin of Altai State Agricultural University*, (1), pp. 72–83 (in Russian).
4. Pomelyaiko, I.S., 2017. Ecological and Geochemical Ranking of Residential Areas in Resort and Industrial Cities of the Russian Federation by Three Soil Contamination Criteria. *Geoekologiya*, (1), pp. 28–39 (in Russian).

5. Pomelyayko, I.S., 2018. The Concentration of a Series of Substances 1-2 Class of Hazards and Long-Living Technogenic Radionuclides ^{137}Cs and ^{90}Sr in Natural Environments of the City-Resorts of the Region of the Caucasian Mineral Waters. *Nedropolzovanie XXI vek = 21 Century Subsoil Use*, (5), pp. 142–151 (in Russian).
6. Gupta, V., Bisht, L., Deep, A. and Gautam S., 2022. Spatial Distribution, Pollution Levels, and Risk Assessment of Potentially Toxic Metals in Road Dust from Major Tourist City, Dehradun, Uttarakhand India. *Stochastic Environmental Research and Risk Assessment*, 36(10), pp. 3517–3533. https://doi.org/10.1007/s00477-022-02207-0
7. Ciarkowska, K., 2018. Assessment of Heavy Metal Pollution Risks and Enzyme Activity of Meadow Soils in Urban Area under Tourism Load: A Case Study from Zakopane (Poland). *Environmental Science and Pollution Research*, 25(14), pp. 13709–13718. https://doi.org/10.1007/s11356-018-1589-y
8. Díaz Rizo, O., Buzón González, F., López, J.O.A. and Denis Alpízar O., 2015. Heavy Metal Levels in Dune Sands from Matanzas Urban Resorts and Varadero Beach (Cuba): Assessment of Contamination and Ecological Risks. *Marine Pollution Bulletin*, 101(2), pp. 961–964. https://doi.org/10.1016/j.marpolbul.2015.10.025
9. Sukhacheva, E.Y. and Revina, Y.S., 2020. Medium-Scale Soil Map of the Crimea Southern Coast. *Eurasian Soil Science*, 53(4), pp. 397–404. https://doi.org/10.1134/S1064229320040146
10. Neaman, A., Schoffer, J.T., Navarro-Villarroel, C., Pelosi, C., Peñaloza, P., Dovletyarova, E.A. and Schneider, J., 2024. Copper Contamination in Agricultural Soils: A Review of the Effects of Climate, Soil Properties, and Prolonged Copper Pesticide Application in Vineyards and Orchards. *Plant, Soil and Environment*, 70(7), pp. 407–417. https://doi.org/10.17221/501/2023-PSE
11. Gabechaya, V.V., Andreeva, I.V. and Morev, D.V., 2024. Ecological and Geochemical Assessment of the Accumulation and Migration of Heavy Metals in the Soil of Intensive Vineyards of Different Ages in the Conditions of the Eroded Landscape of the Southern Coastal Zone of Crimea. *Agroekoinfo*, (6), 16 (in Russian).
12. Lisetskii, F.N. and Zelenskaya, E.Ya., 2023. Differences in the Content of Heavy Metals in the Soils of the Southern Coast of Crimea (Spatio-Temporal Analysis). *Ekosistemy*, (34), pp. 81–91 (in Russian).
13. Saet, Yu.E., Revich, B.A., Yanin, E.P., Smirnova, R.S., Basharkevich, I.L., Onishchenko, T.L., Pavlova, L.N., Trefilova, N.Ya., Achkasov, A.I. and Sarkisyan, S.Sh., 1990. [*Geochemistry of the Environment*]. Moscow: Nedra, 335 p. (in Russian).
14. Vetrova, N.M., Ivanenko, T.A., Sadykova, G.E. and Sudjeva, D.V., 2020. On the Assessment of the Environmental Ecological State in Coastal Cities. In: IOP, 2020. *IOP Conference Series: Materials Science and Engineering. International Scientific Conference "Construction and Architecture: Theory and Practice of Innovative Development" (CATPID-2020) – Part 1 26-30 September 2020, Nalchik, Russian Federation*. IOP Publishing, 2020. Vol. 913, iss. 5 "Mechanics of a Deformable Solid". 052035. https://doi.org/10.1088/1757-899X/913/5/052035
15. Bezberdaya, L., Kosheleva, N., Chernitsova, O., Lychagin, M. and Kasimov, N., 2022. Pollution Level, Partition and Spatial Distribution of Benzo(a)pyrene in Urban Soils, Road Dust and their PM10 Fraction of Health-Resorts (Alushta, Yalta) and Industrial (Sebastopol) Cities of Crimea. *Water*, 14(4), 561. https://doi.org/10.3390/w14040561
16. Bezberdaya, L., Chernitsova, O., Lychagin, M., Aseeva, E., Tkachenko, A. and Kasimov, N., 2024. Pollution of a Black Sea Coastal City: Potentially Toxic Elements in Urban Soils, Road Dust, and their PM10 Fractions. *Journal of Soils and Sediments*, 24(10), pp. 3485–3506. https://doi.org/10.1007/s11368-024-03893-9

17. Kasimov, N.S., Bezberdaya, L.A., Vlasov, D.V. and Lychagin M.Y., 2019. Metals, Metalloids, and Benzo[a]pyrene in pm10 Particles of Soils and Road Dust of Alushta City. *Eurasian Soil Science*, 52(12), pp. 1608–1621. https://doi.org/10.1134/S1064229319120068
18. Kashirina, E.S., Medvedkov, A.A. and Novikov, A.A., 2022. Assessment of the Surface Atmospheric Air State in the Southwestern Crimea According to Lichenoinification Data. *Bulletin of the Tomsk Polytechnic University. Geo Assets Engineering*, 333(8), pp. 126–138. https://doi.org/10.18799/24131830/2022/8/3229 (in Russian).
19. Bezberdaya, L.A. and Kasimov, N.S., 2022. Levels of Accumulation of Heavy Metals and Metalloids in Soils, Road Dust and Their PM10 Fractions in Yalta. In: F. A. Mkrtchyan, ed., 2022. *Proceedings of the XV International Symposium Ecoinformatics Problems, Moscow, 6-8 December, 2022*. Moscow: The Moscow Sciences Engineering A.S. Popov Society for Radio, Electronics and Communication, pp. 189–193 (in Russian).

Submitted 26.02.2025; accepted after review 5.06.2025;
revised 18.12.2025; published 31.03.2026

About the authors:

Anastasia V. Baranenko, Lomonosov Moscow State University (1, Leninskie Gory, 199011, Moscow, Russia), Master, **IstinaResearcherID (IRID): 232201591**, *evpanetka@mail.ru*

Elena I. Golubeva, Professor, Lomonosov Moscow State University (1, Leninskie Gory, 199011, Moscow, Russia), Dr.Sci (Biology), **ORCID ID: 0000-0001-9595-5974, Scopus Author ID: 16546135000, ResearcherID: L-7520-2015**, *egolubeva@gmail.com*

Ekaterina S. Kashirina, Senior Researcher, A. O. Kovalevsky Institute of Biology of the Southern Seas of RAS (2, Nakhimov Ave., 299011, Sevastopol, Russia), CSc (Geogr.), **ORCID ID: 0000-0002-8808-3255, Scopus Author ID: 57204474315, ResearcherID: 3668033**, *e_katerina.05@mail.ru*

Contribution of the authors:

Anastasia V. Baranenko – collection of information for the study, processing, analysis and description of the study results

Elena I. Golubeva – problem statement, discussion of the results, correction of the article text

Ekaterina S. Kashirina – discussion of the results, article text preparation

All the authors have read and approved the final manuscript.

Original paper

International Environmental Standards as a Regulator of Marine Economic Activities in the Arctic

Zh. V. Vasileva [1] *, M. V. Vasekha [2], D. A. Erofeev [1], A. R. Gafurov [1], E. A. Rumiantceva [1]

[1] *Murmansk Arctic University, Murmansk, Russia*

[2] *Kola Scientific Center of the Russian Academy of Sciences, Apatity, Russia*

* *e-mail: kuchugura@mail.ru*

Abstract

Currently, there is a tendency to tighten international environmental regulations in the field of maritime shipping. This study analyzes possible consequences of the introduction of environmental restrictions by the International Maritime Organization (IMO) on marine activities in the Arctic region, including the ban on the use of heavy fuel oil, presented in IMO Resolution MEPC.329(76), and the requirements of the IMO 2023 Strategy to Reduce Greenhouse Gas Emissions. The volume of use of various types of marine fuel on the Northern Sea Route in 2024 was analyzed. An assessment of the use of heavy fuel oil by ships and a risk analysis for the development of large-tonnage Arctic offshore projects were carried out with the implementation of IMO Resolution MEPC.329(76). A forecast calculation of the compliance of greenhouse gas emissions with cargo turnover on the NSR has been made, taking into account the targets of the IMO 2023 Strategy. It is shown that without switching to environmentally friendly fuels and the introduction of innovative emission reduction technologies, the required reduction in emissions by 2030 and 2040 can only be achieved by significantly limiting cargo turnover on the Northern Sea Route. The IMO's greenhouse gas emissions reduction tools and the possibility of legal mechanisms for implementing the IMO Strategy were analyzed.

Keywords: Arctic, arctic water area, Northern Sea Route, maritime shipping, heavy fuel oil, greenhouse gases, International Maritime Organization

Acknowledgements: The work was supported by a grant from the Russian Science Foundation (project No. 25-27-20102).

For citation: Vasileva, Zh.V., Vasekha, M.V., Erofeev, D.A., Gafurov, A.R. and Rumiantceva, E.A., 2026. International Environmental Standards as a Regulator of Marine Economic Activities in the Arctic. *Ecological Safety of Coastal and Shelf Zones of Sea*, (1), pp. 129–145.

© Vasileva Zh. V., Vasekha M. V., Erofeev D. A., Gafurov A. R., Rumiantceva E. A., 2026

This work is licensed under a Creative Commons Attribution-Non Commercial 4.0 International (CC BY-NC 4.0) License

Международные экологические нормативы как регулятор морехозяйственной деятельности в Арктике

Ж. В. Васильева [1] *, М. В. Васёха [2], Д. А. Ерофеев [1], А. Р. Гафуров [1], Е. А. Румянцева [1]

[1] *Мурманский арктический университет, Мурманск, Россия*
[2] *Кольский научный центр Российской академии наук, Мурманск, Россия*
** e-mail: kuchugura@mail.ru*

Аннотация
В настоящее время наблюдается тенденция к ужесточению международных экологических нормативов в сфере морского судоходства. В работе проанализированы возможные последствия введения Международной морской организацией (ИМО) экологических ограничений на морехозяйственную деятельность в Арктическом регионе, включая запрет на использование судового мазута (резолюция ИМО *MEPC*.329(76)) и требования Стратегии ИМО 2023 по сокращению выбросов парниковых газов. Проанализирован объем использования различных видов судового топлива на Северном морском пути в 2024 г., выполнена оценка использования судами мазута и анализ рисков для развития крупнотоннажных арктических шельфовых проектов при введении в действие резолюции *MEPC*.329(76). Сделан прогнозный расчет соответствия выбросов парниковых газов грузообороту на Северном морском пути исходя из целевых показателей Стратегии ИМО 2023. Показано, что без перехода на экологически чистые виды топлива и внедрения инновационных технологий снижения эмиссий требуемое сокращение выбросов к 2030 и 2040 гг. может быть достигнуто лишь путем значительного ограничения грузооборота на Северном морском пути. Выполнен анализ разработанных ИМО инструментов сокращения выбросов парниковых газов с судов и возможностей правовых механизмов реализации Стратегии ИМО.

Ключевые слова: Арктика, арктическая акватория, Северный морской путь, судоходство, судовое топливо, парниковые газы, Международная морская организация

Благодарности: работа выполнена при поддержке гранта Российского научного фонда (проект № 25-27-20102).

Для цитирования: *Васильева Ж. В., Васёха М. В., Ерофеев Д. А., Гафуров А. Р. и др.* Международные экологические нормативы как регулятор морехозяйственной деятельности в Арктике // Экологическая безопасность прибрежной и шельфовой зон моря. № 1. С. 129–145. EDN UMWFAI.

Introduction

In recent years, there has been an increase in the key indicators of maritime activity in the Arctic. The total distance sailed increased by 111% from 2013 to 2024, reaching 12.9 million nautical miles [1)], and the number of unique vessels amounted to 1,782, which is 37% higher than in 2013 [1].

The increase in activity in the Russian sector of the Arctic from 2014 to 2020 is largely attributed to the development of major offshore projects, as evidenced

[1)] PAME, 2024. The Increase in Arctic Shipping: 2013-2023. Available at: https://oaarchive.arctic-council.org/items/01ddf449-9048-4d6a-a056-65303831bb63 [Accessed: 20 February 2026].

by the growth in cabotage traffic along the Northern Sea Route (NSR) from 4 million tonnes in 2014 to 32 million tonnes in 2020 [2]. Increased activity has also been observed in the Canadian Arctic [3], where shipping volumes have nearly tripled over the past decade, and further growth is expected. Against this backdrop, concerns are also growing regarding the negative impact of maritime transport on the vulnerable Arctic natural environment [4].

In 2009 [2] and 2011 [3], the Working Group on the Protection of the Arctic Marine Environment (PAME) of the Arctic Council highlighted the environmental risks associated with spills of heavy fuel oil (HFO) in the Arctic. Furthermore, the International Maritime Organization (IMO) noted that emissions from ships resulting from global maritime trade increased by 9.6%, from 9.77 billion tonnes in 2012 to 10.76 billion tonnes in 2018 [4].

In this context, the IMO, as the specialized agency of the United Nations responsible for the safety and security of shipping and the prevention of marine pollution by ships, developed the Polar Code – the International Code for Ships Operating in Polar Waters. The Code established the first mandatory, enforceable standards and recommended measures for managing Arctic shipping. In 2018, the IMO presented its Initial IMO Strategy on the Reduction of GHG Emissions from Ships, which declared an ambition to reduce greenhouse gas emissions in the long term [5]. This decision received support from environmental organizations and the public, as they encouraged Arctic States to systematically proceed with the decarbonization of the shipping industry and the wider adoption of alternative fuels [6].

However, in 2021, a landmark IMO decision was adopted to prohibit the use and carriage for use of HFO as fuel in Arctic waters [7], and in 2023, the new 2023 IMO Strategy on the Reduction of GHG Emissions from Ships was adopted, introducing significantly stricter environmental requirements concerning ship emission levels. The decisions adopted by the IMO could significantly impact the development dynamics of Arctic territories and have sparked debates regarding a certain lack of foresight and their premature nature [8, 9].

Unlike other sea areas worldwide, shipping in the Arctic has its own specific characteristics: it plays a unique role in ensuring the economic sustainability of remote Arctic regions and the livelihoods of indigenous peoples [10], as well as in the development of Arctic resources, which are critically important for the global economy [11]. The development of maritime activities in Arctic waters is one of the key objectives of the national policy of the Russian Federation

---

[2] Ellis, B. and Brigham, L., eds., 2009. Arctic Marine Shipping Assessment 2009 Report (AMSA). Arctic Council, 2009. 194 p. Available at: https://pame.is/images/03_Projects/AMSA/AMSA_2009_report/AMSA_2009_Report_2nd_print.pdf [Accessed: 28 January 2026].

[3] IMO, 2020. Assessment of the Benefits and Impacts Associated with a Ban on the Use and Carriage of Heavy Fuel Oil as Fuel by Ships Operating in the Arctic: PPR7/Inf.16. IMO, 16 p.

[4] IMO, 2020. Fourth IMO GHG Study 2020. London: IMO, 524 p. Available at: https://wwwcdn.imo.org/localresources/en/OurWork/Environment/Documents/Fourth%20IMO%20GHG%20Study%202020%20-%20Full%20report%20and%20annexes.pdf [Accessed: 28 January 2026].

in the Arctic [5], which determines the transformation of the Arctic zone into a strategic resource base for Russia's economic growth, and the NSR into a global transport artery [12].

Against the backdrop of diminishing ice cover [1] in the Arctic, the development of Arctic projects becomes particularly promising. For instance, plans for the development of the NSR envisage an increase in cargo traffic to 220 million tonnes [6] by 2035. The introduction of environmental regulations on shipping could significantly impact the development and sustainability of economic ties in the Arctic. Currently, there is no clear understanding of the consequences of such environmental requirements.

This article examines the contradictions between the IMO's incoming environmental requirements and the national interests of the Russian Federation related to the sustainable development of the Arctic and the implementation of key directions for the development of maritime activities in the Arctic region. The aim of the work is a comprehensive analysis of the consequences of the introduction of IMO restrictions on maritime activities in the Arctic region, specifically concerning the prohibition on the use of HFO (IMO Resolution MEPC.329(76)) and the requirements of the 2023 IMO Strategy on the Reduction of GHG Emissions from Ships.

Research methods

The study included a legal and regulatory analysis of international and Russian documents regulating the prohibition on the use of HFO in the Arctic and the implementation of requirements for the reduction of greenhouse gas emissions: the United Nations Convention on the Law of the Sea (UNCLOS), the International Convention for the Prevention of Pollution from Ships (MARPOL), the Polar Code, IMO session materials and resolutions, the IMO Strategy on the Reduction of GHG Emissions from Ships, Federal Law no. 155-FZ of July 31, 1998 "On Internal Maritime Waters, Territorial Sea, and Contiguous Zone of the Russian Federation," and Federal Law no. 191-FZ of December 17, 1998 "On the Exclusive Economic Zone of the Russian Federation."

The statistical analysis included processing data [7] on shipping activity in the NSR waters, analyzing the type and volume of fuel consumed by vessels, and identifying the types of vessels and categories of traffic in the NSR waters that are subject to the introduced prohibitions and restrictions.

The dynamics of cargo turnover on the NSR and ship emissions were forecast based on data on cargo turnover on the NSR [4] and the calculated indicators of greenhouse gas emissions per tonne of cargo for 2024.

---

[5] On the Strategy for Developing the Arctic Zone of the Russian Federation and Ensuring National Security for the Period up to 2035: Decree of the President of the Russian Federation no. 645 of October 26, 2020. Garant: Legal Reference System. Available at: https://base.garant.ru/74810556/ [Accessed: 9 February 2026] (in Russian).

[6] Government of the RF, 2022. *On Approval of Plan of Development of the Northern Sea Route by 2035*. Resolution of the RF Government no. 2115-p as of 1 August 2022. Available at: http://government.ru/docs/46171 [Accessed: 9 February 2026] (in Russian).

[7] Unified Platform of Digital Services of the Northern Sea Route. Available at: https://arctica.rosatom.ru [Accessed: 9 February 2026] (in Russian).

Research results and discussion

The IMO prohibition on the use and carriage of heavy fuel oil in Arctic waters

As of July 1, 2024, IMO Resolution MEPC.329(76) (regulation 43A in chapter 9 of MARPOL Annex I) entered into force, amending the legal regime for the use of marine fuel in Arctic waters and introducing a prohibition on the use and carriage for use as fuel of HFO in Arctic waters. In accordance with paragraph 1.2 of regulation 43 of MARPOL Annex I, HFO, subject to the prohibition, is defined as petroleum products with a density exceeding 900 kg/m³ at a temperature of 15°C or a kinematic viscosity exceeding 180 mm²/s at a temperature of 50 °C. This resolution is based on the precautionary approach enshrined in Principle 15 of the 1992 Rio Declaration on Environment and Development, which advocates the adoption of precautionary measures even in the absence of full scientific certainty. The scope of the introduced prohibition applies to all vessels, except those engaged in ensuring the safety of ships, or in search and rescue operations, and vessels dedicated to oil spill preparedness and response.

The Russian legal system incorporates such international obligations through the ratification of the principal maritime conventions. Federal Law no. 155-FZ of July 31, 1998, "On Internal Maritime Waters, Territorial Sea and Contiguous Zone of the Russian Federation" and Federal Law no. 191-FZ of December 17, 1998, "On the Exclusive Economic Zone of the Russian Federation", provide the legal framework for implementing international environmental requirements in the Arctic waters. Currently, IMO Resolution MEPC.329(76) is not in effect for Russia pending specific approval from the Russian government [8)].

To forecast the potential consequences of the entry into force of IMO Resolution MEPC.329(76) for the Russian Federation, an assessment was made of the use of various fuel types by vessels on the NSR, and an analysis of the risks for the development of Arctic offshore projects was conducted.

In total, 392 vessels operated on the NSR in 2024, of which 228 vessels used HFO. As follows from statistical data on the bunkering of vessels for 2024 (Fig. 1), HFO remains the predominant type of fuel.

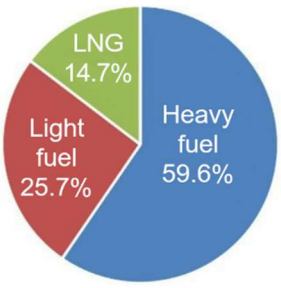

Fig. 1. Use of fuel (thous. t) by vessels of various types in 2024

[8)] Declaration by the Russian Federation pursuant to Article 16 (2)(f)(ii) of MARPOL. Available at: https://portnews.ru/upload/basefiles/2677_PMP.1-Circ.228%20-%20Declaration%20by%20the%20Russian%20Federation%20pursuant%20to%20Article%2016%20(2)(f)(ii)%20of%20MARPOL%20(Secretariat).pdf [Accessed: 9 February 2026] (in Russian).

Its share of total consumption was slightly less than 60%. About a quarter of bunkering volumes accounted for light fuel oil, while the share of LNG (liquefied natural gas) did not reach 15%.

An analysis of HFO consumption by different vessel types on the NSR (Table 1) established that the largest volumes – 37.5% of the total bunkering volume – are consumed by Arctic gas carriers of the Yamalmax class (LNG tankers). Such vessels are equipped with multi-fuel engines capable of running on diesel fuel, HFO, and the LNG they carry. While LNG is considered the primary fuel and HFO a backup option, shipowners find it more profitable to use HFO.

Furthermore, significant volumes of HFO are consumed by oil tankers – 27.93%, dry cargo ships – 9.74%, and icebreakers – 9.23%. The use of HFO by container ships (4.62%), research vessels (4.43%), tugs (2.33%), and bulk carriers (1.31%) constitutes a relatively small share of the total HFO consumption on the NSR.

T a b l e 1. Use of fuel (thousand tonnes) by various vessel types in 2024

Vessel type	Fuel type		
	Heavy fuel	Light fuel	LNG
Tankers	120.48	36.63	–
LNG-tankers	161.68	57.85	106.25
Icebreakers	39.80	23.85	–
Dry cargo ships	42.00	21.38	–
Bulk carriers	5.65	1.94	–
Tow boats	10.05	6.70	–
Container carriers	19.91	3.05	–
Other cargo vessels	4.89	2.80	–
Supply vessels	0.63	4.15	–
Research vessels	19.10	14.05	–
Others	7.14	13.88	–

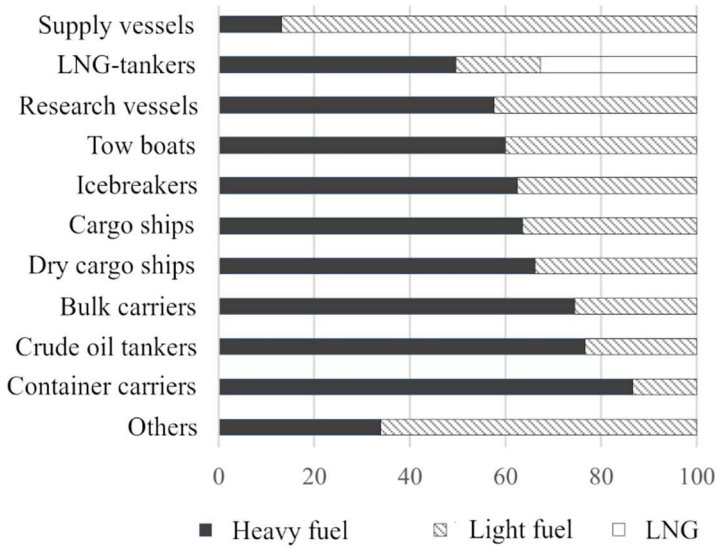

Fig. 2. Fuel consumption by vessels of different types, %

The predominance of heavy fuel oil usage in the NSR water area in 2024 (Fig. 2) is observed for container ships at 86.7%, tankers at 76.7%, and bulk carriers and dry cargo ships at 74.5% and 66.3% respectively.

The prohibition on the use and carriage of heavy fuel oil in Arctic waters affects vessels that are crucial for implementing the objectives outlined in strategic documents for the development of the Russian Arctic and the NSR, and which handle the largest volumes of traffic (Table 2). Primarily, these are vessels supporting projects for the extraction of hydrocarbons (oil, LNG) and mineral raw materials in the Arctic, as well as those performing Northern Delivery tasks.

For instance, cargo transportation for the Norilsk Nickel project on the Murmansk–Dudinka route is provided by a fleet of six vessels of various types, the Aker ACS 650 project with Arc6 ice class, all operating on heavy fuel oil. Oil extracted in the Timan-Pechora oil and gas province is exported year-round via Lukoil's Varandey loading terminal to the port of Murmansk by a fleet of three Arc6 class shuttle tankers with a deadweight of about 70,000 tonnes, also operating on heavy fuel oil. A key element of the Novy Port project logistics is six Arc7 ice-class shuttle tankers of the "Shturman" series (Project SHI 42K Arctic Shuttle Tanker), transporting oil year-round from the "Gate of the Arctic" terminal to a transshipment point in Murmansk. The main engines of the "Shturman" series vessels operated exclusively on heavy fuel oil in 2024. The transportation of liquefied natural gas from the Yamal LNG and Arctic LNG 2 projects is carried out by a fleet of 20 Arc7 ice-class gas carriers. Although the primary fuel for these LNG tankers is intended to be the LNG they carry, in practice, these vessels predominantly use heavy fuel oil.

Table 2. Percentage distribution of fuel types consumed by vessels of Arctic projects in 2024, %

Arctic project	Heavy fuel	Light fuel	LNG
Northern delivery	80.85	19.15	–
New Port Project	98.40	1.60	–
OJSC MMC Norilsk Nickel	98.50	1.50	–
NSR icebreaker support	62.60	37.50	–
LNG Project of PJSC *Novatek* (LNG transportation)	49.60	17.80	32.7
LNG Project of PJSC *Novatek* (SGC transportation)	56.40	43.60	–

Note: SGC – stable gas condensate.

The socially significant Northern delivery ensures food and energy security for populations in remote Arctic regions. A significant portion of these deliveries is carried out by vessels using HFO.

It should be noted that the fleet of major Arctic projects uses HFO due to its availability and relatively low cost. Retrofitting vessels to run on LNG or other alternative fuels requires significant investment. Furthermore, the cost of alternative fuels may be higher than that of HFO, which would increase operating expenses, reduce project profitability, and increase the share of transport costs in the price of goods, including those for Northern delivery.

Reducing the use of HFO is one of the key tasks in the context of ensuring the environmental safety of the Arctic region. However, the restrictions of IMO Resolution MEPC.329(76) must be implemented with due regard to national interests, based on a phased transition to environmentally friendly fuels while maintaining the necessary pace of development of maritime activities in the Arctic waters.

A similar assessment of the consequences of the entry into force of IMO MEPC.329(76) was conducted by Canadian scientists in 2020 [3]. It was found that of the total number of vessels operating in the Canadian Arctic from 2010 to 2018,

about 37% used HFO. These vessels accounted for approximately 45% of the total distance sailed in that water area. The researchers noted that a prohibition on the use and carriage of HFO could significantly impact Canadian Arctic communities and the economy, which depend on maritime shipping.

The authors of work [9] rightly note that the prohibition on the use of HFO will most severely affect Canada and Russia, as the states with the longest coastlines, because it will reduce the attractiveness of new shipping routes and impact regional economic development. It is worth noting that Canada availed itself of a postponement of the entry into force of IMO Resolution MEPC.329(76) until July 1, 2029.

Meanwhile, the geographical zone of application of IMO Resolution MEPC.329(76) is defined according to the Polar Code (Fig. 3, *a*). An analysis of this zone shows that it encompasses the area of active shipping on the NSR. At the same time, the prohibition does not extend to the coast of Scandinavia and the Kola Peninsula but affects the socially and economically significant NSR area for the Russian Federation, while allowing for active trade and navigation in the North Atlantic by vessels using HFO.

Visualization of shipping intensity in the Arctic (Fig. 3, *b*) shows that the Arctic sector including the economic zone of Norwegian waters, where the prohibition on the use of HFO does not apply, is the water area with the highest density of maritime traffic and frequency of voyages, and is characterized by more intensive maritime activity than the NSR.

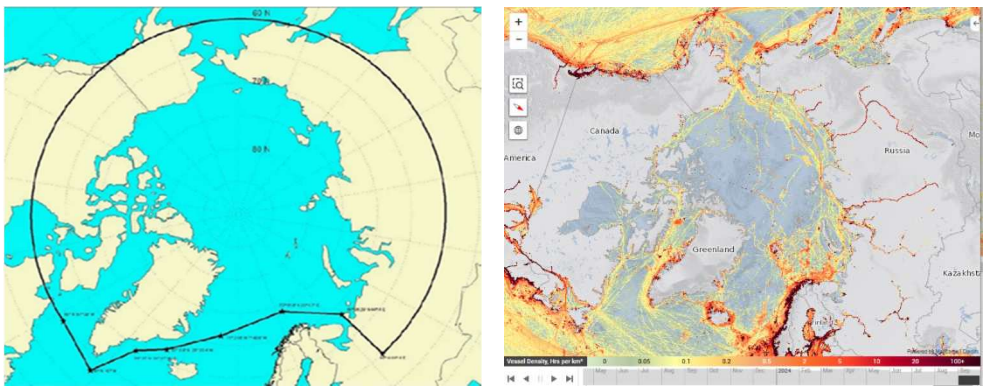

a ***b***

Fig. 3. The zone of prohibition on the use of heavy fuel oil (*a*) and a visualization of arctic navigation intensity, h/km^2, in September 2024. Source: Global Maritime Traffic service (Available at: https://globalmaritimetraffic.org/gmtds.html) (*b*)

Contemporary variants of scientifically based boundaries of the Arctic (Fig. 4), adopted by AMAP (Arctic Monitoring and Assessment Programme), are determined by the physical-geographical features of the region [9]. The zone established in the IMO Resolution does not coincide with any of the existing boundary options proposed by AMAP and lacks scientific justification. It is evident that an HFO spill off the northern coasts of the Scandinavian Peninsula would cause no less harm to Arctic ecosystems than a spill within the prohibition zone according to IMO Resolution MEPC.329(76).

The introduction of IMO restrictions is also justified by the increased risks of petroleum spills in Arctic conditions. However, ice-class vessels that meet the requirements of the Polar Code are structurally adapted for safe navigation in ice, including the prevention of fuel spills. The current navigation regime on the NSR permits only certified vessels and regulates navigation depending on ice conditions. Thus, the necessity for a complete prohibition on the use of HFO requires additional justification, considering existing control mechanisms and technical standards for shipping in polar waters.

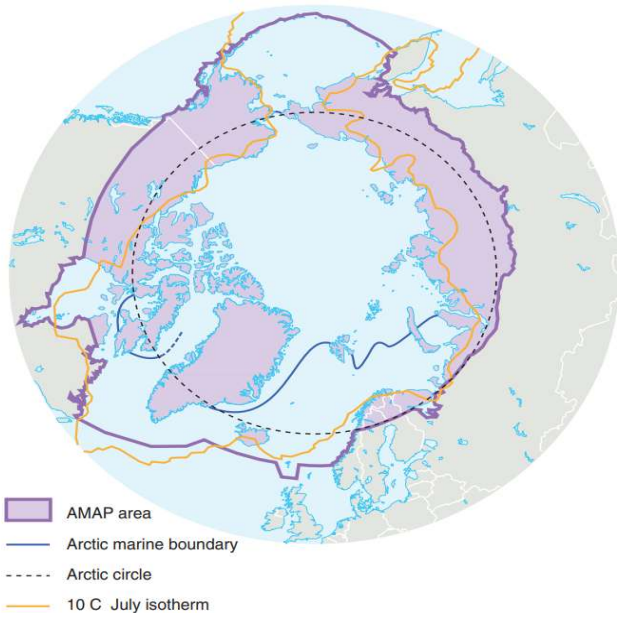

Fig. 4. Arctic borders according to AMAP. Source: Arctic Portal. Available at: https://www.amap.no/documents/download/585/inline [Accessed: 20 February 2026]

[9] Arctic Monitoring and Assessment Programme (AMAP). Geographical coverage. Available at: https://www.amap.no/about/geographical-coverage [Accessed: 9 February 2026].

Since, according to IMO statistics [19], the risk of spills is higher in water areas with more active shipping, vessel traffic in the coastal waters of Scandinavia is more intense than in the NSR waters, making the introduction of a prohibition on the use of HFO only in the NSR zone seem poorly substantiated.

Therefore, the prohibition on the use of HFO currently poses significant risks to domestic Arctic shipping, jeopardizing the implementation of Arctic mineral resource projects, transport accessibility, the energy security of remote Arctic territories, and the socio-economic interests of indigenous populations who depend on seasonal deliveries of goods by sea. The zone of the HFO prohibition does not correspond to existing concepts of Arctic zone boundaries. Moreover, the prohibition does not apply to areas of Arctic shipping with the most intensive traffic, which entails spill risks.

IMO restrictive measures concerning greenhouse gas emissions from ships

The IMO is one of the initiators of the development of regulatory documents related to the regulation of greenhouse gas emissions and decarbonization in global shipping. In 2003, IMO Assembly Resolution A.963(23) on reducing greenhouse gas emissions from ships was adopted, which for the first time officially introduced measures to control greenhouse gas emissions. In 2011, IMO Resolution MEPC.203(62) was approved, which is considered the first regulatory legal act establishing CO_2 emission standards in a global economic sector. In April 2018, the IMO adopted the Initial IMO Strategy on the Reduction of GHG Emissions from Ships, envisioning their complete reduction by the end of this century (2100).

In July 2023, the 80th session of the IMO Marine Environment Protection Committee was held, during which the IMO Strategy on the Reduction of GHG Emissions from Ships was quite sharply and ambitiously revised. It now envisions achieving net-zero GHG emissions by 2050. The revised 2023 IMO Strategy includes indicative checkpoints for the share of fuels/technologies with low or net-zero GHG emissions to be used by 2030, and interim emission reduction targets compared to 2008: “to reduce the total annual GHG emissions from international shipping by at least 20%, striving for 30%, by 2030; ... by at least 70%, striving for 80%, by 2040 [10)], compared to 2008 levels.”

The required reduction in greenhouse gas emissions presents a serious challenge for the development of maritime activities. The entire Arctic fleet, with the exception of eight nuclear-powered vessels of FSUE Atomflot, uses hydrocarbon fuels

[10)] Available at: https://www.imo.org/ru/ourwork/environment/pages/2023-imo-strategy-on-reduction-of-ghg-emissions-from-ships.aspx [Accessed: 20 February 2026].

(HFO, light fuel oil, LNG). Their combustion inevitably produces greenhouse gases, the quantity of which is regulated by the Strategy under discussion.

The scale of the problem affects the entire maritime sector of the Russian economy, while this work considers only the Northern Sea Basin, specifically the NSR waters. The significance of the issue is heightened by the fact that the baseline year for calculating emission reductions is set as 2008. During that period, cargo turnover on the NSR amounted to 2.22 million tonnes, compared to 37.9 million tonnes in 2024. Such a significant increase in cargo turnover inevitably leads to a proportional increase in GHG emissions in the NSR waters, making the task of reducing emissions particularly challenging and requiring a comprehensive approach.

By 2030, the reduction in GHG emissions, according to the 2023 IMO Strategy, must be at least 20% relative to the 2008 level. The methodology for calculating GHG emission volumes in this work is based on the assumption of a constant coefficient of GHG emissions per unit of cargo transported on the NSR (Table 3). Based on data for 2024 – cargo transportation volumes, total fuel consumption, and calculated total emissions – the emission coefficient per tonne of cargo transported was determined. To calculate annual emissions from the known total fuel consumption on the NSR, emission factors for CO_2, CH_4, and NO_x recommended by IMO Resolution MEPC.376(80) were used. A retrospective calculation allowed for determining the GHG emission volumes in 2008, shown in Table 3.

Further analysis showed that without a transition to environmentally friendly fuels and the implementation of innovative technologies by 2030, the required 20% emission reduction could only be achieved by limiting cargo turnover (Fig. 5). Calculations demonstrate that in this case, to meet the GHG emission targets

Table 3. Greenhouse gas emissions relative to cargo turnover on the NSR against the targets of the IMO 2023 Strategy

Indicators	2008	2024	2030	2040	Coefficient of greenhouse gas emission per 1 t of cargo
Emission, thous. t:					
CO_2	130.17	2222.31	104.37	26.03	$5.860 \cdot 10^{-2}$
CH_4	1.81	30.88	1.45	0.54	$8.148 \cdot 10^{-7}$
NO_x	7.63	130.29	6.11	2.29	$3.438 \cdot 10^{-6}$
Cargo turnover, M t	2.22	37.90	1.78	0.44	–

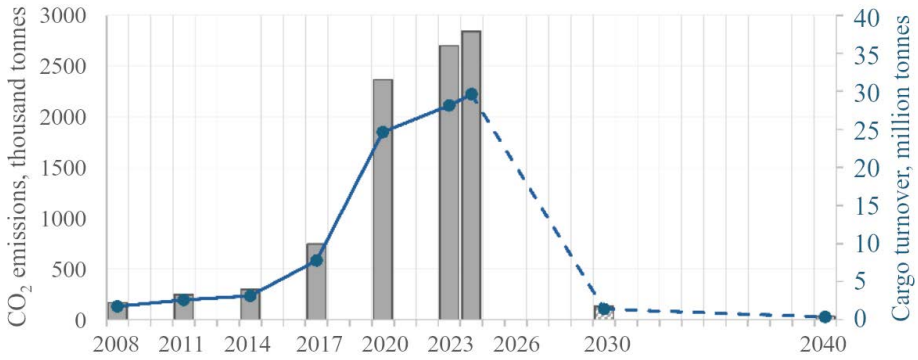

Fig. 5. Projected reduction in CO_2 emissions and cargo traffic on the NSR by 2030 and 2040. The dashed line is estimation

by 2030 and 2040, the volume of traffic along the NSR would have to be reduced to 1.78 million and 0.44 million tonnes per year, respectively, at which point the environmental commitments would be fulfilled.

The emission reduction tools proposed by the IMO are divided into so-called short-term, mid-term, and long-term measures.

The package of short-term measures to reduce GHG emissions from ships includes requirements related to the energy efficiency and operational carbon intensity of existing ships. Amendments to MARPOL Annex VI containing these requirements entered into force on November 1, 2022, were accepted by the Russian Federation under the tacit acceptance procedure, and are currently an integral part of the Russian legal system. The short-term measures are indicated by the IMO as completed, while noting the need for and importance of their review, as defined in regulations 25.3 and 28.11 of MARPOL Annex VI.

The package of mid-term measures includes technical and economic requirements, including the development of a market-based mechanism to equalize the cost of petroleum and alternative marine fuels, the establishment of a standard for the lifecycle GHG intensity of marine fuels, and an emissions pricing mechanism.

Long-term measures are aimed at the progressive development and deployment of non-fossil fuels for the decarbonization of global shipping, as well as the development of technologies with zero GHG emissions to improve the energy efficiency of maritime transport.

An analysis of the short-term, mid-term, and long-term measures proposed by the IMO Strategy revealed several significant limitations in their implementation.

Experts [14] note that the effectiveness of the stated measures does not even come close to achieving the GHG emission target prescribed for 2050. These measures only allow for an improvement in energy efficiency of a few percent.

According to experts [15], fleet renewal is particularly important for achieving the targets of the 2023 IMO Strategy. However, the adopted Strategy lacks clearly defined technical solutions that need to be incorporated into the design of future ships. In these circumstances, owners and shipbuilding companies cannot confidently plan the development of new ship designs in light of future environmental requirements [8].

The package of long-term measures provided for by the Strategy includes the development and use of alternative fuels for shipping. Alternative energy sources for ships include LNG, liquefied biogas, hydrogen, ammonia, methanol, ethanol, wind power, etc. Numerous studies conducted [16–21] show that compared to traditional light fuel oil, alternative marine fuels and energy sources are proclaimed as ideal means for achieving zero emissions, but their use requires correspondingly expensive technical and operational measures to ensure shipping safety.

Experts [8] note that the approved Strategy requires significant scientific and technical refinement, as the document reflects political ambitions more than the real needs of the maritime industry, giving little consideration to the actual necessities and potential consequences for shipping. The proposed mechanisms for limiting emissions are not fully elaborated or substantiated [21].

In addition to the technical and economic solutions discussed above, legal mechanisms for implementing the IMO Strategy must be considered, which could allow for a special approach to its application in the Russian Arctic. For instance, Article 234 of the 1982 United Nations Convention on the Law of the Sea grants coastal states the right to adopt and enforce special environmental requirements for shipping in ice-covered areas within the exclusive economic zone, provided that they are based on scientific evidence and are non-discriminatory. This provision allows for the formation of a differentiated regulatory regime for shipping in Arctic waters, considering local ice conditions and environmental risks.

Furthermore, in accordance with Article 211 of the United Nations Convention on the Law of the Sea, national measures to prevent pollution from ships must conform to international standards but allow for adaptation in light of objective circumstances. International practice confirms the possibility of revising the timelines for implementing new requirements in the presence of technical or economic constraints.

Meanwhile, the 2023 IMO Strategy, despite its recommendatory nature for IMO Member States, currently serves as the basis for developing amendments to IMO instruments, including the mandatory MARPOL Convention.

Amendments to MARPOL Annex VI, currently being developed in line with the indicative checkpoints of the 2023 IMO Strategy, upon ratification by the Russian Federation, will also be mandatory for application and will take precedence over the norms of national legislation in case of conflict with the provisions of MARPOL (Article 15.4 of the Constitution of the Russian Federation).

Conclusions

Currently, there is a trend towards the tightening of international environmental standards in the field of maritime shipping. The regulatory restrictions discussed in the article *de facto* regulate the scale of economic activity in the Arctic region.

The introduction of a prohibition on the use of HFO in polar waters, combined with the implementation of the IMO Strategy for the decarbonization of the fleet, creates significant challenges for the maritime transport industry. Economic actors in the Russian Arctic zone (government bodies, ship-owning companies, and fleet operators) are faced with the need to make comprehensive strategic decisions under new regulatory conditions, lacking a clear understanding of the potential risks and consequences.

Under conditions of sanctions pressure, implementing a set of measures aimed at developing innovative climate technologies in shipping, introducing alternative fuels, and developing the corresponding infrastructure involves significant economic costs, which substantially complicates the process of environmental transformation of Arctic shipping.

The issue raised in this work requires a comprehensive analysis of alternative scenarios for the development of Arctic shipping, an assessment of the economic efficiency of various technological solutions, and the development of a comprehensive program for adapting the industry to the new environmental requirements. It is necessary to create a coherent strategy that takes into account both international commitments and the interests of domestic Arctic transport, which presupposes close cooperation among all interested parties.

Nearly all Arctic projects, transit traffic, and Northern delivery are at risk, which necessitates careful planning of every step in the context of tightening environmental standards and economic sanctions.

References

1. Erokhin, V., 2024. Shipping in the Arctic: A Brief Overview of the Decade's Results. *Marketing and Logistics*, (2), pp. 5–14 (in Russian).
2. Grigoryev, M., 2021. Dynamics of Freight Transport in 2014–2020 and 2020 Results. *The Arctic Herald*, (1), pp. 102–110 (in Russian).
3. Van Luijk, N., Dawson, J. and Cook, A., 2020. Analysis of Heavy Fuel Oil Use by Ships Operating in Canadian Arctic Waters from 2010 to 2018. *FACETS*, 5(1), pp. 304–327. https://doi.org/10.1139/facets-2019-0067
4. Sun, Z., 2019. International Regulation of Heavy Fuel Oil Use by Vessels in Arctic Waters. *International Journal of Marine and Coastal Law*, 34(3), pp. 513–536. https://doi.org/10.1163/15718085-13431095
5. Vasileva, Zh.V., Dzaparov, S.A. and Vasekha, M.V., 2024. Methodology for Estimating Greenhouse Gas Emissions from Arctic Shipping. *Arctic: Ecology and Economy*, 14(4), pp. 596–604. https://doi.org/10.25283/2223-4594-2024-4-596-604 (in Russian).
6. Khoroshev, V.G., Popov, L.N. and Gatin, R.I., 2019. Prospects of Alternative Fuels for Marine Power Plants. *Transactions of the Krylov State Research Centre*, (4), pp. 194–202. https://doi.org/10.24937/2542-2324-2019-4-390-194-202 (in Russian).
7. Tolmachev, S.A., 2021. Ban on the Use of Heavy Fuel Oil on Ships in the Arctic Outcome of IMO Work. *Research Bulletin by Russian Maritime Register of Shipping*, (62/63), pp. 6–13 (in Russian).

8. Tolmachev, S.A., 2023. Questions and Issues Related to the Implementation of the IMO Strategy 2023 on the Reduction of GHG Emissions from Ships. *Research Bulletin by Russian Maritime Register of Shipping*, (72/73), pp. 13–28 (in Russian).
9. Bai, J. and Chircop, A., 2020. The Regulation of Heavy Fuel Oil in Arctic Shipping: Interests, Measures, and Impacts. In: A. Chircop, F. Goerlandt, C. Aporta, R. Pelot, 2020. *Governance of Arctic Shipping. Rethinking Risk, Human Impacts and Regulation*. Cham: Springer. pp. 265–283. https://doi.org/10.1007/978-3-030-44975-9_14
10. Kondratov, N.A., 2015. Experience of Developing the Strategy of Arctic Development by Foreign Countries. *Arctic: Ecology and Economy*, (4), pp. 78–85 (in Russian).
11. Belov, S.V. and Skripnichenko, V.A., 2023. Construction of the Barents-Kara Mineral Resource Center for Non-Ferrous Metals Taking into Account the Development of Sea Communications. *Arctic: Ecology and Economy*, 13(3), pp. 405–416. https://doi.org/10.25283/2223-4594-2023-3-405-416 (in Russian).
12. Pankova, Y.V. and Tarasova, O.V, 2020. On Scenarios of Development of the Arctic Economy and Navigation. *Studies on Russian Economic Development*, 31(5), pp. 514–521. https://doi.org/10.1134/S1075700720050147
13. Yakovlev, V.V., 2003. [*Oil, Gas, Emergency Consequences*]. Saint Petersburg: SpbGPU, 414 p. (in Russian).
14. Magarovsky, V.V., Polovinkin, V.N., Pustoshny, A.V. and Savchenko, O.V., 2023. Novelties in the International Policy Towards Mitigation of Greenhouse Gas Emissions from Ships and Necessary Measures in Marine Industry Part 2. Efficiency Analysis of Power-Saving Measures Intended to Reduce Greenhouse Gas Emissions. *Transactions of the Krylov State Research Centre*, (1), pp. 167–182. https://doi.org/10.24937/2542-2324-2023-1-403-167-182 (in Russian).
15. Shurpyak, V.K., Tolmachev, S.A. and Musonov, M.V, 2021. New IMO Requirements for Reduction of Carbon Dioxide Emissions from Ships Performing Transport Work. *Research Bulletin by Russian Maritime Register of Shipping*, (64/65), pp. 4–18 (in Russian).
16. Wang, Q., Zhang, H., Huang, J. and Zhang, P., 2023. The Use of Alternative Fuels for Maritime Decarbonization: Special Marine Environmental Risks and Solutions from an International Law Perspective. *Frontiers in Marine Science*, 9, 1082453. https://doi.org/10.3389/fmars.2022.1082453
17. Xing, H., Stuart, C., Spence, S. and Chen, H., 2021. Alternative Fuel Options for Low Carbon Maritime Transportation: Pathways to 2050. *Journal of Cleaner Production*, 297, 126651. https://doi.org/10.1016/j.jclepro.2021.126651
18. Salmon, N. and Bañares-Alcántara, R., 2021. Green Ammonia as a Spatialenergy Vector: A Review. *Sustainable Energy Fuels*, 5(11), pp. 2814–2839. https://doi.org/10.1039/D1SE00345C
19. Deniz, C. and Zincir, B., 2016. Environmental and Economical Assessment of Alternative Marine Fuels. *Journal of Cleaner Production*, 113, pp. 438–449. https://doi.org/10.1016/j.jclepro.2015.11.089
20. Karvounis, P., Tsoumpris, C., Boulougouris, E. and Theotokatos, G., 2022. Recent Advances in Sustainable and Safe Marine Engine Operation with Alternative Fuels. *Frontiers in Mechanical Engineering*, 8, 994942. https://doi.org/10.3389/fmech.2022.994942
21. Sardar, A., Islam, R., Anantharaman, M. and Garaniya, V., 2025. Advancements and Obstacles in Improving the Energy Efficiency of Maritime Vessels: A Systematic Review. *Marine Pollution Bulletin*, 214, 117688. https://doi.org/10.1016/j.marpolbul.2025.117688

Submitted 29.08.2025; accepted after review 06.10.2025;
revised 18.12.2025; published 31.03.2026

About the authors

Zhanna V. Vasileva, Head of the Research Laboratory "Eco-engineering and Pollution Monitoring of the Arctic Zone of the Russian Federation", Murmansk Arctic University (13 Sportivnaya St., Murmansk, 183010, Russia), PhD (Techn.), **ORCID ID: 0000-0002-2254-1452, Scopus Author ID: 57226783594**, *kuchugura@mail.ru*

Mikhail V. Vasekha, Leading Researcher, Laboratory of Arctic Logistics, Federal Research Center Kola Science Centre of the Russian Academy of Sciences (14 Fersman St., Apatity, 183010, Russia), DSc (Techn.), **ORCID ID: 0000-0003-0672-5662, Scopus Author ID: 6505839418,** *vasyoha@mail.ru*

Denis A. Erofeev, Lecturer, Department of Theory and History of State and Law, Murmansk Arctic University (13 Sportivnaya St., Murmansk, 183010, Russia), **ORCID ID: 0009-0008-9469-001X,** *zakon.51erofeev@yandex.ru*

Andrey R. Gafurov, Associate Professor, Department of Economics and Management, Murmansk Arctic University (13 Sportivnaya St., Murmansk, 183010, Russia), PhD (Econ.), **ORCID ID: 0000-0002-7901-7694, Scopus Author ID: 572-011-88-298,** *gafurovar-mstu@yandex.ru*

Ekaterina A. Rumiantceva, Senior Researcher, Murmansk Arctic University (15 Kapitan Egorov St., Murmansk, 183038, Russia), PhD (Phys.-Math.), **ORCID ID: 0000-0003-2916-3092, Scopus Author ID: 57205164298,** *rumkate@rambler.ru*

Contribution of the authors:

Zhanna V. Vasileva – overall scientific supervision of the study, formulation of the study goals and objectives, development of methodology and approaches, literature review on the study problem, discussion of the results, formulation of the conclusions, preparation of the article text

Mikhail V. Vasekha – literature review on the study problem, development of methodology and approaches, analysis of the obtained results, discussion of the article materials and study findings, formulation of the conclusions, preparation of the article text, revision of the text

Denis A. Erofeev – processing of regulatory and legal documentation related to the article topic, formulation of conclusions regarding the legal aspects of the scientific problem

Andrey R. Gafurov – information collection and calculations, revision of the text

Ekaterina A. Rumiantceva – material processing, discussion of the results, editing of the manuscript

All authors have read and approved the final version of the manuscript.

Original paper

Methodological Features in Measuring the True Light Absorption Spectrum of Monocultures

S. A. Sholar [1] *, V. V. Suslin [1], L. V. Stelmakh [2], N. V. Minina [2], O. S. Alatartseva [2]

[1] *Marine Hydrophysical Institute of RAS, Sevastopol, Russia*
[2] *A. O. Kovalevsky Institute of Biology of the Southern Seas of RAS, Sevastopol, Russia*

* *e-mail: sa.sholar@mail.ru*

Abstract
This study presents a technique for determining the true light absorption spectrum of a dense culture of the marine coccolithophore *Chrysotila* sp. using a single-beam MS 122A spectrophotometer equipped with an integrating sphere. The main problem with standard measurements is the distortion of the spectrum due to light scattering by cells, which is especially noticeable in the near-infrared region (750–800 nm), where the pigments are not absorbed, but the signal is not zero. To compensate for the scattering effect, the authors used an approach based on recording absorption spectra at two positions from the integrating sphere: standard (close to) and at a distance of 2 mm. The correction factor, independent of wavelength, was calculated from data in the range of 750–800 nm. Its value was 3.77. The true absorption spectrum, stripped of the scattering contribution, was calculated using the proposed formula. The technique has shown its effectiveness for cultures with a high cell density, providing zero absorption values in the near-infrared region. However, with a low cell concentration, the technique is inapplicable due to a significant increase in errors. Thus, the work demonstrates a practical way to correctly determine *in vivo* absorption spectra using available equipment, which is important for ecological and physiological studies of phytoplankton as well as for development of regional remote sensing algorithms.

Keywords: spectrophotometry, integrating sphere, light absorption, coccolithophorides, Chrysotila sp., true absorption spectrum, correction factor, *in vivo*, *in vitro*, acetone extract

Acknowledgments: The work was carried out under state assignment FNNN-2024-0012 “Analysis, diagnosis and real-time forecast of the state of hydrophysical and hydrochemical fields of marine water areas based on mathematical modelling using data from remote and in situ methods of measurements” (code “Operational Oceanology”) and IBSS RAS state assignment no. 124030400057-4 “Transformation of the structure and functions of marine pelagic ecosystems under conditions of anthropogenic impact and climate change”.

For citation: Sholar, S.A., Suslin, V.V., Stelmakh, L.V., Minina, N.V. and Alatartseva, O.S., 2026. Methodological Features in Measuring the True Light Absorption Spectrum of Monocultures. *Ecological Safety of Coastal and Shelf Zones of Sea*, (1), pp. 146–155.

© Sholar S. A., Suslin V. V., Stelmakh L. V., Minina N. V., Alatartseva O. S., 2026

This work is licensed under a Creative Commons Attribution-Non Commercial 4.0 International (CC BY-NC 4.0) License

Методические особенности измерения истинного спектра поглощения света монокультурами

С. А. Шоларь [1] *, **В. В. Суслин** [1], **Л. В. Стельмах** [2], **Н. В. Минина** [2], **О. С. Алатарцева** [2]

[1] *Морской гидрофизический институт РАН, Севастополь, Россия*
[2] *Институт биологии южных морей имени А.О. Ковалевского РАН, Севастополь, Россия*
* *e-mail: sa.sholar@mail.ru*

Аннотация
Представлена методика определения истинного спектра поглощения света плотной культурой морской кокколитофориды *Chrysotila* sp. с использованием однолучевого спектрофотометра МС 122А, оснащенного интегрирующей сферой. Основная проблема стандартных измерений заключается в искажении спектра из-за светорассеяния клетками, что особенно заметно в ближней инфракрасной области (750–800 нм), где поглощение пигментов отсутствует, но измеряемый сигнал не равен нулю. Для компенсации эффекта рассеяния использован подход, основанный на регистрации спектров поглощения при двух положениях кюветы относительно интегрирующей сферы: стандартном (вплотную) и на расстоянии 2 мм. Поправочный коэффициент, не зависящий от длины волны, рассчитывали по данным в области 750–800 нм, его значение составило 3.77. Истинный спектр поглощения, очищенный от вклада рассеяния, вычисляли по предложенной формуле. Методика показала эффективность для культур с высокой численностью клеток, обеспечивая нулевые значения поглощения в ближней ИК-области. Однако при низкой концентрации клеток метод неприменим из-за значительного роста погрешностей. Таким образом, работа демонстрирует практический способ корректного определения спектров поглощения *in vivo* на доступном оборудовании, что важно для экологических и физиологических исследований фитопланктона, а также для развития региональных алгоритмов дистанционного зондирования.

Ключевые слова: спектрофотометрия, интегрирующая сфера, поглощение света, кокколитофориды, *Chrysotila* sp., истинный спектр поглощения, поправочный коэффициент, *in vivo*, *in vitro*, ацетоновый экстракт

Благодарности: работа выполнена в рамках государственного задания ФГБУН ФИЦ МГИ FNNN-2024-0012 «Анализ, диагноз и оперативный прогноз состояния гидрофизических и гидрохимических полей морских акваторий на основе математического моделирования с использованием данных дистанционных и контактных методов измерений» (шифр «Оперативная океанология») и ФГБУН ФИЦ ИнБЮМ «Трансформация структуры и функций экосистем морской пелагиали в условиях антропогенного воздействия и изменений климата» (№124030400057-4).

Для цитирования: *Шоларь С. А., Суслин В. В., Стельмах Л. В., Минина Н. В. и др.* Методические особенности измерения истинного спектра поглощения света монокультурами // Экологическая безопасность прибрежной и шельфовой зон моря. 2026. № 1. С. 146–155. EDN WIERCH.

Introduction

Spectrophotometers are the primary tool for assessing the optical properties of photosynthetic cells. However, the reliability of *in vivo* absorption spectrum measurements is limited by the distorting effect of light scattering, the magnitude of which depends both on the distribution of scattered light within the sample and on the geometry of the cuvette and detector.

The most effective way to minimize the loss of scattered light is to use an integrating sphere (IS) in spectrophotometers [1], the inner surface of which has a high reflection coefficient. When the studied sample is placed inside such a sphere, all scattered light reaches the photodetector, and the measured optical density is determined only by the true absorption of light by the sample [2]. However, in standard spectrophotometers equipped with an IS, the design typically does not allow the sample to be placed inside the sphere, instead, the cuvette is positioned in front of the entrance port. In this configuration, it is impossible to completely eliminate the contribution of scattering.

Two approaches for correction have been proposed in the literature: the use of correction factors and the method of recording spectra at different distances from the IS [3, 4]. The second approach is based on the fact that changing the distance to the IS allows the fraction of scattered light in the recorded signal to vary. Measurements at two distances (one close to and one far from the IS) make it possible to reconstruct the absorption spectrum compensated for scattering, which is confirmed by values approaching zero in the 750–800 nm range, where pigment absorption is absent [5].

Subsequently, such corrected spectra can be used in regional algorithms to separate the contributions of coccolithophores, diatoms, and dinoflagellates from multispectral measurements of the sea surface reflectance coefficient [6], obtained, for example, from satellite data.

For the Black Sea, an urgent task is the development of regional algorithms for interpreting satellite data, which allow the separation of the contribution of various taxonomic groups of phytoplankton (coccolithophores, diatoms, and dinoflagellates) to the total biomass [7]. Solving this problem requires reference absorption spectra of pure cultures of dominant species. In 2023, a series of studies was initiated to investigate the spectral features of the light absorption coefficient of individual Black Sea phytoplankton species of different taxonomic affiliations. However, the quality of the initial *in vivo* spectra obtained using the MS 122A spectrophotometer by the standard method remains unsatisfactory for reliable separation of these contributions, making scattering correction mandatory.

The present paper aims to determine the true light absorption spectrum of a batch culture of the marine coccolithophore *Chrysotila* sp. using a single-beam MS 122A spectrophotometer and the method of measurements at two distances from the IS. This work was carried out using materials from a report presented at the XIII All-Russian Conference with International Participation “Current Problems in Optics of Natural Waters 2025” [8].

Materials and methods

The study used an algologically pure culture of the coccolithophore *Chrysotila* sp. P. L. Anand from the collection of living cultures of marine planktonic microalgae at A. O. Kovalevsky Institute of Biology of the Southern Seas of RAS.

The algae were cultivated in 0.2 L conical flasks in *f*/2 medium [9] prepared with pasteurized seawater. To maintain the culture in the exponential growth phase and at a constant cell density, it was diluted daily with fresh nutrient medium. The cultivation temperature was 18 ± 1°C, which corresponds to the temperature optimum for the studied species.

Absorption spectra were recorded in cuvettes with an optical path length of 1 cm in the range from 300 to 800 nm with a step of 1 nm using a single-beam MS 122A spectrophotometer (SOL instruments, Minsk, Belarus), equipped with a diffuse transmission and reflection attachment with an IS. During the measurements, the cuvette was placed in the cuvette holder of the attachment in front of the IS entrance port [1)]. The inner diameter of the IS is 50.8 mm (2 inches). The inner surface coating of the IS is $BaSO_4$.

Measurements were carried out at two cuvette positions (Fig. 1): the standard position – flush against the IS entrance port ($r = 0$); the distant position – at the maximum possible distance for this setup, $r = 2$ mm from the IS entrance port. The design of the cuvette compartment of the MS 122A spectrophotometer does not allow the cuvette to be placed at a distance greater than 2 mm (a limitation imposed by the mirror in the optical system); therefore, this value was used in the work.

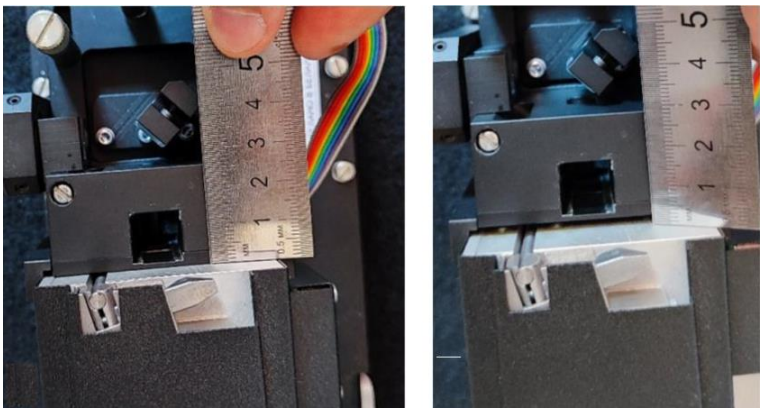

a ***b***

Fig. 1. Top view of the MS 122A cuvette compartment: *a* – in a position close to the integrating sphere (IS); *b* – at a distance of 2 mm from the IS

[1)] Available at: https://solinstruments.by/produkciya/spektrofotometry/mc-122/dopolnitelnoe-oborudovanie/ [Accessed: 14 February 2025].

The true absorption spectrum, compensated for scattering, was determined by the formula [1]:

$$\tilde{a}(\lambda) = a_{ph}(\lambda; r) - L_{att}(r; 0)\cdot\left[a_{ph}(\lambda; r) - a_{ph}(\lambda; 0)\right]. \quad (1)$$

where $a_{ph}(\lambda; r)$ is the light absorption coefficient of the sample located at a distance r from the IS; $L_{att}(r; 0)$ is the correction factor; and $a_{ph}(\lambda; 0)$ is the light absorption coefficient at the standard cuvette position.

Experiments studying the influence of the distance from the IS to the sample on absorption spectra are well described in [3].

It is assumed that the correction factor $L_{att}(r; 0)$ is wavelength-independent and its value can be determined by considering the wavelength region where the sample does not absorb light (i.e., the 750–800 nm region of the visible range):

$$L_{att}(r; 0) = \frac{a_{750-800}(\lambda; r)}{a_{750-800}(\lambda; r) - a_{750-800}(\lambda; 0)}. \quad (2)$$

For comparative analysis, pigments were extracted from the cells with 100% acetone according to the method described in [10]. Absorption spectra of the extracts were recorded on the same instrument using standard 1 cm cuvettes.

Results and discussion

With the standard cuvette position (close to the IS), light absorption by the sample $a_{ph}(\lambda; 0)$ in the 750–800 nm range, where pigments are not absorbing, does not reach zero values. In this region, light absorption increases monotonically with increasing distance between the cuvette and the IS. This phenomenon is caused by non-selective scattering by microbial cells, which arises from abrupt changes in the refractive index at interfaces. Selective scattering likely also contributes, associated with abrupt changes in the refractive index caused by pigments embedded in thylakoid membranes within the spectral regions of their light absorption [4].

Fig. 2 shows the light absorption spectra of a dense culture obtained with the MS 122A spectrophotometer at two cuvette positions: the standard position, $a_{ph}(\lambda; 0)$, and the position at a distance of 2 mm from the IS entrance port, $a_{ph}(\lambda; r)$.

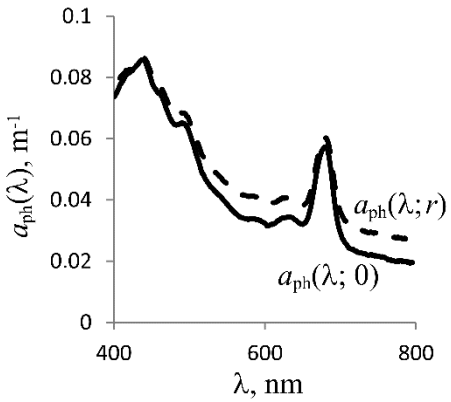

Fig. 2. Examples of light absorption spectra of the *Chrysotila* sp. culture obtained at the standard cuvette position, $a_{ph}(\lambda; 0)$, and at a distance of $r = 2$ mm from the IS input window, $a_{ph}(\lambda; r)$

To correct for the scattering contribution, formula (2) was used, and calculations were performed for several λ values:

$$L_{750} = \frac{a(750; r)}{a(750; r) - a(750; 0)} = \frac{0.0289}{0.0289 - 0.0216} = 3.96,$$

$$L_{775} = \frac{a(775; r)}{a(775; r) - a(775; 0)} = \frac{0.0276}{0.0276 - 0.02} = 3.63,$$

$$L_{800} = \frac{a(800; r)}{a(800; r) - a(800; 0)} = \frac{0.0268}{0.0268 - 0.0196} = 3.72.$$

According to the methods described in [3], the correction factor L was determined as the average value in the 750–800 nm region. For the studied *Chrysotila* sp. culture, the average value of the coefficient $L_{att}(r; 0)$ for the three wavelengths was 3.77 in this work.

Using formula (1), the true absorption value was calculated for each wavelength. As an example, the calculation for the wavelength λ = 443 nm is presented:

$$\tilde{a}(443) = 0.0853 - 3.77 \cdot [0.0853 - 0.0841] = 0.081.$$

Carrying out similar calculations for the remaining wavelengths, the true spectrum of the light absorption coefficient of the *Chrysotila* sp. culture, compensated for scattering, was obtained (Fig. 3). A characteristic feature of this spectrum is the absence of light absorption in the 750–800 nm range (Fig. 3), which confirms the quality of the correction performed.

It should be noted that the described method is effective only at high cell densities, when the culture in the cuvette exhibits a noticeable color, distinguishable visually. At low algae concentrations, the recorded spectra contain (at $a_{ph}(750; 0) > 0.02$ m^{-1}) a significant number of artifacts, which can be mistakenly interpreted as spectral peaks. An attempt to recover the true spectrum under such conditions leads to the amplification of noise spikes and an increase in measurement error. As an example, Fig. 4 shows spectra for two concentrations: the undiluted culture (570,000 cells/mL) (Fig. 4, *a*) and the culture after an eight-fold dilution (71,300 cells/mL) (Fig. 4, *b*).

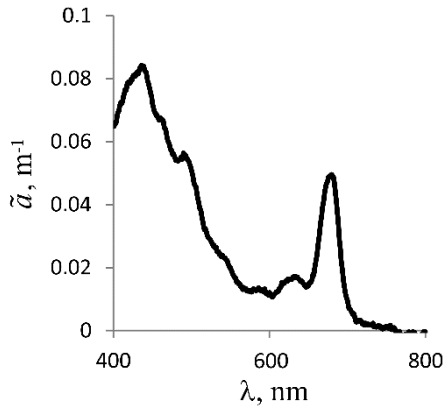

Fig. 3. True light absorption spectrum of the *Chrysotila* sp. culture determined by expression (1)

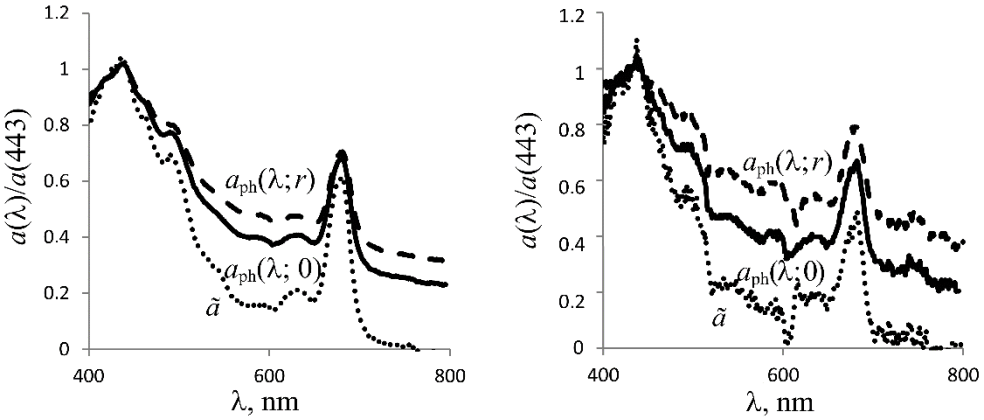

Fig. 4. Absorption spectra of the *Chrysotila* sp. culture normalized to 443 nm, obtained at the standard position of the cuvette, $a_{ph}(\lambda; 0)$, at a distance $a_{ph}(\lambda; r)$ from the IS input window and the true spectra $\tilde{a}$ calculated using expression (1) for a concentration of 570,000 cells/mL (*left*) and 71,300 cells/mL (*right*)

Fig. 5 presents a comparison of the true *in vivo* absorption spectrum (dashed line) and the spectrum of the acetone extract (solid line) for the concentration of 570,000 cells/mL. The spectrum of the acetone extract of the algae is characterized by a shift of the peaks towards shorter wavelengths [11, p. 304] relative to the *in vivo* spectrum. This shift is mainly due to the destruction of pigment-protein complexes during extraction with organic solvents, changes in the polarity of the medium, and aggregation/dissociation of pigments in acetone.

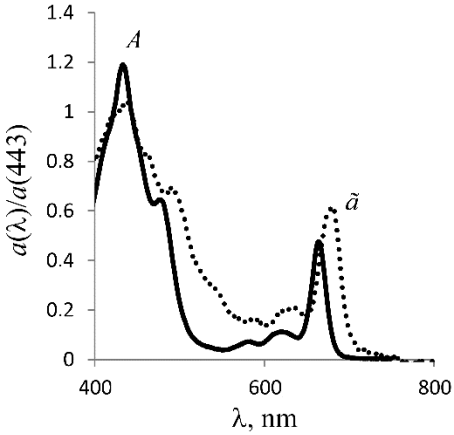

Fig. 5. Light absorption spectra of the *Chrysotila* sp. culture normalized to 443 nm, where the dotted line is the true spectrum calculated using expression (1), the solid line is the spectrum of the acetone extract

This fact is critically important for interpreting remote sensing data, since the calibration of satellite instruments is often based on *in vitro* spectra, whereas *in situ* measurements correspond to the *in vivo* state of pigments. The difference in spectral characteristics is due to the fact that in acetone extracts, some pigments (e. g., chlorophylls) can form aggregates (dimers, oligomers). Aggregation often leads to splitting and shifts of absorption peaks. In the native state, the absorption maximum of chlorophyll is around 660–680 nm (red region), while in acetone extracts the peak can shift to 650–665 nm (hypsochromic shift), which is associated with the loss of interaction with proteins [7].

Conclusions

A method for correcting phytoplankton absorption spectra for scattering has been adapted for the single-beam MS 122A spectrophotometer with an IS. It was established that the maximum possible distance of the cuvette from the IS (2 mm) is sufficient for calculating the correction factor and obtaining the true absorption spectrum, confirmed by values approaching zero in the 750–800 nm range.

For the *Chrysotila* sp. culture, the average value of the correction factor $L = 3.77$ was calculated in the 750–800 nm region. Using this factor, the true *in vivo* absorption spectrum, corrected for the scattering contribution, was obtained.

The applicability limits of the method were determined: it is effective only at high cell densities, when the absorption coefficient at a wavelength of 750 nm $a_{ph}(750; 0)$ exceeds 0.02 m^{-1}. At low concentrations (below 700,000 cells/mL), correction leads to noise amplification and the appearance of artifacts.

It was confirmed that the spectra of acetone extracts of *Chrysotila* sp. pigments are characterized by a hypsochromic shift (shift to shorter wavelengths) relative to *in vivo* spectra, which is caused by the destruction of pigment-protein complexes and pigment aggregation in acetone. This difference must be taken into account when calibrating algorithms for remote sensing of phytoplankton from satellite data.

REFERENCES

1. Ritchie, R.J. and Sma-Air, S., 2020. Using Integrating Sphere Spectrophotometry in Unicellular Algal Research. *Journal of Applied Phycology*, 32(5), pp. 2947–2958. https://doi.org/10.1007/s10811-020-02232-y
2. Klochkova, V.S., Lelekov, A.S., Shiryaev, A.V., Gevorgiz, R.G., Buchelnikov, A.S. and Shupova, E.V., 2021. Change in the Optical Density Spectrum of the Batch Culture *Arthrospira (Spirulina) platensis*. *Russian Journal of Biological Physics and Chemistry*, 6(4), pp. 543–547 (in Russian).
3. Merzlyak, M.N. and Naqvi, K.R., 2000. On Recording the True Absorption Spectrum and the Scattering Spectrum of a Turbid Sample: Application to Cell Suspensions of the Cyanobacterium *Anabaena variabilis*. *Journal of Photochemistry and Photobiology B: Biology*, 58(2–3), pp. 123–129. https://doi.org/10.1016/S1011-1344(00)00114-7
4. Davies-Colley, R.J., Pridmore, R.D. and Hewitt, J.E., 1986. Optical Properties of Some Freshwater Phytoplanktonic Algae. *Hydrobiologia*, 133(2), pp. 165–178. https://doi.org/10.1007/BF00031865

5. Merzlyak, M.N., Chivkunova, O.B., Solovchenko, A.E., Maslova, I.P., Klyachko-Gurvich, G.L. and Naqvi, K.R., 2008. Light Absorption and Scattering by Cell Suspensions of Some Cyanobacteria and Microalgae. *Russian Journal of Plant Physiology*, 55(3), pp. 420–425. https://doi.org/10.1134/S1021443708030199

6. Suslin, V.V., Sholar, S.A., Mansurova, I.M., Alatartseva, O.S. and Stelmakh, L.V., 2023. Absorption Spectra of Diatoms and Dinoflagellates and Their Features: Laboratory Experiment. In: IO RAS, 2023. *Proceedings of the XII All-Russian Conference with International Participation "Current Problems in Optics of Natural Waters"*, Saint-Petersburg: IO RAS, pp. 107–110 (in Russian).

7. Lee, M.E., Shybanov, E.B., Korchemkina, E.N. and Martynov, O.V., 2015. Determination of the Concentration of Seawater Components Based on Upwelling Radiation Spectrum. *Physical Oceanography*, (6), pp. 15–30. https://doi.org/10.22449/1573-160X-2015-6-15-30

8. Sholar, S.A., Suslin, V.V., Minina, N.V., Alatartseva, O.S. and Stelmakh, L.V., 2025. Methodical Features of Measuring Light Absorption Spectra by Monocultures in Laboratory Conditions. In: IO RAS, 2025. *Proceedings of the XII All-Russian Conference with International Participation "Current Problems in Optics of Natural Waters"*, Saint-Petersburg: Publishing House of SpbSUE, pp. 245–250 (in Russian).

9. Guillard, R.R.L. and Ryther, J.H., 1962. Studies of Marine Planktonic Diatoms. I. Cyclotella nana Hustedt, and Detonula confervacea (Cleve) Gran. *Canadian Journal of Microbiology*, 8(2), pp. 229–239. https://doi.org/10.1139/m62-029

10. Kopytov, Yu.P., Lelekov, A.S., Gevorgiz, R.G., Nekhoroshev, M.V. and Novikova, T.M., 2015. Method of Complex Analysis of Biochemical Composition of Microalgae. *Algologia*, 25(1), pp. 35–40. https://doi.org/10.15407/alg25.01.035 (in Russian).

11. Tokarev, Yu.N., Finenko, Z.Z. and Shadrin, N.V., eds., 2008. *The Black Sea Microalgae: Problems of Biodiversity Preservation and Biotechnological Usage*. Sevastopol: ECOSI-Gidrophizika, 454 p. (in Russian).

Submitted 24.10.2025; accepted after review 16.11.2025;
revised 18.12.2025; published 31.03.2026

Declaration of authors' contribution:

Stanislav A. Sholar, Researcher, Marine Hydrophysical Institute of the Russian Academy of Sciences (2 Kapitanskaya St., Sevastopol, 299011, Russia), PhD (Tech.), **ORCID ID: 0000-0002-7242-3403, Scopus Author ID: 57189886286, ResearcherID: GSD-9744-2022**, *sa.sholar@mail.ru*

Vyacheslav V. Suslin, Head of the Department of Oceanic Process Dynamics, Leading Researcher, Marine Hydrophysical Institute of the Russian Academy of Sciences (2 Kapitanskaya St., Sevastopol, 299011, Russia), PhD (Phys.-Math.), **ORCID ID: 0000-0002-8627-7603, Scopus Author ID: 6603566261, ResearcherID: B-4994-2017,** *slava.suslin@mhi-ras.ru*

Lyudmila V. Stelmakh, Head of the Department of Ecological Physiology of Algae, Chief Researcher, A.O. Kovalevsky Institute of Biology of the Southern Seas of the Russian Academy of Sciences (2 Nakhimov Ave., Sevastopol, 299011, Russia), DSc (Biol.), **ORCID ID: 0000-0003-2970-0281, Scopus Author ID: 6603262213, ResearcherID: G-9892-2018,** *lustelm@mail.ru*

Natalya V. Minina, Leading Engineer, A.O. Kovalevsky Institute of Biology of the Southern Seas of the Russian Academy of Sciences (2 Nakhimov Ave., Sevastopol, 299011, Russia), **Scopus Author ID: 57223993379,** *mininachatan@mail.ru*

Olga S. Alatartseva, Junior Researcher, A.O. Kovalevsky Institute of Biology of the Southern Seas of the Russian Academy of Sciences (2, Nakhimov Ave., Sevastopol, 299011, Russia), **ORCID ID: 0000-0002-9671-2285, Scopus Author ID: 57963185300,** *moon-23@mail.ru*

Declaration of authors' contribution:

Stanislav A. Sholar – preparation of graphic materials, literature review on the study problem, manuscript writing, formulation of conclusions, article formatting, collection of study materials

Vyacheslav V. Suslin – formulation and statement of the problem, discussion of the results, concept development, analysis of the results, manuscript writing

Lyudmila V. Stelmakh – formulation and statement of the problem, concept development, analysis of the results, manuscript writing, study supervision

Natalya V. Minina – collection of study materials, primary processing and sorting of data, discussion of the results

Olga S. Alatartseva – collection of study materials, primary processing and sorting of data, discussion of the results

All authors have read and approved the final version of the manuscript.